Canadian
Journal of Chemistry

STRUCTURE OF AN ARABINOGALACTAN FROM TAMARACK (LARIX LARICINA)[1]

S. HAQ[2] AND G. A. ADAMS

ABSTRACT

Partial acid hydrolysis of an arabinogalactan from tamarack wood yielded:
- (I) L-arabinose,
- (II) D-galactose,
- (III) 3-O-β-L-arabinopyranosyl-L-arabinose,
- (IV) 6-O-β-D-galactopyranosyl-D-galactose,
- (V) 3-O-β-D-galactopyranosyl-D-galactose,
- (VI) O-D-galactopyranosyl($1 \rightarrow 6$)-O-D-galactopyranosyl($1 \rightarrow 6$)-D-galactose,
- (VII) 3,6-di-O-(galactopyranosyl)-D-galactopyranose,
- (VIII) O-D-galactopyranosyl($1 \rightarrow 3$)-D-galactose,
- (IX) O-D-galactopyranosyl($1 \rightarrow 6$)-O-D-galactopyranosyl($1 \rightarrow 3$)-D-galactose,
- (X) O-D-galactopyranosyl($1 \rightarrow 6$)-O-D-galactopyranosyl($1 \rightarrow 6$)-O-D-galactopyranosyl ($1 \rightarrow 3$)-D-galactose,
- (XI) O-D-galactopyranosyl($1 \rightarrow 6$)-O-D-galactopyranosyl($1 \rightarrow 3$)-O-D-galactopyranosyl ($1 \rightarrow 3$)-D-galactose.

A previously published structure for the tamarack polysaccharide was revised to show that not more than two consecutive $1 \rightarrow 3$ or $1 \rightarrow 6$ linkages respectively were present in the main core of the repeating unit. Some of the 6-O-β-D-galactopyranosyl-D-galactose units occurred as side chains as well as in the main body of the molecule.

It has been shown previously that the water-soluble polysaccharide of tamarack (*Larix laricina*) is a highly branched arabinogalactan composed of L-arabinose and D-galactose in the ratio of 1:3.8 (1). Evidence was presented to indicate that the galactose residues were joined predominantly by $1 \rightarrow 3$ and $1 \rightarrow 6$ glycosidic linkages. The original view (2) that arabinose was attached as a single molecule in the furanose form in ϵ-galactan polysaccharides was made untenable by the isolation of β-3-O-L-arabinopyranosyl-L-arabinose from a mild hydrolysis of both a larch ϵ-galactan (3) and an arabinogalactan from western larch (*Larix occidentalis*) (4). The present work which describes the fragmentation analysis of arabinogalactan from tamarack was undertaken to provide additional information on the fine structure of the polysaccharide.

The polysaccharide was subjected to a progressive, mild acidic hydrolysis, as it was observed previously (1) that such treatment released arabinose units almost completely from the main body of the polysaccharide, resulting in a degraded galactan. The chromatographic picture of the hydrolyzate (0.01 N H_2SO_4 for 3 hours and .02 N H_2SO_4 for 4 hours) revealed as the main components, L-arabinose, D-galactose, a disaccharide of arabinose, and a disaccharide of galactose. In addition, there were several minor spots of sugars giving pink or reddish-brown colors with p-anisidine hydrochloride spray reagent. Two of these moved on paper chromatograms faster than arabinose and two moved

between galactobiose and arabinobiose and gave a reddish-brown color with p-anisidine hydrochloride. One of the faster-moving components had the same R_F value as L-rhamnose but it was not sufficient in amount to permit further characterization. The components moving between galactobiose and arabinobiose were probably the products of resynthesis because heating of a mixture of arabinose and galactose under the same conditions showed very faint spots having the same flow rates on the chromatogram.

After the foregoing mild hydrolysis, the degraded galactan was subjected to a more rigorous hydrolysis. From the hydrolyzates the various sugars were isolated through a combination of cellulose and charcoal–celite column chromatography. The results are shown in Table I. The preliminary hydrolysis released the monosaccharides, the disac-

TABLE I

Sugars recovered from partial acid hydrolysis of arabinogalactan of tamarack

	Name	Yield (mg)
(I)	L-Arabinose	Not determined
(II)	D-Galactose	Not determined
(III)	3-O-β-L-Arabinopyranosyl-L-arabinose	500
(IV)	6-O-β-D-Galactopyranosyl-D-galactose	850
(V)	3-O-β-D-Galactopyranosyl-D-galactose	390
(VI)	O-D-Galactopyranosyl(1 → 6)-O-D-galactopyranosyl(1 → 6)-D-galactose	17
(VII)	3,6-Di-O-(galactopyranosyl)-D-galactopyranose	32
(VIII)	O-D-Galactopyranosyl(1 → 3)-O-D-galactopyranosyl(1 → 3)-D-galactose	106
(IX)	O-D-Galactopyranosyl(1 → 6)-O-D-galactopyranosyl(1 → 3)-D-galactose	93
(X)	O-D-Galactopyranosyl(1 → 6)-O-D-galactopyranosyl(1 → 6)-O-D-galactopyranosyl(1 → 3)-D-galactose	35
(XI)	O-D-Galactopyranosyl(1 → 6)-O-D-galactopyranosyl(1 → 3)-O-D-galactopyranosyl(1 → 3)-D-galactose	94

charides of arabinose, and galactobiose (IV). The more rigorous hydrolysis released D-galactose (II), additional galactobiose (IV), and all other oligosaccharides. L-Arabinose and D-galactose were crystallized and identified by their physical properties.

The disaccharide of arabinose on complete acidic hydrolysis and chromatographic examination gave arabinose as the only monosaccharide. On complete methylation and hydrolysis, the disaccharide gave (i) 2,3,4-tri-O-methyl-L-arabinose, (ii) 2,4-di-O-methyl-L-arabinose, and (iii) 2,5-di-O-methyl-L-arabinose. These sugars were characterized through their respective crystalline derivatives.

The presence of 2,4- and 2,5-di-O-methyl-L-arabinose in the hydrolyzate of the methylated disaccharide indicated that the disaccharide was a mixture of β-3-O-L-arabinopyranosyl-L-arabinopyranose and β-3-O-L-arabinopyranosyl-L-arabinofuranose. From the amount of 2,4-di-O-methyl-L-arabinose (93 mg) and 2,5-di-O-methyl-L-arabinose (14.2 mg) it was concluded that the two forms of the disaccharide were present in the mixture in the ratio of 6.5:1. Approximately the same ratio was found between the 2,4- and 2,5-di-O-methyl arabinoses by gas–liquid chromatography (5, 6). The lower specific rotation of the disaccharide and that of its methylated derivative compared to those reported by previous workers (3, 4) also indicated the possibility of a disaccharide present in furanose form. The 2,5-di-O-methyl-L-arabinose could not have arisen from incomplete methylation of the disaccharide because the methoxyl content of the methylated derivative agreed with the theoretical value and no adsorption corresponding to $(OH)^-$ group could be detected in the infrared spectrum.

The disaccharide of galactose, which was obtained by mild acid hydrolysis, was crystallized and identified as β-6-O-D-galactopyranosyl-D-galactose and was identical with

galactobiose (IV) described below. The amount released in the preliminary hydrolysis was approximately one quarter of the total amount that was recovered from all hydrolyses. Galactobiose (IV) was obtained in crystalline form and its specific rotation indicated a β-linkage. The mode of linkage in the disaccharide was established by the isolation of 2,3,4,6-tetra-O-methyl-D-galactose and 2,3,4-tri-O-methyl-D-galactose from the hydrolyzate of fully methylated disaccharide. Thus the structure of galactobiose (IV) was confirmed as β-6-O-D-galactopyranosyl-D-galactose.

Galactobiose (V) on complete acidic hydrolysis gave only galactose and its flow rate on a chromatogram indicated that it was a disaccharide. On complete methylation and hydrolysis, the disaccharide gave 2,3,4,6-tetra-O-methyl-D-galactose and 2,4,6-tri-O-methyl-D-galactose, and its structure was established as 3-O-D-galactopyranosyl-D-galactose.

Galactotriose (VI) and galactotriose (VII) were isolated in very small amounts and complete structural studies by methylation were not possible. However, some preliminary experiments revealed their probable structure. Galactotriose (VI) on partial hydrolysis gave galactose, galactobiose (IV), and the original sugar. On reduction and partial hydrolysis of the reduced product, galactose and galactobiose (IV) were obtained as reducing sugars. Therefore galactotriose (VI) is probably O-D-galactopyranosyl (1 → 6)-O-D-galactopyranosyl(1 → 6)-D-galactose. Galactotriose (VII) on partial acidic hydrolysis gave galactose, galactobiose (IV), galactobiose (V), and the original sugar. After reduction and partial hydrolysis of the derived glycitol, galactose was obtained as the only reducing sugar. Therefore the evidence suggests that galactobiose (VII) is probably a branched trisaccharide having the tentative structure 3,6-digalactopyranosyl-D-galactose.

Galactotriose (IX) on complete methylation and hydrolysis of the methylated product gave 2,3,4,6-tetra-O-methyl-D-galactose; 2,3,4-tri-O-methyl-D-galactose; and 2,4,6-tri-O-methyl-D-galactose in equimolar proportion. These results indicated that the trisaccharide was a straight chain containing 1 → 6 and 1 → 3 glycosidic linkages. The trisaccharide on partial acidic hydrolysis gave galactobiose (IV) and galactobiose (V). The sequence of glycosidic linkages was established by the reduction of the trisaccharide and partial hydrolysis of the derived glycitol. On reduction and hydrolysis the trisaccharide gave galactose and galactobiose (IV) as reducing sugars. This finding confirmed that the 1 → 3 linkage was at the reducing end of the molecule while the 1 → 6 linkage was penultimate to the reducing end. Therefore the structure of galactotriose (IX) was established as O-D-galactopyranosyl(1 → 6)-O-D-galactopyranosyl(1 → 3)-D-galactose.

Galactotriose (VIII) was obtained in crystalline form for the first time. The sugar, after partial acidic hydrolysis, gave galactose, galactobiose (V), and the original trisaccharide. After reduction and partial hydrolysis it gave galactose and galactobiose (V) as reducing sugars. Therefore it was probably a straight-chain trisaccharide containing 1 → 3 glycosidic linkages. On methylation and hydrolysis of the methylated product, the trisaccharide gave 2,3,4,6-tetra-O-methyl-D-galactose (1 mole) and 2,4,6-tri-O-methyl-D-galactose (2 moles). Therefore the structure of galactotriose (VIII) was established as O-D-galactopyranosyl(1 → 3)-O-D-galactopyranosyl(1 → 3)-D-galactose.

Galactotetraose (X) on partial acidic hydrolysis produced galactose, galactobiose (IV), galactobiose (V), galactotriose (VI), galactotriose (IX), and the original sugar. On reduction and hydrolysis it gave galactose, galactobiose (IV), and galactotriose (VI). Therefore the structure of galactotetraose (X) was proposed as O-D-galactopyranosyl (1 → 6)-O-D-galactopyranosyl(1 → 6)-O-D-galactopyranosyl(1 → 3)-D-galactose. Similarly,

on the basis of the products of partial hydrolysis of the sugar and its reduced product, the structure of galactotetraose (XI) was proposed as O-D-galactopyranosyl($1 \rightarrow 6$)–O–D-galactopyranosyl($1 \rightarrow 3$)-O-D-galactopyranosyl($1 \rightarrow 3$)-D-galactose. No other galacto-tetraoses were found. Figure 1 shows a diagrammatic representation of the oligosaccharide

$$O_1 \rightarrow {}_6\emptyset$$
galactobiose (IV)

$$O_1 \rightarrow {}_3\emptyset$$
galactobiose (V)

$$O_1 \rightarrow {}_6O_1 \rightarrow {}_6\emptyset$$
galactotriose (VI)

$$O_1 \rightarrow {}_6\emptyset_3$$
$$\uparrow$$
$$O_1$$
galactotriose (VII)

$$O_1 \rightarrow {}_6O_1 \rightarrow {}_3\emptyset$$
galactotriose (IX)

$$O_1 \rightarrow {}_3O_1 \rightarrow {}_3\emptyset$$
galactotriose (VIII)

$$O_1 \rightarrow {}_6O_1 \rightarrow {}_6O_1 \rightarrow {}_3\emptyset$$
galactotetraose (X)

$$O_1 \rightarrow {}_6O_1 \rightarrow {}_3O_1 \rightarrow {}_3\emptyset$$
galactotetraose (XI)
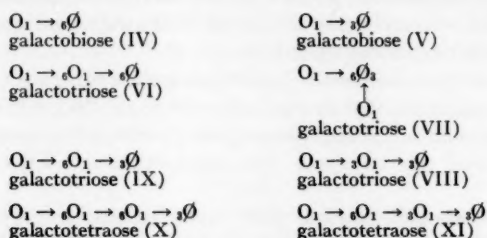
FIG. 1. Diagrammatic representation of D-galactose oligosaccharides from tamarack arabinogalactan: O, galactose; $\emptyset$, galactose (reducing unit).

structures of the various sugars isolated from tamarack in the present study. Of these, (IV), (V), (VI), (VII), and (VIII) have been previously reported as products of partial hydrolysis of European larch galactan (8).

A possible structure for the tamarack arabinogalactan (Fig. 2) was proposed earlier

$$—3 \text{ Ga } 1 \left[\rightarrow 6 \text{ Ga } 1 \rightarrow 6 \text{ Ga } 1 \rightarrow 3 \text{ Ga } 1 \rightarrow 3 \text{ Ga } 1 \rightarrow 3 \text{ Ga } 1 \rightarrow 3 \text{ Ga } 1 — \rightarrow 6 \text{ Ga—} \right]$$

```
                     6        6        6        6
                     ↑        ↑        ↑        ↑
                     1        1        1        1
                     Ga       Ga       Ga       Af
                                                3
                                                ↑
                                                1
                                                Ap
```
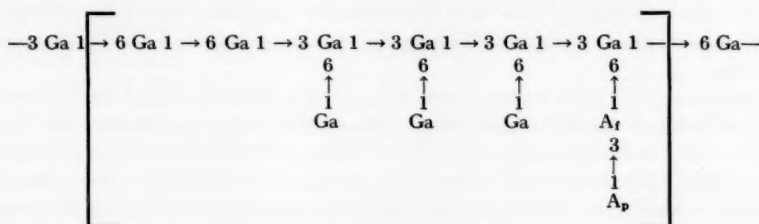
Structure I

FIG. 2. Structure originally proposed for repeating unit of tamarack arabinogalactan.

(1) and was based on methylation and periodate oxidation evidence. The isolation and identification of the oligosaccharides obtained in the present study confirm, in general, most of the main features of this structure. Some revisions, as will be pointed out below, are required. The occurrence of $1 \rightarrow 3$ and $1 \rightarrow 6$ linked galactopyranose units in the core of the molecule was proved by the isolation of galactobiose (IV) and (V). Two galac-tose trisaccharides (VIII) and (VI) joined by 1,3- and by 1,6-linkages respectively were isolated and have established that two consecutive $1 \rightarrow 3$ and $1 \rightarrow 6$ linkages exist in the polysaccharide. In addition, two trisaccharides containing both 1,3- and 1,6-linkages were found. In these, galactotrioses (IX) and (VII), the galactose units constituting the reducing end of the chains were linked to the remainder of the molecule through C_3; in addition, the reducing terminal unit of galactotriose (VII) was branched through C_6. From the structure of galactotetraoses (X) and (XI), it appears that not more than two $1 \rightarrow 3$ or two $1 \rightarrow 6$ linkages occur consecutively in the polysaccharide.

Partial hydrolysis using very dilute acid yielded $1 \rightarrow 6$ linked galactobiose but no

$1 \rightarrow 3$ linked galactobiose. Approximately one quarter of the $1 \rightarrow 6$ linked disaccharide was released by this treatment, the remainder being formed by more rigorous hydrolysis. The $1 \rightarrow 6$ and the $1 \rightarrow 3$ linkages are present in approximately equal proportions (1) and the preferential release of the $1 \rightarrow 6$ linked galactobiose units indicated that some of them were in side chains. This observation was further substantiated by recovery of most of the intact polysaccharide after the preliminary mild acid hydrolysis. The attachment of $1 \rightarrow 6$ linked galactose units as side chains has been proposed also for the ε-galactan of European larch (8). These findings have necessitated changes from structure I (Fig. 2) to structure II (Fig. 3). This latter structure accounts for the formation of all

```
—6 Ga 1 ⎡→ 6 Ga 1 → 3 Ga 1 → 3 Ga 1 → 6 Ga 1 → 6 Ga 1 ⎤→ 3 Ga—
         ⎢        6           6           3           3  ⎥
         ⎢        ↑           ↑           ↑           ↑  ⎥
         ⎢        1           1           1           1  ⎥
         ⎢       Ga          Ga          Ga          A_f ⎥
         ⎢        6                                   3  ⎥
         ⎢        ↑                                   ↑  ⎥
         ⎢        1                                   1  ⎥
         ⎣       Ga                                  A_p ⎦
```
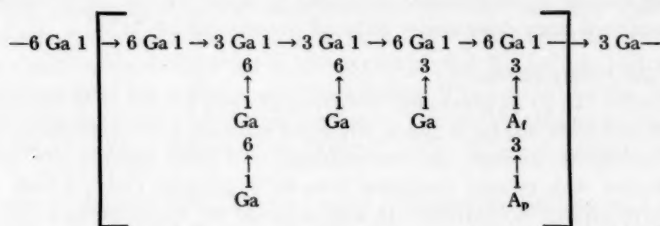
Structure II

FIG. 3.   Modified structure proposed for repeating unit of tamarack arabinogalactan.

the oligosaccharides shown in Fig. 1. In addition, the methylation and periodate oxidation found in a previous study (1) support this structure.

The structure as originally proposed for the tamarack arabinogalactan (1) and shown in Fig. 2 predicted that some of the L-arabinose units were attached in such a way as to yield 3-O-L-arabinopyranosyl-L-arabinofuranose on partial hydrolysis. This disaccharide has now been isolated and identified and found to be identical with that previously isolated from larch ε-galactans (3, 4). In addition, a much larger amount of arabinose occurred as 3-O-L-arabinopyranosyl-L-arabinopyranose. It is presumed that the disaccharide of arabinose existed in the original polysaccharide with its reducing unit in the furanose form and was attached directly to the D-galactose units in the main structure but no positive proof is presently available.

Possible structures for repeating units in galactans from other larch species have been proposed by White (7) and Aspinall (8). The structure proposed by White is characterized by a main chain of 1,6-linked galactose units substituted in position 3 by a secondary chain of three $1 \rightarrow 3$ linked D-galactose residues, the structure proposed by Aspinall consists of a $1 \rightarrow 3$ linked D-galactose main core with two $1 \rightarrow 6$ linked D-galactose units attached to it through position 6. Neither of these formulations would explain the formation of all the oligosaccharides isolated from tamarack arabinogalactan; nor could the proportion of methylated sugars obtained from fully methylated tamarack arabinogalactan be produced from these structures. Assuming the validity of these different proposed structures, it is apparent that some species differences in these polysaccharides must exist.

Further studies of the structural relationships of L-arabinose in the tamarack arabinogalactan are being undertaken through enzymic degradation.

EXPERIMENTAL

The organic phase of the following solvent systems (v/v) was used for chromatography:

- (A) ethyl acetate – pyridine – water (2.5:1:2.5),
- (B) butan-1-ol–ethanol–water (5:1:4),
- (C) benzene–ethanol–water–ammonia (200:47:14:1),
- (D) ethyl acetate – acetic acid – water (9:2:2).

Paper chromatography was carried out on Whatman No. 1 and No. 3MM papers for qualitative and quantitative separations respectively.

A 3% ethanolic solution of p-anisidine hydrochloride was used for detecting reducing sugars (9). All specific rotations were measured in water and at 25° C unless otherwise stated. Evaporations were done under reduced pressure at 32–34° C.

Hydrolysis of the Polysaccharide

Arabinogalactan (20 g) as previously prepared (1) was heated on a boiling-water bath with 0.01 N H_2SO_4 (500 ml) for 3 hours. After the solution had cooled, it was neutralized with barium carbonate, filtered, and concentrated to a small volume (100 ml). The concentrated solution was poured dropwise into 95% ethanol (2 l.), which was rapidly stirred. The precipitated polysaccharide was removed by filtration and the filtrate was evaporated to dryness (1.1 g). The precipitated polysaccharide was hydrolyzed twice more with 0.02 N H_2SO_4 (500 ml) for 2 hours and recovered as above. Chromatograms of all the hydrolyzates showed L-arabinose, D-galactose, a disaccharide of L-arabinose, a disaccharide of D-galactose, and traces of other sugars running faster on paper than L-arabinose.

The sugars (3 g) were separated on a cellulose column (40×6 cm) and eluted with a mixture of butanol–ethanol–water (40:11:19) at a rate of 7 ml per 18 min. The following fractions were collected.

A. (Tube 61–109).—This fraction gave a syrup (30 mg) which contained traces of arabinose and two other sugars, (i) R_{arab} 1.56, (ii) R_{arab} 2.32 in solvent A. L-Rhamnose has R_{arab} 1.56 in solvent A.

B. (Tube 110–114).—This fraction gave a syrup (777 mg) containing mainly arabinose and traces of galactose. The mixture crystallized from aqueous ethanol giving pure L-arabinose which, after three recrystallizations from the same solvent, had m.p. 159–160° C, $[\alpha]_D$ +105° (c, 1.74).

C. (Tube 145–275).—This fraction gave a mixture of sugars (1.63 g) containing L-arabinose, D-galactose, and a disaccharide of L-arabinose. The mixture was separated on a charcoal–celite (1:1) column (27×4.5 cm). The column was washed first with water (2 l.) to remove monosaccharides, and the disaccharide was removed by gradient elution (20% ethanol run into 1.5 l. of water). All the fractions (8–11) showing a single spot on paper chromatogram were combined and evaporated to dryness. A chromatographically pure disaccharide of L-arabinose (500 mg) was obtained.

D. (Tube 293–416).—This fraction on evaporation gave a sugar (220 mg) which contained mainly a galactobiose, R_{gal} 0.32 in solvent A with traces of galactose, a trisaccharide, and another sugar giving a reddish-brown color with p-anisidine reagent and moving on paper slightly faster than galactobiose. A crystalline sugar was obtained by keeping a methanolic solution of the syrup in the cold for 10 days. After recrystallization from methanol, the crystals had m.p. 168–170° C with swelling at 98–100° C and sintering at 120° C. The crystalline sugar was identical with β-6-O-galactopyranosyl-D-galactose (see later).

Identification of Arabinobiose

The syrup (500 mg) had $[\alpha]_D$ +193° (c, 3.77) and R_{arab} 0.74 in solvent A. It gave a characteristic pink color with p-anisidine hydrochloride spray reagent and on complete hydrolysis yielded L-arabinose.

The disaccharide (290 mg) dissolved in water (5 ml), was cooled in an ice bath, and dimethyl sulphate (1 ml) was added. The solution was stirred vigorously and 30% sodium hydroxide solution (2 ml) was added dropwise during 7 hours and the reaction mixture was further stirred for 5 hours. Then 30% sodium hydroxide solution was added 5 ml at a time and dimethyl sulphate (3 ml) was allowed to run in dropwise and the reaction mixture was further stirred for 14 hours. The solution was heated at 60° C for 1 hour to decompose any unreacted dimethyl sulphate, and then the partially methylated sugar was continuously extracted with chloroform for 4 days. After removal of the chloroform the sugar was once again methylated as above except that the sodium hydroxide solution was added first to keep the reaction mixture alkaline. The partially methylated products were then methylated twice with Purdie's reagent. The methylated disaccharide (300 mg) had $[\alpha]_D$ +160° (c, 0.76 in chloroform). (Found: MeO, 50.3%. $C_{16}H_{30}O_9$ requires: OMe, 50.6%.)

The methylated disaccharide (260 mg) was hydrolyzed by heating on a water bath at 100° C for 7 hours with 0.5 N HCl (20 ml). The solution was neutralized with silver carbonate, filtered, and the filtrate was evaporated to dryness. The syrup (240 mg), on examination by paper chromatography in solvent B, showed two spots with R_G 0.81 and R_G 0.63. The sugars were separated on paper in the same solvent.

Fraction I

This fraction proved to be 2,4-di-O-methyl-L-arabinose (93 mg), $[\alpha]_D$ +118° (c, 0.9). (Found: OMe, 33.3. $C_7H_{14}O_5$ requires: OMe, 34.8%.) A portion (32 mg) of the sugar was heated on a water bath with freshly distilled aniline (17 mg) in ethanol (2 ml) for 3 hours. The solvent was removed and the syrup was dissolved in hot butanol, and on cooling, crystals (plates) were formed. After recrystallization from the same solvent the crystals had m.p. and mixed m.p. 135–136° C. (On an uncovered glass plate the crystals melted at 145–147° C; the same behavior was observed with authentic samples of 2,4-di-O-methyl-N-phenyl-L-arabinosylamine.)

Another portion (40 mg) was oxidized with 2 drops of bromine in water (0.5 ml). Barium carbonate (20 mg) was added to the reaction mixture, which was stored in the dark for 72 hours. Bromine was removed by aeration and the acidified solution was extracted with chloroform. After removal of the chloroform the residual syrup was distilled (bath temperature 120–145° C at 0.02 mm). The distillate was dissolved in methanol (10 ml), saturated with ammonia, and kept in the cold overnight. On evaporation of methanol, the amide crystallized and after recrystallization from methanol in the cold the crystals had m.p. 158–159° C (reported m.p. of 2,4-di-O-methyl-L-arabonamide is 160–161° C) (4). (Found: MeO, 32.0%. $C_7H_{14}O_5N$ requires: MeO, 32.3%.)

Fraction II (120.4 mg)

When this fraction was examined by paper chromatography in solvent C it was found to consist of two sugars. This observation was also confirmed when the sugar (2 mg) was refluxed with methanolic hydrogen chloride (2%), and examined by gas–liquid chromatography (5, 6). The sugars were separated on paper in solvent C.

(a) 2,5-Di-O-methyl-L-arabinose (14.2 mg), $[\alpha]_D$ −19.7° (c, 0.71). The sugar was oxidized as above with bromine and the corresponding arabonic acid was distilled (bath temperature 120–140° C at 0.02 mm). The lactone was dissolved in ammoniacal methanol and

kept overnight in the cold. On evaporation of methanol the product crystallized and after recrystallization from ethanol the crystals had m.p. 130–131° C, undepressed on admixture with an authentic specimen of 2,5-di-O-methyl-L-arabonamide.

(*b*) 2,3,4-Tri-O-methyl-L-arabinose (42 mg) (there was some accidental loss of material). The sugar was oxidized with bromine as above and the resulting product was distilled (bath temperature 105–120° C at 0.02 mm). The lactone was heated with phenylhydrazine in methanol (3 ml) for 3 hours. Methanol was removed and the syrup crystallized on seeding. After recrystallization from ethyl acetate the phenylhydrazide of 2,3,4-tri-O-methyl-L-arabonolactone had m.p. and mixed m.p. 156–158° C.

Hydrolysis of the Degraded Polysaccharide

The degraded galactan (20 g) recovered from previous hydrolysis with dilute H_2SO_4 was further hydrolyzed on a boiling-water bath with 0.1 N H_2SO_4 (500 ml) for a total of 6 hours. Three hydrolysis periods of 2 hours each were used, with recovery of polysaccharide after each hydrolysis by precipitation with 92% ethanol. The hydrolysis procedure was again repeated with 0.2 N H_2SO_4 for 2 hours and with 0.5 N H_2SO_4 for 3 hours. The chromatographic picture of all hydrolyzates was similar, showing galactose and oligosaccharides of galactose.

The sugars (12 g) from the combined hydrolyzates were fractionated on a charcoal–celite (1:1) column (48×6.5 cm). The column was first washed with water (3 l.) to remove monosaccharides. Then gradient elution technique was applied in which 10% ethanol was allowed to run into water (4 l.) to elute the oligosaccharides. After 185 fractions had been collected (80–100 ml each), 10% ethanol was replaced by 20% ethanol.

The water eluate on evaporation gave mainly D-galactose (8.1 g) and traces of L-arabinose. D-Galactose was crystallized from aqueous ethanol and after recrystallization had m.p. 165–166° C, $[\alpha]_D$ +80.6° (*c*, 2.02).

The individual sugars were further purified by paper chromatography in solvent A. Galactotriose (VI) gave a single spot in all solvent systems, but when examined by paper electrophoresis in borate buffer at pH 10 it showed two sugars, galactotriose (VI) (M_G 0.81) and galactotriose (VII) (M_G 0.69). These sugars were separated on paper electrophoresis in borate buffer.

Identification of the Oligosaccharides

Galactobiose (IV)

The sugar (650 mg) crystallized from methanol with 2 moles of methanol as solvent of crystallization, m.p. 168–170° C with swelling at 98–100° C and softening at 120° C, $[\alpha]_D$ 28° (*c*, 1.43). (Found: C, 41.39; H, 7.57. $C_{12}H_{22}O_{11},2CH_3OH$ requires: C, 41.30; H, 7.38.) After removal of the solvent of crystallization at 100° C *in vacuo* over P_2O_5, the disaccharide had m.p. 168–170° C with softening at 120° C, $[\alpha]_D$ 34.2° (*c*, 1.52). (Found: C, 41.94; H, 6.54. $C_{12}H_{22}O_{11}$ requires: C, 42.1; H, 6.48.) On complete hydrolysis it gave D-galactose.

The disaccharide (306 mg) was methylated initially with dimethyl sulphate (13 ml) and 30% sodium hydroxide solution (24 ml) as described above for arabinobiose, and subsequently by two methylations with Purdie's reagent. The methylated product (303 mg) crystallized from the syrup as needles but could not be crystallized from any solvent. It had m.p. 68–70° C, $[\alpha]_D$ −5.7° (*c*, 2.4 in methanol). (Found: C, 51.96; H, 8.28; MeO, 52.4%. $C_{20}H_{38}O_{11}$ requires: C, 52.42; H, 8.12; MeO, 54.6%.)

The methylated disaccharide (250 mg) was hydrolyzed with N HCl at 100° C for 5 hours. The solution was neutralized with silver carbonate, filtered, and evaporated to dryness. The individual methylated sugars were separated on paper in solvent C and two fractions were obtained.

(a) 2,3,4,6-Tetra-O-methyl-D-galactose (86.7 mg).—The sugar (40 mg) was heated with freshly distilled aniline (25 mg) in ethanol (3 ml) for 3 hours. When the solution was concentrated and cooled, crystals of 2,3,4,6-tetra-O-methyl-N-phenyl-D-galactosylamine separated which, after recrystallization from ethanol, had m.p. and mixed m.p. 194–196° C.

(b) 2,3,4-Tri-O-methyl-D-galactose (80.3 mg).—A portion of the sugar (20 mg) was heated with freshly distilled aniline (15 mg) for 3 hours in ethanol (3 ml). Ethanol was removed by distillation and the residual syrup was extracted with hot ethyl acetate. After removal of the ethyl acetate the syrup was crystallized from acetone. On recrystallization from the same solvent the crystals (plates) had m.p. 165–167° C, undepressed on admixture with an authentic specimen of 2,3,4-tri-O-methyl-N-phenyl-D-galactosylamine. Another portion of the trimethyl galactose (22 mg) was oxidized with bromine for 48 hours. Bromine was removed by aeration and the acidified solution extracted with chloroform. After removal of the chloroform, the acid was distilled (bath temperature 150–160° C at 0.02–0.01 mm). The distillate was dissolved in methanol (10 ml), saturated with ammonia, and kept at +4° C overnight. After removal of methanol the product crystallized and on recrystallization from ethanol the 2,3,4-tri-O-methyl-D-galactonamide had a m.p. and mixed m.p. 166–167° C.

Galactobiose (V)

This fraction, $[\alpha]_D$ +60.3° (c, 2.1), was a chromatographically pure sugar (390 mg) but it could not be induced to crystallize even by seeding with authentic samples of 3-O-β-D-galactopyranosyl-D-galactose. On complete hydrolysis it gave D-galactose as the only monosaccharide.

The sugar (175 mg), on methylation as described above, gave a methylated product (145 mg). (Found: MeO, 52.37%. $C_{20}H_{38}O_{11}$ requires: MeO, 54.6%.) The methylated sugar (140 mg) was hydrolyzed by being heated on a boiling-water bath with N HCl (15 ml) for 7 hours. The acid was neutralized with silver carbonate, the precipitate was filtered off, and the filtrate was evaporated to dryness. The methylated sugars were separated on paper in solvent B and two fractions were obtained.

(a) 2,3,4,6-Tetra-O-methyl-D-galactose (56.6 mg).—The sugar was converted into its anilide derivative which, after crystallization, had m.p. 195–197° C, undepressed on admixture with an authentic specimen.

(b) 2,4,6-Tri-O-methyl-D-galactose (51.7 mg).—The sugar, on being heated with freshly distilled aniline (30 mg) in ethanol (3 ml) for 3 hours, gave a product which crystallized from acetone on cooling. After recrystallization, the crystals (needles) had m.p. 177–179° C, undepressed on admixture with an authentic sample of 2,4,6-tri-O-methyl-N-phenyl-D-galactosylamine, m.p. 176° C. On the basis of these findings the disaccharide was identified as 3-O-β-D-galactopyranosyl-D-galactose.

Galactotriose (VI) (17 mg)

Galactotriose (VI) was chromatographically pure sugar which had the same R_{gal} value (0.10) as galactotriose (VII) (0.10) in solvent A but which differed in M_G values in borate buffer. The sugar on partial acidic hydrolysis gave galactose, galactobiose (IV), and the original sugar. After reduction (potassium borohydride) and partial acidic

hydrolysis it gave galactose and galactobiose (IV) as reducing sugars. This trisaccharide is probably O-D-galactopyranosyl($1 \rightarrow 6$)-O-D-galactopyranosyl($1 \rightarrow 6$)-D-galactose.

Galactotriose (VII) (31.6 mg)

The sugar on partial acidic hydrolysis gave galactose, galactobiose (IV), and galacto-biose (V). On reduction (potassium borohydride) and partial hydrolysis it gave galactose as the only reducing sugar.

Galactotriose (IX) (93 mg)

This was a chromatographically pure sugar, $[\alpha]_D$ +20.5° (c, 4.0). On partial acidic hydrolysis it gave galactose, galactobiose (IV), galactobiose (V), and the original sugar. On reduction of the trisaccharide (potassium borohydride) and partial acidic hydrolysis of the glycitol only galactose and galactobiose (IV) were found as reducing sugars.

The trisaccharide (80 mg) was methylated twice as described above with dimethyl sulphate (2.5 ml) and 30% sodium hydroxide solution (5 ml). After two further methyla-tions with Purdie's reagent the methylated trisaccharide (66.5 mg) had MeO content 49.37%; $C_{29}H_{54}O_{16}$ requires: MeO, 51.8%. The methylated product was hydrolyzed with N HCl (10 ml) by being heated on a boiling-water bath for 5 hours. The acidic solution was neutralized with silver carbonate, filtered, and evaporated to a syrup (50 mg). The hydrolyzed product on a paper chromatogram in solvent B showed two sugars: (a) the faster-moving, corresponding to tetra-O-methyl-D-galactose, and (b) a slow-moving elongated spot. The mixture was separated on paper in solvent B.

(a) 2,3,4,6-Tetra-O-methyl-D-galactose (18.5 mg).—The sugar gave a crystalline anilide derivative, m.p. and mixed m.p. 195–197° C, when heated with aniline (10 mg).

(b) 2,3,4- and 2,4,6-Tri-O-methyl-D-galactose (29 mg).—Chromatographic separation was done using solvent C. The paper was irrigated and when the solvent front was near the bottom of the paper, the paper was dried and again irrigated. This operation was repeated four times but still gave an imperfect separation. However, about $\frac{3}{4}$ in. of the paper in the middle of the band of sugars was discarded and the top portion of the band was extracted with water to give a sugar (9.2 mg). When heated with a drop of aniline in ethanol the sugar gave a product which crystallized from acetone. After recrystalliza-tion, the crystals (plates) melted at 165° C, undepressed on admixture with an authentic specimen of 2,3,4-tri-O-methyl-N-phenyl galactosylamine. The lower portion of the paper gave a sugar (7.9 mg) which gave a crystalline (needles) anilide derivative, m.p. 176–178° C, undepressed on admixture with an authentic specimen of 2,4,6-tri-O-methyl-N-phenyl galactosylamine.

Galactotriose (VIII) (106 mg)

The sugar crystallized from aqueous ethanol, m.p. 240–245° C (decomposed), $[\alpha]_D$ +51° (c, 0.87). (Found: C, 42.00; H, 6.31. $C_{18}H_{32}O_{16}$ requires: C, 42.10; H, 6.34.) The tri-saccharide after partial acidic hydrolysis gave galactose, galactobiose (V), and the original sugar. After reduction (potassium borohydride) and partial acidic hydrolysis it gave galactose and galactobiose (V) as reducing sugars.

The trisaccharide (75 mg) was methylated as above. The methylated product (75.6 mg) crystallized from ethanol on slow evaporation of the solvent at room temperature, m.p. 158–160° C, $[\alpha]_D$ −10.0° (c, 1.45 in methanol). (Found: MeO, 50.6%. $C_{29}H_{54}O_{16}$ requires: MeO, 51.8%).

The methylated trisaccharide (60 mg) was hydrolyzed in N HCl (10 ml) by being heated on a boiling-water bath for 5 hours. The acid was neutralized with silver carbonate, the precipitate was filtered, and the filtrate evaporated to dryness. The syrup on separa-tion on paper in solvent B gave two fractions.

(a) *2,3,4,6-Tetra-O-methyl-*D*-galactose (17.2 mg)*.—On being heated with aniline (10 mg) in ethanol (2 ml) for 3 hours the product crystallized from ethanol. After recrystallization from the same solvent it had m.p. and mixed m.p. 195–197° C.

(b) *2,4,6-Tri-O-methyl-*D*-galactose (28.6 mg)*.—The syrup was heated with aniline (16 mg) in ethanol (3 ml) for 3 hours. The solvent was removed and the product was crystallized from acetone. After recrystallization, the crystals (needles) had m.p. and mixed m.p. 177–178° C. On the basis of above findings this sugar was identified as O-D-galactopyranosyl(1 → 3)-O-D-galactopyranosyl(1 → 3)-D-galactose.

Galactotetraose (X) (35 mg)

On partial acidic hydrolysis with 0.1 N H_2SO_4 for 1 hour the sugar gave galactose, galactobiose (IV), galactobiose (V), galactotriose (VI), galactotriose (IX), and the original sugar. On reduction and hydrolysis it gave galactose, galactobiose (IV), and galactotriose (VI) as reducing sugars.

Galactotetraose (XI) (94 mg)

On partial acidic hydrolysis the sugar gave galactose, galactobiose (IV), galactobiose (V), galactotriose (IX), galactotriose (VIII), and the original sugar. After reduction of the tetrasaccharide, followed by partial acid hydrolysis, the derived glycitol gave galactose, galactobiose (IV), galactobiose (VI), and galactotriose (IX) as reducing sugars.

REFERENCES

1. G. A. ADAMS. Can. J. Chem. **38**, 280 (1960).
2. E. V. WHITE.   J. Am. Chem. Soc. **64**, 507 (1942).
3. J. K. N. JONES.   J. Chem. Soc. 1672 (1953).
4. H. BOUVENG and B. LINDBERG.   Acta Chem. Scand. **10**, 1515 (1956).
5. A. G. McINNES, D. H. BALL, F. P. COOPER, and C. T. BISHOP.   J. Chromatog. **1**, 556 (1958).
6. C. T. BISHOP and F. P. COOPER.   Can. J. Chem. **38**, 388 (1960).
7. E. V. WHITE.   J. Am. Chem. Soc. **64**, 2838 (1942).
8. G. O. ASPINALL, E. H. HIRST, and ELSE RAMSTAD.   J. Chem. Soc. 593 (1958).
9. L. HOUGH, J. K. N. JONES, and W. H. WADMAN.   J. Chem. Soc. 1702 (1950).

THE CRYSTAL STRUCTURE OF 1,4-DIBROMONAPHTHALENE[1]

J. TROTTER

ABSTRACT

Crystals of 1,4-dibromonaphthalene are monoclinic with eight molecules in a unit cell of dimensions $a = 27.45$, $b = 16.62$, $c = 4.09$ Å; $\beta = 91.9°$; space group $P2_1/a$. The high proportion of bromine in the crystal probably precludes location of the carbon atoms with sufficient precision to give accurate molecular dimensions, and it has therefore not been considered worth while proceeding beyond the detailed examination of the projection along the short c-axis. There are two molecules in the asymmetric unit, and the solution of the structure from $hk0$ Patterson and Fourier projections has indicated that these two molecules are related, at least in projection, by a pseudo center of symmetry. The projected bond distances indicate significant deviations of the bromine atoms from the aromatic plane. Approximate values of the bond lengths in the molecule have been deduced from the projected distances and estimated orientation angles.

INTRODUCTION

The crystal structure of 1,4-dibromonaphthalene has been determined as part of a series of investigations of derivatives of naphthalene (1).

EXPERIMENTAL

Crystals of 1,4-dibromonaphthalene, obtained by crystallization from aqueous ethanol, consist of colorless plates elongated along the c-axis with the (010) face developed. The approximate density was determined by flotation in standard heavy liquids. The unit-cell dimensions and space group were determined from rotation and oscillation photographs of a crystal rotating about the c-axis, $hk0$ and $hk1$ Weissenberg films, and an $h0l$ precession film.

Crystal Data

1,4-Dibromonaphthalene, $C_{10}H_6Br_2$; molecular weight = 286.0; m.p. = 83° C.

Monoclinic, $a = 27.45 \pm 0.08$, $b = 16.62 \pm 0.04$, $c = 4.09 \pm 0.01$ Å; $\beta = 91°55' \pm 10'$.

Volume of the unit cell = 1864.9 Å^3.

Density, calculated (with $Z = 8$) = 2.037 g cm^{-3}, measured $\sim$2.0 g cm^{-3}.

Absorption coefficient for X-rays, $\lambda = 1.542$ Å, $\mu = 105.4$ cm^{-1}; $\lambda = 0.7107$ Å, $\mu = 94.2$ cm^{-1}.

Total number of electrons per unit cell = $F(000) = 1088$.

Absent spectra: $h0l$ when h is odd, $0k0$ when k is odd.

Space group is $P2_1/a$—C_{2h}^5.

The intensities of the $hk0$ reflections* were recorded on Weissenberg exposures for a crystal rotating about the c-axis, using Cu $K\alpha$ radiation, with multiple-film technique to correlate strong and weak reflections. The $h0l$ reflections were recorded on precession films with Mo $K\alpha$ radiation. All the intensities were estimated visually, the range being about 2000 to 1. The cross section of the crystal normal to the c-axis was 0.08×0.02 mm, so that absorption is negligible, and no corrections were applied. The structure amplitudes were derived by the usual formulae for a mosaic crystal, the absolute scale being established later by correlation with the calculated structure factors. Three hundred and sixty-eight independent $hk0$ reflections were observed, representing about 62% of the possible number observable with Cu $K\alpha$ radiation.

STRUCTURE ANALYSIS

The best approach to determining the complete structure was obviously by examination of the c-axis Patterson projection. The $hk0$ Patterson map is shown in Fig. 1. There are

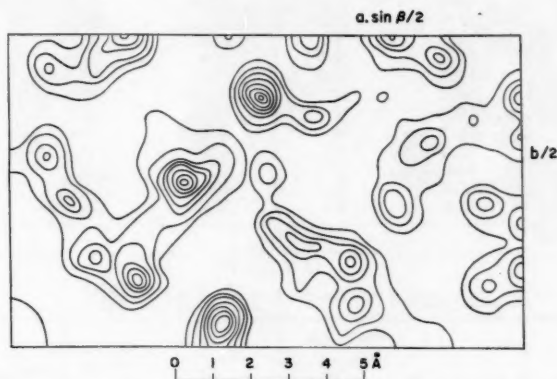

FIG. 1. c-Axis Patterson projection; contours at arbitrary intervals.

two molecules and hence four bromine atoms in the asymmetric unit and the plane group for this projection is pgg, so that the vector distribution is complex, with many multiple peaks. However, the four Harker peaks on each of the lines $x = \frac{1}{2}$ and $y = \frac{1}{2}$ were easily distinguished, and 16 possible positions (x_j, y_j, z_j) for the four bromine atoms readily deduced. A search was then made for single bromine–bromine vectors at positions $(2x_j, 2y_j, 2z_j)$; this eliminated several of the 16 possibilities but ambiguities still remained. However, it was possible to determine the most probable position for one of the bromine atoms, and a minimum function was then constructed by placing the origin of the Patterson function, in turn, at this bromine position and at the three symmetry-related positions. There were only four significant independent peaks on the resulting map, all of about the same height, and these were taken as corresponding to the four bromine atoms. It was noted that they were related in pairs by a pseudo center of symmetry, so that the larger peaks on the Patterson map correspond to fourfold coincidences of Br–Br vectors.

Structure factors were calculated for all the observed $hk0$ reflections using the scattering factor for bromine of the *Internationale Tabellen* (2) with $B = 3.8$ Å^2, and the discrepancy factor was 44.6%. A Fourier series was then summed, using as coefficients the measured structure amplitudes together with the calculated signs. On the resulting electron-density map all the bromine and carbon atoms were well-resolved, although the carbon contours were considerably distorted, as might be expected in the presence of the much heavier bromine atoms. New positions were chosen for the bromine atoms, and co-ordinates also obtained for all 20 carbon atoms in the asymmetric unit. Structure factors were recalculated using the scattering curve for carbon of Berghuis *et al.* (3) with $B = 3.8$ Å^2; the R value was 24.3%. A second Fourier synthesis was then computed, and on the resulting electron-density map (Fig. 2), the resolution of the carbon atoms was much improved. No changes were suggested in the positional parameters of the bromine atoms, but improved co-ordinates were obtained for the carbons. Since it was not considered worth
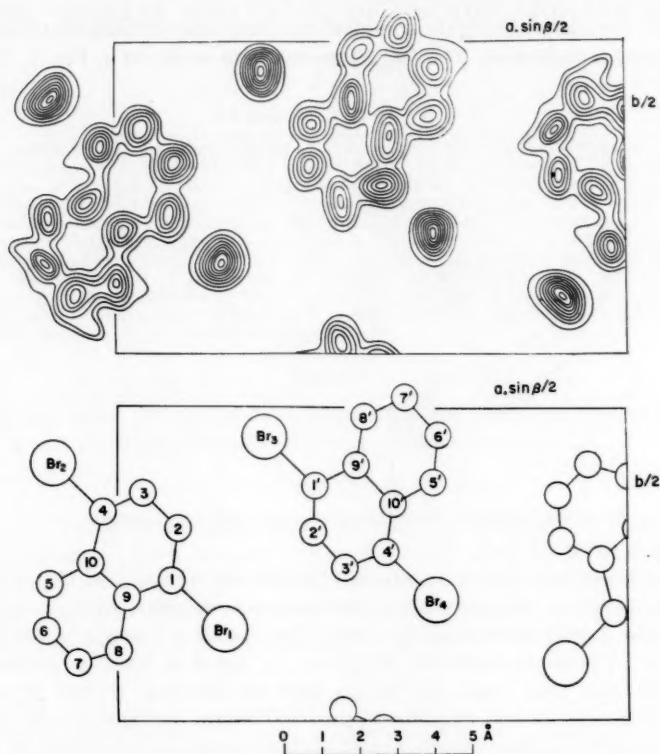
FIG. 2. Electron-density projection along [001] (contours on the carbon atoms at intervals of 1 e Å⁻², starting at 2 e Å⁻², and on the bromine atoms at intervals of 5 e Å⁻², starting at 5 e Å⁻²), and projection of the structure along [001].

while carrying out further intensive refinement, structure factors were not recalculated; the values at the penultimate stage ($R = 24.3\%$) are not included here, to save space, but are available from the author.

It was apparent that no resolution of the individual atoms could be expected in the projections down the long a- and b-axes, so that three-dimensional methods would be required to determine the z-co-ordinates. It was not considered that the results which could be obtained from such an analysis would be sufficiently accurate, nor that the problem was sufficiently important, to justify the great amount of work involved, and so no effort has been made to determine the z-co-ordinates of the atoms.

Co-ordinates and Bond Distances

The final positional parameters are listed in Table I, referred to the crystal axes and expressed as fractions of the unit-cell edges. There is a pseudo center of symmetry at about (0.124, 0.300). The projected bond distances calculated from these co-ordinates are given in the first column of Table II. In order to deduce true bond lengths from these

TABLE I

Final positional parameters

Atom	x	y	Atom	x	y
Br_1	.1037	.1471	Br_3	.1437	.4510
Br_2	−.0620	.4115	Br_4	.3115	.1908
C1	.0525	.2204	C1'	.1931	.3725
2	.0594	.3025	2'	.1918	.2996
3	.0247	.3597	3'	.2214	.2398
4	−.0146	.3295	4'	.2633	.2693
5	−.0658	.2126	5'	.3090	.3799
6	−.0707	.1393	6'	.3146	.4573
7	−.0384	.0893	7'	.2813	.5175
8	.0012	.1098	8'	.2419	.4879
9	.0091	.1906	9'	.2333	.4070
10	−.0260	.2461	10'	.2625	.3458

TABLE II

Bond distances (Å) and orientation angles (θ)

Bond	Projected bond distances, d_{proj}	θ	Bond distances, $d = \dfrac{d_{proj}}{\cos \theta}$	Mean bond lengths	Naphthalene bond lengths
1 —2	1.378	19°	1.459		
1'—2'	1.212		1.283		
5 —6	1.225		1.297		
5'—6'	1.295		1.371		
				1.35	1.36
3 —4	1.189	27°	1.336		
3'—4'	1.250		1.405		
7 —8	1.138		1.279		
7'—8'	1.188		1.335		
4 —10	1.421	19°	1.504		
4'—10'	1.271		1.345		
8 —9	1.360		1.440		
8'—9'	1.366		1.446		
				1.44	1.43
5 —10	1.226	27°	1.378		
5'—10'	1.396		1.569		
1 —9	1.289		1.448		
1'—9'	1.242		1.396		
2 —3	1.344	23°	1.461		
2'—3'	1.283		1.394	1.41	1.42
6 —7	1.215		1.321		
6'—7'	1.355		1.473		
9 —10	1.333	23°	1.449	1.43	1.41
9'—10'	1.294		1.406		
Br_1—1	1.859	12°	1.898		
Br_3—1'	1.881		1.921	1.91	—
Br_2—4	1.884		1.924		
Br_4—4'	1.858		1.897		

projected distances the following assumptions were made:

(i) that the C—Br distances are equal to the normal single bond length (1.91 Å),

(ii) that the naphthalene skeletons are planar and have symmetry *mmm*,

(iii) that the average bond length for each of the three groups of parallel C—C bonds is equal to the corresponding average length in naphthalene (4, 5).

The inclinations of the various bonds from the plane of projection, derived from these assumptions, are listed in the second column of Table II, and the true bond distances in the third column. Although there are some large deviations from *mmm* symmetry, these cannot be considered as significant, and the mean bond lengths are given in the fourth column of the table.

Although it has been assumed, in deriving the true bond distances, that the average distances in the various directions are equal to the corresponding average distances in naphthalene, this does not imply that the individual distances must be equal, and so it is permissible to compare the mean bond lengths in 1,4-dibromonaphthalene with the distances in naphthalene. This comparison is included in Table II; the agreement is extremely good, suggesting, as we might expect, that the mean distances are more accurate than the individual values, and also that the assumptions made are plausible.

Comparison of the inclination angles for the C—Br bonds (12°) and for bonds such as 9—10 (23°) indicates that the bromine atoms are displaced from the naphthalene plane, the two bromine atoms in the molecule being displaced in opposite directions from the aromatic plane by about 0.4 Å. If it had been assumed that the bromine atoms were situated on the naphthalene plane, the true C—Br distances would have been 2.03 Å, considerably longer than the normal single bond length, so that the bromine atom displacements are probably real. The deviations are possibly the result of small steric interactions with the *peri* hydrogen atoms.

Projected distances indicate that all the intermolecular contacts correspond to normal van der Waal's interactions.

REFERENCES

1. J. TROTTER.   Acta Cryst. **13**, 276 (1960).
2. INTERNATIONALE TABELLEN ZUR BESTIMMUNG VON KRISTALLSTRUKTUREN. Vol. 2. Borntraeger, Berlin. 1935.
3. J. BERGHUIS, IJ. M. HAANAPPEL, M. POTTERS, B. O. LOOPSTRA, C. H. MACGILLAVRY, and A. L. VEENENDAAL.   Acta Cryst. **8**, 478 (1955).
4. S. C. ABRAHAMS, J. M. ROBERTSON, and J. G. WHITE.   Acta Cryst. **2**, 238 (1949).
5. D. W. J. CRUICKSHANK.   Acta Cryst. **10**, 504 (1957).

THE EPIMERIZATION OF DELCOSINE[1]

Vinko Skarić[2] and Léo Marion

ABSTRACT

Delcosine has been assigned tentatively the same C—N skeleton as lycoctonine. In lycoctonine, ring A carries at C-1 a methoxyl group which is directed away from the nitrogen ring. In delcosine, C-1 carries a hydroxyl group which has the opposite configuration and is directed towards the nitrogen. An attempt to correlate the two structures first involves epimerization at C-1 in delcosine. This has been carried out by oxidation of desethyldelcosine to an azomethine, the ethiodide of which, by the action of methanolic potassium hydroxide, is converted to oxo-1-epidelcosine in two steps. Oxo-1-epidelcosine in an acid-catalyzed rearrangement is transformed to a pinacone which, after methylation, gives O,O-dimethyl-anhydro-oxo-1-epidelcosine. This compound was compared with O-methyl-anhydro-oxolycoctonine, prepared from oxolycoctonine, but was not identical. Removal of a methoxyl, which in each compound is ortho to a carbonyl, by the action of sodium amalgam, produced O,O-dimethyl-6-desmethoxy-anhydro-oxo-1-epidelcosine and O-methyl-6-desmethoxy-anhydro-oxolycoctonine, which are not identical, but show in their infrared spectra much less dissimilarity than the spectra of the pair of compounds from which they were derived. These results are discussed in terms of the structure of delcosine.

As a working hypothesis, the alkaloid delcosine ($C_{24}H_{39}O_7N$) has been assumed to possess the same C—N skeleton as lycoctonine ($C_{25}H_{41}O_7N$). All the chemical reactions of delcosine studied so far are in agreement with such an assignment. In order to prove or disprove that delcosine has the previously assigned (1, 2, 3) structure I, it has been
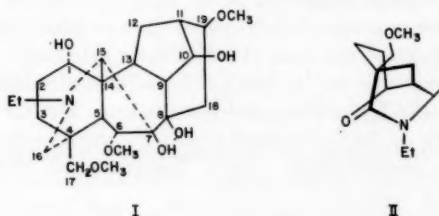
attempted in the work now reported to correlate it with lycoctonine. Although we have failed in our main objective, the results obtained firmly establish the position of all but two of the substituents on the C—N skeleton.

It has been shown earlier (2, 3) that delcosine contains a secondary hydroxyl substituted on the six-membered ring A. Oxidation of delcosine with either silver oxide or N-bromosuccinimide gives rise to a carbinolamine ether, anhydrohydroxydelcosine II (1, 3), the formation of which involves this secondary hydroxyl, which was assumed to occupy position C-1 by analogy with lycoctonine. This conclusion is also supported by the results of the oxidation of oxodelcosine with lead tetraacetate (3). Although the product of this reaction should contain a five-membered and a six-membered cyclic ketone, actually it is a ketohemiketal III in which cyclization has occurred between the secondary hydroxyl of ring A and the carbonyl of the six-membered cyclic ketone (3, 4). Position C-1 for the secondary hydroxyl of ring A is the only one that allows the formation
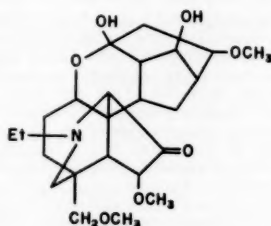
of a six-membered cyclic hemiketal and appears to be the only one where the formation of a ring is geometrically possible. To account for the formation of the carbinolamine ether it is further necessary that the C-1 hydroxyl be directed on the same side of ring A as the nitrogen ring (3). This configuration is different from that of the methoxyl at C-1 in lycoctonine (5).

III

Hence, any attempt to correlate delcosine with lycoctonine would initially involve epimerization at C-1. Sparatore, Greenhalgh, and Marion (6) have attempted this epimerization in delsoline, which is a monomethyldelcosine (2), but their reported result is in error, and the compound that they have described is not epidelsoline but Δ'-anhydro-delsoline ($C_{25}H_{39}O_6N$). Dvornik and Edwards (7) reported the epimerization of a hydroxyl in ajaconine, and Dr. Dvornik suggested to us an adaptation of the method by which it has now proved possible to prepare epidelcosine from N-desethyldelcosine, a previously described oxidation product of the base (1). N-Desethyldelcosine (IV) was oxidized by Sarett's reagent to a mixture of N-desethyl-1,10-didehydrodelcosine-azomethine (V) and the neutral N-desethyl-1,10-didehydro-oxodelcosine. The former was converted to the ethiodide (VI), which on being refluxed with 10% methanolic potassium hydroxide, yielded 10-dehydro-oxo-1-epidelcosine (VII). Reduction of VII with sodium boro-

hydride gave oxo-1-epidelcosine (VIII), m.p. 128–130°, $[\alpha]_D^{25}$ +19.8°, and this on treatment with lithium aluminum hydride produced 1-epidelcosine, m.p. 177–178°, $[\alpha]_D^{26}$ +38.9°, which formed a perchlorate, m.p. 199–201°.
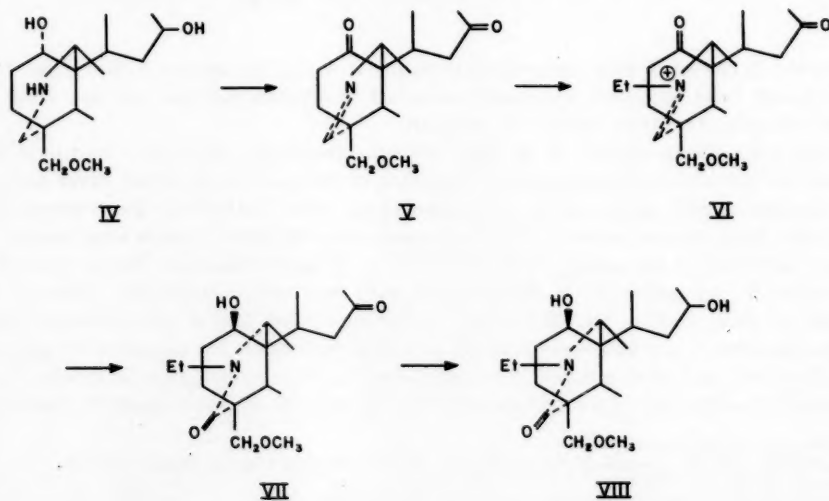
For the purpose of correlating epidelcosine with lycoctonine it was necessary to methylate the primary hydroxyl group in the latter. Although this could be achieved, the yield was poor and it was more usual to obtain a dimethylated product in which one of the two vicinal tertiary hydroxyls had reacted. This complication made it necessary to use derivatives of the two alkaloids in which the tertiary hydroxyls were no longer present. Such derivatives are accessible via the pinacolic rearrangement which these alkaloids undergo readily (8, 9). Oxo-1-epidelcosine was, therefore, heated with acetic acid containing sulphuric acid according to the method described earlier (8, 9), and thus converted to the pinacone anhydro-oxo-1-epidelcosine (IX, R = R′ = H), which was methylated to O,O-dimethyl-anhydro-oxo-1-epidelcosine (IX, R = R′ = CH₃), $C_{26}H_{39}O_7N$, m.p. 178–180°, $[\alpha]_D$ −56.3°, showing in the ultraviolet a maximum at 303 and a minimum at 263 mμ. In the infrared it showed no absorption in the hydroxyl region, but produced a band at 1727 cm⁻¹ due to a six-membered cyclic ketone and a band at 1648 cm⁻¹ attributable to the lactam carbonyl.
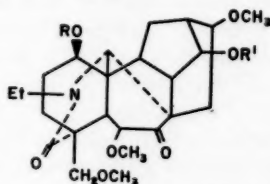
IX

By acid-catalyzed pinacolic rearrangement, oxolycoctonine (previously designated lycoctonam) was converted to anhydro-oxolycoctonine (9), which was methylated to O-methyl-anhydro-oxolycoctonine, $C_{26}H_{39}O_7N$, m.p. 126–128°, $[\alpha]_D^{25}$ +9.2°. In the ultraviolet it showed a maximum at 302 and a minimum at 267 mμ while in the infrared the spectrum contained bands at 1725 and 1642 cm⁻¹. The melting point and optical rotation of this compound are quite different from those of IX (R = R′ = CH₃), and, also, both compounds contain the same functional groups as shown by both the ultraviolet and infrared spectra; the fingerprint region of their I.R. spectra showed marked differences.

It has been shown by X-ray crystallography that the methoxyl at C-6 in lycoctonine is equatorial whereas in aconitine the methoxyl in the same position is axial (5). The non-identity of the two pinacones (IX (R = R′ = CH₃) and O-methyl-anhydro-oxolycoctonine) could be due to a similar difference between lycoctonine and delcosine. Since in the two pinacones the methoxyl at C-6 is vicinal, or α, to the carbonyl, it is removable by the action of sodium amalgam (10, 11). Both O,O-dimethyl-anhydro-oxoepidelcosine and O-methyl-anhydro-oxolycoctonine were, therefore, dissolved in absolute ethanol and demethoxylated at C-6 by treatment with sodium amalgam. O,O-Dimethyl-6-desmethoxy-anhydro-oxoepidelcosine thus produced, m.p. 152.5–154°, $[\alpha]_D^{25}$ −35.2°, showed a maximum at 282 mμ and a minimum at 262 mμ in the ultraviolet. Its infrared spectrum contained an absorption band at 1715 cm⁻¹ due to the six-membered cyclic ketone and one at 1645 cm⁻¹ due to the lactam carbonyl. The O-methyl-6-desmethoxy-anhydro-oxolycoctonine, m.p. 161–163°, $[\alpha]_D^{26}$ +3.4°, showed in the ultraviolet a maximum

at 282 mμ and a minimum at 262 mμ; and in the infrared, a band at 1716 cm^{-1} and one at 1638 cm^{-1}. The two desmethoxy compounds are not identical, but the fingerprint region of their infrared spectra are much more closely alike than the spectra of the preceding pair of compounds in the same region, which may indicate that the C-6 methoxyl in delcosine is axial.

The demethoxylating action of sodium amalgam establishes the location of the methoxyl at C-6. The presence of the two tertiary hydroxyls at C_7 and C_8 is firmly established by the formation of secodiketones from anhydrohydroxydelcosine (5), from oxodelcosine (3), and from the related oxodelsoline (6). The presence of a methoxyl at C-19 is indicated by the elimination of methanol and the formation of $\alpha\beta$-unsaturated ketones from the secodiketones derived from anhydrohydroxydelcosine (5) and oxo-delsoline (6). It has not been established, however, whether the stereochemistry at C-19 is the same as in lycoctonine. None of the many oxidation reactions of delcosine that have been studied has yielded an acid product, thus indicating the absence of a primary alcoholic group. Since, however, according to the N.M.R. spectrum, no methyl group attached to carbon is present besides that of the N-ethyl group, it becomes highly probable that the third methoxyl in the molecule is present in a methoxy-methyl group at C-17. Delcosine contains a secondary hydroxyl attached to a five-membered ring (1, 3). This hydroxyl has been located at C-10 by analogy with lycoctonine, which contains a methoxyl at that position, but besides the fact that it must be a substituent on ring D, there is no proof of its exact location. It could be at C-10 and have a configuration different from that of the C-10 methoxyl in lycoctonine, or it could be at C-12. Although the derivatives of delcosine and lycoctonine that have been compared did not prove to be identical, it still remains that the chemical reactions of delcosine and its transformations all point to the alkaloid possessing the same carbon–nitrogen skeleton as lycoctonine. It is hoped, with work presently underway, to locate the position of the secondary hydroxyl on ring D, and to complete the correlation of delcosine with lycoctonine.

EXPERIMENTAL

Ultraviolet spectra were determined in 95% ethanol and recorded with a Beckman DU instrument. The infrared absorption spectra were recorded with a Perkin–Elmer double-beam model 21 spectrophotometer, and unless it is otherwise mentioned, the samples were suspended in nujol. Melting points were determined on a Kofler hot stage and were uncorrected. Optical rotations were determined in a dm microbore tube and, unless otherwise stated, in chloroform solution. The neutral alumina used for chroma-tography was standardized according to Brockmann, and the eluants were collected in fractions of 20 ml.

Δ'-Anhydrodelsoline

To a solution of delsoline (220 mg) in dried, chilled pyridine (5.5 ml), p-toluenesul-phonyl chloride (440 mg) dissolved in pyridine (5.5 ml) was added, and the mixture allowed to stand at room temperature for 54 hours. It was then concentrated under reduced pressure at room temperature to a syrup which was dissolved in chloroform and extracted with 4% aqueous sodium carbonate. The chloroform solution was dried and evaporated to dryness. The residue was triturated in ether, and the ether-soluble fraction (176 mg) was crystallized from hexane, yield 84 mg, m.p. 135–140°. It was dissolved in benzene and chromatographed on alumina (activity II to III, 1.4 g). Elution with chloroform gave a product which, after crystallization from hexane, melted at 139–141°. For analysis

this sample was sublimed at 145° at 5×10^{-4} mm. $[\alpha]_D^{24}$ $+27.7 \pm 0.7°$ $(c, 1.37)$. Found: C, 66.62; H, 8.81. Calc. for $C_{25}H_{39}O_6N$: C, 66.79; H, 8.75%. Ultraviolet: end absorption. IR: 3470 and 3390 cm⁻¹ (hydroxyl).

Hydrogenation of 1-Dehydro-oxodelcosine

1-Dehydro-oxodelcosine (35 mg obtained by oxidation of monoacetyldelcosine, followed by hydrolysis (3)) in glacial acetic acid (5 ml) was hydrogenated over Adams' catalyst (17 mg) for 1 hour at 3.9 atm. The catalyst was filtered off and the filtrate evaporated to dryness; the residue was dissolved in chloroform and the solution extracted with 4% aqueous sodium carbonate; the chloroform layer was evaporated to dryness and the residue (35 mg) was crystallized from ether from which it separated as colorless prisms, 31 mg, m.p. 241–243.5° undepressed on admixture with authentic oxodelcosine. $[\alpha]_D^{24}$ $+42.2 \pm 1.1°$ $(c, 0.9)$. The infrared spectrum of the product and that of oxodelcosine were superimposable.

Oxidation of N-Desethyldelcosine

(a) *N-Desethyl-didehydrodelcosine-azomethine (V)*.—To freshly distilled pyridine (10 ml) cooled to 0°, chromic anhydride (1.0 g) was added portionwise with stirring. To the precipitated yellow complex a solution of N-desethyldelcosine (1) (500 mg) in pyridine (18 ml) was added and the mixture allowed to stand at room temperature for 12 hours in a stoppered flask. Subsequently sulphur dioxide was bubbled into the reaction mixture and the solvent evaporated under diminished pressure. Ice and 3 N sulphuric acid were added to the residue, and the resulting green solution was extracted with chloroform. The chloroform extract containing the neutral component was set aside. The aqueous acid layer was neutralized by the gradual addition of powdered sodium carbonate and made alkaline by the further addition of 10% aqueous sodium hydroxide. It was then extracted with chloroform, the extract washed with water, dried, and evaporated to dryness. The residue (270 mg) was redissolved in dry, pure, chloroform, chromatographed on alumina grade III (6.0 g), and eluted with chloroform. The eluate, on evaporation, yielded 248 mg of the azomethine which was crystallized twice from acetone–ether from which it separated as rhombohedral prisms, m.p. 219–220°, $[\alpha]_D^{25}$ $+257.5 \pm 1.3°$ $(c, 0.8)$. Found: C, 63.15; H, 6.81. Calc. for $C_{22}H_{29}O_7N$: C, 62.99; H, 6.97%. Ultraviolet: λ_{max} 269 mμ, log ϵ 2.105; λ_{max} 290 mμ, log ϵ 2.123; λ_{min} 281 mμ, log ϵ 2.098. Infrared: 3420 cm⁻¹ (hydroxyl), 1745 cm⁻¹ (five-membered cyclic ketone), 1702 cm⁻¹ (six-membered cyclic ketone), 1633 cm⁻¹ (—CH=N—); in chloroform: 3520, 3470, 1753, 1715, 1635 cm⁻¹.

(b) *N-Desethyl-1,10-didehydro-oxodelcosine*.—The chloroform solution containing the neutral fraction of the product (mentioned above) was washed with 4% aqueous sodium carbonate, dried, and evaporated to dryness. The residue (114 mg) was triturated with ether and the material recrystallized from acetone–hexane from which it separated as colorless prisms, m.p. 274–275.5°, $[\alpha]_D^{28}$ $+139 \pm 0.9°$ $(c, 1.12)$. Found: C, 60.63; H, 6.53. Calc. for $C_{22}H_{29}O_8N$: C, 60.68; H, 6.71%. Ultraviolet: λ_{max} 300 mμ, log ϵ 2.039; λ_{min} 262 mμ, log ϵ 1.312. Infrared: 3430 cm⁻¹ (hydroxyl), 3350 cm⁻¹ (imine), 1740 cm⁻¹ (five-membered cyclic ketone), 1703 cm⁻¹ (six-membered cyclic ketone), 1665 cm⁻¹ (lactamic carbonyl); in chloroform: 3460, 3380 cm⁻¹ (hydroxyl), 3280 cm⁻¹ (imino group).

Ethiodide of N-Desethyl-1,10-didehydrodelcosine-azomethine (VI)

Desethyldidehydrodelcosine-azomethine (290 mg) was dissolved in acetone (30 ml), and ethyl iodide (6 ml) was added to the solution. The mixture was left at room temperature for 24 hours in the dark, after which it was evaporated to dryness under

reduced pressure. The crystalline residue (414 mg) was recrystallized repeatedly from acetone–hexane from which it separated as pale-yellow microcrystals, m.p. 168–171°, $[\alpha]_D^{28}$ +132.4±1.0° (c, 1.02 in methanol). Found: C, 50.27; H, 6.13. Calc. for $C_{24}H_{34}O_7NI$: C, 50.09; H, 5.96%. Ultraviolet: shoulders at λ_{max} 258 mμ, log ϵ 2.918 and λ_{max} 350 mμ, log ϵ 1.851; λ_{max} 300 mμ, log ϵ 2.498; λ_{min} 292 mμ, log ϵ 2.484. Infrared: 3440, 3220 cm^{-1} (hydroxyls), 1755 cm^{-1} (five-membered cyclic ketone), 1713 cm^{-1} (six-membered cyclic carbonyl), 1652 cm^{-1} (—C=N$^+$).

10-Dehydro-oxo-1-epidelcosine (VII)

The ethiodide of desethyldidehydrodelcosine-azomethine (85 mg) was dissolved in 10% methanolic potassium hydroxide (5 ml), and the mixture was refluxed for 90 minutes and evaporated to dryness under reduced pressure. The residue was dissolved in water, and the solution extracted with chloroform. The chloroform extract was washed first with 3 N sulphuric acid, then with water, dried, and evaporated to dryness. The residue (62 mg), which failed to crystallize, was dissolved in chloroform, chromatographed on alumina (activity III), and eluted with chloroform. The product obtained from the eluate could not be induced to crystallize, $[\alpha]_D^{27}$ +10.4±0.8° (c, 1.25). Ultraviolet: λ_{max} 295 mμ, log ϵ 1.456; λ_{min} 265 mμ, log ϵ 0.736. Infrared in chloroform: 3575, 3500, 3420 cm^{-1} (hydroxyls), 1750 cm^{-1} (five-membered cyclic ketone), 1640 cm^{-1} (lactamic carbonyl).

Oxo-1-epidelcosine (VIII)

(a) Sodium borohydride (300 mg) was added to a solution of 10-dehydro-oxo-1-epidelcosine (230 mg) in 80% methanol (20 ml), and the mixture allowed to stand at room temperature for 2 hours and then evaporated to dryness. The residue was dissolved in water and the solution extracted with chloroform. The chloroform extract was washed with 3 N sulphuric acid, with water, dried, and evaporated to dryness. There was left a residue (208 mg) which crystallized from ether, wt. 161 mg, m.p. 124–126°. The crystalline product was dissolved in benzene, chromatographed on alumina (5.0 g, activity III), and eluted with chloroform. From the eluate there was obtained a fraction, m.p. 126–130°, which was recrystallized from acetone–hexane. The colorless hexagonal prisms thus obtained, after being dried at 100° at 5×10^{-4} mm, melted at 128–130°, $[\alpha]_D^{25}$ +19.8±0.9° (c, 1.16). Found: C, 61.39; H, 8.14. Calc. for $C_{24}H_{37}O_8N$: C, 61.65; H, 7.98%. Infrared in chloroform: 3640, 3570, 3490 cm^{-1} (hydroxyls), 1638, 1628 cm^{-1} (double peak due to lactam carbonyl).

(b) The above product was also obtained as follows. 10-Dehydro-oxo-1-epidelcosine (65 mg), dissolved in glacial acetic acid (6.5 ml), was shaken under hydrogen with Adams' catalyst (50 mg) at 3.9 atm for 1 hour. The catalyst was filtered off and the filtrate evaporated to a syrup which was dissolved in chloroform and washed with 4% aqueous sodium carbonate. The dried chloroform solution was evaporated to dryness and the residue (60 mg) crystallized from acetone–ether–hexane, m.p. 126–128°, undepressed by admixture with the sample of oxo-1-epidelcosine obtained above. The infrared spectra of both samples were superimposable.

Didehydro-oxodelcosine from Oxo-1-epidelcosine

To a solution of oxo-1-epidelcosine (69 mg) in glacial acetic acid (5 ml), a solution of sodium dichromate (35 mg) in glacial acetic acid (5 ml) was added dropwise, and the reaction mixture set aside for 1 hour at room temperature. Sulphur dioxide was bubbled in to reduce the excess reagent and the solvent removed under reduced pressure. The

residue was dissolved in chloroform and the solution washed first with 3 N sulphuric acid, then with 4% aqueous sodium carbonate, dried, and evaporated under reduced pressure. It left a residue (63 mg) which crystallized from ether. Recrystallization from acetone–ether–hexane yielded 44 mg, m.p. 208–209° undepressed by mixture with an authentic sample of didehydro-oxodelcosine, $[\alpha]_D^{25}$ +128.0±1.0° (c, 1.0). The infrared spectra of both samples were superimposable.

Epi-1-delcosine

To a solution of oxo-1-epidelcosine (50 mg) in pure dioxane (5 ml), powdered lithium aluminum hydride (60 mg) was added in small portions under a nitrogen atmosphere. The suspension was refluxed and stirred for 1 hour. The excess of reagent was decomposed with methanol, water was added, the precipitated aluminum hydroxide was filtered with suction and washed with acetone and with methanol. The combined filtrate and washings was evaporated to dryness under reduced pressure and the residue dissolved in chloroform. The chloroform solution was washed with several portions of 3 N sulphuric acid, the acid solution made basic with sodium hydroxide and extracted with chloroform. This last chloroform solution when evaporated to dryness left a residue (40 mg) which crystallized from water (2 drops). The product was recrystallized twice from benzene–hexane, from which it separated as colorless prisms, m.p. 177–178°, $[\alpha]_D^{26}$ +38.9±1.0° (c, 0.95). Found: C, 63.69; H, 8.66. Calc. for $C_{24}H_{39}O_7N$: C, 63.55; H, 8.67%. Infrared: 3590, 3504, 3410, 3364 cm^{-1} (hydroxyls).

1-Epidelcosine (30 mg) dissolved in methanol (2 ml) was made just acid to Congo red by the dropwise addition of perchloric acid. The solution was evaporated to dryness under reduced pressure and the crystalline residue recrystallized from methanol–ether from which it separated as colorless hexagonal prisms, m.p. 197–200°. After several recrystallizations the salt melted at 199–201° when immersed in a bath at 193°, $[\alpha]_D^{28}$ +26.8±1.8° (c, 0.56 in methanol). Found: C, 52.15; H, 7.40. Calc. for $C_{24}H_{39}O_7N \cdot HClO_4$: C, 52.03; H, 7.27%.

Anhydro-oxo-1-epidelcosine (IX, R = R′ = H)

Oxo-1-epidelcosine (150 mg) in glacial acetic acid (5 ml, containing 0.1% by volume of sulphuric acid) was heated at 75–80° for 70 minutes. The warm solution was poured onto crushed ice, neutralized with ice-cold 20% aqueous potassium hydroxide, and extracted with chloroform. The chloroform layer was evaporated to dryness and the residue refluxed for 1 hour with 10% methanolic potassium hydroxide (10 ml) and water (1.0 ml). The solution was evaporated to dryness, and the residue dissolved in water and extracted with chloroform. The extract was washed with 3 N sulphuric acid, with water, dried, and evaporated to dryness under reduced pressure. The residue (144 mg) was dissolved in benzene containing 15% of chloroform and chromatographed on alumina, activity III (2.7 g). Chloroform was used to elute the column, and the eluate yielded the pinacone which crystallized from ether, m.p. 225–229°. Recrystallization from acetone–ether–hexane raised the melting point to 227–231°, wt. 86 mg. For analysis the product was recrystallized once more and obtained as colorless long needles, m.p. 230–232°, $[\alpha]_D^{23}$ −23.8±2° (c, 0.55). Found: C, 64.13; H, 7.80; OMe, 20.53. Calc. for $C_{24}H_{35}O_7N$: C, 64.12; H, 7.85; 3OMe, 20.71%. Ultraviolet: λ_{max} 302 mμ, log ϵ 1.810; λ_{min} 265 mμ, log ϵ 0.993. Infrared: 3360 cm^{-1} (hydroxyl), 1725 cm^{-1} (six-membered cyclic ketone), 1625 cm^{-1} (lactam carbonyl); in chloroform: 3578, 3440 cm^{-1} (hydroxyls), 1727 and 1642 cm^{-1} (carbonyls).

O,O-Dimethyl-anhydro-oxo-1-epidelcosine (IX, R = R' = CH₃)

The pinacone described above (93 mg) was dissolved in dioxane (9 ml) and a slight excess of sodium hydride was added to the solution, which was brought to a boil and, after the addition of excess methyl iodide, was refluxed, with stirring, in a hydrogen atmosphere for 10 hours. The reaction product was filtered through a Hyflo-Supercel column, the filtrate evaporated to dryness, and the residue dissolved in water and extracted with chloroform. The chloroform solution was washed with 3 N sulphuric acid, with water, dried, and evaporated to dryness. The residue (quantitative yield) was dissolved in benzene containing 20% hexane and chromatographed on alumina (2.9 g, activity III). Elution of the column was done first with benzene and then with a benzene–chloroform (3:1) mixture. Both eluates yielded the same product, which crystallized from ether, m.p. 177–180°, wt. 71.5 mg. A sample for analysis was recrystallized from ether, m.p. 178–180°, $[\alpha]_D^{22}$ −56.3±1.3° (c, 0.80), and sublimed at 145° at 5×10⁻⁴ mm. Found: C, 65.64; H, 8.40; OMe, 32.41. Calc. for $C_{26}H_{39}O_7N$: C, 65.39; H, 8.23; 5OMe, 32.49%. Ultraviolet: λ_{max} 303 mμ, log ϵ 1.897; λ_{min} 263 mμ, log ϵ 1.423. Infrared: 1727 cm⁻¹ (six-membered cyclic ketone), 1648 cm⁻¹ (lactam carbonyl).

O,O-Dimethyl-6-desmethoxy-anhydro-oxo-1-epidelcosine

Sodium amalgam (5%, 680 mg) was added to a solution of the methylated pinacone, O,O-Dimethyl-anhydro-oxo-1-epidelcosine (74 mg), in absolute ethanol (1.6 ml). The mixture was shaken for 90 minutes, filtered through a Hyflo-Supercel column, and the filtrate diluted with water and extracted with chloroform. Evaporation of the chloroform extract left a residue (67 mg) which was dissolved in benzene–hexane (1:1) and chromatographed on alumina (2.4 g, activity III). From benzene and benzene containing 30% chloroform eluates, there was isolated a middle fraction (36 mg) which crystallized from ether, m.p. 149–154°. Recrystallized from ether–pentane, the product consisted of colorless prisms, m.p. 152.5–154°, $[\alpha]_D^{25}$ −35.2±1.8° (c, 0.54). Found: C, 67.26; H, 8.29. Calc. for $C_{25}H_{37}O_6N$: C, 67.09; H, 8.33%. Ultraviolet: λ_{max} 282 mμ, log ϵ 1.744; λ_{min} 261 mμ, log ϵ 1.533. Infrared: 1715 cm⁻¹ (six-membered cyclic ketone), 1645 cm⁻¹ (lactam carbonyl).

O-Methyl-anhydro-oxolycoctonine

Anhydro-oxolycoctonine was prepared from acetyl-oxolycoctonine by acid-catalyzed rearrangement followed by hydrolysis as described above for the corresponding oxoepi-delcosine derivative. The pinacone (155 mg) was dissolved in dioxane (9 ml) and excess sodium hydride was added to the solution which was brought to a boil and, after the addition of excess methyl iodide, was refluxed, with stirring, for 7 hours under a hydrogen atmosphere. The reaction mixture was filtered through a Hyflo-Supercel column and the product worked up exactly as described above for the corresponding delcosine derivative. The crude product was dissolved in benzene–hexane (4:1), chromatographed on alumina (4 g, activity III), and eluted (a) with benzene, (b) with benzene–chloroform (4:1), and (c) with benzene–chloroform (1:1). The first two eluates (a and b) together yielded a fraction (104 mg) which crystallized from ether and after recrystallization from the same solvent consisted of colorless needles, m.p. 126–128°, $[\alpha]_D^{25}$ +9.2±0.8° (c, 1.2). Found: C, 65.57; H, 8.09; OMe, 32.40. Calc. for $C_{26}H_{39}O_7N$: C, 63.59; H, 8.23; 5OMe, 32.49%. Ultraviolet: λ_{max} 302 mμ, log ϵ 1.856; λ_{min} 267 mμ, log ϵ 1.471. Infrared: 1725 cm⁻¹ (six-membered cyclic ketone), 1642 cm⁻¹ (lactam carbonyl).

The third eluate (c) from the chromatogram yielded a by-product (20 mg) which crystallized from ether, m.p. 185–201°, $[\alpha]_D^{26}$ +85.9±1.6° (c, 0.63). Infrared: 1728 cm⁻¹ (six-membered cyclic ketone), 1650 cm⁻¹ and 1643 cm⁻¹ (lactam carbonyl).

O-Methyl-6-desmethoxy-anhydro-oxolycoctonine

Sodium amalgam (5%, 610 mg) was added to a solution of the above methylated oxolycoctonine pinacone (67 mg) in absolute ethanol (1.8 ml) and the mixture shaken for 2 hours. It was afterwards filtered through a Hyflo-Supercel column and the filtrate diluted with water and extracted with chloroform. The extract was evaporated and the residue (quantitative yield) crystallized from ether, wt. 52 mg, m.p. 159–163°. After recrystallization from ether it consisted of colorless needles, m.p. 161–163°, $[\alpha]_D^{26}$ +3.4±1.1° (c, 0.89). Found: C, 67.26; H, 8.30; OMe, 27.60. Calc. for $C_{25}H_{37}O_6N$: C, 67.09; H, 8.33; 4OMe, 27.73%. Ultraviolet: λ_{max} 282 mμ, log ϵ 1.643; λ_{min} 262 mμ, log ϵ 1.410. Infrared: 1716 cm^{-1} (six-membered cyclic ketone), 1638 cm^{-1} (lactam carbonyl).

ACKNOWLEDGMENTS

REFERENCES

1. R. ANET, D. W. CLAYTON, and L. MARION.   Can. J. Chem. **35**, 397 (1957).
2. V. SKARIĆ and L. MARION.   J. Am. Chem. Soc. **80**, 4434 (1958).
3. V. SKARIĆ and L. MARION.   Can. J. Chem. **38**, 2433 (1960).
4. R. ANET and L. MARION.   Can. J. Chem. **36**, 766 (1958).
5. M. PRZYBYLSKA and L. MARION.   Can. J. Chem. **37**, 1843 (1959).
6. F. SPARATORE, R. GREENHALGH, and L. MARION.   Tetrahedron, **4**, 157 (1958).
7. D. DVORNIK and O. E. EDWARDS.   Proc. Chem. Soc. 280 (1958).
8. R. C. COOKSON and M. E. TREVETT.   Chem. & Ind. (London), 1324 (1954); J. Chem. Soc. 3864 (1956).
9. O. E. EDWARDS, L. MARION, and D. K. R. STEWART.   Can. J. Chem. **34**, 1315 (1956).
10. H. KONDO and E. OCHIAI.   Ann. **470**, 224 (1929).
11. O. E. EDWARDS, L. MARION, and K. H. PALMER.   Can. J. Chem. **36**, 1097 (1958).

THE KINETICS OF REACTION OF 2,2-DIPHENYL-1-PICRYLHYDRAZYL WITH PHENOLS[1]

J. S. Hogg, D. H. Lohmann, and K. E. Russell

ABSTRACT

The kinetics of reaction between 2,2-diphenyl-1-picrylhydrazyl (DPPH) and a wide variety of phenols have been studied. The rate of disappearance of DPPH is of first order with respect to both the DPPH and the reacting phenol. The rates of reaction can be roughly correlated with the Hammett σ value of the phenol substituent in the range $-0.4 < \sigma < 0.2$, a ρ value of -6 being obtained. t-Butyl groups in both ortho positions of the phenol give rise to steric hindrance, the reduction in rate being largely due to a reduction in the A factor. Hydrogen abstraction from the less reactive phenols is strongly retarded by the product, 2,2-diphenyl-1-picrylhydrazine.

The rate-determining step probably involves the abstraction of a hydrogen atom from the phenol by the DPPH to give diphenylpicrylhydrazine and a phenoxy radical. The retardation by diphenylpicrylhydrazine is readily explained if this primary step is reversible.

Hydrogen-abstraction reactions involving 2,2-diphenyl-1-picrylhydrazyl (DPPH) as the acceptor molecule are relatively easily studied and a number of recent publications have been concerned with the rates of reaction of this radical with hydrogen donors. Information has been obtained concerning the reactivities of restricted ranges of donors containing C—H (1), N—H (2, 3), O—H (4, 5, 6), and S—H (7, 8) bonds. Phenols are well suited to an investigation of hydrogen abstraction from O—H-containing compounds (3). A wide range of phenols is available and a detailed study of the effect of substituents is possible.

During the course of the work, a paper by McGowan, Powell, and Raw was published (4) giving rate constants for the second-order reactions of DPPH with a large number of phenols, showing that substituents may exert considerable polar and steric influences on the reaction. Their measurements were normally made at room temperature using carbon tetrachloride as solvent, but with three phenols, measurements were made over a temperature range. In the work described here benzene was used as solvent, activation energies and A factors were obtained for all the phenols studied, and the effect of the product 2,2-diphenyl-1-picrylhydrazine on the rate of reaction was determined. Some additional evidence was obtained that the primary reaction involves the hydrogen atom of the O—H group, and the stoichiometry of the process was investigated.

EXPERIMENTAL

Materials

2,2-Diphenyl-1-picrylhydrazine was prepared by the reaction of picryl chloride and 1,1-diphenylhydrazine (9, 10). DPPH was prepared by the oxidation of diphenylpicrylhydrazine with lead dioxide (9). Complexed solvent was removed by heating *in vacuo* at 60° for several hours.

2-Methylanisole and 1- and 2-methoxynaphthalene (Eastman Kodak) were used without further purification.

Phenols were obtained from the Aldrich Chemical Company or from the Eastman Kodak Company. The liquids were distilled and the solids were either sublimed at reduced pressure or recrystallized; 2,6-di-t-butylphenol was used without further purification.

Procedure

The experimental method has been described elsewhere (3). The rates of disappearance of DPPH were normally followed in the presence of air. With phenol, experiments were performed at various concentrations using degassed solutions and a comparison of rates was made at corresponding extents of reaction. Initial DPPH concentrations were in the range $4-20 \times 10^{-5}$ M. Phenol concentration ranges were chosen to give convenient rates of reaction; a minimum value of 2×10^{-5} M was used with the very reactive 2,4-dichloro-1-naphthol and a maximum value of 2×10^{-2} M with 4-acetylphenol. Measurements were normally performed at 30° C and activation energies were derived from measurements taken over a temperature range of at least 20 degrees.

The stoichiometry of the reaction was investigated by making up solutions containing ratios of DPPH to phenol between 2.5:1 and 1:1 and determining the optical densities of the solutions diluted 10-fold with benzene after appropriate times. If optical density is plotted against DPPH-to-phenol ratio, a break in the curve is observed which gives the stoichiometry applying under the particular experimental conditions. The break is sharp for the more reactive phenols; Fig. 1 shows the results obtained with 1-naphthol
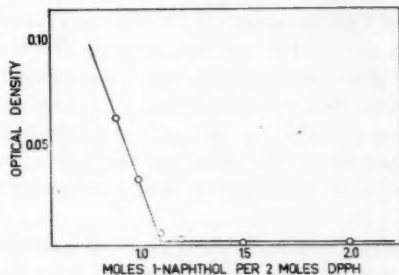

FIG. 1.   Stoichiometry of the reaction of DPPH with 1-naphthol.

after 85 minutes at 50° C and an initial DPPH concentration of 2.5×10^{-3} M. With phenols whose reaction with DPPH is strongly retarded by diphenylpicrylhydrazine, the break in the curve is less sharp and the stoichiometric ratios are probably not known to better than 10% of their value.

Retardation by diphenylpicrylhydrazine was investigated by determining initial rates of reaction for solutions to which the hydrazine had been added at a concentration twice that of the initial DPPH concentration. With the very reactive phenols 4-methoxyphenol, 1-naphthol, and 2,4-dichloro-1-naphthol, the concentration of diphenylpicrylhydrazine was 8×10^{-5} M and with all other phenols it was 2×10^{-4} M.

The yield of diphenylpicrylhydrazine was determined for the reactions between DPPH and phenol and 1-naphthol. Reaction mixtures containing a slight excess of phenol were allowed to react until more than 99% of the DPPH had disappeared, and the products were separated on a column of alumina deactivated by the addition of 4% water. The diphenylpicrylhydrazine, identified by melting point and mixed melting point, was obtained in greater than 80% yield when phenol was the donor and in a yield of 90% to 95% when 1-naphthol was the donor.

Infrared spectra of mixtures obtained by the reaction of DPPH with various phenols in chloroform solution were examined. The high yields of diphenylpicrylhydrazine were confirmed but little information was obtained concerning the structures of the other products.

RESULTS AND DISCUSSION

Diphenylpicrylhydrazine (DPPH—H) is a major product of the reaction of DPPH with phenols, confirming that the main reaction is a hydrogen-abstraction process. The very low rates of reaction observed with the methylated phenols 1-methoxynaphthalene, 2-methoxynaphthalene, and 2-methylanisole indicate that the hydrogen of the O—H is attacked in the rate-determining step.

$$DPPH + XOH \rightarrow DPPH—H + XO \cdot \qquad [1]$$
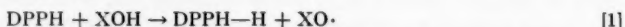
The change in substituent from O—H to O—Me might affect the rate of hydrogen abstraction from C—H but relative rates greater than a thousand would not be expected. Further support is given by the observation that pentachlorophenol, which contains no C—H bonds, reacts with DPPH to give diphenylpicrylhydrazine as a major product, and the rate of reaction is approximately that predicted from reactions involving mono-chlorophenols. In addition, Bickel and Kooyman (6) observed a deuterium isotope effect in the second-order reaction of DPPH with 4-methyl-2,6-di-t-butylphenol and concluded that the rate-determining step involved the simple attack of DPPH on the O—H group. It is probable that a similar conclusion applies in the reactions of DPPH with all phenols.

In this study the rates of disappearance of DPPH were usually found to be of first order with respect to both the DPPH and the phenol. The only exceptions were the reactions involving phenol, pentachlorophenol, and 2,6-di-t-butylphenol where the order was slightly less than one with respect to the phenol. The reactions were normally studied in the presence of air and it is possible that oxygen has some effect on the rate of reaction and on the nature of the products. The effect on the rate of reaction of DPPH with phenol is small, for when degassed solutions are used a reduction in rate of a few per cent is observed.

The kinetic results are summarized in Table I. The rate constants (k) for the hydrogen-abstraction process of reaction [1] have been calculated from the observed initial rates of disappearance of DPPH at 30° C and the stoichiometry of the reaction. The activation energies (E) are probably correct to better than ± 1.0 kcal/mole with phenols which have very high rate constants or which undergo reactions which are strongly retarded by diphenylpicrylhydrazine; with other phenols the activation energies are probably correct to ± 0.5 kcal/mole. The uncertainty in the A factors is determined largely by the uncertainty in the corresponding activation energy.

The rate constant for hydrogen abstraction varies considerably with the nature of the substituent. 4-Methoxyphenol, for example, gives a rate constant some 20,000 times that given by 4-nitrophenol. In Fig. 2 values of $\log_{10}(k/k_0)$, where k is the second-order rate constant for the substituted phenol and k_0 is the rate constant for phenol at 30° C, are plotted against the Hammett σ value (11). For σ values less than 0.2 the relationship

$$\log_{10}(k/k_0) = -6$$

is very roughly obeyed but for values of σ greater than 0.2 the slope is much lower. The high negative value of the slope in the range $-0.4 < \sigma < 0.2$ has been compared with the smaller slopes of -3.7 for hydrogen-abstraction reactions involving phenols and alkylperoxy radicals (12) and of -2.5 for phenols and polystyryl radicals and is interpreted as evidence for the great importance of polar factors in the free-radical reactions between DPPH and phenols (5). However, the referee has pointed out that recent discussions of substituent effects (13, 14) indicate that the substituents from which the

. TABLE I

The reaction of DPPH with phenols and methylated phenols

|	k at 30° (cc/mole sec)	E (kcal/mole)	A (cc/mole sec)	Stoichiometry	Retardation
Phenol	22.4	10.4	7.1×10^8	1.1	0.14
4-Methyl-	377	9.0	1.2×10^9	1.1	0.72
3-Methyl-	68	10.2	1.6×19^9	1.25	0.29
2-Methyl-	180	9.1	6.6×10^8	1.2	0.68
4-t-Butyl-	337	9.5	2.4×10^9	1.2	0.082
4-Phenyl-	936	8.7	1.8×10^9	1.2	0.12
2-Phenyl-	96	9.7	9.5×10^8	1.25	0.22
4-Chloro-	40	10.5	1.5×10^9	1.1	0.23
3-Chloro-	5.0	12.4	4.4×10^9	1.3	0.078
2-Chloro-	10.6	10.6	4.7×10^8	1.2	0.24
4-Fluoro-	92	9.6	7.8×10^8	1.3	0.22
4-Nitro-	1.5	14.6	5.1×10^{10}	1.1	0.11
3-Nitro-	1.0	14.1	1.5×10^{10}	1.2	0.099
4-Methoxy-	29,100	4.8	8.4×10^7	1.1	0.53
3-Methoxy-	134	11.1	1.4×10^{10}	1.2	0.14
4-Acetyl-	3.5	16.1	1.4×10^{12}	1.2	0.051
2,6-Dimethyl-	585	6.1	1.5×10^7	1.1	0.78
2,6-Diisopropyl-	425	6.4	1.8×10^7	1.0	0.95
2,6-Di-t-butyl-	18	6.0	3.8×10^5	1.0	0.87
2,6-Di-t-butyl-4-methyl-	126	6.1	3.2×10^6	1.0	0.96
Pentachloro-	6.1	10.5	2.3×10^8	1.7	0.16
1-Naphthol	33,600	4.9	1.1×10^8	1.1	0.93
2-Naphthol	2,150	6.6	1.2×10^8	1.1	0.24
2,4-Dichloro-1-naphthol	49,800	4.5	8.8×10^7	1.9	0.75
1-Methoxynaphthalene	40	—	—	—	—
2-Methoxynaphthalene	0.01	—	—	—	—
2-Methylanisole	0.01	—	—	—	—
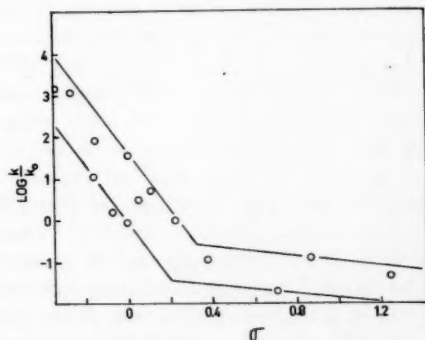
FIG. 2. Variation of rate constant with Hammett σ value of phenol substituent.

value of $\rho = -6$ is deduced are ones for which the unmodified Hammett equation is not valid. Taft (14) has shown that a meaningful measure of the inductive contribution of a substituent to the reactivity of a benzene derivative is the ρ_I value obtained from a Hammett σ plot using only selected meta substituents. The value of ρ_I for the DPPH–phenol reaction obtained from rate constants for phenol, m-chlorophenol, m-cresol, and m-nitrophenol is -2.1. Assuming that the inductive effect is the same for meta and para substituents, it is possible to estimate the resonance contributions of substituents to the reactivities of benzene derivatives. Taft defines a specific resonance parameter $\bar{\sigma}_R$ and

shows that deviations from the Hammett equation which result from a specific dependence of resonance effects on reaction type can usually be detected by deviation of the specific resonance parameter from its "normal" value. In the reaction of DPPH with phenols, considerably enhanced values of $\bar{\sigma}_R$ are observed for p-methoxy, p-methyl, and p-phenyl substituents. Both electrophilic and free-radical reactivities (14) give enhanced values of $\bar{\sigma}_R$ for these substituents and at this stage it is not possible to use $\bar{\sigma}_R$ values to place the DPPH–phenol reaction in one of these classes. More data for the present reaction, and for free-radical reactions generally, would be helpful, but the difficulty largely stems from our use of a highly polar free radical as a hydrogen acceptor. McGowan, Powell, and Raw (4) prefer an ionic mechanism for the DPPH–phenol reaction and suggest that the DPPH abstracts a hydride ion from the phenol. The main evidence for this suggestion is that the relative rates of hydrogen abstraction from phenols by DPPH are remarkably close to those for the solvolysis of dimethylbenzyl chlorides. We believe, however, that the rate-determining step of the reaction of DPPH with phenols is not significantly different from that generally put forward for the reaction of alkylperoxy radicals (12) and polystyryl radicals (5) with phenols and for the reaction of DPPH with hydro-aromatic compounds (1), aromatic amines (4), and mercaptans (7).

The rate constants for the reaction of DPPH with phenols in carbon tetrachloride solution (4) are greater than those obtained using benzene as solvent under similar conditions; the ratio is of the order of three but varies with the phenol. The dielectric constant of the medium has been shown to be important in determining the rate of reaction of DPPH with mercaptans (8) but the similar values for carbon tetrachloride and benzene make it unlikely that the difference in rates can be accounted for in terms of dielectric constant alone. With mercaptans as hydrogen donors it was found that the reactions were approximately twice as fast in cyclohexane as in benzene (7) and it was suggested that the loose complex formed between benzene and DPPH could account for the slower reaction in benzene. This explanation may apply to the reaction of DPPH with phenols since carbon tetrachloride does not complex with DPPH to any great extent.

McGowan, Powell, and Raw have pointed out that alkyl substituents in the two ortho positions of the phenol can cause steric hindrance to the hydrogen-abstraction reaction (4). The effect is small for two methyl groups but the rate of reaction drops to approximately one hundredth of the expected rate when there are t-butyl groups in both ortho positions. The present work shows that the reduction in rate is caused largely by a reduction in the A factor rather than an increase in activation energy. The A factors are normally of the order of 10^9 cc/mole sec but higher values are usually observed in reactions of comparatively high activation energy and lower values in reactions of low activation energy. The expected values for the 2,6-disubstituted phenols would be of the order of 10^8 cc/mole sec and the lower values observed for 2,6-dimethylphenol and 2,6-diisopropylphenol may indicate that some steric hindrance is occurring in these cases. The value of 3.8×10^5 cc/mole sec observed for 2,6-di-t-butylphenol is much lower than the expected value and there is little doubt that steric hindrance is the main factor involved. Some caution must be exercised in arguments of this type as the A factor found for the reaction involving 2,6-di-t-butyl-4-methylphenol is considerably larger (3.2×10^6 cc/mole sec), yet it is not significantly different from that found for di-t-butylphenol because of the wide limits of experimental uncertainty.

The effect of the product 2,2-diphenyl-1-picrylhydrazine on the rate of reaction is shown in Table I. The values recorded are the ratios of the rate constants k_1/k where k

applies to the normal reaction and k_1 to the reaction retarded by the addition of diphenyl-picrylhydrazine at a concentration twice that of the initial DPPH concentration. For the less reactive phenols the values of k_1/k are generally small and in these cases the accumulation of diphenylpicrylhydrazine as the product of a normal reaction will cause a considerable decrease in rate. It is clear that accurate kinetic analyses can only be made using initial rates of reaction where the concentration of retarding product is low. The retardation can be simply explained if reaction [1] is reversible; the rate of production of dehydrogenation products of the phenols is determined by the concentration of XO· radicals and any lowering of this concentration by a reversal of reaction [1] results in a decreased rate of production of dehydrogenation products and a decreased rate of disappearance of DPPH. The quantitative effect of the diphenylpicrylhydrazine on the rate of reaction depends on the reactivity of XO· towards diphenylpicrylhydrazine and also on the further reactions of XO· radicals with themselves, and with DPPH. In many cases these further reactions become rate controlling even at low concentrations of diphenylpicrylhydrazine, and detailed kinetic studies of the retarded reactions may be useful in distinguishing between the alternative secondary processes.

Some indication of the nature of the secondary reactions is given by the stoichiometric results; these are recorded in Table I as the number of moles of phenol reacting with 2 moles of DPPH. In most cases the ratio of DPPH to phenol consumed is approximately 2:1.1 and since the yields of diphenylpicrylhydrazine are high, an average of almost two hydrogen atoms is abstracted from each phenol molecule. The second hydrogen atom is probably in the ortho or para position because if these positions are blocked as in 2,4-dichloro-1-naphthol the DPPH-to-phenol ratio is closer to 1:1. Products of the type I and II are suggested by the stoichiometry and by previous work on the oxidation of

I II
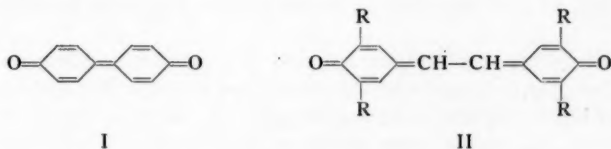
phenols (15, 16). The infrared spectra of the product mixtures do not show a strong absorption in the carbonyl stretching region, however, and there is no direct evidence for the formation of quinonoid compounds. With all phenols examined the OH stretching absorption of the reacting phenol decreases in intensity as the reaction proceeds, but in the case of 1-naphthol a new absorption at a frequency some 40 cm^{-1} below that of the 1-naphthol is observed in the products. It appears that the paths followed in the further reactions of the phenoxy radicals may vary with the phenol.

REFERENCES

1. E. A. BRAUDE, A. G. BROOK, and R. P. LINSTEAD. J. Chem. Soc. 3574 (1954).
2. A. S. KUZ'MINSKII and L. G. ANGERT. Doklady Akad. Nauk S.S.S.R. 96, 1187 (1954).
3. J. E. HAZELL and K. E. RUSSELL. Can. J. Chem. 36, 1729 (1958).

4. J. C. McGowan, T. Powell, and R. Raw.   J. Chem. Soc. 3103 (1959).
5. M. P. Godsay, D. H. Lohmann, and K. E. Russell.   Chem. & Ind. (London), 1603 (1959).
6. A. F. Bickel and E. C. Kooyman.   J. Chem. Soc. 2415 (1957).
7. K. E. Russell.   J. Phys. Chem. 58, 437 (1954).
8. A. H. Ewald.   Trans. Faraday Soc. 55, 792 (1959).
9. S. Goldschmidt and K. Renn.   Ber. 55, 628 (1922).
10. R. H. Poirier, E. J. Kahler, and F. Benington.   J. Org. Chem. 17, 1439 (1952).
11. H. H. Jaffé.   Chem. Revs. 53, 191 (1953).
12. C. E. Boozer, G. S. Hammond, C. E. Hamilton, and J. N. Sen.   J. Am. Chem. Soc. 77, 3238 (1955).
13. H. Van Bekkum, P. E. Verkade, and B. M. Wepster.   Rec. trav. chim. 78, 815 (1959).
14. R. W. Taft, Jr. and I. C. Lewis.   J. Am. Chem. Soc. 81, 5343 (1959); R. W. Taft, Jr.   J. Phys. Chem. 64, 1805 (1960).
15. S. L. Cosgrove and W. A. Waters.   J. Chem. Soc. 388 (1951).
16. A. F. Bickel and E. C. Kooyman.   J. Chem. Soc. 3211 (1953).

AN ALTERNATIVE SYNTHESIS OF 5-O-METHYL-L-ARABINOSE[1]

I. R. SIDDIQUI,[2] C. T. BISHOP, AND G. A. ADAMS

ABSTRACT

5-O-Methyl-L-arabinose has been synthesized by an unambiguous route in which O-benzyl groups were used to block positions 2 and 3 in the L-arabinose molecule. In addition to the usual indirect proofs of structure, a direct proof is described involving isolation of the product from periodate oxidation of the 5-O-methyl-L-arabinose. Two new derivatives, the phenyl-hydrazide and amide of 5-O-methyl-L-arabonic acid, were prepared.

The probable occurrence of 5-O-methyl-L-arabinose among the hydrolysis products of methylated wheat bran hemicellulose (1) prompted the synthesis of this compound by Dutton *et al.* (2). These authors used O-acetyl groups to block positions 2 and 3 in ethyl α-L-arabinofuranoside during methylation by Purdie's reagents and stated that "although sugar acetates may undergo acetyl migration even in the presence of such a weak base as silver oxide there was no indication of such migration in the preparation described here" (2). This result indicated that O-acetyl migrations, which are known to occur in the hexopyranoside series (3–6) and in D-glucose diethyl thioacetal tetracetate (7), may not happen in the pentofuranoside series.

Authentic samples of mono- and di-O-methyl ethers of L-arabinose were required in connection with another problem (8) and were obtained from various laboratories. Examination of the methyl glycosides of these compounds by gas–liquid partition chromatography (9, 10) revealed that all of the samples that were syrups contained more than one component. These samples had been obtained by chromatography on cellulose and the results showed that pure methyl ethers of arabinose may be difficult to isolate by that method.

Because of the unexpected absence of O-acetyl migration in the synthesis of Dutton *et al.* (2), the apparent difficulties in purification of these compounds by cellulose chromatography, and the urgent need for an authentic sample of this important reference sugar, an alternative synthesis of 5-O-methyl-L-arabinose seemed desirable. The present paper reports such a synthesis together with a proof of structure and two new derivatives of this sugar, namely the phenylhydrazide and the amide of 5-O-methyl-L-arabonic acid.

The route followed in this synthesis was similar to that used by Dutton *et al.* (2) except that O-benzyl rather than O-acetyl groups were used to block positions 2 and 3 in the L-arabinose molecule. The sequence of reactions was as follows. Ethyl α-L-arabino-furanoside was tritylated and the product was benzylated to yield ethyl 2,3-di-O-benzyl-5-O-trityl-α-L-arabinoside. This compound was successively detritylated, methylated, debenzylated, and hydrolyzed to yield 5-O-methyl-L-arabinose. Purities of the compounds obtained in each step of the synthesis were checked by analysis and, where possible, by gas–liquid partition chromatography and paper chromatography.

Confirmation that the syrupy mono-O-methyl-L-arabinose from the above synthesis was 5-O-methyl-L-arabinose was obtained from the following evidence. Complete methylation of the methyl glycosides, prepared by refluxing the mono-O-methyl-L-arabinose in methanolic hydrogen chloride, yielded methyl 2,3,5-tri-O-methyl α- and β-L-arabinosides,

readily distinguished from the methyl glycosides of 2,3,4-tri-O-methyl-L-arabinose by gas–liquid partition chromatography (8). Oxidation of the mono-O-methyl-L-arabinose by bromide yielded a lactone that crystallized from the chloroform extract of the reaction mixture. This lactone showed a very slow change in rotation in aqueous solution and had carbonyl absorption at 1773 cm^{-1} in the C=O stretching frequency of its infrared spectrum. Barker *et al.* (11) have shown that γ-lactones of aldonic acids have their carbonyl absorption bands in the range 1765–1790 cm^{-1} while those of δ-lactones are between 1726 and 1760 cm^{-1}. This was confirmed here by observation of the infrared spectra of the following lactones, which showed carbonyl absorption as indicated: D-gluconic acid δ-lactone (1720 cm^{-1}); 2,5-di-O-methyl-L-arabonic acid-γ-lactone (1777 cm^{-1}); and 3,5-di-O-methyl-D-galactonic acid-γ-lactone (12) (1786 cm^{-1}). The results of methylation and the isolation of the γ-lactone showed that the parent mono-O-methyl-L-arabinose was capable of existing in the furanose form and therefore that the O-methyl group could not be located at C$_4$.

The mono-O-methyl-L-arabonic acid-γ-lactone provided a crystalline phenylhydrazide and a crystalline amide on reaction with phenylhydrazine and ammonia respectively. The amide gave a positive Weerman (13) reaction showing the presence of a free hydroxyl at C$_2$. This conclusion was supported by isolation of an osazone from the mono-O-methyl-L-arabinose without loss of methoxyl and by the large M_G value of the parent sugar on paper electrophoresis in borate buffer (14).

On oxidation by periodate the methyl glycosides of the mono-O-methyl-L-arabinose consumed one molar proportion of oxidant and released neither formic acid nor formaldehyde. This result could not have been obtained from methyl 3-O-methyl-L-arabinoside, which would not be oxidized in either the furanoside or pyranoside form, and showed that C$_3$ in the mono-O-methyl-L-arabinose must carry a free hydroxyl.

The foregoing evidence showed that free hydroxyls existed on C$_2$, C$_3$, and C$_4$ of the mono-O-methyl-L-arabinose and constituted indirect proof that the O-methyl group was located on C$_5$. On periodate oxidation the mono-O-methyl-L-arabinose yielded methoxyacetaldehyde, isolated by azeotropic distillation with water and identified as its *p*-nitrophenylhydrazone (15, 16). The isolation of this product, which could have arisen only from the 5-O-methyl isomer, constituted a direct proof of structure.

The physical constants of the 5-O-methyl-L-arabinose, 5-O-methyl-L-arabonolactone, and 5-O-methyl arabinosazone isolated in the present study are in reasonable agreement with the values reported for these derivatives by Dutton *et al.* (2) except for the specific rotations of the free sugar and of its osazone. Although certain partially methylated reducing sugars are known to give anomalous results when oxidized by periodate (17, 18), Dutton *et al.* (2) have shown that 5-O-methyl-L-arabinose behaves normally under these conditions, a conclusion supported by the present work.

EXPERIMENTAL

Paper chromatograms were run by the descending method on Whatman No. 1 paper using the organic phase of butanone saturated with water containing 2% of concentrated ammonium hydroxide. Paper electrophoresis was done on Whatman 3MM paper at 700–800 v for 2 hours using 0.2 M borate buffer, pH 10. Sugars were detected on the papers by the *p*-anisidine hydrochloride spray reagent (19). Infrared spectra were measured in the frequency range 3800–699 cm^{-1} either on chloroform solutions or by the Nujol mull technique. Gas–liquid partition chromatograms were done on a Pye Argon

Chromatograph using straight, 4-ft columns with the following packings:

(a) butanediol succinate polyester on Chromosorb W, 60–80 mesh (1:9 w/w),

(b) polyphenyl ether, m-bis(m-phenoxyphenoxy)-benzene, on Celite 545, 80–100 mesh (1:6 w/w).

Flow rates and temperatures were as cited for individual analyses. Evaporations were carried out at 35° C under diminished pressure unless otherwise stated and melting points are corrected.

Ethyl 5-O-Trityl-α-L-arabinoside

Ethyl α-L-arabinofuranoside (10.8 g, m.p. 48–49° C, $[\alpha]_D^{26}$ −117°±1.5° (c, 1.7% in water) (20)) was dissolved in dry pyridine (100 ml) and triphenylchloromethane (16.85 g) was added. After the solution had been kept at room temperature (25–26° C) for 41 hours isolation of the product (21) yielded ethyl 5-O-trityl-α-L-arabinoside as a syrup (yield 25.0 g or 98%), $[\alpha]_D^{22}$ −51.4° (c, 3.1% in methanol). Anal: Calc. for $C_{26}H_{28}O_5$: trityl, 59.8%; C, 74.26%; H, 6.71%. Found: trityl (22), 59.67%; C, 74.99%; H, 6.92%.

Ethyl 2,3-Di-O-benzyl-5-O-trityl-α-L-arabinoside

Ethyl 5-O-trityl-α-L-arabinoside (23 g) was benzylated according to the procedure of Dennison and McGilvray (23). The syrupy product showed very weak hydroxyl absorption in its infrared spectrum but the high yield (35.0 g, 106%) indicated incomplete removal of benzyl chloride or benzyl alcohol from the reaction mixture. $[\alpha]_D^{22}$ −40.5° ±1° (c, 1.7% in chloroform). Anal: Calc. for $C_{40}H_{40}O_5$: C, 80.0%; H, 6.71%. Found: C, 81.1%; H, 6.71%.

Ethyl 2,3-Di-O-benzyl-α-L-arabinofuranoside

Ethyl 2,3-di-O-benzyl-5-O-trityl-α-L-arabinoside (34.8 g) was dissolved in dry chloroform (100 ml) and the solution was saturated at 0° C with dry hydrogen chloride. After 1 hour, the solution was neutralized with silver carbonate, silver salts were filtered, and the filtrate was evaporated to a syrup. A methanolic solution of this syrup yielded crystals of triphenylcarbinol when kept at 0° C. The crystals (4.0 g) were removed and the filtrate was evaporated to dryness. The residue, slurried in petroleum ether (65–110° C), was added to a column of alumina (3.5×28 cm) which was then eluted with petroleum ether (700 ml) to remove triphenylmethane (10 g, m.p. 93° C). Elution of the column with methanol (500 ml) and evaporation of the eluate then yielded the syrupy product (14.66 g, 74.5%), $[\alpha]_D^{24}$ −28.5°±0.5° (c, 2.4% in chloroform). Anal: Calc. for $C_{21}H_{26}O_5$: C, 70.37%; H, 7.31%. Found: C, 70.53%; H, 7.10%.

Ethyl 2,3-Di-O-benzyl-5-O-methyl-α-L-arabinoside

Ethyl 2,3-di-O-benzyl-α-L-arabinofuranoside (14 g) was methylated with methyl iodide (125 ml) and silver oxide (19 g). Filtration and evaporation of the filtrate yielded a product which still had hydroxyl absorption in its infrared spectrum. One more methylation yielded a product (14.1 g, 96%) with no hydroxyl absorption in the infrared and having $[\alpha]_D^{24}$ −22.3°±0.5° (c, 2.0% in chloroform). Anal: Calc. for $C_{22}H_{28}O_5$: C, 70.94%; H, 7.58%. Found: C, 71.58%; H, 7.08%.

Ethyl 5-O-Methyl-α-L-arabinoside

Ethyl 2,3-di-O-benzyl-5-O-methyl-α-L-arabinoside (13.0 g) was debenzylated by reduction with sodium in alcohol (24) to yield a syrupy product (4.66 g, 78.5%). Analysis of this product by gas–liquid partition chromatography, column A, 170° C, 300 ml argon/min, showed the presence of one major component (68.9%) and four minor

components. The minor components were undoubtedly partially benzylated products that were soluble in water. Because of this evidence of a mixture, no analyses or measurement of specific rotation were done.

Hydrolysis of Ethyl 5-O-Methyl-α-L-arabinoside

The syrupy glycoside obtained above (2.5 g) was heated with 0.05 N sulphuric acid (50 ml) at 100° C and the hydrolysis was followed by gas–liquid partition chromatography using the conditions just described for examination of the products from debenzylation. The glycosides gradually disappeared and none could be detected after 2 hours of hydrolysis. The hydrolyzate was neutralized with barium carbonate, filtered, and the filtrate was evaporated to dryness yielding a syrup (1.9 g, 91.2%). Paper chromatography of this material showed the presence of a major component of R_G 0.39 and minor components of R_G values 1.1, 1.0, 0.77, 0.22, and 0.12 (R_G = movement relative to 2,3,4,6-tetra-O-methyl-D-glucose).

Isolation of 5-O-Methyl-L-arabinose

The syrupy mixture from the hydrolysis (1.9 g) was resolved by chromatography on 22 sheets of Whatman No. 3MM paper (46×57 cm) and elution of the appropriate areas yielded the major component (R_G 0.39), which was recovered as a syrup (0.90 g, 47.4%). The yield was corrected for material lost on the guide strips used to locate the sugars.

Dutton et al. (2) reported $[\alpha]_D^{25}$ −32.0° (c, 0.484% in water) for 5-O-methyl-L-arabinose. The sugar isolated in the present work had $[\alpha]_D^{25}$ −25.3°±1.5° (c, 1.0% in water) and a methoxyl content of 18.7%; a mono-O-methyl pentose requires a methoxyl content of 18.9%. On paper chromatography and paper electrophoresis this sugar gave R_G, R_F, and M_G values of 0.39, 0.32, and 0.74 respectively. Gas–liquid partition chromatography of a methanolyzate of this compound on column B showed only two peaks, which corresponded to the anomeric glycosides of 5-O-methyl-L-arabinose. These results show that 5-O-methyl-L-arabinose is readily purified by chromatography on cellulose despite the apparent difficulties, referred to in the discussion, in obtaining pure samples of arabinose methyl ethers by that procedure.

Methylation of 5-O-Methyl-L-arabinose

The mono-O-methyl pentose (ca. 2 mg) was heated at 100° C in a sealed tube with 2% methanolic hydrogen chloride (1.0 ml) for 12 hours. Acid was neutralized with silver carbonate, and the filtrate from removal of silver salts was evaporated to a syrup which was shaken overnight with silver oxide (20 mg), methyl iodide (0.2 ml), and dimethyl formamide (0.2 ml) (25). The reaction mixture was examined by gas–liquid partition chromatography using column B, 200° C, 85 ml argon/min. Two components were found, in the methylation reaction, with retention volumes (V_R), which were made relative to methyl 2,3,5-tri-O-methyl-α-L-arabinoside, of 1.00 and 1.28 corresponding to the α- and β-methyl glycosides respectively of 2,3,5-tri-O-methyl-L-arabinose. Under the conditions used, the α- and β-methyl glycosides of 2,3,4-tri-O-methyl-L-arabinose ran as one component with V_R = 1.75 and none was found in the methylated product.

5-O-Methyl-L-arabonolactone

A mixture of 5-O-methyl-L-arabinose (300 mg), water (3 ml), barium carbonate (300 mg), and bromine (30 drops) was kept in the dark at room temperature for 70 hours. Bromine was removed by aeration and the aqueous solution was extracted continuously with chloroform for 5 days. The lactone crystallized from the chloroform solution and

evaporation of the solution left more of the lactone as a crystalline residue. Recrystallization from ethanol – petroleum ether (30–60° C) yielded 5-O-methyl-L-arabonolactone (170 mg), m.p. 137–138° C; $[\alpha]_D^{25}$ $-79.1°\pm1°$ → $-71.3°\pm1°$, 6 days incomplete (c, 1.0% in water); ν_{max}^{Nujol} 1773 cm^{-1}. Reported (2) values are m.p. 135° C, $[\alpha]_D^{25}$ $-76.2°$ (c, 0.22% in water). Anal: Calc. for $C_6H_{10}O_5$: C, 44.44%; H, 6.22%; OCH$_3$, 19.3%. Found: C, 44.12%; H, 5.99%; OCH$_3$, 19.1%.

5-O-Methyl-L-arabonamide

5-O-Methyl-L-arabonolactone (50 mg) was dissolved in saturated methanolic ammonia and stored at 5° C for 20 hours. Evaporation of the solution and recrystallization from ethanol–ether yielded the amide, m.p. 141–143° C, $[\alpha]_D^{25}$ $+40.7°\pm2°$ (c, 0.8% in methanol). Anal: Calc. for $C_6H_{13}O_5N$: C, 40.22%; H, 7.31%; N, 7.82%. Found: C, 39.98%; H, 7.09%; N, 7.76%.

A portion of the amide (ca. 5 mg) was oxidized with sodium hypochlorite and on addition of semicarbazide hydrochloride (13) gave a white precipitate of hydrazodicarbonamide.

5-O-Methyl-L-arabonic Acid Phenylhydrazide

5-O-Methyl-L-arabonolactone (40 mg) was dissolved in methanol (3 ml), and freshly distilled phenylhydrazine (30 mg) was added. The solution was refluxed for 3 hours and then evaporated to a syrup which crystallized from ethanol–ether to give the phenylhydrazide, m.p. 176.5–178° C, $[\alpha]_D^{25}$ $+23.6°\pm3°$ (c, 0.38% in methanol). Anal: Calc. for $C_{12}H_{18}O_5N_2$: N, 10.37%. Found: N, 10.58%.

5-O-Methyl-L-arabinose Phenylosazone

A mixture of 5-O-methyl-L-arabinose (50 mg), 20% acetic acid (3 ml), sodium bisulphite (50 mg), and phenylhydrazine (0.5 ml) was heated for 1 hour at 80° C and was then left for 24 hours at room temperature. The yellow, crystalline precipitate (25 mg) was recrystallized from aqueous acetone to give 5-O-methyl-L-arabinose phenylosazone, m.p. 153–155° C, $[\alpha]_D^{25}$ $+3°\pm1°$ (c, 0.97% in methanol). Reported (2) values are m.p. 154.5° C, $[\alpha]_D^{25}$ $-16.6°$ (c, 0.4% in methanol). Anal: Calc. for $C_{18}H_{22}O_3N_4$: C, 63.14%; H, 6.48%; N, 16.4%; OCH$_3$, 9.05%. Found: C, 63.08%; H, 6.51%; N, 16.57%; OCH$_3$, 9.11%.

Periodate Oxidation of 5-O-Methyl-L-arabinose

5-O-Methyl-L-arabinose (90 mg) was dissolved in 0.10 M sodium metaperiodate (20 ml) and the solution was stored in the dark at room temperature for 24 hours. The solution was then distilled and to the distillate was added an aliquot (4 ml) of a solution of p-nitrophenylhydrazine (0.4 g) in water (25 ml) and concentrated hydrochloric acid (0.4 ml) (15). The dense yellow precipitate was filtered after 5 minutes and recrystallized from ethanol:water (2:3) to yield methoxyacetaldehyde-p-nitrophenylhydrazone, m.p. 114–116° C. Reported (15, 16) values are m.p. 116° C and 115–115.5° C. Anal: Calc. for $C_9H_{11}O_3N_3$: C, 51.67%; H, 5.30%; N, 20.09%. Found: C, 51.30%; H, 5.39%; N, 19.95%.

Periodate Oxidation of Methyl 5-O-Methyl-(α,β)-L-arabinoside

5-O-Methyl-L-arabinose (40 mg) was refluxed with 2% methanolic hydrogen chloride (3 ml) for 6 hours. The solution was neutralized with silver carbonate, filtered, and the filtrate was evaporated to a syrup. The syrup (33.7 mg) was oxidized in aqueous solution (25 ml) containing 0.3 M sodium metaperiodate (10 ml); a blank was run concurrently. The consumption of periodate, estimated by the arsenite method (26), was 0.96 mole

per mole of glycoside, constant after 24 hours. No formic acid or formaldehyde could be detected.

REFERENCES

1. G. A. ADAMS. Can. J. Chem. **33**, 56 (1955).
2. G. G. S. DUTTON, Y. TANAKA, and K. YATES. Can. J. Chem. **37**, 1955 (1959).
3. A. P. DOERSCHUK. J. Am. Chem. Soc. **74**, 4202 (1952).
4. W. N. HAWORTH, E. L. HIRST, and E. G. TEECE. J. Chem. Soc. 2858 (1931).
5. R. L. WHISTLER and S. J. KAZENIAC. J. Am. Chem. Soc. **76**, 5812 (1954).
6. H. O. BOUVENG, B. LINDBERG, and O. THEANDER. Acta Chem. Scand. **11**, 1788 (1957).
7. R. U. LEMIEUX and H. F. BAUER. Can. J. Chem. **32**, 362 (1954).
8. G. A. ADAMS and C. T. BISHOP. Can. J. Chem. **38**, 2380 (1960).
9. A. G. MCINNES, D. H. BALL, F. P. COOPER, and C. T. BISHOP. J. Chromatog. **1**, 556 (1958).
10. C. T. BISHOP and F. P. COOPER. Can. J. Chem. **38**, 388 (1960).
11. S. A. BARKER, E. J. BOURNE, R. M. PINHARD, and D. H. WHIFFEN. Chem. & Ind. (London), 658 (1958).
12. I. R. SIDDIQUI and G. A. ADAMS. Can. J. Chem. **38**, 2029 (1960).
13. R. A. WEERMAN. Rec. trav. chim. **37**, 16 (1917).
14. A. B. FOSTER. Advances in Carbohydrate Chem. **12**, 81 (1957).
15. J. K. HAMILTON, G. W. HUFFMAN, and F. SMITH. J. Am. Chem. Soc. **81**, 2173 (1959).
16. N. L. DRAKE, H. M. DUVALL, T. L. JACOBS, H. T. THOMPSON, and H. M. SONNICHSEN. J. Am. Chem. Soc. **60**, 73 (1938).
17. E. L. HIRST and J. K. N. JONES. J. Chem. Soc. 1659 (1949).
18. J. M. BOBBITT. Advances in Carbohydrate Chem. **11**, 1 (1956).
19. L. HOUGH, J. K. N. JONES, and W. H. WADMAN. J. Chem. Soc. 1702 (1950).
20. J. W. GREEN and E. PACSU. J. Am. Chem. Soc. **60**, 2056 (1938).
21. B. HELFERICH and J. BECKER. Ann. **440**, 1 (1924).
22. F. J. BATES and ASSOCIATES. Polarimetry, saccharimetry and the sugars. Circ. Natl. Bur. Standards C440, U.S. Govt. Printing Office, Washington. 1942. p. 512.
23. J. C. DENNISON and D. I. McGILVRAY. J. Chem. Soc. 1616 (1951).
24. K. FREUDENBERG and E. PLANKENHORN. Ann. **536**, 257 (1938).
25. R. KUHN, H. TRISCHMANN, and I. LÖW. Angew. Chem. **67**, 32 (1955).
26. P. P. FLEURY and J. LANGE. J. pharm. chim. **17**, 107 (1933).

THE REACTION OF NITROGEN ATOMS WITH OXYGEN ATOMS
IN THE ABSENCE OF OXYGEN MOLECULES[1]

C. Mavroyannis[2] and C. A. Winkler

ABSTRACT

The reaction has been studied in a fast-flow system by introducing nitric oxide in the gas stream with excess active nitrogen. The nitrogen atom consumption was determined by titrating active nitrogen with nitric oxide at different positions along the reaction tube. The rate constant is found to be $k_1 = 1.83 \, (\pm 0.2) \times 10^{16} \, cc^2 \, mole^{-2} \, sec^{-1}$ at pressures of 3, 3.5, and 4 mm, and with an unheated reaction tube.

The homogeneous and surface decay of nitrogen atoms involved in the above system were studied using the nitric oxide titration method, and the rate constants were found to be $k_3 = 1.04 \pm 0.17 \times 10^{16} \, cc^2 \, mole^{-2} \, sec^{-1}$, and $k_4 = 2.5 \pm 0.2 \, sec^{-1} \, (\gamma = 7.5 \pm 0.6 \times 10^{-6})$, respectively, over the range of pressures from 0.5 to 4 mm with an unheated reaction tube.

INTRODUCTION

The emission spectrum of the blue nitric oxide afterglow has been studied recently by Kaplan and his associates (1). From the sensitivity of its vibrational intensity distribution to the addition of helium, it has been postulated that the spectrum arises from the three-body recombination of a ground-state oxygen atom and a ground-state nitrogen atom, by way of some intermediate state, into the excited upper states of the beta, gamma, and infrared bands,

$$N(^4S) + O(^3P) + He \rightarrow NO \, (\text{intermediate}) + He \rightarrow NO(A^2\Sigma, B^2\Pi) + He.$$
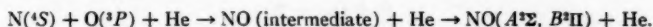
The lifetime of the intermediate, relative to the duration of the collision, is not known. Kaufman and Kelso (2) have obtained support for the above mechanism.

In the present paper, the kinetic characteristics of the reaction between nitrogen atoms and oxygen atoms have been studied, using a fast-flowing system.

EXPERIMENTAL

Active nitrogen was produced by a microwave generator. A quartz tube of 12-mm i.d., and 10 cm long, was used as a discharge tube, and the reaction vessel consisted of a pyrex tube of 20-mm i.d., and 30 cm long. Nitrogen (>99.9% pure) was passed into the discharge tube through a liquid-air trap to remove water, while purified nitric oxide was passed into the reaction tube through small jets, located at four different points along the reaction tube.

Oxygen atoms were produced by addition of nitric oxide at the first jet, to an excess of active nitrogen, at pressures of 3, 3.5, and 4 mm and with an unheated reaction tube. The nitrogen atom consumption, after the first jet, was determined by titrating active nitrogen with nitric oxide (2, 3) at subsequent jet positions along the reaction tube.

The same procedure was used to study the homogeneous and surface decay of nitrogen atoms, that is, the disappearance of nitrogen atoms along the reaction tube was determined by titration with nitric oxide at the different jet positions.
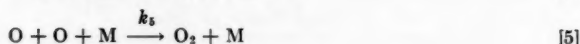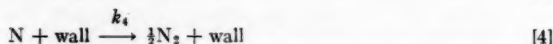
RESULTS AND DISCUSSION

The following reactions may be involved:

$$N + O + M \xrightarrow{k_1} NO + M \tag{1}$$

$$NO + N \xrightarrow{k_2} N_2 + O \tag{2}$$

$$N + N + M \xrightarrow{k_3} N_2 + M \tag{3}$$

$$N + \text{wall} \xrightarrow{k_4} \tfrac{1}{2}N_2 + \text{wall} \tag{4}$$

$$O + O + M \xrightarrow{k_5} O_2 + M \tag{5}$$

$$O + \text{wall} \xrightarrow{k_6} \tfrac{1}{2}O_2 + \text{wall}. \tag{6}$$

The reaction

$$NO + O + M \to NO_2 + M \tag{7}$$

was not taken into account, since NO_2 would react rapidly with oxygen atoms to produce NO (4) and, moreover, reaction [2] is very fast (5) in comparison with reaction [7]. Since the system was free from O_2, except for small amounts formed by reactions [5] and [6], it was assumed that there would be negligible influence from the reactions

$$O + O_2 + M \to O_3 + M \tag{8}$$

$$O + O_3 \to 2O_2 \tag{9}$$

$$N + O_2 \to NO + O. \tag{10}$$

The disappearance of nitrogen atoms in reactions [1] to [4] is given by

$$\frac{-d(N)}{dt} = 2k_1(N)(O)(M) + k_3(N)^2(M) + k_4(N)$$

and

$$k_1 = k_5 \frac{\log \dfrac{(N)_{t_1}}{(N)_{t_2}} - \dfrac{k_4 \Delta t}{2.303} - \log\left[1 + \dfrac{k_3(M)(N)_{t_1}}{k_4}(1 - e^{-k_4 \Delta t})\right]}{\log\left[1 + \dfrac{2k_5(M)(O)_{t_1}}{k_6}(1 - e^{-k_6 \Delta t})\right]}.$$

The rate constant for reaction [5] was assumed to be $k_5 = 1.6 \times 10^{15}$ cc^2 mole^{-2} sec^{-1}, with $\gamma = 1.65 \times 10^{-5}$ (6) which, for the conditions used, corresponds to a value of $k_6 = 0.516$ sec^{-1}. Several values of k_3 and k_4 have been reported; the value of k_4 in particular presumably depends on the condition of the wall of the reaction vessel used. Reinvestigation of reactions [3] and [4], with the procedure described above, gave the results shown in Fig. 1, on the assumption that only homogeneous decay of nitrogen atoms occurred, i.e. that the rate constant, over the pressure range 0.5 to 4 mm, is given by

$$k_3 = \frac{1}{(M)\Delta t}\left[\frac{1}{(N)_{t_2}} - \frac{1}{(N)_{t_1}}\right]. \tag{11}$$

The data indicate that the value of k_3 decreases as the pressure is increased up to about 2.5 mm, then remains essentially constant with further increase of pressure. Hence, the
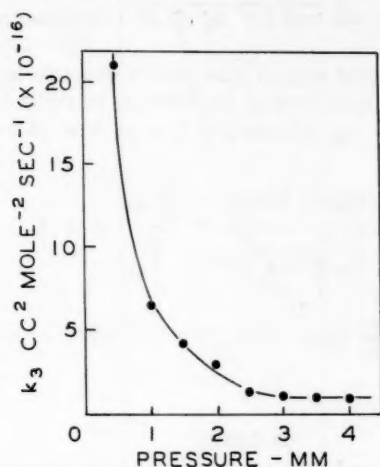
FIG. 1.

surface decay of nitrogen atoms is practically negligible at pressures above about 2.5 mm. A typical plot of $1/((N)_t(M))$ against reaction time at 2.5 mm pressure yields a straight line (Fig. 2).
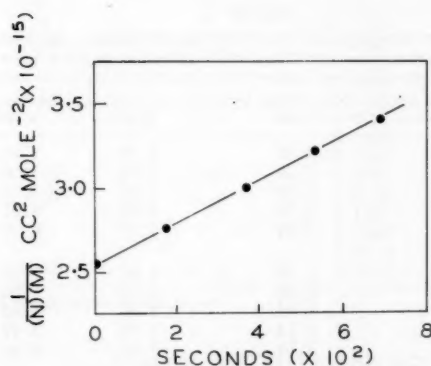

FIG. 2.

To separate the homogeneous and surface decay of nitrogen atoms, plots were made of $\ln (N)$ against time. Approximately straight lines were obtained, the slopes of which depended, of course, on (M). The average slopes of these lines are plotted against (M) in Fig. 3. For pressures of 2.5 mm and above, an extrapolation of the line passes through zero, indicating the small effect of the surface decay at these pressures. For pressures lower than 2.5 mm, an extrapolation gives an intersection corresponding to $k_4 = 2.5 \pm 0.2$ sec^{-1}. The recombination coefficient is given (7) by $\gamma = (2rk_4)/\bar{c}$, where r is the radius of the reaction vessel and $\bar{c}$ is the root mean square atomic velocity, and is found to be $\gamma = (7.5 \pm 0.6) \times 10^{-5}$. The value of γ, and that of k_3 (Table I), are in good agreement
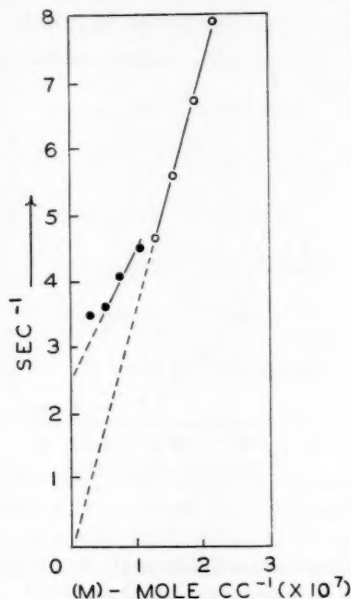
FIG. 3.

TABLE I

Variation of k_3 (from equation [11]) as a function of pressure, reaction time, and
initial reactant concentrations with unheated reaction tube

Total pressure (mm)	(M) (mole/cc) $\times 10^7$	(N)$_{t_1}$ (mole/cc) $\times 10^9$	(N)$_{t_2}$ (mole/cc) $\times 10^9$	t (sec) $\times 10^2$	k_3 (cc^2 mole^{-2} sec^{-1}) $\times 10^{-16}$
2.5	1.34	2.95	2.70	1.80	1.25
,,	,,	2.70	2.50	1.90	1.29
,,	,,	2.95	2.50	3.70	1.20
,,	,,	2.95	2.32	5.35	1.26
,,	,,	2.95	2.20	6.90	1.24
					Average 1.25
3.0	1.6	3.10	2.85	1.50	1.24
,,	,,	3.40	3.10	1.60	1.00
,,	,,	3.74	3.40	1.82	0.93
,,	,,	3.74	3.10	3.42	0.95
,,	,,	3.74	2.85	4.92	1.05
					Average 1.00
3.5	1.87	3.38	3.05	1.48	1.12
,,	,,	3.72	3.38	1.57	0.94
,,	,,	4.25	3.72	1.82	1.00
,,	,,	4.25	3.38	3.39	0.96
,,	,,	4.25	3.05	4.87	1.00
					Average 1.00
4.0	2.15	3.95	3.50	1.50	0.94
,,	,,	4.48	3.95	1.60	0.88
,,	,,	5.20	4.48	1.80	0.86
,,	,,	4.48	3.50	3.10	0.90
,,	,,	5.20	3.95	3.40	0.86
,,	,,	5.20	3.50	4.90	0.87
					Average 0.90

NOTE: Average $k_3 = 1.04$ (± 0.17) $\times 10^{16}$ cc^2 mole^{-2} sec^{-1} (this value is for the disappearance of *two* N atoms). t_1 refers to zero time.

with those of other investigators (8, 9, 10, 11) but not with those previously reported from this laboratory (12, 13).

Since the reaction of nitrogen atoms with oxygen atoms was studied at pressures of 3, 3.5, and 4 mm, the effect of reaction [4] is very small, and has been neglected. The integrated equation for k_1, with $k_4 = 0$, is given by

$$k_1 = k_5 \frac{\log \dfrac{(N)_{t_1}}{(N)_{t_2}} - \log (1 + k_3(M)(N)_{t_1}\Delta t)}{\log \left[1 + \dfrac{2k_5(M)(O)_{t_1}}{k_6}(1 - e^{-k_6\Delta t})\right]}. \tag{12}$$

The results are shown in Table II, with an average value of $k_1 = 1.83(\pm 0.2) \times 10^{15}$ cc^2 $mole^{-2}$ sec^{-1}.

TABLE II

Rate constants for the reaction of nitrogen atoms with oxygen atoms
at various pressures with unheated reaction tube

Total pressure (mm)	$(N)_{t_1}$ (mole/cc) $\times 10^9$	$(O)_t$ (mole/cc) $\times 10^9$	$\log \dfrac{(N)_{t_1}}{(N)_{t_2}}$	t (sec) $\times 10^2$	k_1 (cc^2 $mole^{-2}$ sec^{-1}) $\times 10^{-15}$
3.0	1.47	2.30	0.0701	4.35	1.80
,,	,,	,,	0.0962	6.30	1.75
,,	1.22	2.56	0.0375	2.10	1.85
,,	,,	,,	0.0632	4.35	1.65
,,	,,	,,	0.1239	8.12	2.00
,,	1.15	2.63	0.0555	4.35	1.70
,,	,,	,,	0.0767	6.30	1.60
,,	,,	,,	0.0989	8.12	1.52
3.5	1.58	2.67	0.0457	2.15	1.92
,,	,,	,,	0.0937	4.40	2.03
,,	,,	,,	0.1335	6.40	2.00
,,	,,	,,	0.1659	8.24	1.95
4.0	2.60	2.60	0.0681	2.15	1.70
,,	2.46	2.74	0.0708	2.15	2.15
,,	,,	,,	0.1326	4.40	1.80
,,	,,	,,	0.1844	6.40	1.75
,,	,,	,,	0.2459	8.25	2.05
,,	0.86	4.34	0.1645	8.25	1.70

NOTE: Average $k_1 = 1.83$ (± 0.2) $\times 10^{15}$ cc^2 $mole^{-2}$ sec^{-1}.

COMPARISON WITH THEORY

Using the hard sphere collision model, and assuming the reaction scheme to be

$$N + O \underset{k_{-1}'}{\overset{k_1'}{\rightleftarrows}} NO^*$$

$$NO^* + M \xrightarrow{k_2'} NO + M,$$
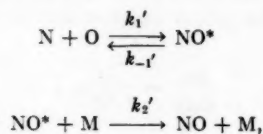
the stationary concentration of the binary complex NO* may be taken approximately as $(NO)^* = Z_{N.O}\tau_{NO}(N)(O)$, where $Z_{N.O}$ is the collision frequency of N and O, and τ_{NO} is the mean lifetime of the complex NO*.

The over-all rate is

$$\frac{d(\text{products})}{dt} = k_1(\text{N})(\text{O})(\text{M}) = k_2'(\text{M})(\text{NO}^*)$$

$$= k_2'(\text{M})(\text{N})(\text{O})Z_{\text{N.O}}\tau_{\text{NO}}$$

from which, by substituting $k_2' = PZ_{\text{NO}^*.\text{M}}e^{-E_2/RT}$, the experimental specific rate constant may be written as $k_{\text{exp}} = PZ_{\text{NO}^*.\text{M}}\tau_{\text{NO}}e^{-E_2/RT}$; τ_{NO} is the reciprocal of a unimolecular rate constant, and it should be about 10^{-13} sec, if we neglect activation energy. If there is any activation energy, it may be absorbed in the exponential term, thus, $Z_{\text{ter}} = Z_{\text{NO}^*.\text{M}}Z_{\text{N.O}}\tau_{\text{NO}}$. The collision frequencies can be calculated, assuming collision diameters of 3.5, 3.75, 2.95, and 1.8×10^{-8} cm for NO, $(\text{M}) = \text{N}_2$, N, and O respectively. For $T = 300°$ K, $Z_{\text{ter}} = 1.65 \times 10^{15}$ cc^2 mole^{-2} sec^{-1}.

The calculated value of Z_{ter} is in good agreement with that given experimentally by $k_1 = 1.83 \ (\pm 0.2) \times 10^{15}$ cc^2 mole^{-2} sec^{-1}.

Wigner (14) has developed an expression which gives an upper limit for the rate of association reactions, by determining the probability of decrease of the relative energy of the two atoms below zero, under the influence of a third body. For the atomic reaction $A_1 + A_2 + A_3 \rightarrow A_1A_2 + A_3$ the rate constant is given by

$$k' = -2\pi \frac{g_{12}}{g_1g_2}\left(\frac{2\pi m_r}{kT}\right)^{1/2} \int_{V_0<0} V_0 q_{12} \left[(a_{13}{}^2 - a_{23}{}^2)(a_{13}/m_1 - a_{23}/m_2)\right. \qquad [13]$$

$$\left. + 2(a_{13}{}^2/m_1 + a_{23}{}^2/m_2)q_{12} + (a_{13}/m_1 + a_{23}/m_2)q_{12}{}^2\right]dq_{12}$$

where k' is the rate constant, k the Boltzmann constant; V_0 is the relative potential energy of the atoms A_1 and A_2 for infinite separation of A_3; m_r, m_1, m_2 are the reduced mass and the masses of A_1 and A_2; g_{12}, g_1, and g_2 are the statistical weight factors of A_1A_2, A_1, and A_2; q_{12} is the separation of the atoms A_1 and A_2; a_{13} and a_{23} are the sum of the collision radii of A_1A_3, and A_2A_3 respectively. The term $T^{-\frac{1}{2}}$ will cause a small fall-off in rate with increasing temperature.

For V_0, the Hulburt–Hirschfelder (15) potential energy curve was used, given by the equation

$$V(r) = 6.609[(1-e^{-x})^2 + 0.0678x^3(1+2.663x)e^{-2x} - 1] \text{ ev,}$$

where $x = 3.1579 \ (r-r_e)/r_e$, $V(\infty) = 0$, and $r_e = 1.1508$ Å, which, according to Vanderslice (16), fits better than a Morse curve for the $X^2\Pi$ state of NO. The adopted radii were 0.89 (17), 1.49, and 1.875 Å (derived from viscosity data) for O, N, and N_2 respectively. The ratio of the statistical weights may be taken as

$$\frac{g_{\text{NO}}}{g_{\text{N}}g_{\text{O}}} = \frac{3.1}{4 \times 8.7},$$

taking into account the separation of the levels. The final result, for $T = 300°$ K, is $k' = 3.4 \times 10^{16}$ cc^2 mole^{-2} sec^{-1}. The agreement between the observed and calculated value might be taken as satisfactory, since equation [13] gives an upper limit for the reaction rate, when only atoms are involved.

REFERENCES

1. C. A. BARTH, W. J. SCHADE, and J. KAPLAN. J. Chem. Phys. **30**, 347 (1959).
2. F. KAUFMAN and J. R. KELSO. J. Chem. Phys. **27**, 1209 (1957).
3. G. B. KISTIAKOWSKY and G. G. VOLPI. J. Chem. Phys. **27**, 1141 (1957).
4. H. W. FORD and N. ENDOW. J. Chem. Phys. **27**, 1156 (1957).
5. G. B. KISTIAKOWSKY and G. C. VOLPI. J. Chem. Phys. **28**, 665 (1958).
6. J. E. MORGAN, L. ELIAS, and H. I. SCHIFF. J. Phys. Chem. **33**, 930 (1960).
7. K. E. SCHULER and K. J. LAIDLER. J. Chem. Phys. **17**, 1212 (1949).
8. G. G. MANELLA, R. R. REAVES, and P. HARTECK. J. Chem. Phys. **29**, 608 (1958).
9. J. HERRON, J. L. FRANKLIN, P. BRADT, and V. H. DIBELER. J. Chem. Phys. **29**, 230 (1958).
10. T. WENTINK, JR., J. O. SULLIVAN, and K. L. WRAY. J. Chem. Phys. **29**, 231 (1958).
11. J. HERRON, S. L. FRANKLIN, P. BRADT, and V. H. DIBELER. J. Chem. Phys. **30**, 879 (1959).
12. R. KELLY and C. A. WINKLER. Can. J. Chem. **37**, 62 (1959).
13. R. BACK, W. DUTTON, and C. A. WINKLER. Can. J. Chem. **37**, 2059 (1959).
14. E. WIGNER. J. Chem. Phys. **5**, 720 (1937); Trans. Faraday Soc. **34**, 29 (1938); J. Chem. Phys. **7**, 646 (1939).
15. H. M. HULBURT and J. O. HIRSCHFELDER. J. Chem. Phys. **9**, 61 (1941).
16. J. T. VANDERSLICE, E. A. MASON, and W. G. MAISCH. J. Chem. Phys. **31**, 738 (1959).
17. LANDOLT-BORNSTEINS TABLES. 1st Erganzungsband. p. 69.

HELMINTHOSPORAL, THE TOXIN FROM HELMINTHOSPORIUM SATIVUM
I. ISOLATION AND CHARACTERIZATION[1]

P. de Mayo,[2] E. Y. Spencer,[3] and Robert W. White[3]

ABSTRACT

The toxin produced by *Helminthosporium sativum* P.K. and B.[4] has been isolated in crystalline form. It has the formula $C_{15}H_{22}O_2$ and has been shown to contain one saturated aldehyde function, one α,β-unsaturated aldehyde, and two carbocyclic rings.

The significance of toxins as agents in plant pathology is now generally recognized, and these substances may be of considerable economic significance. *Helminthosporium sativum*[4] is a fungus which produces a seedling blight, foot and root rot, head blight, and leaf spot of cereals and grasses. The disease is widespread in North America and elsewhere and in particular affects wheat and barley crops. It has been estimated that the loss of the wheat crops in Western Canada caused by the action of this fungus has ranged from 3 to 13% during the past 25 years (2); an estimated loss of the order of $50,000,000.00.

Recently Ludwig (3) has demonstrated that the action of the fungus is dependent on the presence of a toxin produced by the fungus. Means were found for the artificial growth of the fungus, and the cell-free culture filtrates were able to produce many of the general symptoms characteristic of seedling blight, the degree of damage being related directly to the dosage. However, the combined action of spore suspensions, themselves reported innocuous (3), and culture filtrate resulted in the plants becoming diseased and the plants generally died. Ludwig concluded that the nonspecific toxin predisposed the plants to invasion of the organism.

For the preparation of the toxin on a large scale, the fungus was grown (see Experimental) in a 25-gal jacketed fermenter on sucrose–potato infusion. The culture filtrate was then stirred with charcoal upon which the active principle was absorbed. It was eluted with chloroform, and after filtration through alumina it was then distilled at low pressure. The distillate crystallized, and was purified by recrystallization.

The substance so obtained, helminthosporal, showed characteristic absorptions in the ultraviolet (λ_{max} 266 mμ) and infrared (ν_{max} 1715 and 1685 cm^{-1}). The original crude toxin concentrate before heat treatment either did not show these bands or (in certain batches where perhaps inadvertent heating had occurred) they were present but very weak, but, weight for weight, showed essentially the same biological activity. It would seem, therefore, that helminthosporal exists in the fungus as a precursor, from which it is formed by the fungus. This change can also be effected by heat, acid or base.

Helminthosporal analyzed in accordance with the empirical formula $C_{15}H_{22}O_2$. It is unstable to air, even at low temperature, and at room temperature takes up oxygen in a quantity equivalent to half an atom in 5 days. The presence of two bands in the carbonyl region of the infrared at 1715 and 1685 cm^{-1} suggested that these accounted for both oxygen atoms. This was supported indirectly by the absence of any bands in the infrared attributable to hydroxyl or ether groupings. It was demonstrated directly by the preparation of a bis oxime.

The ultraviolet absorption spectrum indicated the presence of conjugation of some sort. That this was due to conjugation of a double bond with one or both of the carbonyl functions and was not to be attributed to a diene system was shown by reduction of helminthosporal with lithium aluminum hydride to the glycol, the latter being characterized as the crystalline bis-3,5-dinitrobenzoate. The glycol showed no high-intensity absorption in the ultraviolet above 210 mμ.
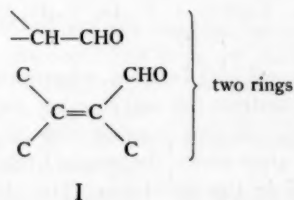
A band in the infrared at 2720 cm^{-1} was suggestive of the presence of an aldehyde. That this was so was shown directly by oxidation of helminthosporal with alkaline silver oxide in good yield to the corresponding monoacid, further characterized as the acid oxime. The acid showed bands in the infrared at 1705 and 1670 cm^{-1}, indicating that the conjugated carbonyl had not been affected. This was confirmed by the fact that the ultraviolet absorption (λ_{max} 265 mμ) was also essentially unchanged.

Attempts at further oxidation, of the remaining carbonyl group, led to intractable material, and a decision between an (second) aldehyde and a ketone function was arrived at by two methods. First, although the presence of a carboxyl group obscured the 2750 cm^{-1} region and rendered the C—H aldehyde stretch undetectable, there was present in the near infrared a band at 4480 cm^{-1} characteristic of aldehydes and very strongly suggestive of a conjugated aldehyde (4).

Secondly, the proton resonance spectrum of helminthosporal (in CCl$_4$) showed a singlet equivalent to one hydrogen at $\tau = 0.1$ and a doublet, also equivalent to one hydrogen at $\tau = 0.5$ ($J \sim 4$ c.p.s.). In the corresponding monoacid the doublet was replaced by a singlet at $\tau = 1.48$ (carboxyl hydrogen), the singlet being unaffected. This provided strong evidence that the remaining carbonyl was aldehydic, and this was confirmed by the spectrum of the derived oxime in which the singlet at $\tau = 0.1$ had been replaced by a singlet at $\tau = 1.93$ in accord with expectance for the grouping —CH=N·OH (5).

Of the five double-bond equivalents indicated by the empirical formula of helminthosporal and its derivatives, three have been accounted for as two carbonyl groups and a double bond. The latter is required to be tetrasubstituted since no bands attributable to vinyl hydrogen appear in the N.M.R. spectrum of helminthosporal or any of its simple derivatives. This was confirmed by the fact that the bis-3,5-dinitrobenzoate already referred to reacted with one molecule of osmium tetroxide to give a tetraol bis-3,5-dinitrobenzoate which was recovered unchanged on attempted acetylation.

That no other tetrasubstituted double bond was present was shown as follows. Reduction of the aldehyde acid with sodium borohydride gave, directly, a lactone. This reacted with one molecule of osmium tetroxide to give a diol which was optically transparent in the ultraviolet above 200 mμ. It must therefore be concluded that helminthosporal contains two carbocyclic rings. This, together with the observation that the band at $\tau = 0.5$ in helminthosporal is a doublet, allow the functions of this substance to be expressed as in I.

$$\begin{array}{c} \diagdown \\ -\text{CH}-\text{CHO} \\ \text{C} \diagdown \qquad \text{CHO} \\ \text{C}=\text{C} \\ \text{C} \diagup \qquad \diagdown \text{C} \end{array} \quad \Bigg\} \ \text{two rings}$$

I

The results of the further work in progress will be reported in due course.

EXPERIMENTAL

Infrared spectra and nuclear magnetic resonance spectra were determined in carbon tetrachloride solution, ultraviolet spectra in ethanol, and optical rotations in chloroform unless otherwise stated. Light petroleum refers to the fraction of b.p. 35–60°. Melting points were taken on the Köfler hot stage.

The N.M.R. spectra were determined in ca. 10% w/v solution with 1% tetramethylsilane using a Varian V-4302 spectrometer. The peak positions were determined using an audio oscillator calibrated with a Hewlett Packard 522-B frequency counter.

Isolation

The same strain of *H. sativum* as used earlier (3) was employed in the production of toxin for isolation and characterization studies. Inoculum for the fermenter tank was prepared by inoculating four 500-ml Erlenmeyer flasks, each containing 150 ml of medium (prepared from 100 ml infusion of 100 g potatoes and 10 g sucrose) with 5 ml of spore suspensions from agar slants of the fungus and incubating the cultures at 27° C on a shaker for 3 to 5 days. The inoculum was then transferred aseptically to 8 l. of sterilized medium similar to the above. The suspension was aerated at room temperature for 3 to $3\frac{1}{2}$ days. This was then used to inoculate 100 l. of a sterilized infusion from 5000 g potatoes and 1500 g sucrose in a 35-gal jacketed fermenter. Aeration with stirring was continued for $3\frac{1}{2}$ days followed by separation of the mycelium from the culture filtrate in a Tolhurst basket centrifuge. The filtrate was adjusted to pH 2 and activated charcoal (Nuchar C 145-A; 400 g) was added and stirred. The charcoal with the absorbed toxin was separated from the liquid in a Tolhurst centrifuge and suspended in ethanol (1500 ml). After filtering on a Buchner funnel the charcoal cake was suspended in chloroform (1200 ml), stirred, and filtered. This process was repeated three times. The chloroform extracts were combined and the solvent removed *in vacuo* to yield between 25 and 35 g of crude extract.

The oil (58 g) was heated under nitrogen at 120° for 12 hours. During this time small amounts of water, ethanol, and chloroform were lost, leaving a residue of 47 g which was dissolved in light petroleum (b.p. 60–80°, 150 ml) and applied to a column of alumina (Merck, acid-washed; 400 g). Elution with the same solvent (4 l.) gave a trace (100 mg) of oil. Elution with ether (8 l.) gave, after evaporation, a brown oil (38 g). Distillation of this oil (b.p. 115–120/0.015 mm) afforded a yellow oil (18 g) which slowly set. A portion was crystallized twice from light petroleum to give helminthosporal, m.p. 56–59°; $[\alpha]_D$ −49° (*c*, 1.18); λ_{max} 266 mμ (ϵ 11,000); ν_{max} 1715, 1685, and 1618 (C=C) cm^{-1}. Calc. for $C_{15}H_{22}O_2$: C, 76.88; H, 9.46; C—Me (2), 12.83%; M.W. 234. Found: C, 76.72; H, 9.27; C—Me, 12.56%; M.W. (isopiestic, av.) 232, (Rast, av.) 247 Biological tests showed little difference in activity between the crude distillate and the recrystallized material.

The bis-*oxime* (hydroxylamine hydrochloride – pyridine at room temperature) had m.p. 177–182° (from aq. EtOH). Calc. for $C_{15}H_{24}O_2N_2$: C, 68.15; H, 9.15; N, 10.60%. Found: C, 68.0; H, 8.87; N, 10.69%.

Reduction of Helminthosporal with Lithium Aluminum Hydride

To lithium aluminum hydride (50 mg) in ether (50 ml) was added slowly with stirring a solution of the aldehyde (50 mg) in ether (100 ml) over 30 minutes. The mixture was refluxed for 30 minutes, after which the excess hydride was decomposed with ice water, and the product isolated in the usual way. The glycol was obtained as a colorless oil showing no high-intensity absorption in the ultraviolet above 210 mμ.

The glycol (40 mg) in pyridine (1 ml) containing 3,5-dinitrobenzoyl chloride (230 mg) was allowed to stand for 24 hours. Isolation of the neutral material with ether, followed by washing the ether with 0.5 N HCl, aqueous NaHCO$_3$ and water, successively, gave, after evaporation of the solvent, a yellow semisolid (78 mg). This was percolated in ethyl acetate solution through a short column of alumina, and the solvent evaporated. The product was crystallized from ethanol to give the bis-3,5-dinitrobenzoate (69 mg), m.p. 151–152.5°. Calc. for C$_{29}$H$_{30}$O$_{12}$N$_4$: C, 55.59; H, 4.83%. Found: C, 55.41, 55.66; H, 4.79, 4.72%.

The glycol diester (39 mg) in dioxan (3 ml) solution with osmium tetroxide (38.5 mg) was allowed to stand 5 days. Pyridine (1 ml) was then added and the mixture allowed to stand a further 5 days. Decomposition of the osmic ester with hydrogen sulphide, filtration, followed by concentration gave the tetraol diester as an amorphous powder. Calc. for C$_{29}$H$_{32}$O$_{14}$N$_4$: C, 52.73; H, 4.73%. Found: C, 52.68; H, 4.96%. Attempted acetylation (acetic anhydride – pyridine) gave back material, the infrared spectrum of which was superposable on that of the diester.

Oxidation with Silver Oxide

To the aldehyde (200 mg) in ethanol (8 ml) was added in one portion, a solution of silver nitrate (320 mg) in water (4 ml). The mixture was stirred while sodium hydroxide (113 mg) in water (2 ml) was added dropwise. After completion of the addition the stirring was continued for 2 hours.

After removal of the silver oxide by filtration the solution was diluted with water and neutral material removed by extraction with ether previously used to wash the silver oxide residue. The aqueous phase was then acidified with sulphuric acid (6 N; 5 ml) and the acidic material isolated with ether. Evaporation of the solvent gave a partly solidified oil (203 mg). This was chromatographed on silica gel (6 g). The material eluted with ether:benzene (1:19) was crystallized from light petroleum (b.p. 60–80°) to give the acid, m.p. 127–128°; λ_{max} 265 mμ (ϵ 7000); ν_{max} 1705, 1670 cm^{-1}; $[\alpha]_D$ −64° (c, 1.07). Calc. for C$_{15}$H$_{22}$O$_3$: C, 71.97; H, 8.86%. Found: C, 72.05; H, 8.98%.

The acid (50 mg) was converted into the oxime (hydroxylamine hydrochloride – pyridine). Crystallized from light petroleum (b.p. 60–80°) it had m.p. 142–143°. Calc. for C$_{15}$H$_{23}$O$_3$N: C, 67.89; H, 8.74; N, 5.28%. Found: C, 68.11; H, 8.63; N, 5.47%.

Reduction of the Aldehyde-Acid with Sodium Borohydride

To the monoacid (695 mg) in aqueous ethanol (50%; 200 ml) was added, in portions, sodium borohydride (1.0 g). The mixture was allowed to stand at room temperature with occasional swirling for 2 hours, after which it was acidified with H$_2$SO$_4$ (6 N), allowed to stand 30 minutes, diluted with water (500 ml), and extracted with ether. The ether extracts were then extracted with 5% sodium carbonate solution. This alkaline solution was then acidified with dilute H$_2$SO$_4$, allowed to stand 30 minutes, and again extracted with ether.

This process was repeated four times and the combined neutral material washed with water, dried, and evaporated to dryness. The product thus obtained (539 mg) was crystallized from light petroleum to yield the lactone (459 mg), m.p. 133.5–135°; ϵ_{200} 6000; ν_{max} 3080, 1780, 1615, 905 cm^{-1}; $[\alpha]_D$ +136° (c, 1.14). Calc. for C$_{15}$H$_{22}$O$_2$: C, 76.88; H, 9.46%. Found: C, 77.00; H, 9.46%. The compound showed bands at τ = 4.74 and 5.03 (doublets, $J \sim$ 5 c.p.s.) (exomethylene group).

Ozonolysis in carbon tetrachloride solution at −15° gave formaldehyde, characterized as the dimedone derivative, in 25% yield.

Reaction of the Lactone with Osmium Tetroxide

To the lactone (320 mg), dissolved in ether (2 ml) was added pyridine (0.5 ml) and osmium tetroxide (383 mg). This mixture was kept in the dark at room temperature for 23 days when it was diluted with ethanol and the osmic ester decomposed with hydrogen sulphide. The precipitate was filtered off on Celite and washed thoroughly with ethanol. The combined filtrate and washings were evaporated to dryness to leave an oil which solidified on standing. Chromatography on silica gel (20 g) gave, on elution with ether–benzene (1:19), unchanged lactone (70 mg). Elution with ether–benzene (1:1) gave a product (250 mg) which on crystallization from ether – light petroleum gave the lactone diol (190 mg), m.p. 159–164°; ϵ_{190} <200; ν_{max} 3600, 3500, and 1785 cm^{-1}; $[\alpha]_D$ +64° (c, 1.01). Calc. for $C_{15}H_{24}O_4$: C, 67.13; H, 9.02%. Found: C, 66.97; H, 8.59%.

ACKNOWLEDGMENTS

REFERENCES

1. R. A. SHOEMAKER. Can. J. Botany, **37**, 879 (1959); R. H. BURRAGE and R. D. TINLINE. Can. J. Plant Sci. **40**, 672 (1960).
2. B. J. SALLANS. Can. Plant Disease Survey, **38**, 11 (1958).
3. R. A. LUDWIG. Can. J. Botany, **35**, 291 (1957).
4. J. F. KING, P. DE MAYO, and B. VIG. In preparation.
5. J. B. STOTHERS. Personal communication.

THE REACTION OF BENZOYL CHLORIDE AND ETHYL BENZOATE WITH SOME ALKALI METAL SALTS OF FLUORENE[1]

G. W. H. Scherf and R. K. Brown

ABSTRACT

In hydrocarbon or ether solvents, the sodium or potassium salt of fluorene or of 9-benzoyl-fluorene reacts with an equimolar amount of benzoyl chloride to form 9,1'-benzoyloxybenzyli-denefluorene (I). The reaction of equimolar quantities of the lithium salt of fluorene or of 9-benzoylfluorene and benzoyl chloride in ether solvents gives rise to a mixture of 9,9-dibenzoylfluorene (II) and 9,1'-benzoyloxybenzylidenefluorene (I), but in hydrocarbon solvents produces only 9,9-dibenzoylfluorene (II).
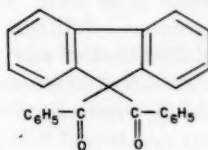
Only 9-benzoylfluorene is isolated from the reactions of the monometal salts of fluorene or of 9-benzoylfluorene with ethyl benzoate.

INTRODUCTION

The dibenzoylation of fluorene at carbon 9 gives rise to two products, the enol ester (I) and the β-diketone (II). The first recorded synthesis of 9,9-dibenzoylfluorene (II) was
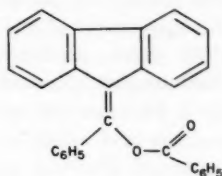
(I)   (II)

that of Schlenk and Bergmann (1, 2), who, from the reaction between 9-fluorenyllithium and benzoyl chloride in benzene, isolated di-(9-fluorenyl)-phenylcarbinol along with a small amount of a compound, m.p. 180°, of unknown structure. This compound, obtained only by painstaking effort, was later identified by Kliegl et al. as the β-diketone (II) (3). Subsequent preparations of II have followed this (4) or similar procedures (5). The enol ester (m.p. 189.5–190°) was first obtained by Kliegl and co-workers (3) from the reaction of benzoyl chloride with 9-fluorenylsodium in ether. The only other product reported from this reaction was unchanged fluorene. No mention was made that 9-benzoylfluorene was obtained as one of the products from the reaction of benzoyl chloride with either 9-fluorenyllithium (1, 2) or 9-fluorenylsodium (3). However, recent work (5) shows that 9-propionyl-fluorene can be prepared in 10% yield by the reaction of 9-fluorenyllithium with propionyl chloride in ether if the reaction is carried out at reflux temperature, whereas at room temperature 9,9-dipropionylfluorene is obtained. The 9-benzoylfluorene can be synthesized quite conveniently by the reaction of fluorene with potassium metal and ethyl benzoate (6, 7).

In view of the finding that the relative amount of mono- and di-alkylation at C_9 of fluorene obtained from the reaction of equimolar quantities of alkyl halide and mono-metalated fluorene depended upon the metal and solvent employed (8), a study was undertaken of the reaction of benzoyl chloride with some of the alkali metal salts of fluorene in ether and in hydrocarbon solvents.

RESULTS

Unless otherwise stated, all experiments involved equimolar proportions of fluorene, metal, and benzoyl chloride or ethyl benzoate in hydrocarbon or ether solvent.

The Reaction of Benzoyl Chloride with 9-Fluorenyl-lithium, -sodium, or -potassium

When 9-fluorenylpotassium (9) was treated at room temperature with benzoyl chloride in either dioxane or diethyl ether, wherein the salt is only partly soluble, the major product consisted of 9,1'-benzoyloxybenzylidenefluorene, I. The expected 9-benzoyl-fluorene was obtained only as a minor product and could be removed quite readily, along with much unreacted fluorene, by boiling the solid reaction product with ethyl alcohol, in which the enol ester is insoluble. The same results were obtained when the solid 9-fluorenylpotassium, freed from dioxane (9), was suspended in pentane and treated with benzoyl chloride. Similar results were obtained when 9-fluorenylpotassium, completely dissolved in dimethoxyethane, or 9-fluorenylsodium dissolved in dimethoxyethane or diethoxyethane (8, 10) was allowed to react with benzoyl chloride.

On the other hand, the reaction of 9-fluorenyllithium and benzoyl chloride gave results quite different from those obtained with the sodium or potassium analogues. Under the heterogeneous conditions obtained in the suspension of the lithium salt in pentane, 9,9-dibenzoylfluorene was produced in 28% yield, uncontaminated by the enol ester (I). The unreacted fluorene, along with a small amount of monobenzoylfluorene, was easily removed by extraction from the insoluble β-diketone (II) with hot ethanol. However, equimolar amounts of 9-fluorenyllithium and the acid halide in diethoxyethane or dimethoxyethane yielded, after removal of unchanged fluorene and some mono-benzoylfluorene, a mixture of 9,9-dibenzoylfluorene and 9,1'-benzoyloxybenzylidene-fluorene. Efforts to separate this mixture were unsuccessful. The infrared spectra obtained for both I and II showed clearly the presence of this mixture.

The infrared spectrum of the enol ester, I, in carbon disulphide showed a strong band at 1738 cm^{-1}, typical of a conjugated ester carbonyl group and a band of medium strength at 1650 cm^{-1} due to the enol double bond (11). The enol ester showed no absorption at 1688 cm^{-1}. The spectrum of the diketone, II, exhibited a strong doublet at 1688 cm^{-1} and 1660 cm^{-1}, but no absorption at 1738 cm^{-1}. The presence of one isomer as an impurity in the other was thus easily detected by the bands at 1738 cm^{-1} and 1688 cm^{-1}. A further distinct difference occurred in the region of aromatic C—H out-of-plane bending frequencies. The β-diketone showed one sharp band of medium intensity at 762 cm^{-1} whereas the enol ester gave two sharp bands, one at 762 cm^{-1}, the other at 775 cm^{-1}.

The spectrum of 9-benzoylfluorene also showed a doublet at 1670 cm^{-1} and 1688 cm^{-1}, though it was not as well resolved as that found for the diketone. In addition, a strong band at 1273 cm^{-1} and a weak band at 1723 cm^{-1} occurred in the spectrum of the mono-benzoylfluorene but not in that of the diketone. The 9-benzoylfluorene is considered to exist in the more stable keto form (12). The double carbonyl band of the keto form of 9-benzoylfluorene is not unusual since this phenomenon has been observed in a number of compounds containing only one carbonyl group (13).

The Reaction of Ethyl Benzoate with 9-Fluorenyl-lithium, -sodium, and -potassium

The reaction of 9-fluorenylpotassium, either in dioxane or in pentane, with ethyl benzoate gave a 40% yield of 9-benzoylfluorene. This is considerably better than the yield of 28% of the monobenzoylated fluorene obtained by Wislicenus and Fehrle (7) from the reaction of fluorene, potassium, and ethyl benzoate mixed in the ratio 1:1:1. The reaction of 9-fluorenyllithium, either partly dissolved in dimethoxyethane or as an

insoluble suspension in pentane, when treated with ethyl benzoate, gave 40–45% of 9-benzoylfluorene. In all cases much fluorene was isolated, but no evidence was found for the formation of the enol ester, I, or the diketone, II.

The Reaction of 9-Benzoyl-9-fluorenyl-lithium, -sodium, or -potassium with Benzoyl Chloride or Ethyl Benzoate

The compound 9-benzoylfluorene was converted readily to the lithium, sodium, or potassium salt, and then brought into reaction with benzoyl chloride or ethyl benzoate. In the ether solvents, dimethoxyethane or diethoxyethane, 9-benzoyl-9-fluorenyllithium and benzoyl chloride produced 55–65% of an inseparable mixture of enol ester and diketone. But when pentane was the solvent, a 54% yield of diketone was obtained, uncontaminated by enol ester. The sodium salt in dimethoxyethane or diethoxyethane, and the potassium salt in dimethoxyethane gave a 50–60% yield of the enol ester uncontaminated by the diketone.

The potassium or sodium salt of 9-benzoylfluorene in dimethoxyethane, reacting with ethyl benzoate, produced only unchanged 9-benzoylfluorene.

DISCUSSION

The results obtained clearly indicate that the following equilibrium occurs in the reaction of 9-fluorenyl-lithium, -sodium, or -potassium with benzoyl chloride in ether or in hydrocarbon solvents and under homogeneous or heterogenous conditions.

M = Li, Na, K
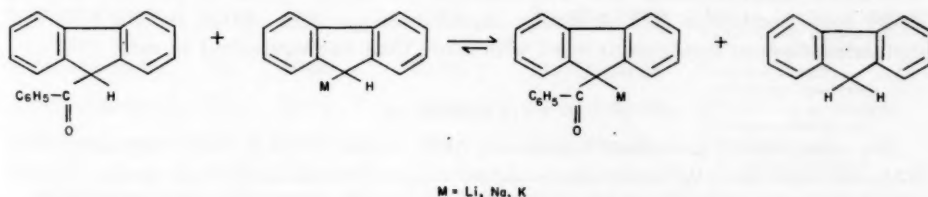
The enhanced acidic character of the remaining hydrogen at C_9 causes 9-benzoylfluorene to react with the remaining monometalated fluorene much more readily than the latter does with the benzoyl chloride.

The sodium and potassium salts of 9-benzoylfluorene will be largely, if not completely, ionic and stabilized by contributing structures A, B, and C. When the reaction with
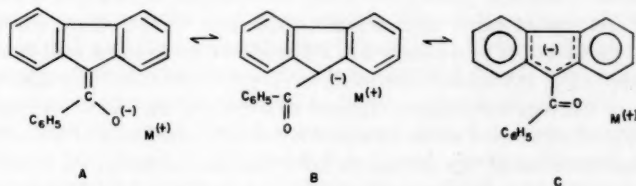
benzoyl chloride occurs, the carbon–metal bond, highly ionic in both hydrocarbon and ether solvents, permits the accumulation of negative charge preferentially on the oxygen atom, the most electronegative atom in the anion. Reaction thus produces the enol ester, I, exclusively.

On the other hand, the carbon–*lithium* bond has considerable covalent character,

especially so in hydrocarbon solvents (14–16). In pentane the attack of benzoyl chloride therefore occurs at the carbon–metal bond directly, yielding only the diketone, II. However, in ether solvents, particularly dimethoxyethane and diethoxyethane, some association occurs between the metal and the unshared electron pairs of the oxygen atoms of the ethers (8), enhancing the ionic character of the carbon–lithium bond. Benzoyl chloride will then have two alternative competitive courses of reaction. Approach to the carbonyl oxygen atom produces the enol ester, with the assistance of the ether associated with the metal. Approach to the carbon–lithium bond results in facile displacement of the ether with consequent reaction directly at the carbon–lithium bond, thus yielding the diketone. The infrared spectra of the inseparable mixture of these two products obtained from the reaction of 9-benzoyl-9-fluorenyllithium and benzoyl chloride in the ethers mentioned indicate that the enol ester and the diketone are formed in the ratio of nearly 1:2.

The formation of only 9-benzoylfluorene along with unchanged fluorene from the reaction of ethyl benzoate and 9-fluorenyl-lithium, -sodium, or -potassium in ether or hydrocarbon solvents is no doubt due to the lower nucleophilic character of the resonance-stabilized anion ABC as compared with that of the ethoxide ion. The ethoxide ion, which must be formed if this anion reacts with ethyl benzoate, readily reacts with the enol ester or β-diketone to reconvert it to the more stable monobenzoylfluorenyl anion ABC. Such a decomposition of an enol ester or diketone by a strong base has been shown previously (4, 7). The failure of the Grignard reagent to form the expected tertiary alcohol from 9-methyl-9-benzoylfluorene also demonstrates the labile nature of 9-benzoylfluorene under basic conditions (17). A similar explanation has been offered for the failure of metalated diphenylmethane to react with more than one equivalent of ester (18).

EXPERIMENTAL

The experimental procedure is generally quite similar in all the reactions performed. A typical experiment for the reactions carried out in ether solvent and one for the reaction conducted with pentane as solvent are shown below. The essential details for the remainder of the experiments carried out are shown in the accompanying table.

All preparations involving organometallic compounds were carried out under nitrogen. Products were identified by mixed melting points with authentic specimens and (or) by comparison of the infrared spectra.

The Reaction of 9-Fluorenylpotassium with Benzoyl Chloride

(1) In dioxane.—Fluorene (16.6 g, 0.1 mole) and potassium (3.9 g, 0.1 mole) were kept for 4 hours in 160 ml of pure, dry, refluxing dioxane. Under these conditions all the potassium was consumed. The mixture was allowed to cool to room temperature and then benzoyl chloride (14 g, 0.1 mole), dissolved in 50 ml of dioxane, was slowly added. The dark red color of the original solution turned to light orange and a viscous solution was formed. Addition of ether and water followed by several washings of the ether layer with water permitted removal of the inorganic salts and the dioxane. At room temperature the ether layer contained yellow crystals which were separated. A second crop of crystals was obtained when the mother liquor was reduced in volume. The yield of crude material was 11.7 g (31%). After unreacted fluorene and 9-benzoylfluorene were removed by trituration with hot ethyl alcohol, pure 9,1'-benzoyloxybenzylidenefluorene, m.p. 189°, was obtained.

(2) In pentane.—Fluorene (8.3 g, 0.05 mole) and potassium metal (1.95 g, 0.05 mole)

TABLE I

Original compound	Metal	Metalation medium[a]	Solvent medium for benzoylation	Benzoylating agent[b]	Product[c]; yield
Fluorene	K	Dioxane	Dioxane	Ethyl benzoate	39% 9-benzoylfluorene + unchanged fluorene
Fluorene	K	Dioxane	Pentane	Ethyl benzoate	42% 9-benzoylfluorene + unchanged fluorene
Fluorene	Li	DEE (10)	DEE	Benzoyl chloride	31% of a mixture of I and II + unchanged fluorene
Fluorene	Li	DEE (10)	Pentane	Benzoyl chloride	28% of II + unchanged fluorene
Fluorene	Li	DEE (10)	DEE	Ethyl benzoate	45% of 9-benzoylfluorene + unchanged fluorene
Fluorene	Li	DEE (10)	Pentane	Ethyl benzoate	41% of 9-benzoylfluorene + unchanged fluorene
9-Benzoylfluorene	Li	DEE (10)	DEE	Benzoyl chloride	67% of a mixture of I and II + unchanged 9-benzoylfluorene
9-Benzoylfluorene	Li	DME	DME	Benzoyl chloride	56% of a mixture of I and II + unchanged 9-benzoylfluorene
9-Benzoylfluorene	Li	DEE	Pentane	Benzoyl chloride	54% of II + unchanged 9-benzoylfluorene
9-Benzoylfluorene	Li	DEE	DEE	Ethyl benzoate	Only unchanged 9-benzoylfluorene
9-Benzoylfluorene	Li	DEE	Pentane	Ethyl benzoate	Only unchanged 9-benzoylfluorene
9-Benzoylfluorene	Na	DME	DME	Benzoyl chloride	60% of I + unreacted 9-benzoylfluorene
9-Benzoylfluorene	Na	DEE	DEE	Benzoyl chloride	Only I (amount undetermined) + unreacted 9-benzoylfluorene
9-Benzoylfluorene	Na	DME	DME	Ethyl benzoate	Only unchanged 9-benzoylfluorene
9-Benzoylfluorene	K	DME	DME	Benzoyl chloride	48% of I + unchanged 9-benzoylfluorene
9-Benzoylfluorene	K	DME	DME	Ethyl benzoate	Only unchanged 9-benzoylfluorene

[a]Metalation was complete in all cases, although the time varied between 0.5 and 2 hours for complete reaction with 9-benzoylfluorene and 4 to 5 hours for the metalation of fluorene. DEE = diethoxyethane. DME = dimethoxyethane.
[b]The slower reaction with ethyl benzoate was allowed to continue overnight, with stirring, to ensure complete reaction. Benzoyl chloride reacted more rapidly but was given a 1- to 3-hour reaction time to ensure completeness.
[c]The 9-benzoylfluorene was freed from fluorene by crystallization from ethanol. Hot ethanol removed fluorene and 9-benzoylfluorene from the alcohol-insoluble enol ester and/or diketone.

were kept for 4 hours in 40 ml of pure, refluxing dioxane. The cooled solution, containing no unreacted potassium, was poured into 500 ml of dry pentane, whereupon the 9-fluorenylpotassium precipitated. The liquid was decanted and the precipitate washed by decantation using pentane, and then suspended in 100 ml of pentane. To this was added slowly a solution of 7 g (0.05 mole) of benzoyl chloride in 50 ml of dry pentane. Reaction occurred immediately but was allowed to continue for 3 hours, with stirring, to assure maximum reaction of the suspended solid. After removal of inorganic substances by water washes, there remained a solid material suspended in the pentane layer. When this was removed and dried it weighed 9.9 g. Contaminating fluorene and 9-benzoylfluorene were removed by extraction of the crude material with hot ethanol, in which both the 9,1'-benzoyloxybenzylidenefluorene and 9,9-dibenzoylfluorene are insoluble. There was obtained 5.1 g (27%) of material analyzing correctly for the enol ester and melting at 189°.

The pentane mother liquor, upon evaporation, yielded a small amount of 9-benzoylfluorene and a considerable quantity of unreacted fluorene.

ACKNOWLEDGMENT

REFERENCES

1. W. SCHLENK and E. BERGMANN. Ann. **463**, 125 (1928).
2. W. SCHLENK and E. BERGMANN. Ber. **62**, 748 (1929).
3. A. KLIEGL, F. WENG, and G. WIEST. Ber. **63**, 1262 (1930).
4. P. PFEIFFER and E. LUBBE. Ber. **63**, 762 (1930).
5. J. A. KING, R. J. MELTZER, and J. DOCZI. J. Am. Chem. Soc. **77**, 2217 (1955).
6. A. WERNER and G. SCHOLER. Ber. **39**, 1287 (1906).
7. W. WISLICENUS and A. FEHRLE. Ber. **48**, 1320 (1915).
8. G. W. H. SCHERF and R. K. BROWN. Can. J. Chem. **39**, 799 (1961).
9. G. W. H. SCHERF and R. K. BROWN. Can. J. Chem. **38**, 697 (1960).
10. G. W. H. SCHERF and R. K. BROWN. Can. J. Chem. **38**, 2450 (1960).
11. L. J. BELLAMY. The infrared spectra of complex molecules. 2nd ed. John Wiley & Sons, Inc., New York. 1958.
12. K. H. MEYER and H. GOTTLIEB BILLROTH. Ber. **54**, 575 (1921).
13. R. N. JONES, C. L. ANGELL, T. ITO, and R. J. D. SMITH. Can. J. Chem. **37**, 2007 (1959).
14. J. HINE. Physical organic chemistry. McGraw-Hill Book Co., Inc., Toronto. 1956.
15. R. L. LETSINGER. J. Am. Chem. Soc. **72**, 4842 (1950).
16. D. Y. CURTIN and E. E. HARRIS. J. Am. Chem. Soc. **73**, 2716 (1951).
17. P. M. G. BAVIN. Can. J. Chem. **37**, 2023 (1959).
18. R. S. YOST and C. R. HAUSER. J. Am. Chem. Soc. **69**, 2325 (1947).

INTERMOLECULAR FORCES AND LIQUID STRUCTURE IN SOME METAL ALKOXIDES[1]

D. C. BRADLEY,[2] CALLIOPE C. A. PREVEDOROU,[2] AND W. WARDLAW[3]

ABSTRACT

The viscosities of some alkoxides of titanium, zirconium, cerium (IV), thorium, and tin (IV) have been measured in the temperature range 25–40° C. The liquid structure in these compounds is discussed in terms of the activation energy, free energy, and entropy of activation for viscous flow, and the energies of cohesion and vaporization.

INTRODUCTION

Previously (1) we investigated the liquid-state properties of a number of germanium tetraalkoxides (alkyl orthogermanates) in order to establish a basis for comparison with similar properties of a number of metal alkoxides. The germanium alkoxides are monomeric whereas some of the metal alkoxides studied in this research are known to be polymeric. It was of interest, in connection with the theory of intermolecular forces in the liquid state, to study the behavior of both monomeric and polymeric metal alkoxides since these large molecules are believed to have globular or quasi-spherical structures. We now report some results on the viscosities of a number of alkoxides of the group IV metals and discuss these in conjunction with related properties of the liquid state.

EXPERIMENTAL

Preparation of the Alkoxides

The alkoxides of titanium (2), zirconium (2), cerium (3), thorium (4), and tin (5) were prepared, purified, and analyzed by the previously described methods. Titanium tetraethoxide is a supercooled liquid at room temperature but it did not change in viscosity when kept in the apparatus over 8 hours.

Viscosity Measurements

All-glass Ostwald viscometers were calibrated using pure benzene at 25, 30, 35, and 40° C. The sample of alkoxide was distilled into the rigorously dried viscometer at 0.1 mm pressure and dry nitrogen was then admitted at atmospheric pressure. The temperature of the viscometer was controlled to ±0.01° C and three separate determinations were carried out on each compound. The reproducibility was of the order of ±0.0001 poises for the least viscous and ±0.01–0.02 poises for the most viscous compounds. The results (viscosity in poises) are presented in Table I.

The activation energies of viscosity E_{vlsc} (kcal/mole) were evaluated graphically from the plot of $\log \eta$ versus $1/T°$ K. The free energies of activation of viscous flow $\Delta F^{\ddagger}$ (kcal/mole) were calculated from Eyring's (6) equation:

$$\eta = (hN/V) . e^{(\Delta F^{\ddagger}/RT)}.$$

The molar volumes were taken from our previous work (8) and the molar heats of vaporization from the results of vapor pressure studies (2).

TABLE I

Viscosities (poises) of metal alkoxides

Compound	25° C	30° C	35° C	40° C
Ti(OEt)$_4$	0.447	0.357	0.285	0.236
Ti(OPr^n)$_4$	1.749	1.306	1.070	0.851
Ti(OBu^n)$_4$	0.692	0.579_5	0.483	0.406_5
Ti(OBu^i)$_4$	0.0352	0.0315	0.0285	0.0258
Zr(OBu^i)$_4$	0.0317	0.0278	0.0246	0.0224
Ti(OCMe$_2$Et)$_4$	0.0808	0.0714	0.0626	0.0537
Zr(OCMe$_2$Et)$_4$	0.0759	0.0673	0.0589	0.0518
Sn(OCMe$_2$Et)$_4$	0.166_5	0.143	0.120_5	0.102
Ti(OCMe$_2$Pr^n)$_4$	0.0479	0.0434	0.0395	0.0362
Zr(OCMe$_2$Pr^n)$_4$	0.0464	0.0419	0.0379	0.0346
Sn(OCMe$_2$Pr^n)$_4$	0.0986	0.0840	0.0716	0.0644
Ce(OCMe$_2$Pr^n)$_4$	8.13	5.89	4.28	3.16
Ti(OCMeEt$_2$)$_4$	0.345	0.299_5	0.260	0.220_5
Zr(OCMeEt$_2$)$_4$	0.281	0.236_3	0.200	0.170_5
Sn(OCMeEt$_2$)$_4$	0.413	0.339	0.265_5	0.225
Ce(OCMeEt$_3$)$_4$	0.216	0.169_5	0.141	0.119
Ce(OCEt$_3$)$_4$	0.526	0.451_5	0.387_5	0.332_5
Th(OCEt$_3$)$_4$	0.492	0.387	0.322	0.269

DISCUSSION

The data on E_{visc}, $\Delta F^{\pm}$, and $\Delta S^{\pm}$ (cal/deg mole), at 25° C, are presented in Table II.

TABLE II

Compound	E_{visc} (kcal/mole)	$\Delta F^{\pm}$ (kcal/mole)	$\Delta S^{\pm}$ (cal/°C mole)
Ti(OEt)$_4$	7.9	5.9	+6.7
Ti(OPr^n)$_4$	8.4	6.9	+5.3
Ti(OBu^n)$_4$	7.1	6.5	+2.0
Ti(OBu^i)$_4$	4.1	4.8	−2.4
Zr(OBu^i)$_4$	4.4	4.8	−1.4
Ti(OCMe$_2$Et)$_4$	5.2	5.4	−0.7
Zr(OCMe$_2$Et)$_4$	5.4	5.4	0
Sn(OCMe$_2$Et)$_4$	6.4	5.8	+2.0
Ti(OCMeEt$_2$)$_4$	6.1	6.3	−0.7
Zr(OCMeEt$_2$)$_4$	6.6	6.2	+1.3
Ce(OCMeEt$_2$)$_4$	7.0	6.1	+3.5
Sn(OCMeEt$_2$)$_4$	8.2	6.7	+5.0
Ti(OCMe$_2$Pr^n)$_4$	3.8	5.2	−5.0
Zr(OCMe$_2$Pr^n)$_4$	4.0	5.2	−4.0
Ce(OCMe$_2$Pr^n)$_4$	12.6	8.1	+15.1
Sn(OCMe$_2$Pr^n)$_4$	5.6	5.6	0
Ce(OCEt$_3$)$_4$	6.3	6.6	−1.3
Th(OCEt$_3$)$_4$	7.6	6.6	+3.5

The errors in E_{visc} and $\Delta F^{\pm}$ were of the order of ± 0.5–1.0%, whilst for $\Delta S^{\pm}$ the errors probably range from about $\pm 5\%$ for values around 5 cal/deg mole to about $\pm 15\%$ for values around 1 cal/deg mole.

Considering first the n-alkoxides of titanium, Ti(OR)$_4$, where R = Et, Pr^n, and Bu^n, it is noteworthy that for both η and E_{visc} there is a maximum value at the n-propoxide. This is in marked contrast to the behavior of the corresponding germanium n-alkoxides where E_{visc} increases steadily with molecular size (1). Moreover, the values of E_{visc} for the titanium derivatives are two to three times greater than for the corresponding germanium derivatives. There is little doubt that this "anomalous" behavior of the titanium compounds is a consequence of their polymeric nature. For example, Caughlan et al. (7)

showed cryoscopically that the number-average degree of polymerization of titanium n-alkoxides in benzene increased with increasing concentration to a limiting value of three. They suggested that the trimer was of structural significance and deduced two possible structures based on octahedral titanium atoms in which 6-co-ordination was attained by intermolecular bonds from oxygen to titanium. It seems reasonable to assume that these alkoxides would also be trimeric in the pure liquid state. Concerning the mechanism of viscous flow, there seem to be two alternatives for the polymeric derivatives. Either the trimers migrate individually or they may dissociate into more mobile monomer units which then migrate. We have already observed that for the germanium n-alkoxides, which are monomeric, E_{visc} increases steadily with increase in molecular size. It is also clear from the data in Table II that for the monomeric tertiary alkoxides of titanium (and zirconium) E_{visc} again increases steadily with molecular size. Hence it might reasonably be expected that E_{visc} for the trimer $Ti_3(OR)_{12}$ would be almost triple that for the monomer $Ti(OR)_4$ if the trimer migrates as a whole. We have estimated, by extrapolation from the values of E_{visc} for the monomeric tertiary alkoxides, that the values of $(E_{visc})_{mon}$ for "monomeric" normal alkoxides of titanium should be approximately: $Ti(OEt)_4$, 2.2; $Ti(OPr^n)_4$, 3.2; $Ti(OBu^n)_4$, 4.1 kcal/mole. These figures are reasonably close to the corresponding values for the work of cohesion W_c (see later) and W_c should be $\simeq E_{visc}$ for simple molecules (9). The ratios $E_{visc}/(E_{visc})_{mon}$ are as follows: $Ti(OEt)_4$, 3.6; $Ti(OPr^n)_4$, 2.6; $Ti(OBu^n)_4$, 1.7. Bearing in mind the approximations involved, it might be agreed that the figures for $Ti(OEt)_4$ and $Ti(OPr^n)_4$ are consistent with these compounds exhibiting flow by migration of trimeric molecules, but such is not the case for $Ti(OBu^n)_4$. Moreover, the alternative mechanism of flow involving depolymerization of the trimers and migration of monomers would also require anomalously high values of E_{visc} because the activation energy for viscous flow would include the energy of depolymerization ΔE. Assuming that $E_{visc} = (E_{visc})_{mon} + \Delta E$, the following values for ΔE are derived: $Ti(OEt)_4$, 5.7; $Ti(OPr^n)_4$, 5.2; $Ti(OBu^n)_4$, 3.0 kcal/mole. The observed order of E_{visc} would then be a consequence of the decrease in depolymerization energy (ΔE) with increase in length of the alkyl chains. We are inclined to the view that the second mechanism, i.e. depolymerization followed by migration of monomers, is the correct one because of the entropies of activation $\Delta S^{\ddagger}$ shown in Table II. Thus the monomeric germanium n-alkoxides had negative entropies of activation and the monomeric titanium tertiary alkoxides also have negative entropies of activation. Hence we should expect the migration of trimeric molecules to involve a similar negative entropy of activation. However, the titanium n-alkoxides have relatively large positive entropies of activation and this is consistent with the proposition that depolymerization is involved in the mechanism of flow since such a process should cause a considerable degree of disorder in attaining the activated configuration. It is noteworthy that the positive $\Delta S^{\ddagger}$ values decrease in the same order as the values of ΔE.

Turning now to the monomeric alkoxides of titanium and zirconium, we note that η and E_{visc} increase with molecular size from $M(OCMe_3)_4$ to $M(OCMe_2Et)_4$ to $M(OCMeEt_2)_4$, with the titanium derivative having a slightly higher viscosity but slightly lower E_{visc} than the corresponding zirconium derivative. The $\Delta S^{\ddagger}$ values are slightly more positive for the zirconium compounds. However, the E_{visc} values for the $M(OCMe_2Pr^n)_4$ derivatives of Ti and Zr are remarkably low and suggest that the mechanism of flow must differ in these molecules from the mechanism of "molecular jumps" which probably occurs in the other tertiary alkoxides. This is reflected in the large negative $\Delta S^{\ddagger}$ values for the $M(OCMe_2Pr^n)_4$ molecules. The behavior of the stannic

alkoxides is surprising since the values for η and E_{visc} are higher and $\Delta S^{\neq}$ more positive than in the corresponding titanium and zirconium derivatives. Previous work (8) showed that the stannic compounds also had anomalously low parachors compared with the Ti and Zr compounds. The reason for this is still not clear. The effect of polymerization is strikingly revealed in the viscosity data for the cerium derivatives of dimethyl n-propyl carbinol and methyl diethyl carbinol. On the other hand the triethyl carbinol derivatives of cerium and thorium, which are monomeric, seem to have η and E_{visc} values of the correct order of magnitude.

Grunberg and Nissan (9) have shown that important structural information on liquids may be deduced from a comparison of the internal energy of vaporization $E_v (\Delta H_v - RT)$, the work of cohesion W_c ($2\gamma N^{1/3} V_1^{2/3}$, where γ is the surface tension and V_1 the molar volume of the liquid), and the activation energy of viscosity E_{visc}. Eyring (6) has shown that for many liquids, $E_v/\Delta F^{\neq} \simeq 2.5$ and E_v/E_{visc} is 3–4, and has interpreted deviations from these values in terms of structural abnormalities. We have calculated the values for W_c (kcal/mole) (8) and the ratios E_v/E_{visc} etc. for some liquid metal alkoxides and the data are given in Table III.

TABLE III

Compound	E_v (kcal/mole)	W_c (kcal/mole)	$E_v/\Delta F^{\neq}$	E_v/E_{visc}	E_v/W_c	E_{visc}/W_c
Ti(OEt)$_4$	21.0	2.84	3.55	2.50	7.39	2.95
Ti(OPr^n)$_4$	15.1	3.78	2.18	1.71	3.99	2.33
Ti(OBu^n)$_4$	19.5	4.39	3.00	2.71	4.44	1.63
Ti(OBu^t)$_4$	14.0	4.92	2.91	3.41	3.00	0.83
Zr(OBu^t)$_4$	14.6	4.47	3.04	3.32	3.27	0.98
Ti(OCMe$_2$Et)$_4$	16.1	6.03	2.98	3.10	2.67	0.86
Zr(OCMe$_2$Et)$_4$	15.7	5.46	2.90	2.91	2.88	0.98
Ti(OCMeEt$_2$)$_4$	18.4	6.92	2.92	3.01	2.66	0.88
Zr(OCMeEt$_2$)$_4$	18.4	6.30	2.96	2.80	2.92	1.05
Ti(OCMe$_2$Pr^n)$_4$	18.9	6.75	3.63	4.97	2.73	0.57
Zr(OCMe$_2$Pr^n)$_4$	18.4	6.28	3.54	4.60	2.93	0.64

In addition, the values of W_c and the ratio E_{visc}/W_c have been calculated for some alkoxides whose latent heats of vaporization are not known: Sn(OCMe$_2$Et)$_4$: W_c 4.96, E_{visc}/W_c 1.31; Sn(OCMe$_2$Pr^n)$_4$: 4.99, 1.13; Ce(OCMeEt$_2$)$_4$: 6.23, 1.12; Ce(OCEt$_3$)$_4$: 7.03, 0.90; Th(OCEt$_3$)$_4$: 6.09, 1.25.

Grunberg and Nissan (9) showed that for various monomeric liquids, $E_{\text{visc}} = W_c$, and it is clear that in these cases the energy requirements for translating a molecule from one equilibrium position to another in viscous flow are the same as in displacing a molecule to expose fresh surface of the liquid. They also noted that for "associated" liquids, $E_{\text{visc}} > W_c$, and suggested that the difference $E_{\text{visc}} - W_c$ could be attributed to the energy of dissociation of the associated molecules since W_c does not contain the dissociation energy but E_{visc} does. This difference presumably arises because E_{visc} is determined from a rate process whereas the determination of W_c involves an equilibrium system. In principle, a higher value of W_c including the energy of dissociation might be obtained by using a dynamic method in which the surface tension was measured during a time interval which was short compared with the lifetime of a "dissociated" molecule. The results for the monomeric tertiary alkoxides $M(OCMe_nEt_{3-n})_4$, where M = Ti or Zr and n = 3, 2, or 1, and also for some of the tertiary alkoxides of tin, cerium, and thorium, show that the ratio E_{visc}/W_c is indeed close to unity. Evidently these large

globular molecules behave similarly to simple molecules in the processes of viscous flow and surface formation. No doubt this is because the intermolecular forces between the monomeric tertiary alkoxides are mainly determined by the peripheral alkyl groups and these forces will be of the dispersion type. It is quite clear that the central metal atom has little influence on the magnitude of these forces and this is in accordance with the earlier theory of Bradley *et al.* (2, 3, 4, 5) that the highly branched tertiary alkoxide groups effectively screen the metal and prevent intermolecular bonding involving the metal. The behavior of the monomeric alkoxides $Ti(OCMe_2Pr^n)_4$ and $Zr(OCMe_2Pr^n)_4$ is extremely interesting. In both cases the ratio E_{visc}/W_c is considerably less than unity and it appears, from a comparison with the data for the other monomeric titanium and zirconium alkoxides, that for $M(OCMe_2Pr^n)_4$ the values of W_c are normal but values of E_{visc} are abnormally low. This suggests that the mechanism of flow for $M(OCMe_2Pr^n)_4$ liquids does not involve the discrete movement of the whole molecule but, more probably, migration occurs by a "molecular wriggle" mechanism. It is noteworthy that these compounds also have fairly large negative entropies of activation for viscous flow and this recalls the mechanism of flow postulated by Moore, Gibbs, and Eyring (10) for straight-chain hydrocarbons. They noted that these compounds had low values of E_{visc} in the low-temperature region and gave negative ΔS^{+}'s. It was suggested that these liquids had a quasi-crystalline structure and that viscous flow involved a co-operative movement analogous to the movement of dislocations in the lattice of a metal.

It is extremely interesting to note that for the polymeric *n*-alkoxides of titanium, the values of E_{visc}/W_c are much greater than unity due to the abnormally high values for E_{visc}. In fact, the values of W_c for the *n*-alkoxides are remarkably close to the values calculated for hypothetical "monomeric" derivatives by extrapolation from the data on the monomeric tertiary alkoxides. From this we deduce that the intermolecular forces which are overcome in the creation of fresh surface are the same in nature for both the polymeric and the monomeric alkoxides and hence must involve predominantly the dispersion forces between the peripheral alkyl groups. Hence the values of W_c for the polymeric alkoxides do not involve the dissociation energy of the polymers whereas we have argued earlier that E_{visc} does include the dissociation energy. Therefore, the difference $E_{visc} - W_c \simeq \Delta E$ and provides an alternative measure for ΔE. The values of ΔE so calculated are: $Ti(OEt)_4$, 5.1 (5.7); $Ti(OPr^n)_4$, 4.6 (5.2); $Ti(OBu^n)_4$, 2.7 (3.0); the values in parentheses are the ones deduced earlier in the paper by the other method.

For the monomeric tertiary alkoxides which exhibit the "molecular jump" mechanism of flow it appears that $E_v/\Delta F^{+}$ is 3.0 rather than 2.5 as found by Eyring (6) for "normal" liquids. This discrepancy may well be due to the fact that Eyring's values of E_v were calculated from heats of vaporization at the normal boiling point whereas in the metal alkoxides our values of E_v are derived from vapor pressure results at lower pressures (where ΔH_v will be larger). For the same compounds E_v/E_{visc} is around 3.0 whereas for the "abnormal" polymeric alkoxides E_v/E_{visc} is low and for $M(OCMe_2Pr^n)_4$ (M = Ti, Zr) the values are rather high.

Finally, it is interesting to explore the application of Grunberg and Nissan's (9) ideas on the structure of liquids to our data. For liquids composed of simple molecules they suggested that there is a statistical structure in which each molecule is surrounded by *n* nearest neighbors and that intermolecular forces may be considered as localized in "bonds" between nearest neighbors. In the process of vaporization all of these "bonds" must be disrupted before a molecule is free to escape into the vapor. However, in surface formation the number of "bonds" which need to be disrupted in order to expose a

"central" molecule depends on the quasi structure in the liquid and this is why $E_v > W_e$. They deduced that the ratio $E_v > W_e$ would be determined by the co-ordination number and the structure of the liquid as follows: for hexagonal (c.p.), cubic (c.p.), and cubic (b.c.) packing, $E_v/W_e = 4$; for octahedral packing, $E_v/W_e = 3$; and for tetrahedral packing, $E_v/W_e = 2$. For the monomeric tertiary alkoxides the data in Table III show that the zirconium compounds have E_v/W_e values about 10% greater than the corresponding titanium derivatives. This is a reflection of the fact that the zirconium compounds have lower values of W_e but about the same values of E_v as the titanium compounds. Nevertheless, the value of E_v/W_e for all of these compounds is around 3.0 and suggests that the molecules have an average co-ordination number of 6. This figure must be treated with caution since the molecules under consideration are large and complicated in structure and hence may not conform to the requirements of the theory.

CONCLUSIONS

1. From considerations of the energies of intermolecular attraction as deduced from the processes of vaporization, viscous flow, and surface formation, it appears that the monomeric tertiary alkoxides behave rather like simple covalent molecules which are bound by dispersion forces in the liquid state. This agrees with the conclusions from other work that the steric effect of the branched alkoxide groups largely precludes the central metal atom from being involved in intermolecular interaction.

2. In the n-alkoxides of titanium, which are polymeric due to intermolecular bonding between titanium and oxygen, it appears that the mechanism of viscous flow involves dissociation of the polymers with consequent abnormally high activation energy. On the other hand the process of surface formation appears to involve only the relatively weak dispersion forces between the molecules.

REFERENCES

1. D. C. BRADLEY, L. J. KAY, J. D. SWANWICK, and W. WARDLAW. J. Chem. Soc. 3656 (1958).
2. D. C. BRADLEY, R. C. MEHROTRA, J. D. SWANWICK, and W. WARDLAW. J. Chem. Soc. 2025 (1953);
   D. C. BRADLEY, R. C. MEHROTRA, and W. WARDLAW. J. Chem. Soc. 4204 (1952).
3. D. C. BRADLEY, A. K. CHATTERJEE, and W. WARDLAW. J. Chem. Soc. 2600 (1957).
4. D. C. BRADLEY, M. A. SAAD, and W. WARDLAW. J. Chem. Soc. 3488 (1954).
5. D. C. BRADLEY, E. V. CALDWELL, and W. WARDLAW. J. Chem. Soc. 4775 (1957).
6. H. EYRING. J. Chem. Phys. 4, 283 (1936).
7. C. N. CAUGHLAND, H. S. SMITH, W. KATZ, W. HODGSON, and R. W. CROWE. J. Am. Chem. Soc. 73, 5652 (1951).
8. D. C. BRADLEY, C. C. A. PREVEDOROU, J. D. SWANWICK, and W. WARDLAW. J. Chem. Soc. 1010 (1958).
9. L. GRUNBERG and A. H. NISSAN. Trans. Faraday Soc. 45, 125 (1949).
10. R. J. MOORE, P. GIBBS, and H. EYRING. J. Phys. Chem. 57, 172 (1953).

MOLECULAR INTERACTIONS

I. INFRARED SPECTRA OF SOME CARBOXYLIC ACIDS IN CARBON TETRACHLORIDE AND BENZENE SOLUTIONS[1]

F. E. MURRAY[2] AND S. SUNDARAM

ABSTRACT

Infrared spectra of benzoic, o-chlorobenzoic, and salicylic acids in the range 700 to 3800 cm^{-1} have been studied. Measurements have been made on the three acids in carbon tetrachloride and benzene solutions, at a number of concentrations in each case. The results are interpreted in terms of the molecular species present in each solution and the effect of the solvents on these species. Assignments have been made of the observed bands to the various vibrational modes characteristic of the COOH group.

INTRODUCTION

Dimeric carboxylic acids have been the subject of study by a number of investigators in the past. The infrared and Raman spectra have been used to show the presence of strong hydrogen bridges between the carbonyl and the hydroxyl groups of the two molecules. Even in dilute solutions in certain solvents, the association between the molecules persists.

The abnormally strong hydrogen bonds in these acids is an advantage in correlating the characteristic distortions of the O—H stretching modes with the association. There are also other regions of the spectra that are equally important. The C=O region (1700 cm^{-1}) gives indications of the immediate environment of the COOH group. The other regions that provide additional useful data are 1300–1400 cm^{-1}, corresponding to C—O stretching and O—H in-plane deformation, and near 950 cm^{-1}, attributed to the O—H out-of-plane mode.

The infrared spectra of benzoic acid in solution in carbon tetrachloride have been studied by Davies and Sutherland (1), Harris and Hobbs (2), and Bratoz et al. (3). Hadzi and Sheppard (4) have also observed the infrared spectrum of solid benzoic acid below 1500 cm^{-1}. Among others, Murty and Seshadri (5) have reported the Raman spectrum of benzoic acid in solution in benzene and indicated the presence of ring dimers. Brooks et al. (6, 7) have recently investigated the C=O and O—H frequencies in the infrared spectra of benzoic and o-chlorobenzoic acid in ether–CCl$_4$ and CCl$_4$ solutions respectively and of substituted salicylic acids and their esters in CCl$_4$ solutions. The Raman spectrum of salicylic acid in benzene solution has been studied by Murty and Seshadri (8). They concluded that some chelate monomer is present in benzene solution but the major molecular species is a polymer, the structure of which was not clear.

The present study was begun to obtain information on the effect of the ortho substituents in benzoic acid on the tendency of this compound to form dimers in solution. The presence of an ortho substituent in benzoic acid makes possible the formation of chelate monomers. This tendency for chelation depends on the donor or acceptor strength of the ortho substituent group. Thus, for these compounds there are two competing processes for the formation of donor–acceptor bonds leading to the production of chelate monomers or to associated polymers. The effect of the solvent on the type of the molecular species present in solution has also been investigated.

Three acids, benzoic, o-chlorobenzoic, and salicylic were chosen for study. The spectra for these three compounds were obtained at various concentrations in solution in carbon tetrachloride and in benzene.

EXPERIMENTAL

All the spectra were recorded using a Perkin–Elmer Model 21 double-beam spectrometer equipped with sodium chloride optics. The instrument was calibrated against atmospheric absorption bands and a polystyrene film. The accuracy in the O—H stretching band region is estimated at ± 10 cm^{-1}. Measurements were made using 5-mm matched cells. The solvents used, carbon tetrachloride and benzene, were spectrograde and the acids used were analytical reagent grade. All of the above compounds were used without any attempts at further purification.

RESULTS

(a) Infrared spectral data for benzoic acid in carbon tetrachloride solution at a concentration of 8.2 millimoles per liter.—Principal absorption bands (cm^{-1}): 3650, 3545, 3060, 3020, 3005, 2875, 2658, 2590, 2540, 2080, 1970, 1927, 1912, 1815, 1780, 1737, 1692, 1620, 1455, 1420, 1352, 1320, 1287, 1177, 1125, 1090, 1065, 1025, 935.

(b) Infrared spectral data for benzoic acid in benzene solution at a concentration of 17.2 millimoles per liter.—Principal absorption bands (cm^{-1}): 3660, 3630, 3470, 3220, 3000, 2780, 2665, 2630, 2540, 2345, 2300, 2197, 2080, 1902, 1725, 1690, 1650, 1640, 1355, 1290, 1272.

(c) Infrared spectral data for salicylic acid in carbon tetrachloride solution at a concentration of 6.58 millimoles per liter.—Principal absorption bands (cm^{-1}): 3535, 3060, 2918, 2870, 2590, 2530, 1690, 1660, 1612, 1482, 1462, 1442, 1382, 1297, 1180, 1162, 1152, 1135, 1072, 1033, 903.

(d) Infrared spectral data for salicylic acid in benzene solution at a concentration of 4.4 millimoles per liter.—Principal absorption bands (cm^{-1}): 3655, 3450, 3240, 3000, 2820, 2635, 2570, 2540, 1787, 1687, 1655, 1642, 1417, 1342, 1330, 1290, 1265.

(e) Infrared spectral data for o-chlorobenzoic acid in carbon tetrachloride solution at a concentration of 12.8 millimoles per liter.—Principal absorption bands (cm^{-1}): 3585, 3080, 3030, 3000, 2910, 2655, 2555, 1977, 1947, 1755, 1700, 1565, 1480, 1442, 1410, 1297, 1180, 1165, 1145, 1130, 1100, 1050, 1042, 925.

(f) Infrared spectral data of o-chlorobenzoic acid in benzene solution at a concentration of 12.8 millimoles per liter.—Principal absorption bands (cm^{-1}): 3655, 3460, 3210, 2775, 2670, 2530, 1717, 1690, 1332, 1270.

DISCUSSION

In the following discussion of the spectra observed, the absorption bands in the various regions are assigned to the molecular species which appear to exist for each of the acids in the two solvents. The assignments are based on the position of the band and on the behavior of the intensity of the band with changing concentration of the solute. In some cases, the positions of the bands change significantly as the concentration of the solute is changed. This effect, which must be caused by an interaction between solvent molecules and the functional group which gives rise to the vibrational band, has not been considered in any detail.

1. Region of the O—H Stretching Fundamental

The results obtained in the region of the O—H stretching vibrational frequency are shown in Fig. 1. The acids in solution in carbon tetrachloride show sharp monomer
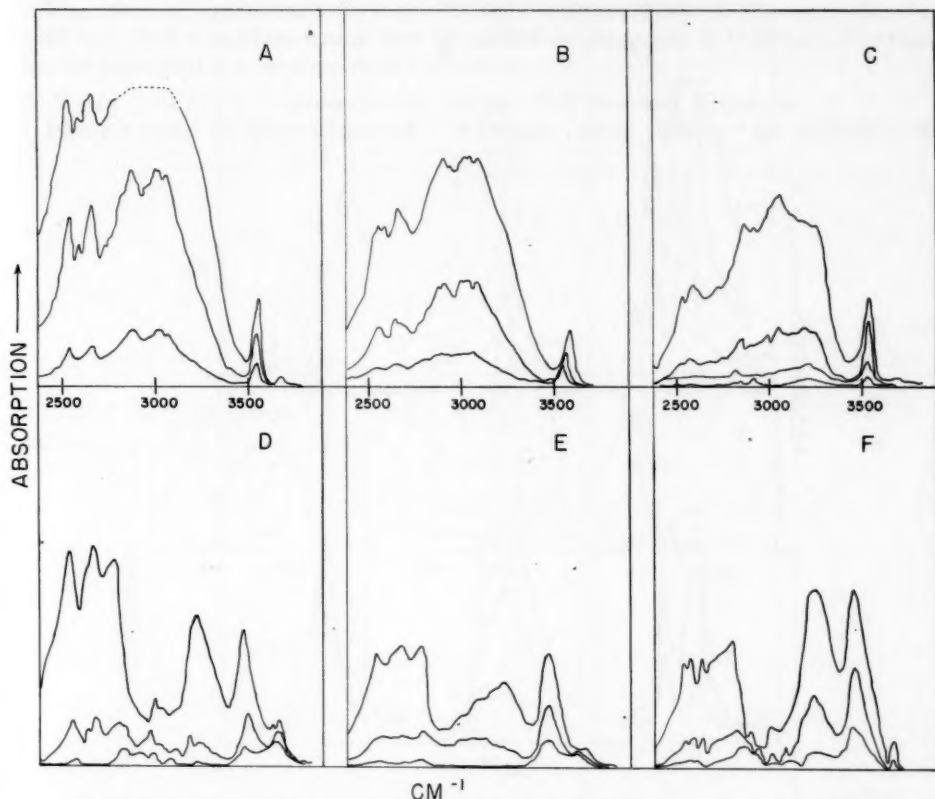
FIG. 1.   Region of the O—H stretching fundamental bands: A, benzoic acid in carbon tetrachloride at concentrations 32, 8.2, and 1.3 millimoles per liter; B, orthochlorobenzoic acid in carbon tetrachloride at concentrations 12.8, 3.84, and 1.15 millimoles per liter; C, salicylic acid in carbon tetrachloride at concentrations 6.58, 1.98, 0.59, and 0.18 millimoles per liter; D, benzoic acid in benzene at concentrations 17.2, 3.4, and 0.68 millimoles per liter; E, orthochlorobenzoic acid in benzene at concentrations 12.8, 3.84, and 1.15 millimoles per liter; F, salicylic acid in benzene at concentrations 14.5, 4.4, and 1.32 millimoles per liter.

O—H bands at 3545, 3585, and 3535 cm^{-1} for benzoic, o-chlorobenzoic, and salicylic acids, respectively. In this solvent, the band of the associated form is strong and broad with the actual position of the peaks obscured by the overlapping C—H bands.

In benzene solution, the monomeric bands appear at lower frequencies than the bands for the same acids in carbon tetrachloride solution. The monomer bands are at 3470, 3460, and 3450 cm^{-1} respectively for the benzoic, o-chlorobenzoic, and salicylic acids. The bands for the associated species are clearly defined for each acid and appear at 3220, 3210, and 3240 cm^{-1} for the benzoic, o-chlorobenzoic, and salicylic acids.

Subsidiary maxima, with somewhat narrower half-band widths, have been observed in all the solutions in the region 2500–3000 cm^{-1}. These bands have been very satisfactorily accounted for by a summation-band hypothesis by Hadzi and Sheppard (4).

2. Region of the C=O Stretching Fundamental

The spectra obtained for the three acids in both the solvents, in the region of the C=O stretch, are shown in Fig. 2. The effect of the solvent change on the C=O stretching
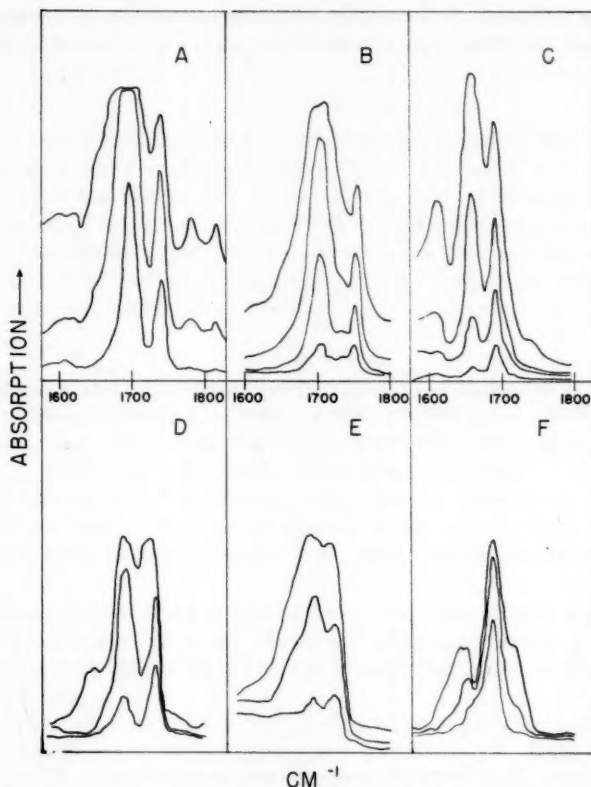
FIG. 2. Region of the C=O stretching fundamental bands: A, benzoic acid in carbon tetrachloride at concentrations 32, 8.2, and 1.3 millimoles per liter; B, orthochlorobenzoic acid in carbon tetrachloride at concentrations 12.8, 3.84, 1.15, and 0.35 millimoles per liter; C, salicylic acid in carbon tetrachloride at concentrations 6.58, 1.98, 0.59, and 0.18 millimoles per liter; D, benzoic acid in benzene at concentrations 17.2, 3.4, and 0.68 millimoles per liter; E, orthochlorobenzoic acid in benzene at concentrations 12.8, 3.84, and 1.15 millimoles per liter; F, salicylic acid in benzene at concentrations 14.5, 4.4, and 1.32 millimoles per liter.

vibration is not nearly as great as it is on the O—H stretching vibration. Thus, the C=O bands are shifted only slightly in changing from the solvent carbon tetrachloride to benzene. This region yields considerable information regarding the molecular species present in each case.

Monomer bands for the benzoic, o-chlorobenzoic, and salicylic acids in carbon tetrachloride appear at 1737, 1755, and 1690 cm^{-1} respectively. In the case of the salicylic acid, the peak at 1690 cm^{-1} is characteristic of the chelated form of the acid as shown in Figs. 5e and 5f, and the small shoulder at 1730 cm^{-1} arises from the presence of some unchelated monomer. The peaks for the associated forms of the benzoic, o-chlorobenzoic, and salicylic acids in carbon tetrachloride solution appear at 1692, 1700, and 1660 cm^{-1} respectively.

In benzene solution, the benzoic acid shows a monomer band at 1725 cm^{-1} and the bands for the associated forms of the acid at 1690 and 1650 cm^{-1}. The monomer peak for the o-chlorobenzoic acid in benzene solution appears at 1717 cm^{-1} with the peak for the associated species at 1690 cm^{-1}.

The chelated form of salicylic acid in benzene solution shows an absorption band at 1687 cm^{-1} with a shoulder arising from the unchelated monomer at 1710 cm^{-1}. The band for the associated species appears at 1655 cm^{-1}.

3. Region of the O—H In-plane Bending and the C—O Stretching Vibrations

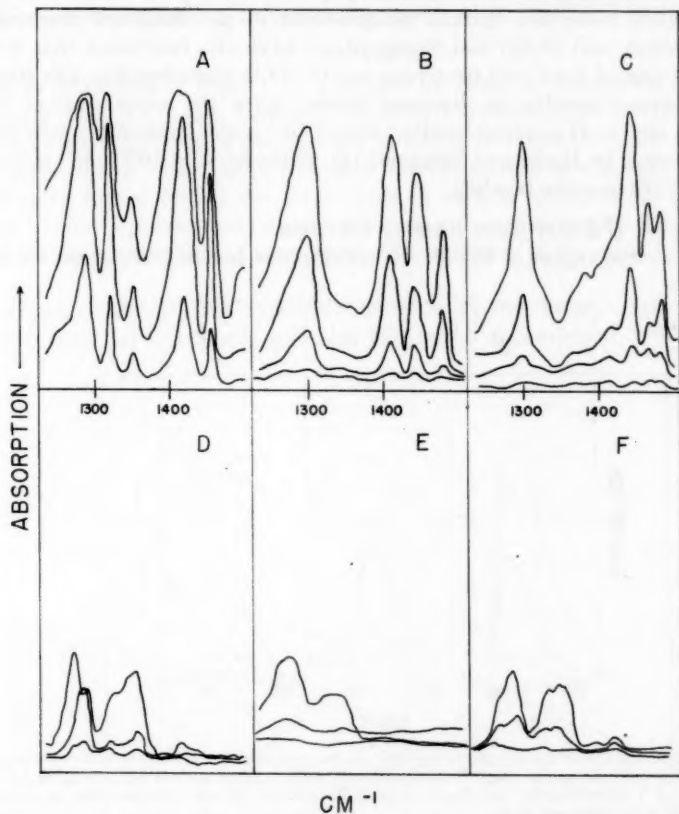Figure 3 shows the spectra observed in the region 1250 to 1500 cm^{-1} for the three acids

FIG. 3. Region of the O—H in-plane bending and C—O stretching: A, benzoic acid in carbon tetrachloride at concentrations 32, 8.2, and 1.3 millimoles per liter; B, orthochlorobenzoic acid in carbon tetrachloride at concentrations 12.8, 3.84, 1.15, and 0.35 millimoles per liter; C, salicylic acid in carbon tetrachloride at concentrations 6.58, 1.98, 0.59, and 0.18 millimoles per liter; D, benzoic acid in benzene at concentrations 17.2, 3.4, and 0.68 millimoles per liter; E, orthochlorobenzoic acid in benzene at 12.8, 3.84, and 1.15 millimoles per liter; F, salicylic acid in benzene at concentrations 14.5, 4.4, and 1.32 millimoles per liter.

in both the solvents. The spectra in benzene are rather poorly defined in this region as a result of the solvent absorption. It is noteworthy, however, that the bands appearing between 1400 and 1500 cm^{-1} in carbon tetrachloride solution are essentially absent for the acids in benzene solution. Hadzi and Sheppard (4) have reported 1420 and 1287 cm^{-1} in this region for the characteristic frequencies of the COOH group of solid benzoic acid.

The internal co-ordinates of the COOH group which might account for the frequencies in the region between 1500 and 800 cm^{-1} are the C—O stretching, O—H motion perpendicular to the plane of the dimer, or the torsional motion of the O—H band about the

C—O linkage for the monomeric molecule. The assignment of these modes to this frequency range has been confirmed by Hadzi and Sheppard (4), who observed the behavior of the two bands corresponding to the in-plane and the out-of-plane O—H bending on deuteration. One is, however, left with the ambiguity with regard to distinguishing the C—O stretching and the O—H in-plane bending frequencies in the region of 1450–1300 cm^{-1}. They both belong to the same symmetry species and might be expected to interact appreciably. While there is a marked disagreement in the literature concerning their precise assignments, and Hadzi and Sheppard (4) have also concluded that a clear-cut assignment in terms of the C—O stretching and O—H in-plane bending vibrations is not possible, the present results, as discussed below, favor the assignment of the band ⌣1400 cm^{-1} to the O—H in-plane bending mode. This is also compatible with the unambiguous assignment, by Hadzi and Sheppard (4), of the band at 1050 cm^{-1} in the COOD group to the O—D in-plane bending.

4. Region of the O—H Out-of-plane Bending Vibration

Figure 4 shows the region of the O—H out-of-plane bending vibration for the three
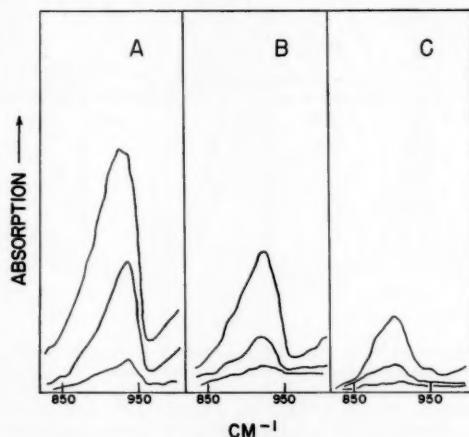

FIG. 4. Region of the O—H out-of-plane bending: A, benzoic acid in carbon tetrachloride at concentrations 32, 8.2, and 1.3 millimoles per liter; B, orthochlorobenzoic acid in carbon tetrachloride at concentrations 12.8, 3.84, and 1.15 millimoles per liter; C, salicylic acid in carbon tetrachloride at concentrations 6.58, 1.98, and 0.59 millimoles per liter.

acids in carbon tetrachloride solution. That this region is definitely that of the O—H out-of-plane bending has been suggested on less direct experimental evidence by Davies and Sutherland (1) and confirmed by Hadzi and Sheppard (4). The changes in this band caused by dilution in carbon tetrachloride solutions are as spectacular as those occurring for the O—H stretching frequencies. The interest in the study of this band also stems from the energy change implied by the deviation from a linear hydrogen bond configuration. This band was absent in benzene solution.

The absence of these bands in the benzene solution may be caused by the relatively strong absorption of the solvent in this region. However, data from the region of the O—H stretching vibration indicate that benzene interacts with the O—H sufficiently to shift the monomer O—H bands by about 100 cm^{-1} on changing from carbon tetrachloride to benzene solution. This interaction may also act to suppress the O—H bending vibrations in both the in-plane and the out-of-plane modes. This possible explanation for the

absence of appreciable bands for all the three acids in benzene solution at about 900 cm⁻¹ and at 1400 cm⁻¹ requires further study but appears reasonable.

On the basis of the above explanation for the absence of the O—H in-plane and out-of-plane bending modes in benzene solution, it appears that the absorption peaks appearing in the region of 1400 to 1500 cm⁻¹ (Fig. 3A, B, and C) in carbon tetrachloride solutions arise from the O—H in-plane bending modes for the various molecular species. The bands at ⌄1300 cm⁻¹ therefore can be reasonably assigned to the C—O stretching mode.

CONCLUSIONS

The data presented in Figs. 1 to 4 cannot be considered accurate enough to yield quantitative intensity values. However, the results are semiquantitative and conclusions may be drawn on the basis of the intensity changes with concentration.

An examination of Figs. 1 and 2 indicates that the ratio of associated to monomer form is appreciably higher for all the three acids in carbon tetrachloride than in benzene solutions. Thus, it appears that benzene interacts more strongly with the solute molecules in every case and suppresses to some extent the tendency of the acids to form associated species.

It has been established by cryoscopic methods (9) that benzoic acid exists primarily as a dimer (Fig. 5b) in benzene solution. The peaks appearing at 1692 cm⁻¹ in carbon
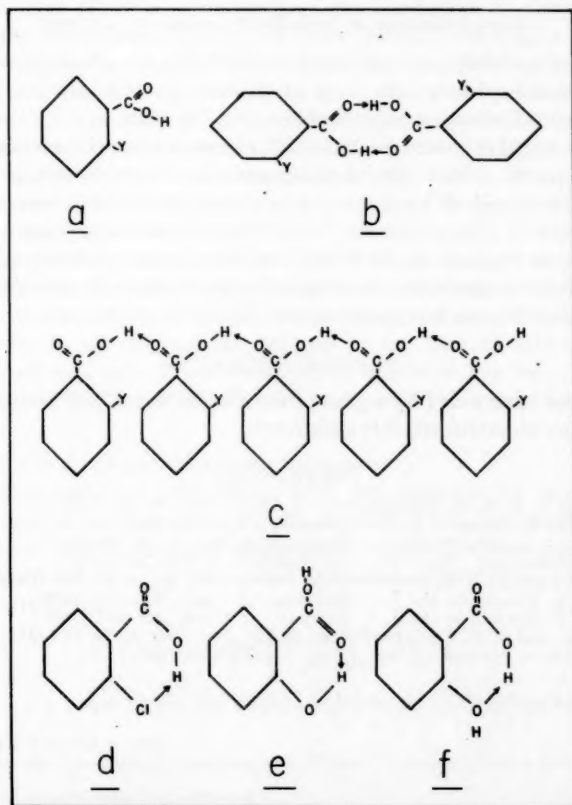

FIG. 5. Various molecular species which may be present in the ortho-substituted benzoic acids.

tetrachloride solution (Fig. 2A), and at 1690 cm^{-1} in benzene solution (Fig. 2D), appear to be the dimer peaks. The results shown in Figs. 1D and 2D indicate that appreciable amounts of the monomer are also present in benzene solution and the C=O peak at 1650 cm^{-1} (Fig. 2D) indicates that some polymer (Fig. 5c) or open dimer is also present.

Only two molecular species are present in the o-chlorobenzoic acid solution in carbon tetrachloride or benzene. The associated form is most probably a dimer. The results obtained in carbon tetrachloride solution are in agreement with those of Brooks et al. (6).

It is noteworthy that the position of the monomer band for the o-chlorobenzoic acid in benzene solution is lower by about 40 cm^{-1} than the corresponding band in carbon tetrachloride solution. This large decrease in frequency that occurs on changing the solvent is not apparent in the case of the benzoic or the salicylic acids and may well indicate that the monomer of o-chlorobenzoic acid in benzene solution is a chelate form such as that shown in Fig. 5d.

The results shown in Fig. 2F indicate that the most stable form of salicylic acid at low concentrations in benzene is the chelate form (Fig. 5e or f). As the acid concentration is increased, the appearance of the peak at 1655 cm^{-1} indicates the formation of some polymer and the appearance of the shoulder at 1710 cm^{-1} indicates the presence of some unchelated monomer. This unchelated monomer would be expected as an intermediate species arising from the equilibrium

chelated monomer ⇌ unchelated monomer ⇌ polymer.
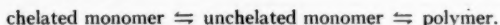
The strong band at 1660 cm^{-1} for the salicylic acid in carbon tetrachloride solution indicates the presence of large amounts of polymer in this solvent. The presence of unchelated monomer is shown by the shoulder at 1730 cm^{-1}.

As pointed out by Murty and Seshadri (7), the peaks for the associated form of the salicylic acid (Figs. 2C and F) occur at appreciably lower frequency than the dimer peaks for the benzoic acid or for the o-chlorobenzoic acid. This raises some question of whether these peaks at about 1655 cm^{-1} arise from dimers or polymers. The occurrence of a polymer peak in the case of the benzoic acid in benzene solution (Fig. 2D) at 1650 cm^{-1} seems to favor the conclusion that the associated species in salicylic acid solution is a polymer form probably of the type shown in Fig. 5c.

REFERENCES

1. M. M. Davies and G. B. B. M. Sutherland. J. Chem. Phys. **6**, 755 (1938).
2. J. T. Harris and M. E. Hobbs. J. Am. Chem. Soc. **76**, 1419 (1954).
3. S. Bratoz, D. Hadzi, and N. Sheppard. Spectrochim. Acta, **8**, 249 (1956).
4. D. Hadzi and N. Sheppard. Proc. Roy. Soc. (London), A, **216**, 247 (1953).
5. G. V. L. N. Murty and T. R. Seshadri. Proc. Indian Acad. Sci. A, **16**, 264 (1942).
6. C. J. W. Brooks, G. Eglinton, and J. F. Morman. J. Chem. Soc. 106 (1961).
7. C. J. W. Brooks, G. Eglinton, and J. F. Morman. J. Chem. Soc. 661 (1961).
8. G. V. L. N. Murty and T. R. Seshadri. Proc. Indian Acad. Sci. A, **19**, 17 (1944).
9. B. C. Barton and C. A. Kraus. J. Am. Chem. Soc. **73**, 4561 (1951).

INFRARED SPECTRA AND THE STRUCTURES OF
XANTHATES AND DIXANTHOGENS[1]

M. L. SHANKARANARAYANA AND C. C. PATEL[2]

ABSTRACT

The infrared spectra of representative dialkyl dixanthogens and a few xanthates have been examined. All these compounds have two strong absorption bands in the regions 1140–1265 and 1010–1080 cm^{-1}. On the basis of the shift of the bands with the changes in the substituents in the xanthic acid, the former band is assigned to the C=S group, while the latter to the CO group. Except in the ionic compounds, the canonical structure $---\bar{S}_2C=\overset{+}{O}R$ contributes very little to the structures of dixanthogens and covalent metal complexes.

Although infrared spectra of some of the xanthates and dixanthogens have been reported (1–5), an interpretation of the vibration frequencies of C=S and C—O groups of these compounds has not been attempted. The assignment of these group frequencies is somewhat difficult since both of them lie in the same region 1000 to 1275 cm^{-1}. Further, the absorption bands of both these groups are intense and very susceptible to the environmental changes in the molecules. In fact, Bellamy (6, p. 355) has pointed out that the location of the C=S absorption frequency has been a matter of some difficulty in organic thio compounds. Bak (7) *et al.* have assigned the band close to 1200 cm^{-1} to the C=S stretching mode of vibration in dithioesters, while Bellamy and Rogasch (8) have assigned the frequencies between 1000 and 1200 cm^{-1} for different types of thio compounds. These examples point out that the CO and C=S group frequencies fall in the same region. The CO symmetrical stretching vibration takes place around 1030 cm^{-1} in alkyl esters, alcohols, and silicon ethers and around 1200 cm^{-1} in aryl esters (9). In the present paper, it is assumed that the higher frequency around 1200 cm^{-1} is due to the C=S group, while the lower one around 1030 cm^{-1} is due to the CO group. The validity of this assumption is considered later.

Felumb (1) reported the infrared spectra of dimethyl, diethyl, and di-*n*-propyl dixanthogens and arbitrarily located the C=S frequency in the region 1210–1230 cm^{-1}. Little and Leja (2) gave the spectra of diethyl dixanthogen and some xanthates but could not make assignments to the frequencies because of the lack of information of infrared data. The infrared spectrum of potassium ethyl xanthate has been lately reported by several investigators (3–5) but they have not located the group frequencies for C=S and CO groups.

Gordy's Relation and C=S and CO Group Frequencies

Gordy's relation (10), in combination with the equation for the simple harmonic oscillator, has been helpful in assigning the P—S and PO frequencies (11). The same relations have been tried here to get the probable spectral regions for the C=S and CO vibrations. Gordy's relation [1] (10) gives the bond-stretching force constant, $k \times 10^{-5}$ in dynes/cm, as follows:

$$[1] \qquad k = 1.67N\left(\frac{\chi_A \cdot \chi_B}{d^2}\right)^{3/4} + 0.30,$$

where χ_A and χ_B are respectively the electronegativities (in Pauling's scale) of the atoms
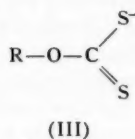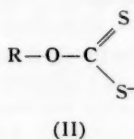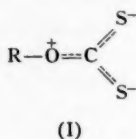
involved, d is the internuclear distance between the atoms in Å, and N is the bond order. The values of $k \times 10^{-5}$ for C=S and CO are 6.88 and 5.26 dynes/cm respectively (d for C=S is 1.6 Å) (12). By substituting these values in the equation for the simple harmonic oscillator, the frequencies for C=S and CO are 1161 and 1147 cm^{-1} respectively. In the above calculation for CO, d is taken as 1.43 Å, as given by Pauling (12). If, however, the average value of d for CO (1.38 Å) is taken, as deduced by Carrai and Gottardi (13), the ν_{CO} falls at 1170 cm^{-1}. These values of $\nu_{C=S}$ and ν_{CO} are so close to each other, and overlapping, that it is difficult to make assignments to C=S and CO groups when they occur in the same molecule, as in the derivatives of xanthic acids. In the following discussion, an alternative approach is, therefore, made to assign the frequencies on the basis of the effect of the substituents in xanthic acid.

Assignment of C=S and CO Frequencies of Xanthates

The xanthate ion can be represented in the following three forms.

involved, the π-bond character of C=S will be lowered while the σ bond of CO will acquire a partial π-bond character. This is expected to result in the lowering of the C=S frequency and the enhancing of the CO frequency. This expectation has come true when the corresponding absorption frequencies of sodium ethyl xanthate are compared with those of the symmetrical compound di-*n*-butyl dixanthogen (Table I). The C=S frequency in sodium xanthate is lowered to 1179 cm^{-1}, while that of CO is raised to 1040

Dithiocarbamate ion, which is similar to the xanthate ion, is also represented in the same way (14). Analogous to the structure of ionic salts of carboxylic acids, investigated in detail by Lecomte and co-workers (15) from the infrared studies, the structure of xanthate ion in ionic compounds can mainly be represented as a canonical structure (I). In such a case, the π-bond character of C=S will be lowered while the σ bond of CO will acquire a partial π-bond character. This is expected to result in the lowering of the C=S frequency and the enhancing of the CO frequency. This expectation has come true when the corresponding absorption frequencies of sodium ethyl xanthate are compared with those of the symmetrical compound di-*n*-butyl dixanthogen (Table I). The C=S frequency in sodium xanthate is lowered to 1179 cm^{-1}, while that of CO is raised to 1040

TABLE I

Characteristic frequencies of C=S and CO groups of the derivatives of xanthic acid

Substance	Medium	C=S frequency (cm^{-1})	CO frequency (cm^{-1})
Sodium ethyl xanthate (2)	Nujol mull	1179	1040
Potassium ethyl xanthate (3–5)	KCl disk (3) ⎫ KBr disk (4) ⎭	1143	1055
Potassium *n*-butyl xanthate (2)	Nujol mull	1153	1077
Cuprous ethyl xanthate (2)	"	1200	1037
Zinc ethyl xanthate (2)	"	1212	1035
Lead ethyl xanthate (2)	"	1220	1020
Diethyl dixanthogen	CCl₄ solution	1242 ⎫ (split 1262 ⎭ band)	1026
Diisopropyl dixanthogen	"	1258	1010
Di-*n*-butyl dixanthogen	"	1258	1026
Diisoamyl dixanthogen	"	1258	1024
Ethyl xanthic S-ethyl ester (5)	—	1190	1053–1000 (triply split band)

cm^{-1}, as compared to the respective frequencies of the dixanthogen at 1258 and 1026 cm^{-1}. Now, if sodium is replaced by potassium in the ethyl compound, the ionic character of the xanthate ion will increase according to the Fajan's rule and also according to the lower electronegativity of the bigger potassium ion. We thus expect the π-bond character of C=S to decrease further while that of CO to increase, resulting in further lowering of the C=S frequency and enhancement of the CO frequency. This expectation has also been realized, which is evident from the comparison of the C=S and CO frequencies of the sodium and potassium ethyl xanthates (Table I). The frequency for C=S in the potassium salt is lowered to 1143 cm^{-1} while that for CO is raised to 1055 cm^{-1}. When the ethyl group is replaced by the n-butyl group in the potassium xanthate both the C=S and CO bands move to higher frequencies (Table I), probably due to the greater electron-releasing tendency of the n-butyl group.

In a covalent compound such as cuprous ethyl xanthate, resonating structures (II) and (III) predominate. No bonding is expected between the covalent copper and π-bonded sulphur. This non-bonding is similar to the behaviors of arsenic (III) (13) and lead (II) (16) in their xanthates, studied by X-ray and electron diffraction respectively. Under such circumstances, the π-bond character of C=S and σ-bond character of CO are greatly enhanced in cuprous xanthate, as compared to those in the alkali metal xanthates. A shift of the C=S to the higher frequency and of the CO to the lower one could be expected for cuprous xanthate. A comparison of the C=S and CO frequencies of cuprous xanthate and of alkali metal xanthates confirms the above reasoning. It is seen from the above discussion that as the metal–sulphur bond strengthens, the CO vibration frequency and its bond order are lowered.

Much experimental data are not available on the spectra of the divalent metal xanthates. The relative shifts of C=S and CO frequencies of zinc and lead ethyl xanthates (Table I) are not in accordance with the electronegativities of their metal atoms. It is possible that other considerations such as the thermodynamic stability and the stereochemistry of the metal xanthates may also be contributory factors in determining the shifts of the C=S and CO frequencies in such compounds.

Apart from the discrepancy encountered in the divalent metal xanthates, the results of the alkali metal and cuprous xanthates are sufficient to indicate that the strong band around 1200 cm^{-1} is due to C=S and the band around 1030 cm^{-1} is due to CO absorption.

C=S and CO Group Frequencies of Dixanthogens

The dixanthogen absorption spectra (Table I and Fig. 1) do not show any appreciable change in the C=S and CO frequencies, even though the alkyl groups of different dixanthogens vary. The C=S group frequency is practically constant at 1258 cm^{-1} while that of CO, at 1025 cm^{-1}. A small shift of CO frequency to 1010 cm^{-1} in the case of diisopropyl dixanthogen is probably due to the vibrational coupling of the CO group with the C—C skeletal stretching vibration. Diisoamyl dixanthogen has also a similar branched alkyl group, but its remoteness from the CO group probably prevents the analogous interaction. The constancy of the C=S group frequency at 1258 cm^{-1} in the dixanthogens is due to the symmetry of the groups in either parts of the molecules. It is interesting to note that the asymmetric ethyl xanthic S-ethyl ester gives the C=S frequency at 1190 cm^{-1}. The splitting of the C=S band of diethyl dixanthogen (Fig. 1) is interesting and peculiar to this dixanthogen. Such a splitting has been observed with this compound both in the solid state (2) and in the carbon tetrachloride solution.
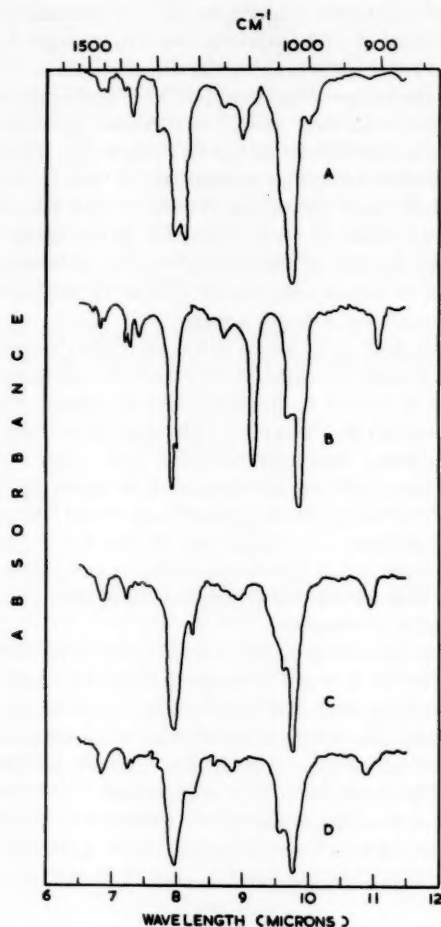
FIG. 1.   Infrared spectra of dialkyl dixanthogens. A, diethyl dixanthogen; B, diisopropyl dixanthogen; C, di-*n*-butyl dixanthogen; D, diisoamyl dixanthogen.

EXPERIMENTAL

Dixanthogens

Diethyl, diisopropyl, di-*n*-butyl, and diisoamyl dixanthogens were prepared by oxidation of the respective high-purity potassium alkyl xanthates by iodine and were purified by extraction with petroleum ether (b.p. 40–60° C). The purity of the dixanthogens was over 99.7% as analyzed by the method developed in this laboratory (17).

Spectra

The spectra of the dixanthogens in the region 700–4000 cm^{-1} were obtained in carbon tetrachloride solution (0.1 M), with a Perkin–Elmer double-beam recording Infracord spectrophotometer, Model 137. The spectra in the range 850–1500 cm^{-1} with NaCl prism are reproduced in Fig. 1. The infrared spectrum of diethyl dixanthogen in carbon

tetrachloride solution agrees well with that of the solid substance given by Little and Leja (2).

Diisopropyl dixanthogen gives rise to a characteristic intense band at 1087 cm^{-1}. This band is peculiar to this dixanthogen and may be due to the rocking mode of vibration of methyl groups, coupled strongly with the skeletal vibration of isopropyl group. A similar band is found around 1100 cm^{-1} in the derivatives of isopropyl alcohol as in isopropyl nitrate (6, p. 368) and diisopropyl ether (18). In the spectrum of the diethyl dixanthogen alone a medium band occurs at 1105 cm^{-1} owing to the rocking mode of vibration of C—CH$_3$.

ACKNOWLEDGMENT

REFERENCES

1. R. FELUMB.   Bull. soc. chim. France, 890 (1957).
2. L. H. LITTLE and J. LEJA.   Proceedings of the second international congress of surface activity. Vol. III. Butterworths Scientific Publications, London. 1957. p. 261.
3. J. I. JONES, W. KYNASTON, and J. W. HALES.   J. Chem. Soc. 614 (1957).
4. D. A. ANDREWS, F. G. HURTUBISE, and H. KRASSIG.   Can. J. Chem. 38, 1381 (1960).
5. E. KLEIN, J. K. BOSARGE, and I. NORMAN.   J. Phys. Chem. 64, 1666 (1960).
6. L. J. BELLAMY.   The infra-red spectra of complex molecules. 2nd ed. Methuen & Co. Ltd., London. 1958.
7. B. BAK, L. H. NYGAARD, and C. PEDERSEN.   Acta Chem. Scand. 12, 1451 (1958).
8. L. J. BELLAMY and P. E. ROGASCH.   J. Chem. Soc. 2121.(1960).
9. V. A. A. STUART, C. L. LAU, and H. BREEDERVELD.   Rec. trav. chim. 74, 747 (1955).
10. W. GORDY.   J. Chem. Phys. 14, 305 (1946).
11. R. C. GORE.   Discussions Faraday Soc. 9, 138 (1950).
12. L. PAULING.   The nature of the chemical bond. Cornell Univ. Press, Ithaca. 1960. p. 224.
13. G. CARRAI and G. GOTTARDI.   Z. Krist. 113, 373 (1960).
14. J. CHATT, L. A. DUNCANSON, and L. M. VENANZI.   Suomen Kemistilehti, B, 29, 75 (1956).
15. J. LECOMTE.   Discussions Faraday Soc. 9, 125 (1950).
16. H. HAGIHARA, H. UCHIKOSHI, and H. YAMASHITA.   Proceedings of the second international congress of surface activity. Vol. III. Butterworths Scientific Publications, London. 1957. p. 343.
17. M. L. SHANKARANARAYANA and C. C. PATEL.   Analyst, 86, 98 (1961).
18. R. B. BARNES, U. LIDDEL, and V. Z. WILLIAMS.   Ind. Eng. Chem. Anal. Ed. 15, 659 (1943).

THE CRYSTAL AND MOLECULAR STRUCTURES OF
m-DINITROBENZENE AND p-DINITROBENZENE[1]

J. TROTTER

ABSTRACT

The structures of m-dinitrobenzene and p-dinitrobenzene have been refined by three-dimensional $(F_o - F_c)$ syntheses. The results indicate that both nitro groups in each molecule are twisted 11° out of the aromatic plane, about the C—N bonds, in contrast to nitrobenzene, where the whole molecule is completely planar. These molecular configurations are shown to be in accord with those which might be expected from intramolecular steric effects. The dimensions of the three molecules have also been compared.

INTRODUCTION

The crystal structure of m-dinitrobenzene has recently been reinvestigated using new three-dimensional data, the refinement of positional and anisotropic temperature parameters proceeding by use of the block diagonal least-squares method (1). This analysis yielded a reasonably precise account of the geometry of the molecule: all the carbon and nitrogen atoms are situated on one plane, but each of the oxygen atoms is displaced from this plane by about 0.2 Å, the deviations being in such a sense that the molecular symmetry is m within the limits of experimental error. The nitro groups are thus rotated about the C—N bonds out of a completely planar configuration, the angles of rotation being about 11°.

The results of this least-squares refinement are, however, unsatisfactory in several respects. Firstly, there was a large increase (of about 20%) in the over-all scale factor during the three cycles of refinement. Secondly, the final anisotropic temperature parameters vary widely, haphazardly, and do not appear to correspond to any physically reasonable rigid-body vibrations of the molecule. Thirdly, although the deviations of the oxygen atoms from coplanarity suggest that the molecule has symmetry m, detailed study of the bond lengths and valency angles indicates that this is very far from being so, the measured values of two chemically identical bonds, for example, differing by 0.12 Å. It seems unlikely that these large bond length differences and large temperature factor variations can be real, and probably they result from some inadequacy of the refinement process. One possible source of error is unsuitability of the weighting system, but the weights used were those normally adopted, and there would appear to be no reason for supposing that they are unsuitable in this case. A second source of error is termination of the refinement process before shifts become negligible, but again the positional and temperature parameter changes in the final cycle were very small, and were not generally in directions which indicated that continued refinement would make the final results more reasonable. Thirdly, introduction of anisotropic thermal parameters at too early a stage in the refinement might introduce errors in positional parameters, but it is difficult to comment on this possible source of inaccuracy; the DEUCE least-squares program used automatically produces anisotropic temperature parameters, although it is, of course, possible to reinsert isotropic ones manually. Another obvious source of error might be inaccuracies in the measured structure factor data, but it is considered that this can be completely discounted, as the photographic records were

all very good, and inaccuracies in visual intensity estimation are unlikely to produce such wide variations in molecular dimensions and temperature factors as are observed.

In view of all these uncertainties it seemed that some useful information might be obtained by repeating the whole refinement process, using a different method. In order that the results might be comparable with those obtained for nitrobenzene (2), it seemed that differential syntheses would be most convenient, but since no program was available for computing these, it was decided to proceed, instead, by calculating three-dimensional $(F_o—F_c)$ syntheses. The final results should then be equivalent to those which would be obtained from differential syntheses with backshift corrections.

It also seemed that some useful information might be derived from a similar refinement of the crystal structure of *p*-dinitrobenzene. This structure had been investigated previously (3) and the molecular geometry had been established with considerable precision (4), but it was decided that it would be useful to refine it further so that the results would be directly comparable with those obtained for nitrobenzene and *m*-dinitrobenzene.

REFINEMENT OF THE STRUCTURES

m-Dinitrobenzene

Structure factors were calculated for all the observed reflections from the previous final positional parameters of the carbon, nitrogen, and oxygen atoms, but using an isotopic temperature factor $B = 4.5$ Å² for all the atoms. The discrepancy factor R was 22%, and the over-all scale factor had returned to the value prior to the anisotropic least-squares refinement. Further refinement proceeded by computing successive $(F_o—F_c)$ syntheses and altering the positional and isotropic temperature parameters to minimize the difference–density slopes and magnitudes at the atomic centers. After two cycles, R had been reduced to 19% and no further significant changes in atomic co-ordinates or temperature factors were indicated. Refinement was terminated at this point so that the results would be directly comparable with those for nitrobenzene. Any further work would require introduction of a contribution from the hydrogen atoms and of anisotropic thermal parameters for the heavier atoms, and in view of the unsatisfactory results which had already been obtained with the only program available to us for carrying out the refinement of anisotropic temperature factors, it was not considered worth while proceeding any further with the refinement. The measured structure factor data previously listed (1) should be multiplied by a scale factor 0.822 to convert them to an absolute scale.

p-Dinitrobenzene

No new structure factor data were collected for *p*-dinitrobenzene, but structure factors were calculated for all the reflections measured by Llewellyn (3), using the positional parameters of the carbon, nitrogen, and oxygen atoms listed by Abrahams (4), with $B = 4.6$ Å² for all the atoms. R was 25%. Refinement proceeded as for *m*-dinitrobenzene, and after two cycles of three-dimensional $(F_o—F_c)$ syntheses, R had been reduced to 19% and no further changes were indicated in any of the parameters.

CO-ORDINATES AND MOLECULAR DIMENSIONS

m-Dinitrobenzene

The positional and temperature parameters of the carbon, nitrogen, and oxygen atoms are listed in Table I. The atomic co-ordinates are referred to the principal crystallographic

TABLE I

Final positional and temperature parameters for m-dinitrobenzene (and deviations, Δ, from the aromatic plane)

Atom	x	y	z	B (Å²)	Δ (Å)
C_1	.1416	.3667	$-.0055$	3.5	-0.02
C_2	.1788	.4513	$-.1408$	3.5	$+0.02$
C_3	.2795	.4568	$-.1093$	3.5	-0.01
C_4	.3478	.3884	.0226	4.0	-0.01
C_5	.2999	.3032	.1363	4.0	$+0.01$
C_6	.1956	.2929	.1187	4.0	$+0.01$
N_1	.0297	.3535	$-.0197$	5.2	-0.02
N_2	.3282	.5479	$-.2419$	5.2	$+0.01$
O_1	$-.0065$	.2857	.1424	7.0	-0.25
O_2	$-.0189$	.4109	$-.1945$	7.0	$+0.21$
O_3	.2759	.6021	$-.4038$	7.0	$+0.21$
O_4	.4152	.5609	$-.1900$	7.0	-0.15

axes, x, y, z being expressed as fractions of the unit-cell edges.

The equation of the best plane through the carbon atoms is

$$0.0836X - 0.3945Y - 0.9151Z + 1.8230 = 0,$$

where X, Y, Z are expressed in Å units; the deviations of the atoms from this plane are listed in the final column of Table I. The equations of the planes of the nitro groups are

$$N_1O_1O_2: \ 0.1098X - 0.5803Y - 0.8070Z + 2.7621 = 0,$$

$$N_2O_3O_4: \ 0.2218X - 0.4850Y - 0.8459Z + 1.9737 = 0.$$

The angle between the plane of the carbon atoms and the $N_1O_1O_2$ plane is 12.4°, and between the carbon atom plane and the $N_2O_3O_4$ plane, 10.3°.

The bond distances and valency angles in the m-dinitrobenzene molecule, calculated from the co-ordinates of Table I, are shown in Fig. 1a. The estimated standard deviations of the atomic positions (5) are $\sigma(x) = \sigma(y) = \sigma(z) = 0.02$ Å for all the atoms.
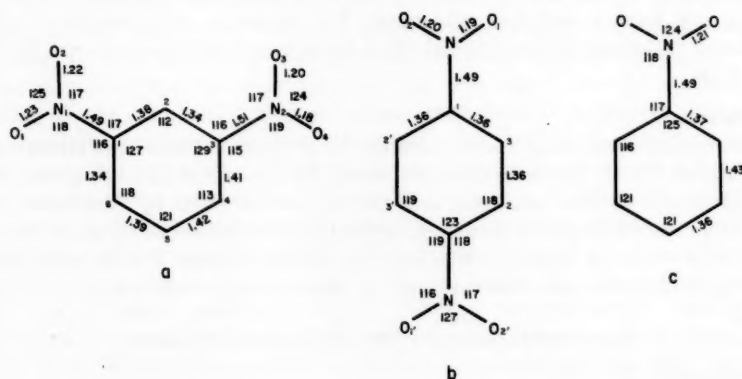

Fig. 1. Measured bond lengths (Å) and valency angles (deg) in (a) m-dinitrobenzene, (b) p-dinitrobenzene, and (c) nitrobenzene.

p-Dinitrobenzene

The final positional and thermal parameters are listed in Table II, *x*, *y*, *z* being

TABLE II

Final positional and temperature parameters for *p*-dinitrobenzene (and deviations, Δ,
from the aromatic plane)

Atom	x	y	z	B (Å²)	Δ (Å)
C_1	.0688	.1819	.0885	3.6	+0.01
C_2	.0317	−.1177	−.2042	4.2	+0.01
C_3	.1006	.0725	−.1165	4.2	−0.01
N	.1440	.3903	.1858	3.6	−0.01
O_1	.2171	.4719	.0587	5.5	−0.24
O_2	.1231	.4624	.3811	4.9	+0.18

co-ordinates referred to the principal crystallographic axes and expressed as fractions of the unit-cell edges.

The equation of the plane through the six carbon atoms of the aromatic ring is

$$0.5285X' - 0.6577Y + 0.5367Z' = 0,$$

where X', Y, Z' are co-ordinates expressed in Å units and referred to orthogonal axes a, b, and c'; the deviations of the atoms from this plane are given in the last column of Table II. The equation of the nitro group plane is

$$0.6697X' - 0.6313Y + 0.3911Z' = 0.1123,$$

and the angle between this plane and the plane of the aromatic ring is 11.8°.

The bond lengths and valency angles in the molecule were calculated from the co-ordinates of Table II, and are shown in Fig. 1*b*. The standard deviations of the atomic positions are about 0.02 Å for all the atoms.

DISCUSSION

The molecule of nitrobenzene in the crystalline state is completely planar within the limits of experimental error, the maximum deviation from the mean molecular plane being 0.03 Å, and the root mean square deviation, 0.016 Å (in comparison with an e.s.d. in atomic position of 0.014 Å). This suggests that the most stable configuration of a typical aromatic nitro compound, with only hydrogen atoms ortho to the nitro group, is a completely planar one. This is, of course, the configuration required by resonance theory, since maximum resonance interaction between the aromatic π-electrons and the substituent nitro group is obtained when the nitro group is coplanar with the aromatic ring. This situation may be contrasted with that in a molecule which has bulky substituents ortho to the nitro group; in a molecule of this type the steric effects of the bulky ortho groups cause the nitro group to be twisted markedly out of the aromatic plane, about the C—N bond. In nitromesitylene, for example, the angle of twist is 66° and the oxygen atoms lie one above and one below the aromatic plane at perpendicular distances of 0.95 Å from it.

The six-membered ring of carbon atoms in the *m*-dinitrobenzene molecule is completely planar within the limits of experimental error, the maximum deviation from the mean plane (Table I) being 0.02 Å and the root mean square deviation, 0.015 Å (e.s.d. of atomic position 0.02 Å). The nitrogen atoms also lie on this aromatic plane (deviations only

-0.02 Å for N_1 and $+0.01$ Å for N_2), but the oxygen atoms of each nitro group lie one above and one below the plane, so that each group is twisted about the C—N bond, out of the plane of the carbon and nitrogen atoms, the angles of twist being $12.4°$ for $N_1O_1O_2$ and $10.3°$ for $N_2O_3O_4$. The small difference between these two angles is probably not significant, so that each nitro group may be considered to be rotated out of the aromatic plane by $11.4°$. The mean oxygen atom displacement from this plane is 0.21 Å, and these displacements are in directions such that the symmetry $mm—C_2$, which would pertain in a completely planar model is reduced to $m—C_h$ (neglecting, for the moment, variations in bond distances and valency angles).

In the p-dinitrobenzene molecule all the carbon atoms lie in one plane, within experimental error, the maximum and root mean square deviations being 0.01 Å (Table II). The nitrogen atoms also lie on this aromatic plane, but the oxygen atoms of a nitro group are displaced one above and one below the plane, so that the group is rotated about the C—N bond $11.8°$, out of the plane of the carbon and nitrogen atoms. The differences between the oxygen atom displacements are probably not significant, the mean value being 0.21 Å. The displacements are in directions such that the symmetry $mmm—D_{2h}$ possessed by a planar model is reduced to $2/m—C_{2h}$ (only a center of symmetry being required from space group considerations).

We see then that while the nitrobenzene molecule is completely planar, in m-dinitrobenzene and p-dinitrobenzene the groups are all twisted out of the aromatic planes by about $11°$. Since the most stable configuration for the nitrobenzene molecule is apparently a completely planar one, and since the steric considerations in all three molecules are very similar, the author has previously considered that the deviations from planarity in m-dinitrobenzene and p-dinitrobenzene are probably the result of intermolecular forces (1, 2). However, it is now evident that all the nitro groups in m- and p-dinitrobenzenes are twisted out of the aromatic planes by about the same amount, although their environments in the crystals are not similar, and this suggests that perhaps some intramolecular steric effects, which are similar for both these molecules but absent in nitrobenzene, are operative.

In order to investigate intramolecular steric effects, planar models were constructed for all three molecules, using for the values of the van der Waal's radii: 1.40 Å for the oxygen atoms and 1.20 Å for hydrogen (Fig. 2). In all three molecules there is apparently

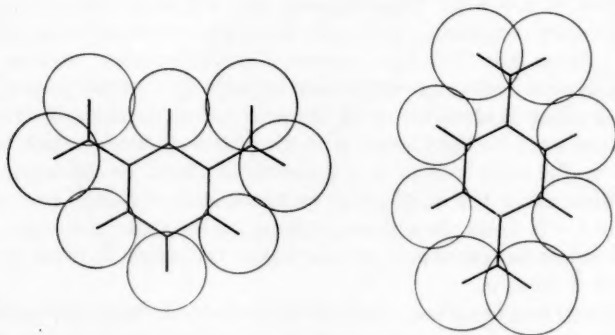Fig. 2. Coplanar configurations of m-dinitrobenzene and p-dinitrobenzene, drawn to scale with van der Waals radii: oxygen = 1.40 Å, hydrogen = 1.20 Å.

a small steric interference between the oxygen atoms and the neighboring ortho hydrogen atoms. For nitrobenzene, however (the model is similar to that for *p*-dinitrobenzene, but with one nitro group replaced, of course, by a much smaller hydrogen atom), this steric repulsion can be relieved by small in-plane displacements of the hydrogen atoms, and no displacements of the oxygen atoms from the aromatic plane are necessary. In-plane displacements would clearly be inadequate in the *m*-dinitrobenzene molecule (Fig. 2), where relief of steric repulsions between the oxygen atoms and that hydrogen atom which is ortho to both nitro groups can be accomplished only by out-of-plane displacements. The steric effects in *p*-dinitrobenzene are apparently very similar to those in nitrobenzene, but closer examination of Fig. 2 indicates that any in-plane displacements of the hydrogen atoms would result in steric interferences between these atoms, so that relief of oxygen–hydrogen steric effects would again have to involve deviations of the oxygen atoms from the aromatic plane. These simple considerations of the steric effects are certainly in accord with the experimentally determined molecular configurations.

The variations in the measured bond lengths for *m*-dinitrobenzene (Fig. 1*a*) are smaller than those previously noted in the least-squares refinement, but there is still quite a large difference between the values for two chemically identical bonds. However, a χ^2 test of the differences between the chemically equivalent bonds (Table III) shows

TABLE III

χ^2 test

	Least-squares refinement	Fourier refinement
$\Sigma\,[\Delta(l)]^2$	0.0219 Å^2	0.0107 Å^2
$\sigma^2(l) = [\sqrt{2}\sigma(x)]^2$	<0.0004 Å^2	0.0008 Å^2
$\chi^2 = \Sigma\,\Delta^2/\sigma^2$	>55	13.4
Degrees of freedom	6	6
Probability P	$0.001 > P$	$0.05 > P > 0.01$
Significance level	Highly significant	Possibly significant

clearly that these differences were in the highly significant range in the least-squares refinement, but have now been reduced to the possibly significant range. This improvement is still evident even if $\sigma(x)$ is taken as 0.02 Å for both sets of results. For *p*-dinitrobenzene the measured molecular dimensions (Fig. 1*b*) suggest that the molecule does not deviate from symmetry 2/*m*. When the mean bond distances in nitrobenzene (Fig. 1*c*), *m*-dinitrobenzene, and *p*-dinitrobenzene are compared, the most significant feature is that all the C—N distances are greater than the value usually quoted for the C(sp^2)—N single-bond length (1.475 Å). The measured molecular configurations indicate that some force, possibly resonance interaction, is tending to keep the molecules planar, or as nearly planar as steric effects will allow, so that the non-observance of any reduction of the C—N bond distances below the single-bond lengths might be due to the fact that any such reduction would further increase the steric repulsions.

ACKNOWLEDGMENTS

REFERENCES

1. J. Trotter. Acta Cryst. **14**, 244 (1961).
2. J. Trotter. Acta Cryst. **12**, 884 (1959).
3. F. J. Llewellyn. J. Chem. Soc. 884 (1947).
4. S. C. Abrahams. Acta Cryst. **3**, 194 (1950).
5. D. W. J. Cruickshank. Acta Cryst. **2**, 65 (1949).

THE OXIDATION OF NITRITE AND IODATE IONS BY HYPOCHLORITE IONS[1]

M. W. LISTER AND P. ROSENBLUM

ABSTRACT

The oxidation of nitrite ions and of iodate ions by hypochlorite ions in aqueous solution has been examined. The oxidation of nitrite is really a reaction of hypochlorous acid, with the slow stage $HOCl + NO_2^- + H_2O \rightarrow H_3O^+ + Cl^- + NO_3^-$. The rate constant is given by $\log k = 7.36 - 6450/RT$ (time in minutes, and the activation energy in calories). The oxidation of iodate is chiefly a reaction of hypochlorite ions, probably $ClO^- + IO_3^- \rightarrow Cl^- + IO_4^-$, although the rate is somewhat increased by a higher concentration of hydroxide ions. The rate constant is given by $\log k = 16.15 - 26,100/RT$. These results are compared with other oxidations by hypochlorite ions, to see if any general trends are apparent.

Sodium hypochlorite solution will oxidize many substances, and the mechanisms of these oxidations have been the subject of considerable investigation, e.g. ref. 1–4. Some of these reactions have, in fact, turned out to be reactions of free hypochlorous acid, but at present it does not seem possible to predict whether any particular reaction will go through hypochlorite ions or the free acid. On the other hand, there does seem to be a rough correlation between the heats of these reactions and their rates; for instance, the very exothermic oxidation of sulphite ions is very fast, while the slightly endothermic oxidation of iodate ions is slow. This is certainly what might be expected; however, there are one or two notable exceptions, and this matter will be briefly discussed later. The present work was undertaken in order to increase the information on which any generalizations about the reactions of hypochlorites could be based.

1. REACTION OF NITRITE AND HYPOCHLORITE IONS

This reaction has been known in relatively acid solution for a long time, and is the basis of one method for estimating nitrites. Some measurements on the reaction under these conditions have been made by Shilov (5), who found a considerable dependence of the rate on pH over the range 5 to 8. However, he gives very little detail about his results.

The present work was on the reaction in alkaline solution, where it was thought that a reaction of two ions might occur. As will be seen in what follows, this also proved to be a reaction of hypochlorous acid.

Experimental Method

Mixtures in solution of sodium hypochlorite, sodium nitrite, and sodium hydroxide of various concentrations were made up; these were then kept at constant temperature, and analyzed at intervals as described below.

The sodium hypochlorite was made in the usual way from sodium hydroxide and chlorine. The solutions consequently contained sodium chloride in amounts at least equimolar to the sodium hypochlorite. Sodium nitrite and hydroxide stock solutions were made from reagent grades of these chemicals. Reagent grade sodium chloride was added to control the ionic strength.

The solutions were kept stirred in a water thermostat, and, at intervals, 10-ml samples were pipetted out and analyzed as follows. The cooled sample was diluted to a known

volume in a volumetric flask, and the optical density of the diluted solution was measured at 292 mμ, where there is a maximum in the absorption spectrum of hypochlorite ions, and at 360 mμ, which is close to the maximum in the absorption spectrum of nitrite ions. A Beckmann DU spectrophotometer was used. The known extinction coefficients for the various ions at these wave lengths were checked on separate samples, and the following values were used in the calculations:

| Ion	$\lambda = 292$	360 mμ
OCl^-	345	10.2
NO_2^-	8.8	21.8
NO_3^-	6.4	0.01

It was assumed that all nitrogen was present either as nitrite or nitrate; hence, if the original concentration of nitrite is known, measurements at these two wave lengths suffice to determine the concentrations of hypochlorite, nitrite, and nitrate ions. This assumption was justified by the consistency of the results. Most of the disappearance of hypochlorite ions is due to reaction with nitrite, but a small part (between 0.1 and 0.5%) is due to their decomposition to chlorate and chloride ions. This is shown by the slow increase of the difference, $[NO_2^-]-[OCl^-]$. Results from a typical run are given in Table I. The

TABLE I

(Run 1; at 60° C; ionic strength 1.46; $[NaOH] = 0.3901$ M)

Time, min	$[OCl^-]$, M	$[NO_2^-]$, M	Difference, M	$\log [OCl^-]/[NO_2^-]$
0	0.0951	0.3255	0.2304	$\bar{1}.466$
60.4	0.0834	0.3139	0.2305	$\bar{1}.424$
120.2	0.0745	0.3050	0.2305	$\bar{1}.388$
210.7	0.0622	0.2927	0.2305	$\bar{1}.327$
331.0	0.0505	0.2811	0.2306	$\bar{1}.254$
481.2	0.0392	0.2698	0.2306	$\bar{1}.162$
692.2	0.0281	0.2587	0.2306	$\bar{1}.036$
1411.6	0.0100	0.2407	0.2307	$\bar{2}.619$

last column gives $\log [OCl^-]/[NO_2^-]$, which should give a straight line when plotted against time if the reaction is first order in hypochlorite and in nitrite ions. This was found to be the case for all runs.

The evaluation of the rate constants was done as follows. Two reactions are occurring simultaneously in the mixture:

$$NO_2^- + OCl^- \rightarrow NO_3^- + Cl^-, \quad k_1,$$

$$2OCl^- \rightarrow ClO_2^- + Cl^-, \quad k_2,$$
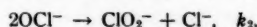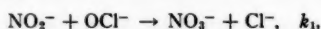
where the rate constants are respectively k_1 and k_2. The second reaction is followed by further oxidation of chlorite to chlorate ions. Then if $[OCl^-] = x$, and $[NO_2^-] = y$, these equations require that

$$\frac{dx}{dt} = -k_1 xy - \frac{3}{2} k_2 x^2,$$

$$\frac{dy}{dt} = -k_1 xy.$$

The rigorous solution of these equations is difficult; but since k_2 is small, an approximate solution can be obtained as follows.

If $k_2 = 0$, it is easily shown that the solution is

$$\ln \frac{x_0 y}{y_0 x} = -k_1(x_0-y_0)t,$$

where x_0 and y_0 are the initial concentrations. Under these conditions a plot of $\ln(x/y)$ against time would give a straight line of slope $k_1(x_0-y_0)$.

If k_2 is not zero, the equations above give

$$\frac{d \ln(x/y)}{dt} = k_1(x-y) - \frac{3}{2} k_2 x,$$

and since $(x-y)$ is very nearly constant and k_2 is small, in practice a plot of $\ln(x/y)$ against time does in fact give a virtually straight line. Table I, for instance, shows that in run 1, $(x-y)$ varied by only 0.13%; and the slope of the graph is such that k_1 is of the order of 100 times as large as k_2. If s is the slope of the graph of $\ln(x/y)$ against time, then approximately

$$s = k_1\overline{(x-y)} - \frac{3}{2} k_2 \bar{x},$$

where the bar over the symbols indicates the average value during a run. The rate constant k_1 was calculated from this equation, with the results given in Table II; k_2 was

TABLE II

Run	Temp., °C	Ionic strength	Initial concentrations, g-mol./l.			$k_1 \times 10^3$, (g-mol./l.)$^{-1}$ min^{-1}
			[OCl$^-$]	[NO$_2^-$]	[OH$^-$]	
1	60.0	1.46	0.0978	0.3283	0.390	6.18
2	"	1.46	0.0978	0.3283	0.390	6.12
3	"	1.53	0.2942	0.1028	0.391	5.98
4	"	1.53	0.2942	0.1028	0.391	5.94
5	"	1.43	0.0966	0.3283	0.196	15.93
6	"	1.42	0.0966	0.3283	0.196	15.89
7	"	1.50	0.0963	0.2462	0.117	26.59
8	"	1.50	0.0963	0.2462	0.117	26.48
9	"	2.65	0.0957	0.3283	0.390	7.28
10	"	2.65	0.0957	0.3283	0.390	7.28
11	70.0	1.45	0.0949	0.3265	0.388	13.17
12	"	1.45	0.0949	0.3265	0.388	13.15
13	50.0	1.47	0.1215	0.3299	0.397	2.645
14	"	1.47	0.1215	0.3299	0.397	2.674

taken from reference 1, the following values being used:

T, °C	50	60	70
$k_2 \times 10^3$, (g-mol./l.)$^{-1}$ min^{-1}	1.5	5.0	15.5

The values in Table II show that the rate is dependent on the hydroxide concentration; and, in fact, [OH$^-$].k_1 is approximately constant, as shown by the following values, all for 60° C:

Runs	1, 2	5, 6	7, 8
[OH$^-$].$k_1 \times 10^3$	2.40	3.11	3.11

This is equivalent to saying that the rate is proportional to the hydrogen ion concentration, and the most probable explanation is that this is really a reaction of hypochlorous acid, with

$$\text{rate} = k[\text{HOCl}].[\text{NO}_2^-].$$

Nitrous acid is a much stronger acid than hypochlorous, so it is much more likely that the H^+ is attached to the hypochlorite. On this assumption, the true rate constant, k, is given by

$$k = \frac{k_1[\text{OH}^-]}{K_h},$$

where K_h is the equilibrium constant for the hydrolysis of hypochlorite ions:

$$\text{OCl}^- + \text{H}_2\text{O} \rightleftharpoons \text{HOCl} + \text{OH}^-.$$

The ionization constant of hypochlorous acid is 3.8×10^{-8} at $27°$ C (6), and combining this with the ionization constant of water, K_h is 3.1×10^{-7} at $27°$ C. At $25°$ C, ΔH for this hydrolysis is 11.0 kcal; if we assume that this value holds up to $60°$ C, then K_h is 1.92×10^{-6} at $60°$ C. This value cannot be claimed to be very accurate, but is the best available on the present data. Hence $k = 1.61 \times 10^3$ (g-mol./l.)$^{-1}$ min^{-1} at $60°$ C.

The data in Table II make the apparent activation energy 17.4 kcal/g-mol. However, since the heat of hydrolysis of hypochlorite ions is 11.0 kcal, the true activation energy is 6.4 kcal. If k is given by the usual formula $k = Ae^{-E/RT}$, then $\log A = 7.41$. This is a rather small value, but there are others as small (see e.g. ref. 7).

Runs 7 and 8, in conjunction with the others, show that the rate constant increases with ionic strength, though the change is fairly small.

2. REACTION OF HYPOCHLORITE AND IODATE IONS

The total reaction here is

$$\text{NaOCl} + \text{NaIO}_3 + 2\text{NaOH} \rightarrow \text{NaCl} + \text{Na}_3\text{H}_2\text{IO}_6.$$
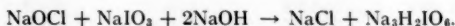
It was checked, by analytical methods given below, that the number of gram-molecules of periodate formed was within 1/2% of the number of gram-molecules of iodate disappearing. This confirms the stoichiometry of the reaction, and also checks the analytical methods. In alkaline solution a precipitate of sodium periodate forms. This was analyzed and found to be $\text{Na}_3\text{H}_2\text{IO}_6$, in agreement with the phase diagram for the system sodium hydroxide, periodic acid, water, as found by Hill (8).

The reaction was followed by mixing solutions of sodium hypochlorite and reagent grade sodium iodate and sodium hydroxide, with sodium chloride added to keep the ionic strength constant. The mixture was kept at constant temperature, and samples for analysis were taken at intervals. It was found that both hypochlorite and periodate ions absorb light strongly at about 300 mμ, so spectrophotometric analysis was not possible. The following titrations were therefore used.

Methods of Analysis

A sample was taken, cooled in ice for a short time, and any sodium periodate was filtered off. The solution was then allowed to warm up to room temperature, and aliquots were pipetted out for analysis. This procedure was necessary, as, otherwise, sodium periodate crystallized from the solution after pipetting. The aliquots were analyzed by the following methods.

(a) The aliquot was diluted and mixed with a known volume of standardized arsenious oxide solution and a large excess of sodium bicarbonate. Then 3 g of potassium iodide was added, and the excess arsenious oxide was titrated with standard iodine solution. In this titration the hypochlorite first oxidizes the arsenite to arsenate; and then, on adding potassium iodide, the periodate liberates iodine (which reacts with the arsenite):

$$Na_2H_2IO_6 + 2KI + H_2O \rightarrow NaIO_3 + 2KOH + 2NaOH + I_2.$$
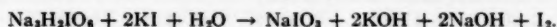
Hence this titration measures hypochlorite plus periodate. It is essential to allow the sodium hypochlorite to react before adding potassium iodide.

(b) The aliquot was mixed with excess dilute (about 0.7 N) sulphuric acid and boiled for 10 minutes. This treatment destroys hypochlorite, but did not affect the iodate and periodate present. The solution was then cooled, excess potassium iodide was added, and the liberated iodine was titrated with sodium thiosulphate. This titration measures iodate plus periodate.

(c) The aliquot was boiled with dilute sulphuric acid as in (b). Borax was added in considerable excess (the pH being about 8); then potassium iodide was added and the liberated iodine was titrated with arsenious oxide. This measures the periodate alone.

From these titrations the concentrations of hypochlorite and iodate ions in the solution could be calculated. The constancy found for the difference, $[OCl^-]-[IO_3^-]$, besides being evidence of the stoichiometry of the reaction, is a check on the reliability of the analytical methods. In this reaction, chlorate formation accounted for less than 0.1% of the total decomposition.

The results show that the reaction is first order in hypochlorite and iodate ions; hence the equations that governed the reaction with nitrite apply here also. The results of a typical run are given in Table III.
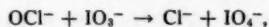
TABLE III

(Run at 60.0° C; ionic strength 1.23; $[NaOH] = 0.4328\ M$)

Time, min	$[OCl^-]$, M	$[IO_3^-]$, M	Difference	$\log[OCl^-]/[IO_3^-]$
0	0.1798	0.06009	0.1197	1.0826
34.0	0.1630	0.04321	0.1198	1.3277
68.5	0.1511	0.03233	0.1188	1.5423
107.8	0.1430	0.02295	0.1200	1.8300
151.5	0.1359	0.01732	0.1186	2.0605
196.5	0.1319	0.01246	0.1194	2.3603
241.0	0.1284	0.00901	0.1194	2.6572
291.0	0.1260	0.00657	0.1194	2.9547

The values of the rate constant, k_1, are given in Table IV. Inspection of these values shows that there is little change of the rate constant with hydroxide concentration. Apart from a degree of scattering in the constants, there seems to be a definite upward drift of the rate constant with hydroxide concentration. Roughly the constants at 60° C obey the equation

$$k_1 = 5.08 \times 10^{-2}(1+0.195[NaOH]_0).$$

The main reaction is therefore one of hypochlorite ions, presumably

$$OCl^- + IO_3^- \rightarrow Cl^- + IO_4^-,$$

but there is some third-order reaction with hydroxide ions as well.

TABLE IV

Run	Temp., °C	Initial				Final [OH⁻]	$k_1 \times 10^2$, (g-mol./l.)⁻¹ min⁻¹
		Ionic strength	[OCl⁻]	[IO₃⁻]	[OH⁻]		
15	60.0	1.40	0.1798	0.06009	0.433	0.325	5.35
16	,,	1.41	0.1913	0.07688	0.418	0.309	5.39
17	,,	1.35	0.0690	0.1887	0.392	0.299	5.48
18	,,	1.36	0.0656	0.1864	0.406	0.315	5.57
19	,,	1.31	0.0667	0.1916	0.574	0.495	5.67
20	,,	1.34	0.0683	0.1885	0.582	0.511	5.91
21	,,	1.31	0.0648	0.1887	0.190	0.110	5.13
22	,,	1.31	0.0649	0.1884	0.190	0.110	5.36
23	50.0	1.36	0.0597	0.2043	0.383	0.305	1.64
24	,,	1.36	0.0598	0.2037	0.384	0.305	1.60
25	40.0	1.38	0.0606	0.2042	0.389	0.299	0.441
26	,,	1.36	0.0602	0.1958	0.386	0.299	0.450
27	60.0	1.36	0.0627	0.1608	1.014	0.929	6.02
28	,,	1.36	0.0627	0.1608	1.014	0.929	6.11

The dependence on temperature corresponds to an activation energy of 26.1 kcal/g-mol. Expressing k_1 as $Ae^{-E/RT}$, $\log A = 15.83$. This is a relatively high value, though not unprecedentedly high.

3. DISCUSSION OF RESULTS

A number of oxidations by hypochlorite have now been examined by various workers, and it is of interest to see whether any generalizations can be made. Table V gives a

TABLE V

Reaction	$\log A^*$	Activation energy, kcal	ΔH^0, kcal	Ref.
OCl⁻ + IO₃⁻	16.15	26.1	2.8	—
HOCl + NO₂⁻	7.36	6.45	−36.2	—
OCl⁻ + OCl⁻	12.03	24.8	− 5.7	1
OCl⁻ + ClO₂⁻	11.52	20.8	−21.6	1
HOCl + OCN⁻	12.30	15.1	—	9
HOCl + Br⁻	8.55	4.5	− 7.5	3
OCl⁻ + MnO₄⁻³ †	13.96	14.1	—	4
HOCl + HC₂O₄⁻	15.76	15.0	−82.5	10
OCl⁻ + ClO₃⁻	Very slow		−22.5	—
OCl⁻ + SO₃⁻⁻	Very fast		−82.1	—
OCl⁻ + CN⁻	,, ,,		−84.0	—
OCl⁻ + I⁻	,, ,,		−28.4/OCl⁻	—

*Time in minutes.
†This rate is proportional to [H₃O⁺]³.

summary of these reactions. The first column gives the reagents indicating whether hypochlorous acid or hypochlorite ions are involved. The activation energies and $\log A$ values refer to the reactions as written, allowing for hydrolysis to HOCl where necessary. The ΔH^0 values also refer to the reactions as written, and assume that the reagents and products are all in aqueous solution. The last four entries are for reactions producing, respectively, perchlorate, sulphate, cyanate, and iodate ions. Here only qualitative observations on the rates are available, but the rates are either very fast or very slow.

Table V perhaps chiefly emphasizes our limited knowledge of the reactions of hypochlorites, but slight indications of trends are apparent. In the first place, log A generally falls when E does, so the actual rate constants are not as different as the activation energies would suggest. The fall in log A is not great enough to offset the change in activation energy; in fact it is about half as large as would be necessary for this. At present no general explanation is suggested.

There is some indication that, if the reaction is relatively exothermic, the activation energy is lower. This is perhaps to be expected, since if the new bond to oxygen is strong, this would tend to lower the energy of the activated complex as it is formed. However, this trend is not universal; for instance, the very exothermic oxidation of oxalate has quite a high activation energy. This particular reaction may be a little different from the others, since it is apparently not an oxygen transfer but an electron transfer; although it could be formulated either way. A more puzzling case is the reluctance of hypochlorite ions to oxidize chlorate ions to perchlorate, although this would be a fairly exothermic process. Some of these reactions involve hypochlorous acid, and some hypochlorite ions, but at present no general explanation can be offered for this distinction.

REFERENCES

1. M. W. LISTER. Can. J. Chem. **34**, 465 (1956).
2. F. FOERSTER and P. DOLCH. Z. Elektrochem. **23**, 127 (1917).
3. L. FARKAS, M. LEWIN, and R. BLOCH. J. Am. Chem. Soc. **71**, 1988 (1949).
4. M. W. LISTER and Y. YOSHINO. Can. J. Chem. **39**, 96 (1961).
5. E. A. SHILOV. J. Appl. Chem. (U.S.S.R.), **17**, 354 (1944).
6. M. W. LISTER. Can. J. Chem. **30**, 879 (1952).
7. E. A. MOELWYN-HUGHES. The kinetics of reactions in solution. 2nd ed. Oxford University Press. p. 76.
8. A. E. HILL. J. Am. Chem. Soc. **50**, 2678 (1928).
9. M. W. LISTER. Can. J. Chem. **34**, 489 (1956).
10. R. O. GRIFFITH and A. MCKEOWN. Trans. Faraday Soc. **28**, 518 (1932).

THE ELECTRONIC STATES OF LINEAR METHYLENE[1]

G. W. KING AND G. L. MALLI[2]

ABSTRACT

The electronic energy levels of the linear methylene radical, with r(C—H) = 1.0295 Å, have been calculated by the LCAO/MO/CI procedure. The state of lowest energy has $^3\Sigma_g^-$ symmetry, and is accompanied by low-lying $^1\Delta_g$ and $^1\Sigma_g^+$ states. Allowed intravalence shell transitions from the ground state ($^3\Pi_u-^3\Sigma_g^-$, $^3\Sigma_u^--^3\Sigma_g^-$) are too high in energy to account for the observed transition at 8.6 ev, indicating that the latter is of Rydberg type if it is between linear combining states.

INTRODUCTION

A spectroscopic transition in absorption at 8.6 ev, obtained during the flash photolysis of diazomethane, has been assigned to the elusory methylene radical by Herzberg and Shoosmith (1), who showed that the lower combining state has a bond angle between 140° and 180° and is non-totally symmetrical. Although experimental data did not permit a complete analysis, it appeared very likely (2) that the spectrum arises from a $^3\Sigma_g^-$ linear ground state, with r''(C—H) in the range 1.029–1.034 Å. Photolysis of diazomethane in solid inert gas matrices at low temperatures has also yielded a product, tentatively identified as methylene, with absorption bands in the near ultraviolet (3, 4). More recently, further flash photolysis work on diazomethane vapor has revealed an extensive absorption spectrum between 6000 and 9000 Å, which may also be due to methylene (2). This spectrum resembles the α-band system of NH_2 (5) and is probably due to an analogous transition ($^1B_1-^1A_1$) between states differing in geometry, but with the $^1A_1$ state lying above the triplet ground state.

Theoretical predictions of the shape and electronic structure of methylene present a divergence of views (6, 7, 8). Apart from these and other qualitative discussions on the nature of the ground state (9, 10), quantitative LCAO/MO/SCF calculations by Padgett and Krauss (11) indicated a $^3B_1$ ground state with an equilibrium bond angle of 120°, while more extensive calculations by Foster and Boys (12) gave the same ground state with an angle of 129°; but in the latter work, the calculated energy of the corresponding $^3\Sigma_g^-$ linear state was greater by only 0.3 ev, a difference that is not significant when compared with the accuracy of the calculation. In both these papers, electronic energy was determined as a function of bond angle, the results confirming Walsh's prediction (13) that if the ground state is a triplet it has linear, or nearly linear, geometry. Walsh also concluded that for such a ground state, the allowed transition at longest wavelengths would occur in the far ultraviolet, but could be either intra- or extra-valence shell in character. However, Padgett and Krauss predicted a low-energy $^3\Pi_u$ state permitting a non-Rydberg ($^3\Pi_u-^3\Sigma_g^-$) allowed transition at 1.5 ev; for slightly bent states, the corresponding ($^3B_1-^3A_1$) transition would also be expected to lie at fairly long wavelengths.

It is clear that further theoretical work on methylene is desirable. Padgett and Krauss and Foster and Boys have both calculated the energies of a few excited states. We report here the values of a much larger number of these for the linear molecule, obtained by procedures which, on the basis of previous work, give useful semiquantitative results.

By the Franck–Condon principle, calculated energies for transition in absorption should give the positions of vibrational bands of maximum intensity in such excited states as may prove to be bent.

THEORETICAL

The LCAO/MO/CI method is outlined in previous papers (14, 15), whose notation is followed here. Accurate wave functions $\Psi'_k(q_0 \ldots {}_N)$ for the stationary states of a molecular system can be constructed as sums of Slater determinants Φ_p only if a complete set of basic single-electron molecular spin orbitals $\phi_{i_0}(\mathbf{r}_e)$ are available. In practice it is necessary to use a restricted number of MSO's as the basic set for approximating to the wave functions of a system. Foster and Boys (12) used exponential functions expanded into a limited number of configurational determinants. On the other hand, in the SCF calculations of Padgett and Krauss (11), Ψ_k was approximated by a single Slater determinant or by a small number of these in linear combination, a modified Hartree–Fock procedure being used to obtain the best MSO's. In general, minimization of the expectation values E_k and E_l for the energies of two states Ψ_k and Ψ_l (necessarily obeying the orthogonality restriction $\int \Psi^*_k \Psi_l d\tau = \delta_{kl}$) will lead to different values of parameters and scaling factors within a restricted set of MSO's from which wave functions are constructed, and energy minimization for each separate state presents a formidable problem in computation. Best SCF ground-state orbitals cannot be assumed suitable for calculating excited-state energies; Padgett and Krauss made this assumption, although they introduced a limited perturbation treatment to compensate for errors.

In the calculation reported here, the basic MSO's were symmetry orbitals constructed from Slater AO's with fixed parameters, and had the same form for all the electronic states considered. This relatively crude approximation simplifies the orthogonalization of wave functions and reduces computation for a large number of electronic states to manageable proportions: errors are reduced by allowing for the interactions between large numbers of configurations. In view of the difficulty of evaluating multicenter integrals over AO's that occur in the calculation, a more sophisticated procedure does not seem justified at present.

Application to Methylene

A linear centrosymmetric geometry was assumed for the radical, with $r(\text{C—H}) = 1.0295$ Å. With Cartesian axes centered on the carbon atom and hydrogen atoms H' and H'' on the positive and negative z-axis respectively, the basic Slater AO's have the following form:

$$h' \equiv \text{H}'(1s) = (\delta_\text{H}/\pi)^{1/2} \exp(-\delta_\text{H} r')$$
$$h'' \equiv \text{H}''(1s) = (\delta_\text{H}/\pi)^{1/2} \exp(-\delta_\text{H} r'')$$
$$1s \equiv \text{C}(1s) = (\delta'_c/\pi)^{1/2} \exp(-\delta'_c r_c)$$
$$s \equiv \text{C}(2s) = (\delta_c^{5/3}\pi)^{1/2} r_c \exp(-\delta_c r_c)$$
$$\left.\begin{array}{l} \pi \equiv \text{C}(2p_x) = \\ \bar\pi \equiv \text{C}(2p_y) = \\ \sigma \equiv \text{C}(2p_z) = \end{array}\right\} (\delta_c^5/\pi)^{1/2} r_c \exp(-\delta_c r_c) \left\{\begin{array}{l} x_c \\ y_c \\ z_c \end{array}\right.$$

with $\delta_\text{H} = 1$, $\delta'_c = 5.70$, $\delta_c = 1.57$. The latter value and that for $r(\text{C—H})$ were chosen together to facilitate interpolation in tables of molecular integrals (16); the internuclear separation is itself only defined approximately by experiment. The carbon 2s orbital was used in the orthogonalized form,

$$s^0 = (s - 0.20848.1s)/0.97803,$$

in evaluating all carbon mononuclear integrals (14). The AO's h', h'', s, π, $\bar{\pi}$, and σ form a reducible representation of the $D_{\infty h}$ point group for the linear molecule

$$\Gamma = 2\Sigma_g{}^+ + 2\Sigma_u{}^+ + 2\Pi_u,$$

and the set of orthogonal LCAO/MO's, which form bases for the irreducible representations and were used in the calculation, are given in Table I.

TABLE I

LCAO/MO's for linear methylene

	Symmetry	Analytical form
ϕ_0	$\sigma_g{}^+$	$0.5280s + 0.3400(h' + h'')$
ϕ_1	$\sigma_u{}^+$	$0.5300\sigma + 0.4200(h' - h'')$
$\phi_2 = \phi_3{}^*$	π_u	$2^{-\frac{1}{2}}(\pi + i\bar{\pi})$
$\phi_3 = \phi_2{}^*$	π_u	$2^{-\frac{1}{2}}(\pi - i\bar{\pi})$
ϕ_4	$\sigma_g{}^+$	$1.5500s - 0.9995(h' + h'')$
ϕ_5	$\sigma_u{}^+$	$1.4990\sigma - 1.1875(h' - h'')$

The carbon $1s$ electrons were taken as screening the nucleus, leaving a total of 924 different ways of distributing the remaining six electrons among the MSO's ϕ_i to satisfy the Pauli principle. Since each way of doing this gives one determinantal function Φ_p, a very large secular equation would have to be solved for the energy, but the order can be reduced in various ways. A somewhat similar procedure to that used here has been outlined by Slater (17) for the diatomic oxygen molecule. We need only select in the first place those determinantal functions Φ_k with eigenvalue $M_S = 0$ (three α and three β spins for the electrons) of S_z, the z-component of the spin operator, since every electronic state has a component with this eigenvalue. The MSO's ϕ_i and the determinants Φ_k constructed from them are eigenfunctions of the symmetry operators i and C_ϕ of the $D_{\infty h}$ point group, which commute with the Hamiltonian for the system and each other, thus factorizing the secular determinant. Further factorization is achieved by recombining the Φ_k as eigenfunctions of S^2; suitable linear combinations Ω^s are readily found for states with up to four singly occupied MO's, but the 20 states with six singly occupied orbitals were not included owing to the complexity of the wave functions resulting from their spin degeneracy. These states, energetically high in LCAO/MO approximation, should only contribute negligibly to the wave functions $\Psi_k{}^S$ of the states considered below. Finally, for configurations containing partly filled orbitals ϕ_2 and ϕ_3, the Ω^s are not eigenfunctions of the operator σ_v (reflection in a plane through the nuclei), and fresh linear combinations are taken to remedy this. Thus the original secular determinant can be factored into blocks, each referring to one particular symmetry class and multiplicity. These reduced equations were rigorously solved on a Bendix D-15G computer to obtain their lowest roots.

Evaluation of Matrix Elements

The elements of the secular determinants expand into sums of integrals over the AO's, on either one, two, or three nuclear centers. Mononuclear and two-center integrals were obtained from analytic expressions (18, 19) and tables (16, 20), each integral being calculated by more than one method where possible, to minimize errors.

Of the various approximations available, the Ruedenberg–Mulliken method (21) was used for evaluating three-center integrals, by which the latter are expanded as sums of

one- and two-center integrals. The nuclear attraction integrals $(\sigma:h'h'')$ and $(H'':h'\sigma)$, of form

$$(A:\chi_b\chi_c) = \int \chi_b{}^*(1) \; |Z_a/r_a| \; \chi_c(1)d\tau_1,$$

were evaluated by the method of Barker and Eyring (22). The Ruedenberg–Mulliken approximation for the integral

$$(h'\pi:h''\pi) = \iint h'(1)\pi(1) \; |1/r_{12}| \; h''(2)\pi(2)d\tau_1 d\tau_2$$

fails here, giving the value zero. Gray, Ross, and Yates (23) found an analogous situation in their work on benzene, and give an approximate formula for the integral which was used in this calculation.

RESULTS

The relative energies of all the states considered are given in Table II. These include: the three states $^3\Sigma_g{}^-$, $^1\Delta_g$, and $^1\Sigma_g{}^+$ of lowest energy; the $^3\Pi_u$ and $^3\Sigma_u{}^-$ states, which can

TABLE II

Calculated energy levels

	Calculated energy (ev)		
Symmetry	This work	Padgett and Krauss	Foster and Boys
$^3\Sigma_g{}^-$	0.00	0.00	0.00 ev
$^1\Delta_g$	2.17	2.0	2.6
$^1\Sigma_g{}^+$	3.30	3.7	
$^5\Sigma_g{}^-$	15.94		
$^3\Delta_g$	19.99		
$^3\Pi_u$	20.35	1.5	
$^3\Sigma_g{}^+$	21.60		
$^1\Pi_u$	25.56		
$^1\Sigma_g{}^-$	27.17		
$^3\Sigma_u{}^-$	27.65		
$^1\Sigma_u{}^-$	34.46		

spectroscopically combine with the ground $^3\Sigma_g{}^-$ state; and a number of other states differing in multiplicity from these, whose calculation used many of the same basic integrals. Detailed energy calculations were not carried out for the Π_g states, which cannot combine with any of the three low-lying states, or for the $\Sigma_u{}^+$ states, which cannot combine with the ground state and which, preliminary LCAO/MO calculations showed, were some 40 ev higher in energy.

The low-lying group of states $^3\Sigma_g{}^-$, $^1\Delta_g$, and $^1\Sigma_g{}^+$ all arise, in LCAO/MO approximation, from the configuration $(\sigma_g{}^2\sigma_u{}^2\pi_u{}^2)$; similar states occur in the oxygen and boron molecules which also have two electrons in degenerate π-orbitals. The calculated energies agree well with those found by Padgett and Krauss (11) and by Foster and Boys (12), which are also shown in Table II. However, the $^3\Pi_u$ state is found to be 20 ev above the ground state, much higher energetically than in the former authors' calculations, and in accordance with Walsh's predictions (13).

In calculations such as these, the basic set of MSO's does not include extravalence shell orbitals, formed from AO's with quantum number $n > 2$, since values for all the necessary integrals are not readily available. Experimentally it is known that many simple organic molecules have Rydberg states some 10 ev above the ground state, leading

to ionization potentials in the 10–15 ev region. These Rydberg states should properly be included in a configuration interaction scheme. In the methylene radical, there are no low-lying excited states which can combine with the ground state; and since the ionization potential is 11.7 ev (24), it must be concluded that the lowest excited states of many species shown at high energy in Table II are in fact largely Rydberg in character, and occur at lower energies. In particular the observed transition at 8.6 ev, if it indeed arises from the $^3\Sigma_g^-$ linear ground state, must be of Rydberg type, as has been suggested (2).

If the absorption spectrum of methylene in the visible region is similar to that of NH_2, then it may well be between the two components ($^1A_1$ and $^1B_1$) into which the $^1\Delta_g$ state transforms on bending. If, as in NH_2, the upper state is linear, the electronic origin of the transition cannot be at energies greater than 2.2 ev, else the actual ground state of the molecule will be bent ($^1A_1$). Both CH_2 and NH_2 show this type of transition in the same spectral region, and detailed analysis for the latter molecule gives the origin at 1.24 ev (5). An origin of similar value for the methylene spectrum is therefore consistent with a linear ground state.

REFERENCES

1. G. HERZBERG and J. SHOOSMITH. Nature, **183**, 1801 (1959).
2. G. HERZBERG. Robert A. Welsh Foundation Symposium, Texas, November 1959. Personal communication.
3. G. W. ROBINSON and M. McCARTY. J. Am. Chem. Soc. **82**, 1859 (1960).
4. T. D. GOLDFARB and G. C. PIMENTEL. J. Am. Chem. Soc. **82**, 1865 (1960).
5. D. A. RAMSAY. Advances in spectroscopy. Vol. I. Interscience Publishers Inc., New York. 1959.
6. G. A. GALLUP. J. Chem. Phys. **26**, 716 (1957).
7. B. F. GRAY. J. Chem. Phys. **28**, 1252 (1958).
8. G. A. GALLUP. J. Chem. Phys. **28**, 1252 (1958).
9. J. LENNARD-JONES. Trans. Faraday Soc. **30**, 70 (1934).
10. K. J. LAIDLER and E. J. CASEY. J. Chem. Phys. **17**, 213 (1949).
11. A. PADGETT and M. KRAUSS. J. Chem. Phys. **32**, 189 (1960).
12. J. M. FOSTER and S. F. BOYS. Revs. Mod. Phys. **32**, 305 (1960).
13. A. D. WALSH. J. Chem. Soc. 2260 (1953).
14. H. HOWARD and G. W. KING. Can. J. Chem. **37**, 700 (1959).
15. G. W. KING. Can. J. Chem. **38**, 365 (1960).
16. M. KOTANI, A. AMENIYA, E. ISHIGURO, and T. KIMURA. Tables of molecular integrals. Maruzen Company, Ltd., Tokyo. 1955.
17. J. C. SLATER. Solid-state and molecular theory group. Technical Report No. 3. Massachusetts Institute of Technology, Cambridge, Massachusetts. 1953.
18. C. C. J. ROOTHAN. J. Chem. Phys. **19**, 1445 (1951).
19. M. P. BARNETT and C. A. COULSON. Trans. Roy. Soc. A, **243**, 221 (1951).
20. J. O. HIRSCHFELDER and J. W. LINNETT. J. Chem. Phys. **18**, 130 (1950).
21. K. RUEDENBERG. J. Chem. Phys. **19**, 1433 (1951).
22. R. S. BARKER and H. EYRING. J. Chem. Phys. **21**, 912 (1953); **22**, 1177 (1954).
23. F. A. GRAY, I. G. ROSS, and J. YATES. Australian J. Chem. **12**, 347 (1959).
24. A. LANGER, J. A. HIPPLE, and D. P. STEVENSON. J. Chem. Phys. **22**, 1836 (1954).

SULPHONIUM SALT SOLVOLYSIS

PART II. COMMON-ION EFFECT AND THE ION-PAIR MECHANISM IN THE SOLVOLYSIS OF DIMETHYL-t-BUTYL SULPHONIUM SALTS[1]

J. B. HYNE and J. W. ABRELL[2]

ABSTRACT

The kinetic effect of added common anion in the solvolysis of dimethyl-t-butyl sulphonium halides in ethanol–water mixtures is analyzed in terms of a mechanism involving solvolysis through an ion-pair intermediate. The simple ion-pair role, however, does not account for the kinetic behavior at higher added common-anion concentrations. A normal salt effect and further involvement of the ion pair in S_N2 attack by common anion are compared as possible explanations for the observed kinetic behavior.

INTRODUCTION

Evidence presented in the previous paper of this series (1) was interpreted as indicative of the increasing role of an ion-pair mechanism in the solvolysis of dimethyl-t-butyl sulphonium salts as the dielectric constant of the medium is reduced. Further experimental

[1]
$$R_3S^+ + X^- \underset{}{\overset{K_A}{\rightleftarrows}} R_3S^+X^-$$
$$\downarrow k_+ \qquad\qquad \downarrow k_{ip}$$
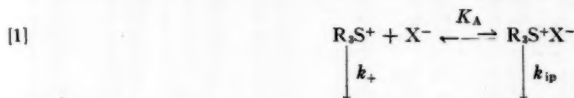
evidence in support of this proposed mechanism is presented in this paper. It is clear from equation [1] that such a mechanism should be affected by the concentration of common anion X^-. Higher concentrations should favor ion-pair formation and a higher proportion of the over-all solvolysis should proceed through the ion-pair intermediate. The over-all rate of solvolysis (k_{obs}) of dimethyl-t-butyl sulphonium iodide and chloride has therefore been measured as a function of both added common anion and solvent composition.

In the previous paper of this series it was shown that if the ion-pair mechanism is correct, $k_{ip} > k_+$. Consequently, added common anion should increase the over-all rate of solvolysis (k_{obs}) since a greater proportion of the solvolytic process will proceed through the faster ion-pair pathway. As the dielectric constant of the solvolytic medium is reduced, the ion-pair association constant (K_A) will increase and together with increasing concentration of common anion these factors will result in virtually complete conversion of the sulphonium ion to the ion-pair state. The over-all rate of solvolysis should therefore increase with added common anion and lower dielectric constant but should approach an upper limiting value as the degree of ion pairing approaches 100%.

EXPERIMENTAL METHOD AND RESULTS

All rates were measured by the radiochemical flow counting technique of Hyne and Wolfgang (2). C^{14}-labelled dimethyl-t-butyl sulphonium iodide was prepared as described previously (2) and converted to the chloride by metathesis with freshly prepared silver chloride. Solvent mixtures were prepared by weight from doubly distilled water (10^{-7} mhos) and redistilled absolute ethanol. Reagent grades of lithium chloride and iodide

TABLE I

Rates of solvolysis of dimethyl-*t*-butyl sulphonium iodide, at 75.75° C, as a function of added common anion and solvent mole fraction composition

(Letters on each column refer to data-fit plots in Fig. 1)

(a) 0.954 EtOH				(b) 0.845 EtOH				(c) 0.713 EtOH				(d) 0.550 EtOH				(e) 0.000 EtOH			
Sulphonium salt, $M \times 10^3$	Added LiI, $M \times 10^3$	Corrected I⁻, $M \times 10^3$	$k_{obs}^{75.75}$ $\times 10^4$, sec⁻¹	Sulphonium salt, $M \times 10^3$	Added LiI, $M \times 10^3$	Corrected I⁻, $M \times 10^3$	$k_{obs}^{75.75}$ $\times 10^4$, sec⁻¹	Sulphonium salt, $M \times 10^3$	Added LiI, $M \times 10^3$	Corrected I⁻, $M \times 10^3$	$k_{obs}^{75.75}$ $\times 10^4$, sec⁻¹	Sulphonium salt, $M \times 10^3$	Added LiI, $M \times 10^3$	Corrected I⁻, $M \times 10^3$	$k_{obs}^{75.75}$ $\times 10^4$, sec⁻¹	Sulphonium salt, $M \times 10^3$	Added LiI, $M \times 10^3$	Corrected I⁻, $M \times 10^3$	$k_{obs}^{75.75}$ $\times 10^4$, sec⁻¹
0.16	0.00	0.14	4.35	0.08	0.00	0.07	4.15	0.16	0.00	0.14	4.03	1.00	0.00	0.88	3.75	1.00	0.00	0.88	2.52
0.32	0.00	0.28	4.46	0.16	0.00	0.14	4.24	1.00	0.00	0.88	4.12	1.00	10.2	11.1	3.88	1.00	15.0	15.9	2.53
1.00	0.00	0.88	4.74	0.32	0.00	0.28	4.37	1.00	0.00	0.88	4.07		19.8	20.7	3.98		35.0	35.9	2.50
1.00	0.00	0.88	4.72	1.00	0.00	0.88	4.51	1.00	1.01	1.89	4.18		30.1	31.0	4.14				
1.00	0.50	1.40	4.75	1.00	1.05	1.93	4.58		4.07	4.95	4.33		40.4	41.3	4.15				
	0.58	1.46	4.85		1.96	2.84	4.66		4.13	5.01	4.34								
	1.03	1.91	5.09		2.47	3.35	4.69		4.37	5.25	4.39								
	1.04	1.92	5.03		3.98	4.86	4.87		7.04	7.92	4.41								
	2.69	3.57	5.28		5.98	6.86	5.06		9.97	10.8	4.54								
	5.00	5.88	5.40		9.25	10.3	5.30		19.7	20.6	4.70								
	5.50	6.38	5.42		15.9	16.8	5.51		30.1	31.0	4.74								
	8.64	9.52	5.72		21.0	21.9	5.45		40.7	41.6	4.95								
	13.0	13.88	5.82		30.3	31.2	5.82												
	15.7	16.6	6.07		42.2	43.1	6.11												
	16.2	17.1	5.99																
	18.3	19.2	6.18																
	22.9	23.8	6.33																
	23.9	24.8	6.40																
	26.9	27.8	6.69																
	38.9	39.8	7.25																
	46.0	46.9	7.58																

were used as sources of the common anion. ~~The concentration of sulphonium~~ salt used throughout was 1×10^{-3} M except in a few cases noted where rates at concentrations of anion less than 10^{-3} M were required. Observed rates as a function of concentration of added anion and solvent composition are shown in Tables I (a)–(e) for the sulphonium iodide and II (a)–(c) for the sulphonium chloride. All rates were measured at 75.75° C.

TABLE II

Rates of solvolysis of dimethyl-t-butyl sulphonium chloride, at 75.75° C, as a function of added common anion and solvent mole fraction composition
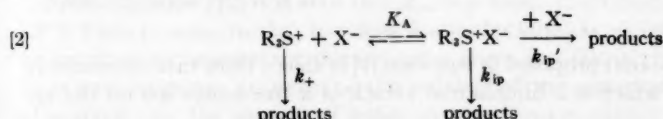
(Letters on each column refer to data-fit plots in Fig. 2)

(a) 0.973 EtOH				(b) 0.800 EtOH				(c) 0.550 EtOH			
Sulpho-nium salt, $M \times 10^3$	Added LiCl, $M \times 10^3$	Correc-ted Cl⁻, $M \times 10^3$	$k^{75.75}_{obs}$ $\times 10^4$, sec⁻¹	Sulpho-nium salt, $M \times 10^3$	Added LiCl, $M \times 10^3$	Correc-ted Cl⁻, $M \times 10^3$	$k^{75.75}_{obs}$ $\times 10^4$, sec⁻¹	Sulpho-nium salt, $M \times 10^3$	Added LiCl, $M \times 10^3$	Correc-ted Cl⁻, $M \times 10^3$	$k^{75.75}_{obs}$ $\times 10^4$, sec⁻¹
0.50	0.00	0.45	4.27	1.00	0.00	0.88	4.09	1.00	0.00	0.88	3.64
1.00	0.00	0.88	4.47	1.00	0.00	0.88	4.19	1.00	7.45	8.33	3.73
1.00	0.80	1.68	4.79	1.00	2.80	3.68	4.36	1.00	18.7	19.5	3.83
1.00	1.40	2.28	4.90	1.00	5.70	6.58	4.57	1.00	29.6	30.4	3.99
1.00	2.90	3.78	4.98	1.00	10.1	11.0	4.61	1.00	50.5	51.4	4.24
1.00	5.70	6.58	5.27	1.00	20.0	20.9	4.75				
1.00	19.7	20.5	5.59	1.00	32.4	33.3	5.01				
1.00	26.9	27.8	5.76	1.00	40.4	41.3	5.23				
1.00	35.0	35.9	6.05								

The rate data plotted in Figs. 1 and 2 show the predicted increase in rate as common anion is added. The observed initial increase, furthermore, becomes more pronounced as the dielectric constant of the solvent decreases. These phenomena are in keeping with the mechanism proposed in equation [1] since the ion-pair association constant increases as the dielectric constant decreases and consequently the effect of added common anion in displacing the equilibrium to the ion pair will also be greater. However, it is seen from these plots that the k_{obs} does not approach a limiting value as the added anion concentration is increased but becomes linearly dependent upon the anion concentration. Two possible explanations of this effect are offered and the relative merits of each considered in the subsequent sections of this paper. Both interpretations involve the equilibrium between free sulphonium ions and sulphonium ion pairs with the anion as postulated in equation [1]. The values of the ion-pair association constant K_A, obtained by analysis of the kinetic data, are both similar in magnitude and in variation with solvent composition to those obtained conductimetrically for similar sulphonium salt systems. There appears to be little doubt, therefore, that such an ion-pair equilibrium is involved in the solvolysis.

MECHANISM INVOLVING S_N2 ATTACK BY THE ANION ON THE ION PAIR

In this interpretation of the observed kinetic behavior the following extended form of equation [1] is proposed.
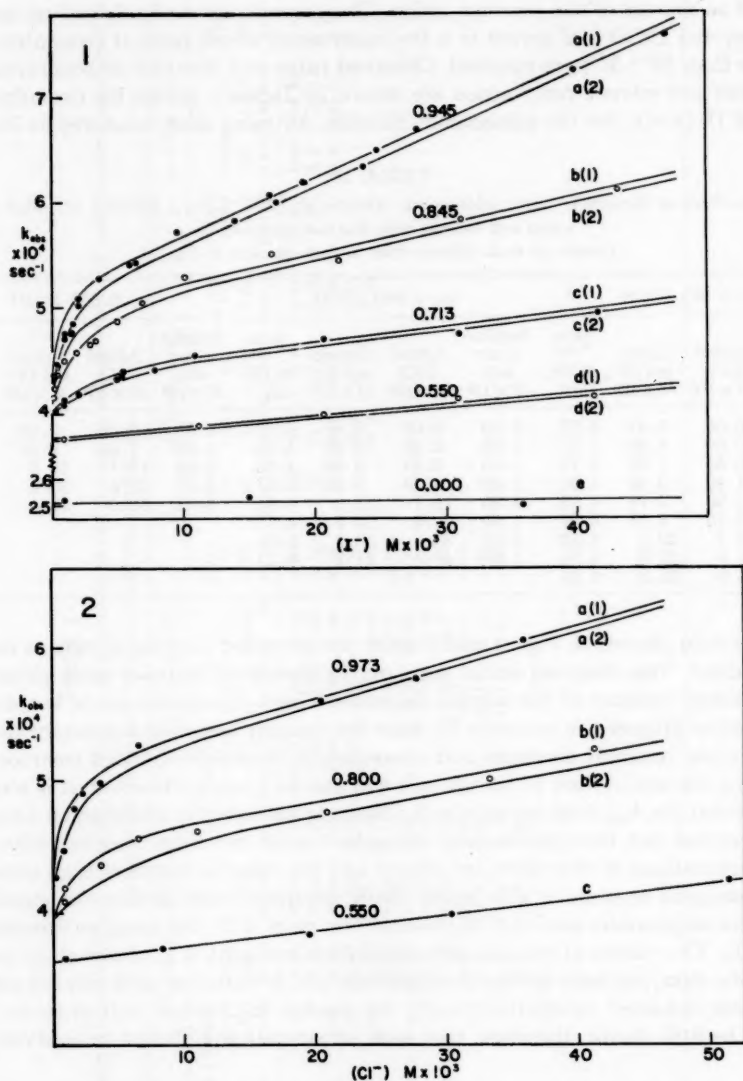
[2]
$$R_2S^+ + X^- \underset{k_+ \downarrow}{\overset{K_A}{\rightleftharpoons}} R_2S^+X^- \xrightarrow{+ X^-}_{k_{ip}} \text{products}$$

products   products

FIG. 1. Fit of experimentally determined k_{obs} (Table I) for dimethyl-t-butyl sulphonium iodide solvolysis to calculated curves from kinetic-expression equations [10] or [17]. (See Table III for values of constants for each calculated line.)

FIG. 2. Fit of experimentally determined k_{obs} (Table II) for dimethyl-t-butyl sulphonium chloride solvolysis to calculated curves from equations [10] or [17]. (See Table III for values of constants for each calculated line.)

This mechanism differs from that proposed in equation [1] in that a third rate-determining step, k_{ip}', has been added, which is a bimolecular attack of a free halide ion on the ion pair.

Derivation of Rate Equation

Assuming the mechanism proposed in equation [2] above, a rate expression for k_{obs} can be derived. Consider the three paths available for the reaction of the sulphonium salt to dimethyl sulphide and other products; in each case the only assumption made is that dimethyl sulphide is produced in the rate-determining step of each path. From equation [2] the observed rate of production of dimethyl sulphide is

[3] $$r = k_+[R_3S^+] + k_{1p}[R_3S^+X^-] + k_{1p}'[R_3S^+X^-][X^-].$$

However,

[4] $$[R_3S^+X^-] = K_A[R_3S^+][X^-],$$

and substituting [4] in [3],

[5] $$r = k_+[R_3S^+] + k_{1p}K_A[R_3S^+][X^-] + k_{1p}'K_A[R_3S^+][X^-]^2.$$

The observed pseudo first-order over-all rate of production of dimethyl sulphide, r, must be equal to the rate of removal of the salt (total) if dimethyl sulphide is produced in the rate-determining step of all paths, hence

[6] $$r = k_{obs}[R_3SX]_T.$$

Substituting [6] in [5] and rearranging,

[7] $$k_{obs} = \{[R_3S^+]/[R_3SX]_T\}\{k_+ + k_{1p}'K_A[X^-] + k_{1p}K_A[X^-]^2\}.$$

But at all times,

[8] $$[R_3SX]_T = [R_3S^+] + [R_3S^+X^-]$$

[9] $$= [R_3S^+] + K_A[R_3S^+][X^-].$$

Substitution of [9] for $[R_3SX]_T$ in [7] and rearranging,

[10] $$k_{obs} = \frac{k_+ + k_{1p}K_A[X^-] + k_{1p}'K_A[X^-]^2}{1 + K_A[X^-]}.$$

Equation [10] requires that k_{obs} increases as $[X^-]$ increases due to the k_{1p} and k_{1p}' terms. However, it does not predict a leveling off of the rate at high $[X^-]$ as in equation [1] since when $K_A[X^-]$ becomes large compared with unity and k_+, equation [10] reduces to

[11] $$k_{obs} \doteq k_{1p} + k_{1p}'[X^-],$$

showing a continued linear dependence of k_{obs} on $[X^-]$.

Analysis of Data by Equation [10]

Equation [10] may be rearranged to

[12] $$k_{obs} = k_+ + K_A\{k_{1p}[X^-] - k_{obs}[X^-] + k_{1p}'[X^-]^2\},$$

which has the general form of a straight line with slope K_A and intercept k_+.

From equation [12] it is seen that k_{obs} is a linear function of a complex term involving $[X^-]$. Thus in order for k_{obs} to follow first-order kinetics, as indeed it does, the $[X^-]$ must be assumed to be constant throughout a given run (i.e. a given determination of k_{obs}). It is now necessary to examine the validity of this assumption for, during the course of a given run, the amount of halide involved in ion pairing will change. On solvolysis

the sulphonium salt liberates halide, previously tied up in ion pairs, as HX; as a result the free [X$^-$] does not remain constant over the entire run. However, inspection of the plots of the basic experimental data (see e.g. ref. 2) shows that first-order behavior of the rate is not observed until some three half lives of reaction have elapsed. This is due to an artifact of the method and not a fundamental change in reaction order (2). Consequently, some 88% of the sulphonium salt has reacted by this point, freeing the halide from ion pairs, and the following half lives over which the rate is determined liberate such a small amount of X$^-$ that the concentration change cannot be detected as affecting the rate of reaction. This concentration effect was corrected for by assuming the total halide concentration present in a given run to be the amount of added lithium halide *plus* 88% of the initial concentration of the sulphonium salt. This corrected halide ion concentration is shown in Tables I and II. It is obvious that this correction is most important at low concentrations of added halide.

An additional complication arises in the computation of the anion concentration, due to the incomplete dissociation of the lithium halide in low dielectric media. Data of sufficient detail is not available to enable precise corrections to be made for this effect. However, the dissociation of lithium chloride in ethanol has been studied (3) and these results show that the salt is still 90% dissociated at 10^{-2} M. Although the neglect of this effect will introduce errors in the analysis presented here these errors will not affect the internal consistency of the treatment although they will be reflected in the absolute values of the constants computed.

The values for k_{1p} and k_{1p}' must be known if K_A and k_+ are to be found graphically. Upon inspection of the data given in Tables I and II and plotted in Figs. 1 and 2, it is noted that after an initial steep rise in k_{obs} with added X$^-$ the relationship approximates linearity. After addition of a sufficient amount of common ion (LiX) the sulphonium ion is present almost entirely in the form of an ion pair, especially in the lower dielectric media where K_A is large. At this point equation [11] should hold. Thus, upon back extrapolation of the linear sections of the plot to zero [X$^-$], the intercept gives an approximate value for k_{1p} and the slope yields a value for k_{1p}'. Approximate values for k_+ were obtained by back extrapolation of the initial steep section of the plots to zero X$^-$ concentration. As noted in Tables I and II several rate determinations were made at salt concentrations less than 10^{-3} M in order to permit more accurate back extrapolations. Using the approximate values of k_+, k_{1p}, and k_{1p}' so obtained, and arbitrarily chosen values of K_A, best-fit curves, as shown in Figs. 1 and 2, were calculated by successive approximation. In some cases the values of k_{1p} and k_{1p}' had to be altered slightly to obtain better fits. It should be noted that k_+ and K_A are theoretically obtainable from a plot of the experimentally determined values of k_{obs}, [X$^-$], k_{1p}, and k_{1p}' according to equation [12]. It was found, however, that a plot of this type is extremely sensitive to [X$^-$] and that the value of the bracketed term in equation [12] is a very small difference between very large numbers. The experimental errors in k_{obs} and [X$^-$] are therefore too great to permit analysis on the basis of a plot of the function as described in equation [12]. Consequently, resort to the technique of successive approximation to a best fit was necessary.

Figure 1 is a composite of the experimental data for the sulphonium iodide (Table I) and the upper and lower limiting theoretical curves for each set of points computed from equation [10] using the values for the constants shown in Table III. Figure 2 is a similar composite for the sulphonium chloride data (Table II), the values for the constants being shown in Table III.

TABLE III

Values of constants in theoretical kinetic expressions (equations [10] and [17]) for solvolysis of dimethyl-t-butyl sulphonium salts

Mole fraction ethanol	D (75.75°) (12)	Curve No. (Figs. 1 and 2)	K_A, l./mole	k_+ (or k_+^0) $\times 10^4$, sec^{-1}	k_{ip} (or k_{ip}^0) $\times 10^4$, sec^{-1}	$k_{ip}' \times 10^2$, l./mole sec	b
Iodide							
0.945	17.5	a (1)	3500	4.15	5.15	5.40	1.05
		a (2)	1500				
0.845	19.3	b (1)	900	4.10	5.10	2.46	0.48
		b (2)	500				
0.713	22.0	c (1)	340	4.00	4.51	1.20	0.27
		c (2)	250				
0.550	25.7	d (1)	180	3.75	3.85	0.929	0.24
		d (2)	120				
0.000	62.0	e	<20	2.51	—	—	—
Chloride							
0.973	16.8	a (1)	2000	4.15	5.08	2.65	0.52
		a (2)	1000				
0.800	20.3	b (1)	600	3.95	4.60	1.53	0.34
		b (2)	200				
0.550	25.7	c	~100	3.63	3.70	1.30	0.35

Discussion of Analysis by Equation [10]

The fit of experimental data to curves calculated from equation [10], as shown in Figs. 1 and 2, supports the kinetic model for the solvolysis from which equation [10] was derived. The formal similarity of the rate behavior in this case to that observed by Fainberg and Winstein (4) for the special salt effect in alkyl halide and benzene sulphonate solvolysis is immediately obvious. The similarity arises from the fact that in this case an initial-state ion can solvolyze by ion-pair formation whereas in the alkyl halide and benzene sulphonates a covalent initial state can solvolyze by passing to the ion-pair intermediate.

The ion-pair association constants (K_A) obtained from the kinetic analysis and shown in Table III exhibit the same form of dependence on solvent dielectric as those reported from conductance measurements on the trimethyl sulphonium iodide system (5, 6). The orders of magnitude are also comparable. This observation can be interpreted as further support for the proposed mechanism. It is also noted that K_A (I$^-$) > K_A (Cl$^-$) in a given solvent medium, which is in keeping with the observed order of ion-pair association constants for lead (7) and lithium halides (8). The probable error associated with the K_A values determined by the kinetic analysis is large compared with the accuracy attainable in modern conductimetric methods. It should be noted, however, that in cases such as the sulphonium salt under study here the kinetic method is the only available technique for K_A determination since the salt reacts with the solvent.

In Table IV the percentages of the sulphonium salt (10^{-3} M) present as ion pairs in various solvents with 10^{-2} M added common anion are shown. These values are calculated

TABLE IV

Percentage association to ion pairs for 10^{-3} M
sulphonium salt with 10^{-2} M added common
anion as a function of K_A (iodide)

Mole fraction ethanol	K_A (median)	% association
0.945	2.5×10^3	96
0.845	7×10^2	88
0.713	3×10^2	75
0.550	1.5×10^2	60
0.000	~ 20	~ 25

from the median values of K_A for each solvent composition shown in Table III for the iodide case. A similar table may be constructed for the chloride system but the iodide case suffices for illustration. The concentration of added common anion of 10^{-2} M was chosen since inspection of Fig. 1 will show that in all solvent compositions the dependence of k_{obs} on added common anion has become linear at this point. It is seen from Table IV that in all solvent compositions above 0.550 mole fraction ethanol more than half of the sulphonium salt is present as ion pairs at this concentration of added common anion. It is beyond this concentration of added anion that the S_N2 attack of the anion on the ion pair is postulated to be important. The fact that most of the sulphonium salt is present as the ion pair and that there is at least a 10-fold excess of anion over sulphonium salt establishes that the necessary species for such a mechanism are present in abundance.

The early interest in the solvolysis of sulphonium salts was primarily due to the fact that such systems represent the case where charge is dispersed on passing to the transition state and the rate would be expected to increase with decreasing dielectric constant. It is clear from the data presented here, however, that the observed rate (k_{obs}) is not the rate of solvolysis of the ion in lower dielectric media. Hence previous attempts to correlate the observed rate with dielectric constant have been unsuccessful. In this analysis, however, values for k_+ are obtained (as shown in Table III) over the whole solvent composition range. These values are plotted versus dielectric constant in Fig. 3 and describe a linear relationship. The additional points in Fig. 3 at $D = 37$ (0.324 mole
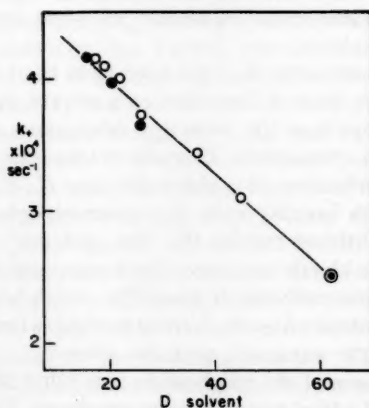

FIG. 3. k_+ versus dielectric constant of solvent: O, iodide; ●, chloride.

fraction ethanol) and $D = 45$ (0.203 mole fraction ethanol) are computed from rates for the solvolysis of dimethyl-t-butyl sulphonium iodide at 50.3° and 78.4° (9). Figure 3 also shows that the k_+ values for both the chloride and iodide salts lie on the same line, an observation consistent with the kinetic model proposed, since k_+ is a measure of the rate of solvolysis of the free sulphonium ion and does not involve the anion in the rate-determining step.

The dependence of k_{ip} and k_{ip}' on dielectric constant of the solvent is shown in Fig. 4(a
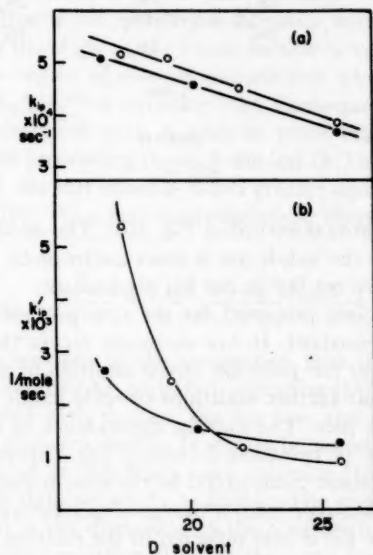
FIG. 4. (a) k_{ip}, (b) k_{ip}' versus dielectric constant of solvent: $\bigcirc$, iodide; $\bullet$, chloride.

and b). According to the kinetic model presented previously, both rates should show a dependence on the nature of the anion since this species is involved in the rate-determining step. Such a dependence is noted in both cases but is considerably greater in the k_{ip}' than in the k_{ip} rate. Furthermore the dielectric-constant dependence of k_{ip}' is larger than that of k_{ip}. The mechanism proposed to account for these observations together with the other features of the over-all solvolytic process are summarized in Fig. 5.

The S_Ni-type mechanism proposed for the rate process k_{ip} is in keeping with the first-order character of the rate constant. Formal charge is presumably partially dispersed in the initial ion-pair state so that little change in charge character results on passing to a transition state involving intramolecular nucleophilic attack of the halide component of the ion pair on the adjacent t-butyl carbon atom; hence the relative insensitivity of k_{ip} to solvent dielectric constant changes. Dimethyl sulphide is liberated in the rate-determining step as assumed in the kinetic analysis and t-butyl halide is also formed. Subsequent solvolysis or elimination of the t-butyl halide to yield alcohol or olefin will not be rate determining since the rates of such reactions under the experimental conditions used in this work are considerably greater than those of the sulphonium salt rates (10, 11). It is perhaps a little surprising that the rate differences between the iodide and chloride
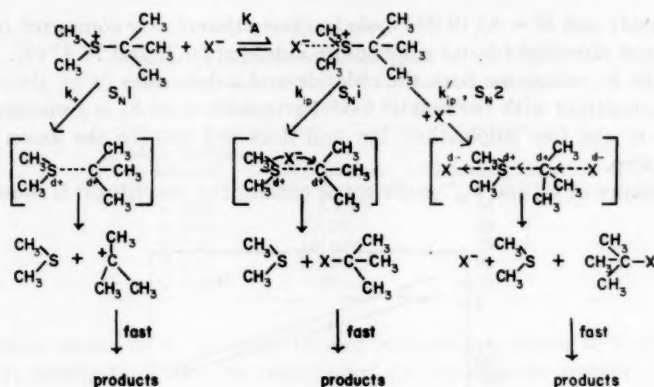
FIG. 5.

salts are not greater than those observed in Fig. 4(a). The small differences, however, are in the expected order since the iodide ion is more nucleophilic than the chloride ion and should react somewhat more readily in the $S_N i$ mechanism.

The bimolecular mechanism proposed for the rate process k_{1p}' is in accord with the second-order form of this constant. In low-dielectric media the bulk of the sulphonium ions are readily converted to ion pairs by initial addition of small amounts of common anion (see Table IV) so that further additions provide halide ions which participate in $S_N 2$-type attack on the ion pair. The marked dependence of k_{1p}' on dielectric constant (Fig. 4(b)) is characteristic of reactions involving the dispersal of ionic charge in the formation of the transition state. Such would be the case in the mechanism proposed here where a halide ion and an ion pair form a charge-dispersed transition state. The greater nucleophilicity of the iodide ion is also reflected in the relative magnitudes of k_{1p}' for the two salts. It is questionable whether the apparent crossover in Fig. 4(b) is real, due to the accuracy with which k_{1p}' can be determined from the best-fit analysis. Dimethyl sulphide is again liberated in the rate-determining step and the subsequent t-butyl halide solvolysis is fast.

MECHANISM INVOLVING NORMAL SALT EFFECT

The alternative explanation for the linear dependence of k_{obs} on added common anion at higher concentrations is based on the possible role of normal salt effects. The derivation of the rate expression in this case is exactly similar to that shown previously in equations [3] through [10] except for the omission of the additional k_{1p}' term. The resulting rate equation obtained is

[13]
$$k_{obs} = \frac{k_+ + k_{1p} K_A [X^-]}{1 + K_A [X^-]}.$$

If a normal salt effect is considered, however, k_+ and k_{1p} are not constants independent of $[X^-]$. Using the approximation favored by Fainberg and Winstein (13) for salt effects in other than pure aqueous media these effects can be expressed as a linear function of anion concentration, i.e.

[14] $$k_+ = k_+^0 (1 + a[X^-])$$

[15] $$k_{1p} = k_{1p}^0 (1 + b[X^-]).$$

Hence

$$[16] \qquad k_{\text{obs}} = \frac{k_+^{\ 0} + k_{\text{ip}}^{\ 0} K_A[X^-] + k_+^{\ 0} a[X^-] + k_{\text{ip}}^{\ 0} b K_A[X^-]^2}{1 + K_A[X^-]}.$$

In the derivation of this equation we have made no simplifying assumptions regarding the nature of the normal salt effect. It would be unjustifiable to assume that the constants a and b are equal since they represent the salt effect on two different processes: one, the solvolysis of an ion and the other, of an ion pair. However, from the experimental data plotted in Fig. 1 it is seen that in the more aqueous media, where the bulk of the solvolysis proceeds via the ion (k_+), the slope of the linear section is very small and in pure water virtually zero. This is the region of solvent composition where the salt effect is largely determined by the term $k_+^{\ 0} a[X^-]$ in equation [16]. Consequently it seems reasonable to assume that a is small compared with b since in more ethanolic solvents, where the proportion of the solvolysis proceeding through the ion (k_+) is small compared with that through the ion pair (k_{ip}), the salt effect is much greater and is determined by the term $k_{\text{ip}}^{\ 0} b K_A[X^-]^2$ in equation [16]. As a first approximation, therefore, equation [16] may be written as

$$[17] \qquad k_{\text{obs}} = \frac{k_+^{\ 0} + k_{\text{ip}}^{\ 0} K_A[X^-] + k_{\text{ip}}^{\ 0} b K_A[X^-]^2}{1 + K_A[X^-]}.$$

This approximation is tantamount to the assumption that the normal salt effect on the free sulphonium ion reaction may be neglected (equation [14]) due to the smaller magnitude of this effect compared with that on the ion pair and the diminishing role of the free-ion reaction in lower dielectric media. It should be noted that a simplifying assumption of this kind is necessary at this stage since equation [16] has more unknowns than can be evaluated from the data presently available. The possible errors inherent in this assumption are considered in the discussion of the b values in a subsequent section.

It is seen immediately that equation [17] has the same form as equation [10] derived for the alternative S_N2-type mechanism explanation for the non-limiting rate behavior. Consequently $k_{\text{ip}}' = k_{\text{ip}}^{\ 0} b$, and since $k_{\text{ip}}^{\ 0} = k_{\text{ip}}$ of equation [10], $b = k_{\text{ip}}'/k_{\text{ip}}$. Values of b so calculated are shown in Table III.

Discussion of Analysis by Equation [17]

The normal salt effect b values obtained from analysis of the experimental data by equation [17] and shown in Table III indicate that a normal salt effect would be one of acceleration since all values are positive. It is further seen that the b values decrease as the dielectric constant of the medium increases. It should be noted, however, that at mole fractions of ethanol of 0.550 and lower, the first-order approximation made in order to simplify equation [16] may become invalid since the $k_+^{\ 0} a[X^-]$ term may now be significant compared with the $k_{\text{ip}}^{\ 0} b K_A[X^-]^2$ term. This suspicion is warranted since in the more aqueous media a larger contribution to the over-all k_{obs} is made by the k_+ term and furthermore, we have no knowledge of how the normal salt effect constant, a, varies with solvent composition. Consequently, while the contribution to k_{obs} from the free-ion pathway (k_+) is still significant, the assumption that the salt effect on this pathway (viz. a) is negligible is a dubious one. This error may be the reason for the apparent similarity of the b values at 0.713 and 0.550 mole fraction ethanol in the iodide case and at 0.800 and 0.550 mole fraction in the chloride case. In both systems the b values at 0.550 mole fraction may be in error due to the increasing significance of the a value.

There can be no doubt, however, that if a normal salt effect is responsible for the linear dependence of k_{obs} on added anion concentration then this effect is one of acceleration, i.e. a positive salt effect. The prediction of the sign of normal salt effects depends upon a knowledge of the relative charge character of the initial and transition states in the rate-determining step. It is known, however, that for reactions in aqueous media, positive salt effects are observed for reactions between two ions of like sign where the transition state has a higher charge density than the initial state while negative salt effects are noted for reactions between oppositely charged ions where the transition state has a lower charge density due to partial neutralization of the two charges. Since all kinetic evidence indicates that the solvolysis of sulphonium salts involves charge delocalization in going to the transition state, it therefore seems reasonable to expect a *negative* normal salt effect and not a positive one. The validity of extension of these principles to systems in non-aqueous media is supported in the work of Fainberg and Winstein on the solvolysis of toluene-sulphonates (4) in ethanol and acetic acid, which demonstrated a positive salt effect, in keeping with the fact that charge is created in moving from the polar initial state to a more ion-like transition state. The b values obtained here refer to the salt effect on a reaction proceeding from an ion-pair initial state to a charge-dispersed transition state. Here the difference in charge character between the two states is presumably even smaller than that between a free sulphonium ion initial state and a charge-dispersed transition state. Yet the b value for the ion-pair process appears to be greater than the a value for the solvolysis from the free ion, as indicated by the virtual independence of k_{obs} on anion concentration in water. There is every indication, therefore, that if our interpretation of the charge character of the sulphonium salt solvolysis is correct, then the observed linear dependence of the rate on salt concentration has the wrong sign for an explanation based on a normal salt effect. Regarding the observed increase in b with lowering of dielectric constant, it is clearly impossible to offer an explanation for this behavior until the more fundamental question of the sign of the effect can be answered.

CONCLUSIONS

There seems little doubt that in the solvolysis of sulphonium salts in media of dielectric constant less than 25, a reaction pathway involving ion pairs plays a significant role. The correspondence between ion-pair association constants obtained from the kinetic analysis and those for similar systems determined conductimetrically appears to be too close to be fortuitous. There still remains considerable doubt, however, about the explanation for the observed linear dependence of the over-all rate of solvolysis on added salt at higher concentrations when the sulphonium salt is largely in the form of ion pairs. The evidence at the moment would appear to favor an explanation based upon the onset of a third S_N2-type attack by anion on the ion pair but there is as yet insufficient evidence to exclude conclusively an explanation based on a normal salt effect. Further work on the effect of added non-common ions and investigation of the stereochemistry of the solvolysis of salts with optically active alkyl groups should provide the necessary information to enable a distinction or an assignment of relative roles of the two phenomena to be made.

REFERENCES

1. J. B. HYNE. Can. J. Chem. **39**, 1207 (1961).
2. J. B. HYNE and R. WOLFGANG. J. Phys. Chem. **64**, 699 (1960).
3. J. R. GRAHAM, G. S. KELL, and A. R. GORDON. J. Am. Chem. Soc. **79**, 2352 (1957).
4. A. H. FAINBERG and S. WINSTEIN. J. Am. Chem. Soc. **78**, 2767 (1956).
5. E. D. HUGHES, C. K. INGOLD, R. MOK, and Y. POCKER. J. Chem. Soc. 1238 (1957).
6. A. L. JACOBSON and J. B. HYNE. J. Am. Chem. Soc. **82**, 2418 (1960).
7. A. I. BIGGS, M. H. PANCKHURST, and H. N. PARTON. Trans. Faraday Soc. **51**, 802, 806 (1955).
8. J. KENTTAMMA. Suomen Kemistilehti, B, **32**, 9 (1959).
9. J. B. HYNE and R. E. WONKKA. To be published.
10. S. WINSTEIN and A. H. FAINBERG. J. Am. Chem. Soc. **79**, 5937 (1957).
11. A. H. FAINBERG and S. WINSTEIN. J. Am. Chem. Soc. **79**, 1602 (1957).
12. G. AKERLOF. J. Am. Chem. Soc. **54**, 4125 (1932).
13. A. H. FAINBERG and S. WINSTEIN. J. Am. Chem. Soc. **78**, 2763 (1956).

THE VELOCITY OF RATE-CONTROLLING SURFACE DIFFUSION REACTIONS IN THE ELECTRODEPOSITION OF METALS AS A FUNCTION OF DISLOCATION DENSITY[1]

H. Kita, M. Enyo, and J. O'M. Bockris

ABSTRACT

The rate constant for the surface diffusion velocity of Cu adions in the deposition of Cu appears to depend on the current density of measurement. An interpretation is suggested in which it is proposed that the number of growth sites during the deposition of Cu under "monolayer" conditions depends upon potential, owing to the dependence of the critical radius for growth upon supersaturation. Calculations based upon this hypothesis are compared with experiment. The dependence of the shape of the Tafel relation in metal deposition (transient conditions) is related to the effect of changing the number of "active" growth sites.

1. INTRODUCTION

It has been recently suggested (1, 2) that in the buildup of the first few layers of a metal surface at low current densities in electrodeposition, the surface diffusion of adions (2), from the sites at which they land on the metal from the solution to growth steps on the metal surface, is the rate-determining step in the over-all reaction $M^{z+}+ze_0^- = M$. Evidence for a similar rate-determining step in dissolution is available (1). The velocity of surface diffusion may be expressed approximately by

$$[1] \qquad V_{\text{diff}} = v_0\left(\frac{c_x - c_0}{c_0}\right)$$

where $v_0{}^* = D(c_0/x_0{}^2)$, c_x is the concentration of adions at distance x from a growth step, c_0 is their concentration at $x = 0$ or the concentration at equilibrium, D is the surface diffusion coefficient, and x_0 is the half distance between growth steps. If the concentration of growth steps is independent of the current density, i, of deposition and dissolution, x_0 and hence v_0 should be independent of i, and this was the approximation made in the first quantitative theory of surface diffusion control for metal deposition or dissolution (1).

Evidence is now available (3, 4) which shows that on Cu and Ag, v_0 increases with i; at low current densities, there is a rough proportionality between v_0 and i. It will be shown here that this result is consistent with the model of rate-controlling surface diffusion already discussed, if the dependence on potential of the number of dislocations which may form growth steps is taken into account.

The assumption of the independence of dc/dx with x, implicit in [1], may be dropped (4); whereupon $\partial^2 c_x/\partial x^2 \neq 0$, so that, during steady-state deposition at a constant overpotential, and assuming a surface far from saturation in respect to adion concentration,

$$[2] \qquad D\left(\frac{\partial^2 c_x}{\partial x^2}\right)+\frac{i_0}{ZF}\exp(-\alpha_c F\eta/RT)-\frac{i_0}{ZF}\exp(\alpha_a F\eta/RT) = 0,$$

where i_0 is the exchange current density, α_c and α_a the transfer coefficients for the electrochemical reaction, and η the overpotential; F, R, and T have their usual meaning and x is counted from the growth step.

The rate of surface diffusion at $x = 0$ is also equal to the rate of the over-all reaction of deposition and dissolution. In mass per unit area per unit time it is given by

[3]
$$V_{z=0} = \frac{D}{x_0} \left(\frac{\partial c}{\partial x} \right)_{z=0}.$$

2. DEPENDENCE OF "EQUILIBRIUM SURFACE DIFFUSION FLUX" UPON CURRENT DENSITY

The critical diameter (5), l_c, which must be exceeded before a nucleus can grow on a surface, is related to the surface free energy of the edge, γ, and the degree of supersaturation, $RT \ln c/c_0$, by (6)

[4]
$$l_c = \frac{2A\gamma}{\rho RT \ln \dfrac{c}{c_0}}$$

where A is the atomic weight, ρ the density, c the concentration of surface adions at the condition considered, and c_0 that at equilibrium. The surface of a real crystal contains a certain concentration of screw dislocations, which constitute surface steps. All steps of length l, the distance between pairs of dislocations, which provide steps having $l > l_c$, will grow when they receive material by means of surface diffusion. Assuming a random distribution of steps of various lengths, it may be shown that (6)

[5]
$$\frac{dN_l}{N_0} = 2\frac{l}{\bar{l}^2} \exp\left[-\left(\frac{l}{\bar{l}} \right)^2 \right] dl$$

where dN_l is the number of steps of length between l and $l+dl$, $\bar{l}$ is the average length of a step, and N_0 is the total number of steps per unit area. Further, on the assumption of a random distribution, one has that

$$\left(\frac{1}{N_{dis}} \right)^{1/2} = \bar{l}$$

where N_{dis} = mean number of dislocations cm^{-2}. Hence $\bar{l}^2 N_{dis} = 1$. But $2N_0 = N_{dis}$ and hence $\bar{l}^2 2N_0 = 1$, or

[6]
$$\bar{l}^2 N_0 = \tfrac{1}{2}.$$

Thus, the number of steps which are active in crystal growth is

$$N_{l>l_c} = \int_{l=l_c}^{l=\infty} 2N_0 \frac{l}{\bar{l}^2} \exp\left[-\left(\frac{l}{\bar{l}} \right)^2 \right] dl = N_0 \exp\left[-\left(\frac{l_c}{\bar{l}} \right)^2 \right].$$

Using [4] and [6],

[7]
$$N_{l>l_c} = N_0 \exp\left[-\left(\frac{2\sqrt{2}A\gamma N_0^{1/2}}{\rho RT \ln \dfrac{c}{c_0}} \right)^2 \right].$$

This number, $N_{l>l_c}$, of steps which will take part in lattice growth influences the rate

of surface diffusion because increase of $N_{l>l_c}$ decreases x_0 and hence increases v_0 (cf. equation [1]).* A relation between i and v_0 arises because, in steady-state metal deposition or dissolution,

[8] $$V_{\text{diff}} = \frac{i}{ZF}.$$

Or, using [1],

[9] $$\ln\frac{c}{c_0} = \ln\left(1+\frac{i}{ZFv_0}\right).$$

Further,

[10] $$v_0 = \frac{Dc_0}{x_0^2} = 8Dc_0N_{l>l_c}$$

[11] $$= 8Dc_0N_0 \exp\left[-\left\{\frac{2\sqrt{2}A\gamma N_0^{1/2}}{\rho RT \ln\left(1+\frac{i}{8ZFDC_0N_{l>l_c}}\right)}\right\}^2\right]$$

from which v_0 can be determined for a given N_0, $N_{l>l_c}$ being determined graphically from [7], [9], and [10].

3. THE TAFEL RELATION AS A FUNCTION OF DISLOCATION DENSITY

It has been shown (Mehl and Bockris (1)) that the $i-\eta$ relation for a metal exchange reaction (adion coverage far from saturation) is

[12] $$i = \frac{i_0[\exp(-\alpha_c F\eta/RT)-\exp(\alpha_a F\eta/RT)]}{1+\frac{i_0}{ZFv_0}\exp(\alpha_a F\eta/RT)}.$$

Correspondingly, the expression for the concentration of adions as a function of x can be found from [2] for certain boundary conditions. Thus, if

$$c = c_0, \qquad x = 0$$
$$\partial c/\partial x = 0, \qquad x = x_0$$

then (4)

[13] $$\frac{c_x}{c_0} = \exp[-(\alpha_a+\alpha_c)F\eta/RT]$$
$$+\frac{1-\exp[-(\alpha_a+\alpha_c)F\eta/RT]}{1+\exp[-2X]}\left[\exp(-2X)\exp\left(X\frac{x}{x_0}\right)+\exp\left(-X\frac{x}{x_0}\right)\right],$$

where

[14] $$X = \left(\frac{i_0}{ZFv_0}\right)^{1/2}\exp(\alpha_a F\eta/2RT).$$

Hence, from [3] and [13],

[15] $$\frac{i}{ZF} = V_{x=0} = \frac{Dc_0}{x_0^2}\cdot X\cdot[1-\exp(-2F\eta/RT)]\left[1-\frac{2}{1+\exp(-2X)}\right].$$

Equation [15] reduces to the normal Butler–Volmer equation for transfer control if $v_0 \gg i_0$, i.e. the rate-controlling reaction is transfer. Hence, qualitatively, it is clear

*The model is applicable only under the condition total quantity of electricity passed = less than one monolayer under which the measurements recorded here were taken.

from [11] and [15] that if surface diffusion is the rate-controlling reaction at low current densities, transfer control will tend to be rate determining at some higher current density,* as has indeed been experimentally found (1, 4). (It is assumed that the experimental conditions are such that diffusion in solution is always "fast".)

4. COMPARISON WITH EXPERIMENT

Comparison will be made for experimental material on Cu (3). Thus, $A = 63$, $z = 2$, $\rho = 8.9$ g cc^{-1}. Values of $c_0 D$, γ, and N_0 require discussion and no measured values of D for surface diffusion on metals in contact with aqueous solutions exist at room temperature.

One can take the value of c_0, in order of magnitude terms, to be 10^{-10} mole cm^{-2}. The value depends sensitively on surface conditions: an intermediate value of those known experimentally (3, 7) was taken here.

D may be roughly estimated by extrapolation from high-temperature values obtained in the gas phase on Cu (8) by using an activation energy† of the order of 1/20th of the heat of sublimation (6). By this method, one obtains $10^{-6} \sim 10^{-7}$ cm^2/sec. The values thus calculated are, however, concerned with *adatom* movement whilst in the electro-deposition case one is concerned with the movement of adions which have a fractional charge (2). The activation energy for the adions is expected to be higher than that of adatoms, and from considerations of an energy cycle, similar to that described by Conway and Bockris (2); the value of D is found to be reduced by about 10^{-1} from the adatoms to the adion case.

Values of the number of dislocations per square centimeter of metal surface recorded in the literature vary from about 10^8–10^{12} dislocation lines cm^{-2}, the upper limit being for cold-worked material (9). The value of N_0 on a quenched surface would be likely to be some 100 less than that on a cold-worked surface. On the latter type of surface, for Cu, the mean number of dislocation from two methods (energy and density measurements) is about 4×10^{11} cm^{-2} (10). Hence it sounds reasonable to accept 4×10^9 cm^{-2}. In the present calculation, 10^{10} cm^{-2} for N_0 was taken. This higher value seems possible to accept for the following reasons. (i) The basis of the estimate of 4×10^9 cm^{-2} is very approximate (i.e., it is the generally observed order of magnitude for the ratio of the number of dislocations for a quenched, compared with a cold-worked, material). (ii) In the preparation of the specimens, SiO_2 or SiO may evaporate from the Vycor tube or diffuse from the glass sheath of the electrode and introduce increased dislocations into the surface. (iii) According to Hirsch and Silcox (11), 10^{10} dislocations cm^{-2} was observed on the rapidly quenched Al.

γ for Cu has been determined by Udin *et al.* (12), who found 1800 ergs cm^{-2} for a Cu surface at 1100° K. The value for Cu at 300° K can be approximately estimated by use of the Ramsey-Shields equation, using $T_C = 0.6 \times T_B$ (cf. *Textbook of physical chemistry* by Glasstone). The value is 2250 ergs cm^{-2}. However, this value refers to surface atoms and it is necessary to have a value of γ corresponding to atoms in the edges to which the surface adions diffuse. The value of γ for a site at which the co-ordination number

---

*An earlier explanation of the change in the rate-controlling step at higher current densities (1) involved a qualitative interpretation in terms of potential-dependent nucleation. This process does not seem a likely path in metal deposition or dissolution on surfaces such as those discussed here until current densities are much higher than those used (except on metals, e.g. vapor-phase dendrites, in which the dislocation density is particularly low).

†Obtained from calculation of the intersection points of potential energy – distance curves using both a Lennard Jones potential (Burton and Cabrera (6)) or a Morse function (Conway and Bockris (2)).

is $c_{s,1}$ may be related to that of a surface atom through Stefan's relation, according to which one finds

$$\frac{\gamma_{s,1}}{\gamma_{s,2}} = \frac{1 - \dfrac{c_{s,1}}{c_B}}{1 - \dfrac{c_{s,2}}{c_B}},$$

where $c_{s,2}$ is the co-ordination of the surface atoms and c_B is that of the bulk liquid. Taking $c_{s,1} = 7$, $c_{s,2} = 9$, and $c_B = 12$, one obtains $\gamma_{s,1} = 3750$ ergs cm^{-2}.

Comparison with experiment is shown in Fig. 1. It is seen that, having the above deduced parameters, we can achieve a moderate agreement with experiment.
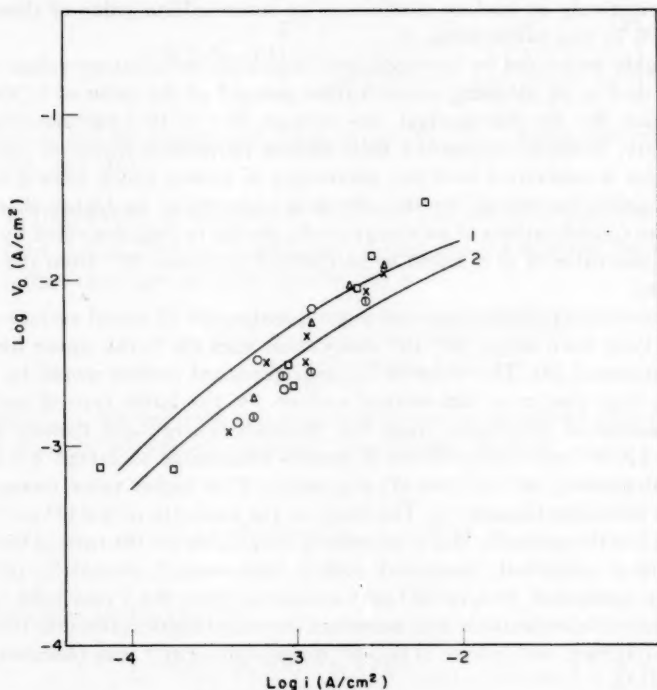
FIG. 1. Change of observed (3) and calculated v_0 with i.
Electrode: quenched electrode in He.
Solution: 0.5 ± 0.1 mole/l. H_2SO_4 and $\times$, 0.46; $\bigcirc$, 0.30; $\square$, 0.096; $\triangle$, 0.073; $\oplus$, 0.012 mole/l. $CuSO_4$.
———: Calculated v_0 using numerical values of $N_0 = 10^{10}$/cm^2, $DC_0 = 10^{-18}$ mole/sec; (1) $\gamma = 2250$ ergs/cm^2, (2) $\gamma = 3750$ ergs/cm^2.

The existence of deviations from the Butler–Volmer equation at low current densities that are due to rate-determining surface diffusion is also well rendered (Fig. 2). With an increasing number of dislocations, the Tafel lines at a given current density (Fig. 2) become increasingly coincident with those for the Tafel equation expected from transfer control. The disappearance of diffusion control with increase of current density, previously reported (1, 7), is thus satisfactorily described.
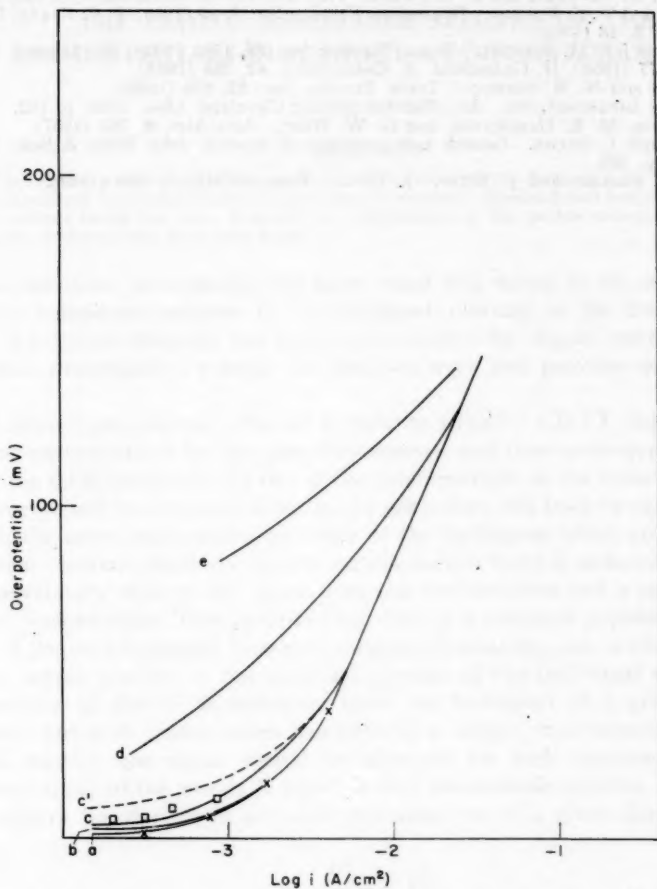
FIG. 2. Deviation from Tafel line due to "surface diffusion". a, Tafel line (transfer rate-controlling); b, $N = 10^{10}/cm^2$, $D = 10^{-8}$ cm²/sec; c, $N = 10^8/cm$, $D = 10^{-8}$ cm²/sec; d, $N = 10^6/cm$, $D = 10^{-8}$ cm²/sec; e, $N = 10^8/cm$, $D = 10^{-9}$ cm²/sec; c', the case where N changes with applied current; $\times$, experimental results on electrodeposited electrode; $\square$, experimental results on quenched electrode.

ACKNOWLEDGMENTS

REFERENCES

1. H. GERISCHER and W. VIELSTICH. Z. Elektrochem. **56**, 380 (1952). H. GERISCHER. Z. physik. Chem. **201**, 55 (1952). W. LORENZ. Z. physik. Chem. **202**, 275 (1953). W. MEHL and J. O'M. BOCKRIS. J. Chem. Phys. **27**, 818 (1957); Can. J. Chem. **37**, 190 (1959).
2. B. E. CONWAY and J. O'M. BOCKRIS. Proc. Roy. Soc. (London), A, **248**, 394 (1958); H. GERISCHER. Z. Elektrochem. **62**, 256 (1958).
3. J. O'M. BOCKRIS and M. ENYO. J. Chem. Phys. In press.
4. A. R. DESPIC and J. O'M. BOCKRIS. J. Chem. Phys. **32**, 389 (1960).
5. M. VOLMER and A. WEBER. Z. physik. Chem. **119**, 277 (1926).

6. W. K. Burton, N. Cabrera, and F. C. Frank. Phil. Trans. Roy. Soc. London, A, **263**, 299 (1951).
   N. Cabrera and W. K. Burton. Discussions Faraday Soc. **5**, 40 (1949). F. C. Frank. Discussions
   Faraday Soc. **5**, 48 (1949).
7. E. Mattson and J. O'M. Bockris. Trans. Faraday Soc. **55**, 1586 (1959). W. Lorenz. Z. physik.
   Chem. **19**, 377 (1959). H. Gerischer. Z. Elektrochem. **62**, 256 (1958).
8. N. Hackerman and N. H. Simpson. Trans. Faraday Soc. **52**, 628 (1956).
9. Impurities and Imperfections. Am. Soc. for Metals, Cleveland, Ohio. 1955. p. 162.
10. M. Llarebrough, M. E. Hargeaves, and G. W. West. Acta Met. **5**, 783 (1957).
11. P. B. Hirsch and J. Silcox. Growth and perfection of crystals. John Wiley & Sons, Inc., New
    York. 1958. p. 262.
12. H. Udin, A. J. Shaler, and J. Wulf. J. Metals, Trans. AIME, **1**, 186 (1949).

THE PROTON RESONANCE SPECTRA OF THE
2,5-DIMETHYL-2,5-DIMETHOXY-3,4-DIPHENYLHEXANES[1]

S. Brownstein

ABSTRACT

The relative free energies of the various conformations for the diastereomeric 2,5-dimethyl-2,5-dimethoxy-3,4-diphenylhexanes have been determined. Hindered and free rotation about the various bonds has been observed and assignments of the proton resonance signals to specific conformations have been made.

Proton resonance spectroscopy has been found well suited to the study of hindered rotation in substituted ethanes (1, 2). Hindered rotation in the 2,5-dimethyl-2,5-dimethoxy-3,4-diphenylhexanes has been demonstrated by dipole moment studies (3). The present investigation extends the previous work and provides some quantitative data.

For a substituted ethane with the symmetry CHXY—CHXY there are two non-equivalent conformations for the meso diastereomer and three non-equivalent conformations for the d,l diastereomer. In one of the conformations of the meso diastereomer the two hydrogens will be non-equivalent. In the other they will both be equivalent, but will not be in the same environment as either of the hydrogens which are non-equivalent. Therefore if rotation about the central carbon–carbon bond is sufficiently hindered one could theoretically observe one signal from one conformation and a pair of peaks from the other conformation. This assumes that there is a sufficient population of molecules in each of the conformations. However, with rapid rotation, only a single signal will be observed, whose position is the weighted average of the individual signals. All three conformations of the d,l diastereomer have the hydrogens of a given conformation equivalent; but each conformation has them in a unique environment. Therefore with hindered rotation one signal should be observed for each conformation. The same conclusions apply to the groups X and Y if they also contain protons.

The relative populations in any two conformations of a given diastereomer will be given by

$$\frac{P1}{P2} = e^{-\frac{\Delta E}{RT}}$$

where ΔE is the free energy difference between the two conformations. Therefore if rotation is sufficiently hindered so that proton resonance signals are observed for the individual conformations, but sufficiently rapid so that thermal equilibrium of the populations is obtained in a reasonable time, then the variation in relative intensities of the signals as the temperature is varied will yield the free energy differences between the conformations.

The rotations and conformations will be discussed with respect to the numbering shown in the following formula.
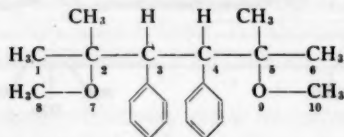
The methyl groups attached to carbon atoms 2 and 5 may be considered as part of a system of symmetry CX_2Y—$CPQR$. It has been shown that regardless of the rate of rotation about the central carbon–carbon bond the two groups X will always be magnetically non-equivalent (4). However, if rotation is hindered it may be possible to observe two peaks for each conformation.

The spectra of the meso and d,l isomers at 296° K are shown in Figs. 1 and 2. Some of the peaks of the less abundant conformations are too weak to be observed at this temperature but become apparent in spectra obtained at higher temperatures. The chemical
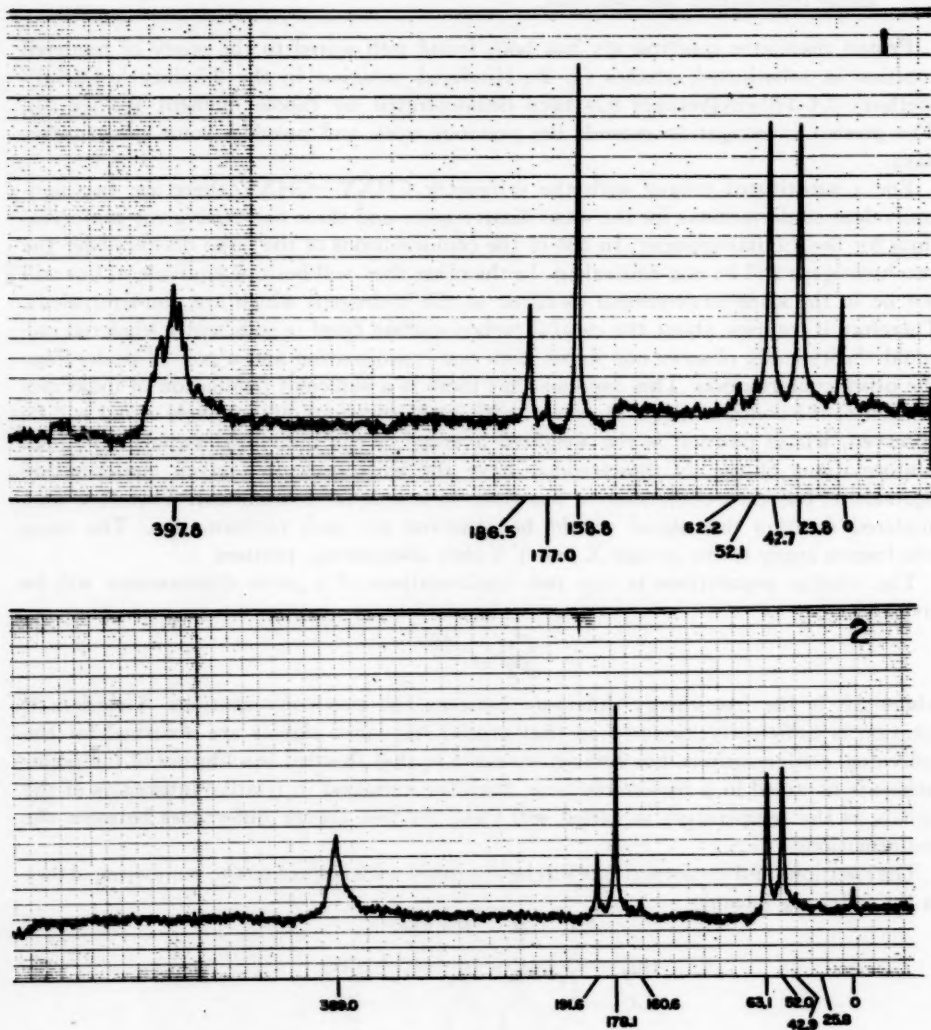
FIG. 1.   meso-2,5-Dimethyl-2,5-dimethoxy-3,4-diphenylhexane.
FIG. 2.   d,l-2,5-Dimethyl-2,5-dimethoxy-3,4-diphenylhexane.

shifts which may be assigned to definite conformations are listed in Table I. The conformations are designated as shown in Fig. 3.

TABLE I

Peak positions of the 2,5-dimethyl-2,5-dimethoxy-3,4-diphenylhexanes

Assignment	meso		Conformation	d,l		Conformation
Intense CH₃	23.8	42.7	A	52.0	63.1	D
Weak CH₃	52.1	62.2	B	25.8	42.9	C
Intense OCH₃		158.8	A		178.1	D
Weak OCH₃		177.0	B		160.6	C
Intense CH		186.5	A		191.6	D
Weak CH	179.9	188.9*	B		188.5*	C

*Position likely due to a hydrogen which is between the dimethylmethoxy group and the hydrogen attached to the opposite carbon atom of the central carbon–carbon bond.
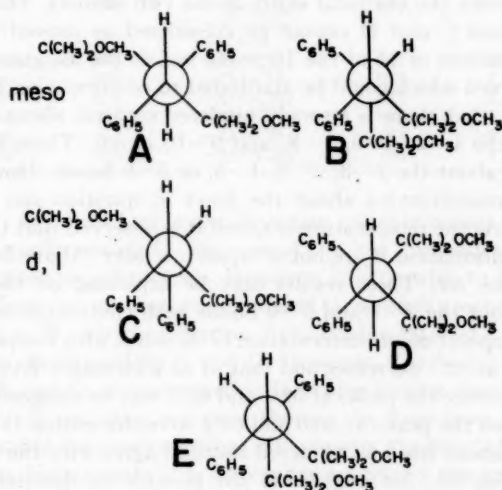
FIG. 3. Conformations of the diastereomeric 2,5-dimethyl-2,5-dimethoxy-3,4-diphenylhexanes.

The assignment to the individual conformations was done according to the following reasoning. Conformation B is the only one with non-equivalent hydrogens on the central carbon atoms; therefore the weak CH peaks must arise from this conformation. The assignment of the other peaks of the meso isomer necessarily follows. The positions reported for the weak CH peaks are those they would have in the absence of spin coupling. Actually, a four-line AB-type spectrum is obtained. Analysis yields the peak positions shown and a spin coupling constant of 1.55 ± 0.2 cycles/sec (5). The dihedral angle between these protons in conformation B is 60°. For this angle the Karplus theory of spin coupling predicts a coupling constant of 1.7 cycles/sec, which agrees nicely with this observation (6).

For the d,l isomer, the dimethylmethoxy group in conformation C is located between the phenyl and the hydrogen attached to the opposite carbon atom of the central carbon–carbon bond. It is in a similar environment for conformation A of the meso isomer.

Therefore the peaks in the d,l isomer which occur in the same position as those of conformation A may be assigned to conformation C. In conformation D the dimethylmethoxy group is located between the hydrogen and the dimethylmethoxy group attached to the opposite carbon atom of the central carbon–carbon bond. It is in a similar environment for conformation B of the meso isomer. Therefore the remaining methyl and methoxyl peaks of the d,l isomer are in good agreement with an assignment to conformation D.

Because it is impossible to assign the C—H peaks of conformation B to a given hydrogen of that conformation, one cannot compare the agreement with the position for the C—H peak of conformation C. However, because of the close similarity in chemical shifts it seems likely that the positions marked with an asterisk in Table I are both due to a hydrogen which is between the dimethylmethoxy group and the hydrogen attached to the opposite carbon atom of the central carbon–carbon bond. In both conformations A and D the C—H is located between the phenyl group and the dimethylmethoxy group attached to the opposite carbon atom of the central carbon–carbon bond. In this case there is not very good agreement between the chemical shifts in the two isomers. The assignment of the peaks to conformations C and D cannot be considered as proved; however, excellent agreement in the positions of 14 of the 16 peaks makes the assignment quite probable. No peaks were observed which could be attributed to conformation E.

So far one can say that there is strongly hindered rotation about the 3—4 bond and free rotation about the 1—2, 5—6, 7—8, and 9—10 bonds. There could be either free or hindered rotation about the 2—3, 2—7, 4—5, or 5—9 bonds. However, if rotation is hindered, only one conformation about the bond in question can be present in any appreciable amount. As the temperature is raised it is observed that the peaks due to the methyl groups in conformation B are not of equal intensity. Above 345° K another peak appears at 56.0 cycles/sec. These results may be explained on the basis of strongly hindered rotation about the 2—7 and 5—9 bonds with conformation F of Fig. 4 as the most stable. As the population of conformation G increases with temperature, the relative intensity of the peak at 52.1 decreases and that at 62.2 increases. Eventually the peak at 56.0 is observed. Therefore the peaks at 52.1 and 62.2 may be assigned to conformation F of conformation B, and the peaks at 56.0 and 62.2 to conformation G of conformation B.

These conclusions about free and hindered rotation agree with the results obtained by dipole moment studies (3). Although it is not possible to determine the freedom of rotation about the 2—3 and 4—5 bonds, examination of Fisher–Hirschfelder models indicates that free rotation is likely.

The variation in the relative intensities of the peaks with temperature is shown in Table II. From this, one can calculate that conformation A is more stable than conformation B by 1.72 ± 0.11 kcal/mole. Similarly conformation D is more stable than
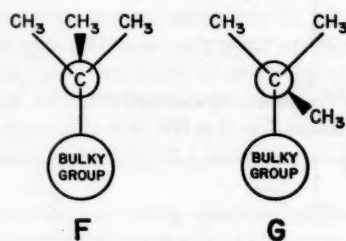

FIG. 4. Conformations about the carbon–oxygen bonds 2—7 and 5—9.

TABLE II
Temperature variation of the relative peak intensities

Isomer	T, °K	Protons measured	P1/P2	ΔE, kcal/mole
d,l	296	—O—CH$_3$ —C—CH$_3$ —C—H	.050	1.76
d,l	302	—O—CH$_3$ —C—CH$_3$ —C—H	.056	1.72
d,l	321	—O—CH$_3$ —C—CH$_3$ —C—H	.053	1.87
d,l	345	—O—CH$_3$ —C—CH$_3$ —C—H	.056	1.97
d,l	371	—O—CH$_3$ —C—CH$_3$ —C—H	.067	1.99
d,l	390	—O—CH$_3$ —C—CH$_3$ —C—H	.059	2.18
meso	296	—O—CH$_3$	.067	1.58
meso	302	—O—CH$_3$	.071	1.58
meso	321	—O—CH$_3$	.071	1.68
meso	345	—O—CH$_3$	.083	1.70
meso	371	—O—CH$_3$	.074	1.91
meso	389	—O—CH$_3$	.091	1.85

conformation C by 1.92 ± 0.13 kcal/mole. It is also possible to say that conformation F is more stable than conformation G. Because of the low intensities involved it was not possible to get quantitative information. However, it is possible to state that the energy difference between these two conformations, F and G, is much greater for conformation A than for conformation B. No contribution from conformation G was detected in the spectra attributed to conformations C and D. However, it is very likely that the energy difference between F and G in conformation D is also greater than for conformation B since no lines due to G are observed even though the lines from conformation D are quite intense. Because of the greater energy difference of the d,l conformations compared to those of the meso diastereomer it is impossible to extend this comparison to conformations B and C.

Only a single signal was seen for the C—H protons in both meso- and d,l-1,2-dibromo-1,2-diphenylethane. Their limited solubility did not allow observations below 350° K for the meso isomer and 225° K for the d,l isomer. Replacement of the dimethylmethoxy group by bromine, or other less bulky groups, would lower the energy of the barrier to rotation, but would not be likely to decrease the energy difference between conformations. At a temperature low enough for hindered rotation it is quite possible that the more stable conformation would predominate to such an extent that no signals could be observed for the other conformation. Therefore this system does not seem to be a suitable one for determining the relative sizes of groupings by determining the change in the barrier to rotation as these groupings replace dimethylmethoxy.

EXPERIMENTAL

The proton resonance spectra were obtained on a Varian Associates high-resolution nuclear magnetic resonance spectrometer Model V4300C operating at 56.4 Mc/sec. The spectra were calibrated using side-band modulation (7) counted with a Hewlett Packard

Model 521C frequency counter. The thermostated probe assembly has been described previously (8). The chemical shifts are listed in cycles per second to low field from tetramethylsilane as an internal reference. Solutions in carbon tetrachloride, saturated at room temperature, were used throughout, except for meso-1,2-dibromo-1,2-diphenylethane which was dissolved in bromoform. Since comparisons of intensity were only made for the same grouping in a somewhat different environment, peak heights rather than peak areas were used to determine intensities. For a given grouping the line width at half height was the same in both conformations. The line width for the C-methyl group was significantly greater than for the O-methyl group. This is unlikely to arise from hindrance to rotation about the 1—2 and 5—6 bonds since the line width did not decrease significantly at the higher temperatures. Both diastereomers of 1,2-dibromo-1,2-diphenylethane were prepared as reported in the literature (9).

ACKNOWLEDGMENT

REFERENCES

1. J. J. Drysdale and W. D. Phillips.   J. Am. Chem. Soc. 79, 319 (1957).
2. J. A. Pople.   Mol. Phys. 1, 3 (1958).
3. H. Sawatzky, G. K. White, and G. F Wright.   Can. J. Chem. 37, 1132 (1959).
4. P. M. Nair and J. D. Roberts.   J. Am. Chem. Soc. 79, 4565 (1957).
5. J. A. Pople, W. G. Schneider, and H. J. Bernstein.   High-resolution nuclear magnetic resonance. McGraw-Hill Book Co., New York. 1959.
6. M. Karplus.   J. Chem. Phys. 30, 11 (1959).
7. J. T. Arnold and M. E. Packard.   J. Chem. Phys. 19, 1608 (1951).
8. S. Brownstein.   Can. J. Chem. 37, 1119 (1959).
9. J. Wislicenus and F. Seeler.   Ber. 28, 2693 (1895).

AN EXTRACELLULAR POLYSACCHARIDE FROM
GIBBERELLA FUJIKUROI (FUSARIUM MONILIFORME)[1]

I. R. SIDDIQUI[2] AND G. A. ADAMS

ABSTRACT

Growth of *Gibberella fujikuroi* (*Fusarium moniliforme*) on a glucose medium produced an extracellular polysaccharide containing D-glucose, D-mannose, D-galactose, D-glucuronic acid (molar ratio 1.0:1.1:1.3:0.6), and possibly D-mannuronic acid. Protein was retained tenaciously by the polysaccharide and several deproteinization methods reduced the nitrogen content only slightly. Methylation studies showed that the polysaccharide was highly branched with D-glucose and D-mannose forming the non-reducing ends in the molecule. Most of the D-mannose and D-galactose units were joined by $1 \rightarrow 2$ and $1 \rightarrow 6$ linkages with some branching also at C_2 and C_6 positions; D-galactose occurred exclusively in the furanose form. D-Glucose units were joined by $1 \rightarrow 2$ and $1 \rightarrow 3$ linkages. The D-glucuronic acid residues were mainly non-terminal and were attached to both D-galactose and D-mannose units. Periodate oxidation studies supported the foregoing conclusions.

Although there are many reports in the literature dealing with the isolation of polysaccharides from a variety of fungi (1–4), few investigations of the structural features of fungal polysaccharides have been made. Galactocarolose, a polysaccharide elaborated by *Penicillium charlesii*, has been shown to contain 9–10 β-galactofuranose units linked through the $1 \rightarrow 5$ position (5). A polysaccharide (varianose) containing $1 \rightarrow 4$ linked galactose units terminated by glucose and idose or altrose has been isolated from *Penicillium varians* (6). Barker *et al.* (7) have shown that an extracellular polyglucosan isolated from *Aspergillus niger* consisted of D-glucose units linked α $1 \rightarrow 4$ and α $1 \rightarrow 3$. A recent survey by Martin and Adams (8) of the polysaccharides produced by 31 species of fungi showed a wide variation in sugar components in both the intracellular and extracellular polysaccharides. In this laboratory, four strains of *Fusarium* (*Fusarium lini* NRC 666, 9593; *Fusarium moniliforme* NRC F73; *Fusarium* species NRC 68) and one strain of *Trichoderma viride* NRC v139 were examined for polysaccharide production, using procedures described by Martin and Adams (8). Following this preliminary study, a more intensive investigation was made of the preparation, isolation, and structural features of the polysaccharide from *Gibberella fujikuroi* (*Fusarium moniliforme*) NRC F73, ATCC 10052. The results of this investigation form the basis for the present communication.

G. fujikuroi was grown on buffered enriched salts medium with glucose as the carbon source. The crude polysaccharide was precipitated from the concentrated culture medium by ethanol after the removal of the cells and salts. Addition of 'Cetavlon' (9) to an aqueous solution of the acidic polysaccharide gave a small oily precipitate, an acid hydrolyzate of which showed equal amounts of the same sugar components as were in an acid hydrolyzate of the Cetavlon-soluble fraction. Since no amino sugars were detectable in an acid hydrolyzate of the polysaccharide, it was assumed that the nitrogen content (3.96%) represented mainly protein contaminants. This observation was confirmed by the presence of amino acids (ninhydrin test) in the acid hydrolyzates. Attempts to remove or reduce the protein content of the crude polysaccharide material by the Sevag method (10) were not practicable since considerable quantities of the polysaccharide were removed

along with the denatured protein. The conclusion that the protein was firmly bound to the polysaccharide was substantiated by the failure of prolonged tryptic digestion (11) to remove it. The use of phenol–water partition (12), however, produced some purification as shown by the lower nitrogen content of the water-soluble fraction (2.9%) as compared with that of the phenol-soluble fraction (3.8%).

The sugar components of the partially purified acidic polysaccharides were glucose, mannose, galactose, and hexuronic acid (1.0:1.1:1.3:0.6). This sugar ratio was determined in an acid hydrolyzate of the polysaccharide obtained by heating the mixture at 100° C for 3 hours with 2 N sulphuric acid, and does not take into account the sugars bound in the uronic acid complexes. Boundary electrophoresis (13) of the polysaccharide in borate buffer showed one major peak along with a smaller stationary peak (Fig. 1) which was

173 MIN

⊢──→ DESC.
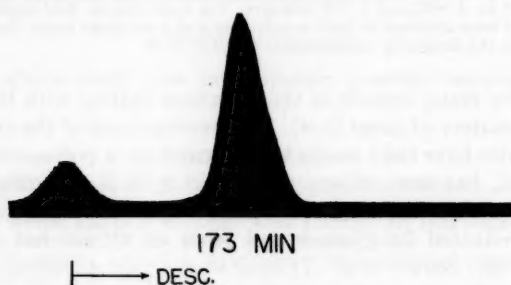
FIG. 1. Electrophoretic pattern of polysaccharide in acetate buffer (pH 5).

presumably a boundary anomaly. The major peak, however, was not symmetrical and hence the polysaccharide may not be homogeneous. The infrared spectrum confirmed the presence of carboxylic acid groupings. The spectrum of the sodium salt showed absorption at 1615 cm⁻¹ and 1405 cm⁻¹, which is characteristic of the carboxylate ion. Amide bands (C=O, 1650 cm⁻¹; and —N—H, 1520 cm⁻¹), such as those given by proteins, were also detected. The absence of absorption at 1735 cm⁻¹ in the spectrum of the sodium salt of the acidic polysaccharide precluded the existence of O-acetyl groups. The ultraviolet absorption spectrum showed an absorption peak at 275 mμ which is characteristic of proteins containing aromatic amino acids (14).

The mixture of sugars produced by heating the polysaccharide with 2 N sulphuric acid at 100° C for 3 hours was fractionated first on an anion exchange resin and subsequently on paper chromatograms. From the hydrolysis products, D-glucose, D-mannose, and D-galactose were recovered and characterized either in crystalline form or as crystalline derivatives. The acidic components were identified as D-glucuronic acid, and an aldo-biouronic acid which was a glucuronosyl-galactofuranose as established by reduction, methylation, and hydrolysis. Two aldotriouronic acids were isolated in amounts too small to establish their structure; one contained galactose, mannose, and glucuronic acid, the other, galactose, mannose, and a hexuronic acid, which appeared to be mannuronic acid.

The polysaccharide was methylated and the hydrolysis products were separated by chromatography on an anion exchange column and then on paper chromatograms. The weights of the fractions finally isolated, together with that of the di-O-methyl uronic acid, corresponded to the following approximate molar ratios: tetra-O-methyl hexose, 3;

tri-*O*-methyl hexose, 2; di-*O*-methyl hexose, 2. The components of each of the above fractions along with their relative ratios are listed in Table I. All of these sugars, with the

TABLE I
Yield of methylated sugars

Fraction	Weight (mg)	Components	Molar ratio
Tetra-*O*-methyl hexose	680	2,3,4,6-Tetra-*O*-methyl-D-glucose 2,3,4,6-Tetra-*O*-methyl-D-mannose	3
Tri-*O*-methyl hexose	390	2,4,6-Tri-*O*-methyl-D-glucose 3,4,6-Tri-*O*-methyl-D-glucose 3,5,6-Tri-*O*-methyl-D-galactose 2,3,5-Tri-*O*-methyl-D-galactose 2,3,4-Tri-*O*-methyl-D-mannose 3,4,6-Tri-*O*-methyl-D-mannose	2
Di-*O*-methyl hexose	380	3,5-Di-*O*-methyl-D-galactose 3,4-Di-*O*-methyl-D-mannose 3,6-Di-*O*-methyl-D-mannose	2

exception of 3,5,6-tri-*O*-methyl-D-galactose and 3,6-di-*O*-methyl-D-mannose, were obtained either in crystalline form or were characterized by the isolation of crystalline derivatives.

The ratio of glucose:mannose:galactose, calculated from the weights of the methylated sugars, was 1.0:1.4:1.1, in reasonable agreement with that found for the original polysaccharide (1.0:1.1:1.3).

The number and proportion of methylated sugars indicated, in general, that the molecule was highly branched. The relatively large amount of tetra-*O*-methyl sugars represented a high proportion of non-reducing terminal units in the molecule. Of these, there was a predominance of glucose over mannose end groups; galactose units were apparently not present on the periphery of the molecule.

A considerable proportion of the main body of the molecule was made up of D-mannose units linked $1 \rightarrow 2$ and $1 \rightarrow 6$ as shown by the occurrence of 3,4,6-tri-*O*-methyl-D-mannose and 2,3,4-tri-*O*-methyl-D-mannose. Lesser amounts of glucose were linked $1 \rightarrow 2$ and $1 \rightarrow 3$. Galactose was recovered as 2,3,5-tri-*O*-methyl-D-galactose and 3,5,6-tri-*O*-methyl-D-galactose on hydrolysis and showed that the D-galactofuranose units were linked glycosidically $1 \rightarrow 6$ and $1 \rightarrow 2$. The presence of 3,5-di-*O*-methyl-D-galactose showed that some of the galactofuranose units formed branch points through C_2 and C_6. Smaller amounts of 3,4-di-*O*-methyl-D-mannose likewise showed that some of the mannopyranose units formed branch points through C_2 and C_6. The tentative identification of 3,6-di-*O*-methyl-D-mannopyranose indicated that some D-mannose units had some minor branching through C_2 and C_4.

Mild acid hydrolysis of the polysaccharide as provided by heating in 0.01 *N* sulphuric acid at 100° C for periods as long as 6 hours did not release any sugars, showing that no more than two furanoside units were contiguous and that no terminal furanoside ring forms were present. This latter observation was further substantiated by the fact that no 2,3,5,6-tetra-*O*-methyl-D-galactose was detected in the cleavage products of the methylated polysaccharide.

Evidence that the major portion of the D-glucuronic acid residues were non-terminal was provided by the identification of 2,3-di-*O*-methyl-D-glucose as a hydrolysis product of the reduced methylated uronic acid isolated from the fully methylated polysaccharide. A small amount of D-glucuronic acid was identified also as 2,3,4-tri-*O*-methyl-D-glucose

after separation, reduction, and hydrolysis of the methylated uronic acid components of the fully methylated polysaccharide. The conclusion that some of the uronic acid was attached to the galactose unit was provided by the isolation of a glucuronosyl galactose by partial hydrolysis of the polysaccharide. Hydrolysis of a methylated aldobiouronic acid fraction yielded 3,4-di-O-methyl-D-mannose and a methylated uronic acid, showing that some of the uronic acid was attached to D-mannose through C_2 or C_6. Following methanolysis, reduction, and hydrolysis, the uronic acid portion appeared as 2,3-di-O-methyl-D-glucose. Hydrolysis of a methylated aldotriouronic acid yielded 3,4-di-O-methyl-D-mannose, 3,5-di-O-methyl-D-galactofuranose, and 2,3,4-tri-O-methyl-D-glucuronic acid. This observation showed that some D-glucuronic units were attached terminally to either unit of contiguous D-galactose and D-mannose residues.

On periodate oxidation, the acidic polysaccharide consumed 1.3 moles of periodate and produced 0.5 mole of formic acid. Acid hydrolysis of the periodate-oxidized polysaccharide gave large amounts of galactose and small amounts of acidic components. Examination of the oxidized polysaccharide by the procedure of Smith et al. (15) showed, in addition to the components detected in the acid hydrolyzate, small amounts of arabinose, traces of two components ($R_{glucose}$ 1.01 and 1.23), glycerol, but no erythritol. The absence of erythritol precluded 1,4 linkages in the polysaccharide but the presence of arabinose clearly indicated that at least some of the galactose residues were in the furanose form with C_5 and C_6 unsubstituted. This is in accord with the isolation of 3,5,6-tri-O-methyl-D-galactose from the methylated polysaccharide. Galactose units in the furanose form that were not oxidized by periodate were linked through C_2 and C_6 and gave rise to 3,5-di-O-methyl-D-galactofuranose as a product of methylation and hydrolysis. The yield of 0.5 mole of formic acid indicated that 50% of the sugar units (pyranose form) were either linked $1 \rightarrow 6$ or were present in non-reducing end groups. Approximately 30% of the residues consumed periodate but did not produce formic acid; such units could be either in the pyranose or furanose form and could be linked $1 \rightarrow 2$. The remainder of the sugar residues did not consume periodate; of these, the pyranose sugars must be linked $1 \rightarrow 3$ or be branched, and the furanose forms must be attached through C_2 and C_6. Such an attachment of the galactofuranose units would account for the relatively high yield of 3,5-di-O-methyl-D-galactofuranose obtained on hydrolysis of the fully methylated polysaccharide.

Present data do not permit formulation of a unique structure for the polysaccharide, although certain structural features have been established. However, no certainty exists that the polysaccharide examined was a homogeneous molecule. Electrophoretic examination indicated that minor amounts of other materials were present. On the basis of methylation and periodate oxidation results, it is suggested that an average general repeating unit consisted of seven sugar units arranged in the following pattern.

$$
\begin{array}{ccc}
O\!-\!O\!-\!O \\
| \quad | \\
O \quad O \\
| \quad | \\
O \quad O
\end{array}
$$

Such a formulation would not only account for the molar ratio (3:2:2) obtained for the tetra-, tri-, and di-O-methyl ethers but would also yield the periodate oxidation result of 1.3 moles periodate consumed, and 0.5 mole formic acid produced. It is suggested that the polysaccharide may consist of repeating units conforming to the general pattern

shown above and containing various sugars. Fragmentation studies now being planned are necessary to reveal further fine features of this polysaccharide.

EXPERIMENTAL

The following solvents (v/v ratios) were used for chromatographic separations: (A) n-butanol:ethanol:water (5:1:4); (B) butanone saturated with water containing 2% ammonia; (C) benzene:ethanol:water:ammonia (200:47:14:1); (D) n-butanol:acetic acid:water (40:1:5); (E) pyridine:ethyl acetate:water (1:2.5:2.5); (F) n-butanol:ethanol: water (40:11:19). Sugars, as their borate complexes, were separated by electrophoresis in 0.2 M borate buffer (pH 10) and uronic acids were analyzed in acetate buffer (pH 5) (17). All electrophoretic examinations were made on Whatman No. 3MM paper at 700–800 v. Uronic acid content was determined by the method of Barker *et al.* (17). Reducing sugars were detected on paper chromatograms or electrophoretograms with *p*-anisidine hydrochloride spray (18); non-reducing sugars were detected by alkaline silver nitrate (19). Evaporations were carried out at 35° C on a rotary film evaporator. Melting points are corrected and rotations are equilibrium values unless otherwise stated.

Cultural Conditions

The organism *G. fujikuroi* was grown on a culture medium as described by Martin and Adams (8), the glucose solution (20 l.) and the other nutrients were sterilized separately and then mixed aseptically in a bottle of 40-l. capacity. The culture was grown on a malt–agar slant and the spores were used to prepare successively larger batches of inoculum. The final inoculated medium was grown at 29° on a rotary shaker with aeration provided by an air stream of about 1 l. per minute passing over the surface of the solution. The cultures were harvested when 80–85% of the sugar had been consumed.

Isolation of the Polysaccharide

The mycelium was removed by filtration through paper and the filtrate was concentrated about 10-fold at 30° C in a Majonnier evaporator and then dialyzed against cold water (2° C) for 2 days. The non-dialyzable material was poured into 3 volumes of ethanol with vigorous stirring. The precipitate was removed by centrifugation, washed with ethanol and ether, and dried *in vacuo* over phosphorus pentoxide (yield 300 mg/l., 7% based on glucose consumed).

The crude polysaccharide (12 g) was extracted with water to yield a water-soluble fraction (6.4 g) and a water-insoluble residue (5.6 g). Chromatographic and electrophoretic examination of hydrolyzates of each fraction showed that the water-soluble material contained glucose, galactose, mannose, and uronic acid components; the residue contained only traces of glucose and mannose, and was discarded.

Attempted Removal of Protein from the Polysaccharide

The crude, water-soluble polysaccharide had a nitrogen content of 3.96%. Since its acid hydrolyzate gave a negative test for amino sugars (20) and a positive test (ninhydrin) for amino acids, it was concluded that the contaminant was protein.

Fractionation by Cetavlon (9) gave a small oily precipitate which on electrophoretic examination in borate buffer gave the same pattern as the unprecipitated material. Examination, by chromatography, of hydrolyzates of the two materials showed that the same sugars were present in each.

Fractionation by phenol (12) gave a water-soluble fraction having a nitrogen content

of 2.9% while that of the phenol-soluble material was 3.8%, but the two fractions had identical sugar components.

Digestion with trypsin (11) for 5 days at 35° C did not lower the nitrogen content of the polysaccharide preparation significantly.

Analysis of Acidic Polysaccharide

The polysaccharide ($[\alpha]_D^{28}$ +12.7±1° (*c*, 1.02 in water)) on analysis gave the following: N, 2.9%; ash, 3.9%; P, nil; and uronic acid, 15%. Electrophoretic examination in a Spinco apparatus model H in 0.5 *M* borate buffer (pH 9.2) showed a single asymmetric peak (Fig. 1). The polysaccharide (10 mg) was hydrolyzed with 2 *N* sulphuric acid for 4 hours at 100° C. The sugars were recovered and determined quantitatively according to Nelson (21), giving a ratio of glucose:mannose:galactose of 1.0:1.1:1.3.

Acid Hydrolysis of the Polysaccharide

Polysaccharide (1.5 g) was hydrolyzed with 2 *N* sulphuric acid (30 ml) for 3 hours at 100° C. After neutralization (BaCO₃) and filtration, the filtrate was slurried with ion exchange resin Dowex 1 (carbonate form, 35 g) for 24 hours. The resin was then washed with water (1 l.) in a column to remove the neutral sugars (0.95 g). The uronic acid fraction was eluted with *N* ammonium carbonate (500 ml) and recovered (0.250 g) by removing excess ammonium carbonate by distillation *in vacuo* at 65–70° C and the remainder with Amberlite IR-120 (H) resin.

A. Neutral Sugars

A portion of the neutral sugars was separated on Whatman 3MM paper using solvent E. Elution with water yielded glucose, mannose, and galactose as syrups.

(i) D-*Glucose*

The syrup was refluxed for 15 minutes with an aliquot (1 ml) of a solution containing *p*-nitroaniline (9 g), methanol (200 ml), and concentrated hydrochloric acid (0.14 ml). The mixture was filtered while hot and after it had cooled, crystallization occurred. Two recrystallizations from methanol gave *N*-*p*-nitrophenyl-D-glucopyranosylamine dihydrate having m.p. and mixed m.p. 184° C. Reported (22): m.p. 184° C.

(ii) D-*Mannose*

The syrup was similarly characterized as *N*-*p*-nitrophenyl-β-D-mannopyranosylamine dihydrate having m.p. 219° C and $[\alpha]_D^{26}$ −330° (*c*, 0.112 in dry pyridine). Reported (22): m.p. 219° C.

(iii) D-*Galactose*

The sugar crystallized from methanol to give m.p. 164–167° C and $[\alpha]_D^{26}$ +80.2±1° (*c*, 0.445 in water), and was therefore D-galactose.

B. Uronic Acid Fraction

The acidic sugars (0.25 g) were separated on Whatman No. 1 paper with solvent A. Three main components were recovered corresponding to hexuronic (A), aldobiouronic (B), and aldotriouronic acid (C) respectively. Two very minor components, one (D) near the starting line and another (E) which moved ahead of (A), were recovered in trace amounts.

(i) Hexuronic Fraction (A)

This fraction (20 mg) was converted to its methyl ester glycoside form by refluxing with methanolic hydrogen chloride (2%) for 6 hours. Reduction with lithium aluminum hydride (23) (80 mg) in tetrahydrofuran:ethyl ether solution (4:1) yielded the corresponding methyl hexoside. Acid hydrolysis and paper chromatography showed glucose

with traces of mannose and galactose. The main hexuronic acid was therefore glucuronic acid.

(ii) Aldobiouronic Acid Fraction (B)

A portion of this fraction (7.5 mg) was hydrolyzed with 2 N sulphuric acid for 3 hours at 100° C. Paper chromatography in solvent A showed glucuronic acid, galactose, and some original material. A portion of the acid (70 mg) was converted to its methyl glycoside methyl ester and reduced with lithium aluminum hydride as described above. Examination of the acid hydrolyzate (solvent E) showed glucose and galactose. The methyl bioside (43 mg) was dissolved in tetrahydrofuran (5 ml) and methylated by the Falconer and Adams procedure (24). The product was recovered by extraction with chloroform. Three methylations by this method followed by one methylation by Purdie's method (methyl iodide, 10 ml; silver oxide, 1 g) gave a fully methylated product, as indicated by its infrared spectrum. Hydrolysis of the methylated disaccharide and separation of the sugars by paper chromatography (solvent B) yielded 2,3,4,6-tetra-O-methyl-D-glucose and a tri-O-methyl galactose (R_g 0.86).

(iii) Aldotriouronic Acid Fraction (C)

Paper chromatography of this fraction in solvent A for 4 days showed the presence of two components C_I ($R_{glucose}$ 0.23) and C_{II} ($R_{glucose}$ 0.17). Acid hydrolysis (2 N sulphuric at 100° C for 3 hours) and chromatographic examination of the hydrolyzates (solvents A and E) showed the components of C_I to be galactose, mannose, and hexuronic acid (which appeared to be mannuronic acid); the components of C_{II} were galactose, mannose, and glucuronic acid.

Spectra of the Polysaccharide

The ultraviolet absorption spectrum of an aqueous solution (0.5%) of the polysaccharide showed a peak at 275 mμ. The infrared spectrum was determined in potassium chloride disks on the free acid form and also the sodium salt of the polysaccharide. The main characteristics of the spectra of both forms were bands ν_{max} 1615, 1405, 1520, and 1650 cm^{-1}; the free acid had an additional band at 1735 cm^{-1}.

Periodate Oxidation

The polysaccharide was oxidized according to the method of Jeanes and Wilham (25). The number of moles of periodate consumed and formic acid produced per 162 g of polysaccharide are given in the following table:

Time (hours)	24	48	72	96	112
Periodate consumption	0.93	1.00	1.20	1.33	1.36
Formic acid production	0.36	0.47	0.54	0.58	0.60

Extrapolation of these values to 0 time showed a ratio of periodate consumed:formic acid produced of 1.3:0.5 mole per 162 g of polysaccharide.

The remaining solution of oxidized polysaccharide was treated with ethylene glycol, dialyzed against tap water, and the product recovered by freeze-drying. A portion was hydrolyzed and on paper chromatographic examination showed large amounts of galactose and small amounts of uronic acid. The remainder of the periodate-oxidized material (40 mg) was dissolved in water (4 ml) and after deionization with Amberlite ion exchange resins IR-45 and IR-120, a solution of potassium borohydride (150 mg in 1 ml of water) was added. After 24 hours, the solution was neutralized with acetic acid, dialyzed for

24 hours, and the reduced product was recovered by freeze-drying. A small amount was hydrolyzed with 2 N sulphuric acid for 3 hours at 100° C. After neutralization, the hydrolyzate was examined by paper chromatography in solvent E and contained galactose, arabinose, and two spots ($R_{glucose}$ 1.01 and 1.23) which gave a light green color with p-anisidine spray reagent. A chromatogram of the same hydrolyzate in solvent F and sprayed with silver nitrate reagent (19) showed glycerol but no erythritol.

Methylation

The polysaccharide (3.0 g), dissolved in water (30 ml), was methylated by the dropwise addition of 30% sodium hydroxide (160 ml) and dimethyl sulphate (60 ml) and was stirred for 24 hours. The reagents were added at such a rate that the reaction mixture was always alkaline. The addition of the methylating agents was repeated twice. The methylation mixture was heated for 75 minutes at 80° C, then cooled, and finally neutralized with sulphuric acid. The precipitated salts were dissolved in water, and the partly methylated polysaccharide was extracted with chloroform. The recovered methylated polysaccharide (2.78 g) showed a definite hydroxyl band at 3500–3600 cm⁻¹ in its infrared spectrum. The partially methylated polysaccharide was dissolved in tetrahydrofuran (150 ml) containing pulverized sodium hydroxide (15 g), and dimethyl sulphate (18 ml) was added dropwise over 6 hours with constant stirring. The mixture was stirred for 18 hours, and then sufficient water was added to dissolve the solids. The pH was adjusted to 9.0 and the solution was extracted with chloroform. The recovered methylated polysaccharide still contained free hydroxyl groups as shown by its infrared spectrum: consequently, the previous methylation was repeated twice more. The methylated product still showed a small hydroxyl group in the infrared spectrum and was methylated further by Purdie's method (methyl iodide, 100 ml; silver oxide, 20 g). After two Purdie methylations there were no free hydroxyl groups shown in the infrared spectrum. Yield 3.1 g, methoxyl content 39.0%.

Hydrolysis of Methylated Polysaccharide

The methylated polysaccharide (3.1 g) was refluxed with 4% methanolic hydrogen chloride (100 ml) for 24 hours. The solution was neutralized with silver carbonate, filtered, and evaporated in vacuo to a syrup, which was hydrolyzed with N sulphuric acid for 30 hours at 100° C. Periodic analysis of aliquots of the hydrolyzate by gas–liquid partition chromatography (26) showed that the prolonged hydrolysis period was necessary to hydrolyze the glycosides completely. The hydrolyzate was neutralized with barium carbonate, filtered, and concentrated to about 100 ml.

Separation of Acidic and Neutral Sugars

The above hydrolyzate (100 ml) was stirred for 30 hours with Dowex 1 (carbonate form) (35 g). The resin was then poured into a column and washed with water (1.5 l.) to elute neutral methyl sugars (1.99 g) and with N ammonium carbonate (700 ml) to elute the methylated uronic acid fraction (0.34 g). The latter was recovered by removing most of the ammonium carbonate by sublimation in vacuo at 65–70° C and the remainder by passing the solution over Amberlite resin IR-120.

A. Separation of Tetra-, Tri-, and Di-O-methyl Sugars

The mixture of neutral methyl sugars (1.6 g) was separated on large sheets of Whatman No. 3 MM papers using solvent A. The three bands located on the papers corresponded to tetra-O-methyl, tri-O-methyl, and di-O-methyl sugars having R_g values of 1.0, 0.84,

and 0.64 respectively. The weights were: tetra-O-methyl, 680 mg; tri-O-methyl, 390 mg; and di-O-methyl, 380 mg, which corresponds to an approximate molar ratio of 3:2:2.

B. Examination and Identification of Tetra-O-methyl Fraction

The syrupy tetra-O-methyl fraction had $[\alpha]_D^{25}$ +48.8° (c, 2.06% in water) and a methoxyl content 50.8% (theoretical value for $C_{10}H_{20}O_6$, 52.5%). Demethylation with boron trichloride (27) gave glucose and mannose as the parent sugars. The tetra-O-methyl fraction (2–3 mg) was heated in a sealed tube with 2% methanolic hydrogen chloride for 12 hours and neutralized with silver carbonate. The mixture of glycosides was examined by gas–liquid partition chromatography (26) using a 4-ft column of 20% Apiezon M on Celite 545 at 150° C and an argon flow rate of 150 ml/min. The examination showed the presence of the methyl glycosides of 2,3,4,6-tetra-O-methyl-D-glucose and 2,3,4,6-tetra-O-methyl-D-mannose in a ratio of 58.9:41.1. Optical rotation measurements of the original mixture indicated a ratio of 2,3,4,6-tetra-O-methyl-D-glucose:2,3,4,6-tetra-O-methyl-D-mannose of 57.3:42.7.

(i) 2,3,4,6-Tetra-O-methyl-D-glucose

The foregoing tetra-O-methyl fraction (550 mg) was dissolved in ethyl ether, small amounts of impurities were centrifuged off, and petroleum ether was added drop by drop. On being cooled, the solution deposited crystals (70 mg) which, after several recrystallizations from ether – petroleum ether (1:1), gave 2,3,4,6-tetra-O-methyl-D-glucose, m.p. 95–96° C; $[\alpha]_D^{25}$ +82.6±2° (c, 0.605% in water). An aliquot of the mother liquor (27 mg) was heated with aniline (15 mg) in methanol (2 ml) and the solution refluxed for 2 hours. The anilide crystallized on partial removal of the solvent and on recrystallization from ethanol gave 2,3,4,6-tetra-O-methyl-N-phenyl-D-glucosylamine, m.p. 134–137° C. Reported value: 137–138° C (28).

(ii) 2,3,4,6-Tetra-O-methyl-D-mannose

A portion of the original tetra-O-methyl hexose mixture was run on sheets of Whatman No. 1 paper using solvent B until the solvent front reached the bottom of the papers. The sugars were located on the papers, the appropriate strips cut out and attached to the top of new sheets of paper, and the chromatograms again run with solvent B. The sugar band was located and the slower-moving fourth of the area was cut out and eluted with water. The syrupy product (20 mg) in methanol (2 ml) was refluxed with aniline (10 mg) to yield crystalline 2,3,4,6-tetra-O-methyl-N-phenyl-D-mannosylamine, which was recrystallized from ethyl ether to give a melting point of 144–146° C, undepressed on admixture with an authentic specimen. Reported (29): m.p. 142–143° C. The X-ray diffraction pattern of the crystals was identical with that of the authentic specimen of 2,3,4,6-tetra-O-methyl-N-phenyl-D-mannosylamine.

C. Examination and Identification of Tri-O-methyl Fraction

The tri-O-methyl fraction (390 mg) ($[\alpha]_D^{26}$ +12.6° (c, 2.53 in water)) yielded galactose, mannose, and a minor amount of glucose on demethylation by boron trichloride (26). Paper electrophoresis (17) (borate buffer, pH 10) separated the sugars into two borate-complexing fractions (0.154 g and 0.0125 g respectively) and a non-complexing fraction (0.126 g).

(i) Borate Non-complexing Fraction

This fraction, when demethylated as before, showed the presence of galactose, mannose, and a small amount of glucose. Paper chromatography in solvent B separated three components, two of which had the same R_g values (0.57 and 0.65) and color reactions with

p-anisidine hydrochloride as 2,4,6-tri-*O*-methyl-D-glucose and 2,3,4-tri-*O*-methyl-D-mannose respectively. The third component had an R_g of 0.74.

2,4,6-Tri-O-methyl-D-glucose.—The syrup (5 mg) was refluxed with aniline (3 mg) in methanol (1 ml) for 3 hours. The product crystallized on partial evaporation of the solvent and on recrystallization from ether gave 2,4,6-tri-*O*-methyl-*N*-phenyl-D-glucosylamine, m.p. 159–162° C. Reported value: 162–166° C (30).

2,3,4-Tri-O-methyl-D-mannose.—The syrup (33.5 mg) was oxidized with bromine (0.1 ml) in the presence of barium carbonate (30 mg) for 70 hours. Bromine was removed by aeration and the acidified solution was extracted with chloroform for 2 days. The chloroform extract was dried with anhydrous sodium sulphate and concentrated to a syrup, which was distilled (bath temperature 130–160° C at 0.01 mm). The distilled syrup was dissolved in methanol saturated with ammonia (5 ml) and allowed to stand for 24 hours at 5° C. Removal of the solvent gave a syrup which crystallized from ethanol:ethyl ether solution giving 2,3,4-tri-*O*-methyl-D-mannosamide, m.p. and mixed m.p. 143° C. Reported (31): m.p. 143° C.

2,3,5-Tri-O-methyl-D-galactose.—The syrup (33 mg) (R_g 0.74, solvent B) was oxidized by bromine as described above. The syrupy lactone showed a strong C≡O stretching peak at 1786 cm^{-1} in its infrared spectrum and was therefore a γ lactone. Treatment with methanolic ammonia gave a crystalline amide, m.p. 145–146° C; $[\alpha]_D^{26}$ −5.1±1.5° (*c*, 0.72 in methanol). Anal. Calc. for $C_9H_{19}O_6N$: C, 45.5%; H, 8.02%; N, 5.9%; OMe, 39.2%. Found: C, 45.15%; H, 8.3%; N, 6.04%; OMe, 38.9%. Since the galactose was in the furanose form this sugar was either 2,3,5- or 2,5,6-tri-*O*-methyl-D-galactose. Periodate oxidation of its amide by the method of Baddiley *et al.* (32) showed a negative test, thus eliminating 2,5,6-tri-*O*-methyl-D-galactofuranose, and hence the sugar was tentatively identified as 2,3,5-tri-*O*-methyl-D-galactofuranose.

(ii) Borate-complexing Fraction I

This fraction on demethylation gave mannose and glucose as the parent sugars. Paper chromatography in solvent C separated two components having R_t values and color reactions with *p*-anisidine spray reagent (18) identical with 3,4,6-tri-*O*-methyl-D-mannose (75 mg) and 3,4,6-tri-*O*-methyl-D-glucose (10 mg).

3,4,6-Tri-O-methyl-D-mannose.—The syrup (75 mg) crystallized on seeding with an authentic specimen of 3,4,6-tri-*O*-methyl-α-D-mannose. On recrystallization from ether: hexane the sugar had a melting point of 102–103° C (undepressed on admixture with an authentic sample) and $[\alpha]_D^{25}$ +32±2° (*c*, 0.875 in methanol). Reported values (33): m.p. 101–102° C; $[\alpha]_D$ +36° (methanol).

3,4,6-Tri-O-methyl-D-glucose.—On seeding with an authentic specimen of 3,4,6-tri-*O*-methyl-D-glucose, the syrup (10 mg) crystallized. Recrystallization from ether:hexane at 0° C gave 3,4,6-tri-*O*-methyl-α-D-glucose, m.p. 76–77°. Reported value (34): m.p. 76–77° C.

(iii) Borate-complexing Fraction II (12 mg)

3,5,6-Tri-O-methyl-D-galactose.—The syrup had $[\alpha]_D^{25}$ −16.2±1.5° (*c*, 1.23 in water). Demethylation by boron trichloride showed galactose as the only parent sugar. Movement on electrophoresis in borate buffer showed that C_2 was unsubstituted and the sugar was tentatively identified as 3,5,6-tri-*O*-methyl glucose. An aliquot (2 mg) was converted to the methyl glycoside by heating in 2% methanolic hydrogen chloride. The glycoside was methylated by the Kuhn procedure (35), and examination of the product by gas–liquid chromatography yielded the glycoside of 2,3,5,6-tetra-*O*-methyl-D-galactose.

D. Examination and Identification of Di-O-methyl Sugars

The fraction had $[\alpha]_D^{20}$ −12.5° (c, 1.35 in water); OMe, 28.7%. Calculated for $C_8H_{16}O_6$: OMe, 29.8%. Demethylation by boron trichloride (26) and examination of the sugars showed mainly galactose with small amounts of mannose. Paper electrophoresis in borate buffer showed the presence of two components (M_G values, 0.66, 0.52). Paper chromatography in solvent B showed three components (R_g values, 0.28, 0.33, and 0.41). The syrup (0.35 g) was separated on Whatman No. 1 paper using solvent B to give the three fractions (R_g 0.28, 14 mg; R_g 0.33, 28 mg; and R_g 0.41, 242 mg).

(i) 3,5-Di-O-methyl-D-galactose

This new sugar (R_g 0.41) was characterized, and the results have been published previously (36).

(ii) 3,4-Di-O-methyl-D-mannose

The syrup (R_g 0.33) (28 mg) crystallized from ethyl acetate, giving 3,4-di-O-methyl-D-mannose, m.p. and mixed m.p. 70–73° C. Reported (37): m.p. 70–73° C.

(iii) 3,6-Di-O-methyl-D-mannose

Demethylation of a portion of the sugar (R_g 0.28) and examination of the products showed mannose as the parent sugar. Paper electrophoresis in borate buffer showed three components; two of these were in trace amounts and had the same M_g values as 2,3- and 2,4-di-O-methyl-D-mannose. The main component was assumed to be 3,6-di-O-methyl-D-mannose since its M_g value did not correspond to that of either 2,6- or 4,6-di-O-methyl-D-mannose. A small sample (1–2 mg) was converted to its methyl glycoside by heating for 12 hours in 2% methanolic hydrogen chloride. The glycoside was methylated by Purdie's reagents (methyl iodide, 2 ml, and silver oxide, 20 mg). Examination of the fully methylated sugar by gas–liquid partition chromatography (26) showed the glycosides of 2,3,4,6-tetra-O-methyl-D-mannose. On the basis of the foregoing evidence, the sugar was tentatively identified as 3,6-di-O-methyl-D-mannose. Scarcity of material precluded further identification.

E. Examination of Methylated Uronic Acid Fractions

The methylated uronic fraction, separated from the neutral sugars, weighed 300 mg. Separation on filter paper using solvent D gave three fractions (R_g 0.85, 0.61, and 0.50).

(i) Fraction 1

Yield 30 mg, R_g value 0.85. A small portion (2 mg) was hydrolyzed with N sulphuric acid (0.5 ml) for 8 hours at 100° C. Chromatographic examination of the hydrolyzate in solvent B failed to show the presence of any neutral sugars. The remainder of the fraction was then converted to its methyl ester methyl glycoside by being heated in 2% methanolic hydrogen chloride in a sealed tube for 12 hours. After reduction with lithium aluminum hydride in ether solution, the disaccharide was recovered and hydrolyzed with N sulphuric acid. Paper chromatography (solvent B) and paper electrophoresis (borate buffer) showed one spot having R_g and M_g values of 0.30 and 0.13 respectively. These values corresponded to those of 2,3-di-O-methyl glucose. Demethylation of the sugar yielded glucose. The methylated uronic acid was therefore 2,3-di-O-methyl-glucuronic acid.

(ii) Fraction 2

Yield 22 mg, R_g value 0.61. Paper chromatography and paper electrophoresis (solvent B and borate buffer, pH 10) of an acid hydrolyzate of this material showed the presence of 3,4-di-O-methyl mannose as the only neutral sugar. As described above, the sugar acid was converted into the methyl ester methyl glycoside, reduced with lithium aluminum

hydride, and hydrolyzed with acid. The sugars, identified by chromatography and electrophoresis, were 2,3-di-O-methyl-D-glucose and 3,4-di-O-methyl mannose with traces of 2,3,4-tri-O-methyl-D-glucose. Demethylation of the reduced sugar produced glucose and mannose.

(iii) Fraction 3

Yield 28 mg, R_g 0.50. Acid hydrolysis and chromatographic examination of the sugars showed 3,4-di-O-methyl mannose, 3,5-di-O-methyl galactose, and trimethyl glucuronic acid. Methanolysis, reduction, and hydrolysis as described for earlier fractions produced 2,3,4-tri-O-methyl-D-glucose, 3,4-di-O-methyl mannose, and 3,5-di-O-methyl galactose. Demethylation of the reduced trisaccharide yielded glucose, mannose, and galactose.

ACKNOWLEDGMENTS

REFERENCES

1. A. W. DOX and R. E. NIEDIG. J. Biol. Chem. 19, 235 (1914).
2. P. W. CLUTTERBUCK, W. N. HAWORTH, H. RAISTRICK, G. SMITH, and M. STACEY. Biochem. J. 28, 94 (1934).
3. P. W. CLUTTERBUCK. J. Soc. Chem. Ind. (London), 55, 551 (1936).
4. L. HOUGH and M. B. PERRY. Biochem. J. 61, 8 (1955).
5. W. N. HAWORTH, H. RAISTRICK, and M. STACEY. Biochem. J. 31, 640 (1937).
6. W. N. HAWORTH, H. RAISTRICK, and M. STACEY. Biochem. J. 29, 2668 (1935).
7. S. A. BARKER, E. J. BOURNE, and M. STACEY. J. Chem. Soc. 3084 (1953).
8. S. M. MARTIN and G. A. ADAMS. Can. J. Microbiol. 2, 715 (1956).
9. A. S. JONES. Biochim. et Biophys. Acta, 10, 607 (1953).
10. H. G. SEVAG. Biochem. Z. 273, 419 (1934).
11. G. S. BERENSON. Biochim. et Biophys. Acta, 28, 176 (1958).
12. O. WESTPHAL, O. LUDERITZ, and F. BISTER. Z. Naturforsch. Pt. b, 7, 148 (1952).
13. D. H. NORTHCOTE. Biochem. J. 58, 353 (1954).
14. G. H. BEAVAN and E. R. HOLLIDAY. Advances in Protein Chem. 7, 320 (1952).
15. M. ABDEL-AKHER, J. K. HAMILTON, R. MONTGOMERY, and F. SMITH. J. Am. Chem. Soc. 74, 4970 (1952).
16. A. B. FOSTER. J. Chem. Soc. 982 (1953).
17. S. A. BARKER, A. B. FOSTER, I. R. SIDDIQUI, and M. STACEY. Talanta, 1, 216 (1958).
18. L. HOUGH, J. K. N. JONES, and W. H. WADMAN. J. Chem. Soc. 1702 (1950).
19. W. E. TREVELYAN, D. P. PROCTER, and J. S. HARRISON. Nature, 166, 444 (1950).
20. S. M. PARTRIDGE. Biochem. J. 42, 240 (1948).
21. N. NELSON. J. Biol. Chem. 153, 375 (1944).
22. F. WEYGARD, W. PERKOW, and P. KUHNER. Chem. Ber. 84, 594 (1951).
23. M. A. ABDEL-AKHER and F. SMITH. Nature, 166, 1037 (1950).
24. E. L. FALCONER and G. A. ADAMS. Can. J. Chem. 34, 338 (1956).
25. A. JEANES and C. A. WILHAM. J. Am. Chem. Soc. 72, 2655 (1950).
26. A. G. MCINNES, D. H. BALL, F. P. COOPER, and C. T. BISHOP. J. Chromatog. 1, 556 (1958).
27. S. ALLEN, T. G. BONNER, E. J. BOURNE, and N. M. SAVILLE. Chem. & Ind. (London), 630 (1958).
28. J. C. IRVINE and A. M. MOODIE. J. Chem. Soc. 93, 95 (1908).
29. J. C. IRVINE and D. MCNICOLL. J. Chem. Soc. 97, 1449 (1910).
30. H. GRANICHSTÄDTEN and E. G. V. PERCIVAL. J. Chem. Soc. 54 (1943).
31. W. N. HAWORTH, E. L. HIRST, F. A. ISHERWOOD, and J. K. N. JONES. J. Chem. Soc. 1878 (1939).
32. J. BADDILEY, J. G. BUCHANAN, R. E. HANSCHUMACHER, and J. F. PRESCOTT. J. Chem. Soc. 2818 (1956).
33. H. G. BOTT, W. N. HAWORTH, and E. L. HIRST. J. Chem. Soc. 1395 (1930).
34. R. L. SUNDBERG, C. M. MCCLOSKEY, D. E. REES, and G. H. COLEMAN. J. Am. Chem. Soc. 67, 1080 (1945).
35. R. KUHN, H. TRISCHMANN, and I. LOW. Angew. Chem. 67, 32 (1955).
36. I. R. SIDDIQUI and G. A. ADAMS. Can. J. Chem. 38, 2029 (1960).
37. P. A. J. GORIN and A. S. PERLIN. Can. J. Chem. 34, 1796 (1956).

THE REDUCTION OF NITROBENZENE BY SODIUM SULPHIDE IN AQUEOUS ETHANOL[1]

O. J. COPE AND R. K. BROWN

ABSTRACT

The reduction of nitrobenzene by sodium sulphide in aqueous ethanol has been examined. Hydrosulphide and hydrodisulphide ions give rise to quite similar, though slow, rates of reduction. Sulphide ion appears to be two to three times as effective as the hydrosulphide ion. Both the sulphide and hydrosulphide species are considered to be responsible for the initial, very slow reduction with possibly some contribution from traces of polysulphide ions. The reduction is markedly accelerated by the addition of elemental sulphur to form di- and polysulphide, a much more reactive reducing species. The formation of "active" elemental sulphur during the course of the reduction produces disulphide and thus gives rise to an autocatalytic reaction. Some of this elemental sulphur is lost as thiosulphate by reaction with hydroxyl ions produced by the reduction itself, and by hydrolysis of sulphide and disulphide ions. The addition of base increases the rate of reduction due to a shift in the equilibria $S^- + H_2O \rightleftharpoons HS^- + OH^-$ and $S_2^- + H_2O \rightleftharpoons HS_2^- + OH^-$, but this is offset somewhat by greater loss of the active elemental sulphur as thiosulphate, thus decreasing the autocatalytic acceleration of rate.

Although, from its absorption at 265 mμ, nitrobenzene concentration could be accurately measured, no satisfactory method was found for estimating the concentration of disulphide ions during the course of the reduction.

INTRODUCTION

In order to understand the variable results obtained in this laboratory in the alkaline sulphide reduction of nitro compounds and to rationalize the well-known selectivity observed in the sulphide reduction of mono- and poly-nitro compounds (1–4), a detailed study of the sulphide reduction of nitrobenzene was undertaken.

Reduction of aromatic nitro compounds by such reagents as titanous chloride or stannous chloride under acidic conditions has been followed by measurement of the consumption of reducing agent (5–7). Since the disappearance of the nitro compounds was not followed directly, one must either determine or assume that certain definite changes occur in the reducible substance and that all the reducing agent has been consumed by this process and no other. This approach has revealed that the reaction is first order with respect to both nitro compound and reducing agent, and agrees with the generally accepted course of the reaction suggested by Haber (8) and shown as follows.

$$RNO_2 \xrightarrow{\text{slow}} RNO \xrightarrow{\text{fast}} RNH(OH) \xrightarrow{\text{fast}} RNH_2 \qquad (a)$$
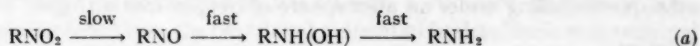
There is a considerably greater difficulty in following the reduction by measuring change in concentration of reducing agent when sulphide ions are employed, since the composition of the reduction mixture is more complex than it is in the case of stannous chloride. It is known that a solution of sodium sulphide contains a number of species including sulphide, hydrosulphide, disulphide, hydrodisulphide, and thiosulphate ions, the relative composition of which depends upon the source of the sodium sulphide used for its preparation and the conditions under which the solution is made. The particular species responsible for the reduction, as well as its concentration, must be determined.

Since a method which measured the disappearance of nitrobenzene directly would

possess obvious advantages, attention was directed to the development of a spectro-photometric method which followed the change in extent of absorption at λ_{max} 265 mμ with change in nitro concentration. Such a method was indeed obtained. However, during the course of our experiments, Ogata *et al.* (9) reported an investigation of the kinetics of the reduction of aromatic nitro compounds by sodium disulphide in aqueous methanol (40% volume methanol:water). The choice of sodium disulphide stemmed from their observations that reduction with the monosulphide was too slow for satisfactory kinetic study. These authors followed the course of the reaction by measurement of the changes in the absorption of nitrobenzene at λ_{max} 270 mμ, although in cases where a large excess of nitrobenzene was employed, the spectrophotometric method was checked by an electrometric titration of the sodium disulphide with silver ion. Their results showed that the reduction was first order in nitrobenzene. A second-order dependence upon disulphide ion was found also, but when allowance was made for hydrolysis, the reaction was reported to be first order with respect to disulphide ion as well.

Bullock and Forbes (10) have also studied the reduction of certain nitrobenzene sulphonates in aqueous solution by sulphide, disulphide, and polysulphide ions. From their measurements of polysulphide concentration by iodometric titration, they concluded that the reduction was first order in both nitro compound and polysulphide, although no allowance for the extent of hydrolysis of the polysulphide appeared to have been made.

The present work describes the results of a study of the reduction of nitrobenzene with sodium sulphide in aqueous ethanol by following the change in absorption of the nitro-benzene at λ_{max} 265 mμ.

EXPERIMENTAL

Chemicals and Solvents

Sodium sulphide (Na$_2$S.9H$_2$O), obtained from the Nichols Chemical Company, was of reagent grade. It was colorless and apparently free from the yellowish polysulphide impurities found in sodium sulphide obtained from some other sources.

Nitrobenzene was Fisher certified reagent grade material. This was distilled, before use, at 85–86° C at 10 mm.

Sulphur was Merck sublimed material, used without further purification.

Aqueous ethanol (40%) was prepared by addition of the requisite amount of distilled water to 95% ethanol. This solution was deaerated before use by gentle reflux and subsequent cooling under an atmosphere of oxygen-free nitrogen.

Solutions

The stock solution of sodium sulphide was prepared by the addition of sufficient Na$_2$S.9H$_2$O (neglecting the change in the water concentration due to the water of hydration) to the 40% aqueous ethanol to make the solution 0.960 molar with respect to the Na$_2$S. This stock solution was then diluted appropriately with the 40% aqueous ethanol in the preparation of a 0.160 M solution of sodium sulphide. A 0.160 M solution of sodium sulphide made in this manner contained 61.2% of water and 38.8% of ethanol.

Apparatus

A Beckman Model DU spectrophotometer, equipped with a power pack, was used to make the absorption measurements. Matched, glass-stoppered quartz cells of 10-mm light path were used for all measurements.

The pH determinations were made with a Beckman Zeromatic meter equipped with

a high pH electrode. The standardization was made with a saturated solution of pure calcium hydroxide which has a pH of 12.45 at 25° C (11), and also with standard buffers at lower pH.

The reaction was carried out in a 500-ml, four-necked flask fitted with an efficient, water-cooled reflux condenser, a stirrer, an inlet for the addition of sodium sulphide solutions, and an inlet for a nitrogen bleed. In addition, a tube dipping below the surface of the solutions held a 1-ml pipette and thus permitted sampling so that there was a minimum of exposure of the solution surface to air. The apparatus was thermostatted at 50.0° C.

A calibrated dropping funnel was used to introduce the solution of sodium sulphide into the reaction vessel.

Procedure

The reaction vessel was first flushed with nitrogen and subsequently a slight positive pressure of nitrogen was maintained in the apparatus above the solution throughout the entire reaction period.

About 50 ml of the stock solution (0.960 M sodium sulphide in aqueous ethanol) was added to the reaction vessel, followed by a sufficient volume of the mixed solvent to give a final concentration of 0.160 M sodium sulphide. For the cases which required the addition of sodium hydroxide or elemental sulphur, the necessary quantity of the reagent was added before the diluting solvent had been completely added, followed by the remainder of the solvent needed to make up the required volume. The solutions made by the addition of sodium hydroxide or sulphur were allowed to stand for $\frac{1}{2}$ hour to ensure equilibration of the species in the solution. No change in absorption was noted in such an equilibrated solution, even upon prolonged standing. Finally the nitrobenzene was introduced by means of a Victor Meyer bottle into the rapidly stirred solution.

For following the change in absorption at 450 mμ, the Beckman DU cell container was thermostatted at 50.0° C. The glass-stoppered cell was completely filled with freshly prepared initial reaction solution obtained from the reaction flask and the change in absorbance was measured continuously and directly. This eliminated errors due to cooling and air oxidation which would occur if fresh samples were taken periodically from the reaction flask.

To follow the change in nitrobenzene concentration, 1-ml samples were withdrawn from time to time and immediately diluted to 100 ml with a standard mixture of 40% aqueous ethanol containing four times the calculated amount of hydrochloric acid required to convert all the sodium sulphide to H_2S and the amine to the hydrochloride. These solutions, properly protected and capped, were allowed to stand for the duration of the experiment (2–4 hours) before measurements were made, and then the absorbances were obtained at 25° C at 265 mμ. The period of standing produced no alteration in absorption and thus permitted the choice of a more convenient time for the absorption measurements. Interfering absorption at 265 mμ due to polysulphide was subtracted from the total absorption at this wave length to give a measure of the nitrobenzene concentration. The magnitude of this interfering absorption due to polysulphide was evaluated by measurement of the polysulphide concentration from its absorbance at 450 mμ at 50° C and conversion of this reading to the corresponding (and lower) one at 25° C using calibration plots of concentration of polysulphide versus absorbance at 450 mμ at these two temperatures. From this value of absorption at 450 mμ, the corresponding interfering absorption

at 265 mμ was obtained from a plot relating absorption at 450 mμ to absorption of the same solution at 265 mμ after having been diluted 100-fold and acidified with the standard aqueous ethanolic solution of hydrochloric acid. These measurements were all made at 25° C.

The solutions required for the comparative absorption of disulphide and hydro-disulphide ions were made up as follows. All preparations were carried out in an atmosphere of nitrogen. To the stock solution of 0.960 M sodium sulphide was added the requisite amount of elemental sulphur. Ten-milliliter aliquots of the resulting solution were then separately treated with base, acid, or bicarbonate as required and then diluted to 60 ml with the 40% aqueous ethanol. The aliquot which was to supply the solution of disulphide was first basified by addition of the necessary amount of solid sodium hydroxide to give a concentration of added base equal to 4 M and then the volume made up to 60 ml. One of the aliquots which was to supply the solution of hydrodisulphide was acidified by careful addition of the requisite quantity of constant-boiling hydrochloric acid to the rapidly stirred solution. The pH of the solution was followed during this addition and found to be 10.7 when all the necessary hydrochloric acid had been added. To the other aliquot was added sufficient solid sodium bicarbonate to convert all the sodium sulphide and sodium disulphide to the corresponding hydrosulphide and hydro-disulphide (12) and then the volume made up to 60 ml. This solution was cooled to 0° C and the sodium carbonate allowed to precipitate. The supernatant solution of sodium hydrosulphide and sodium hydrodisulphide (pH = 10.7) was removed from the flask, under nitrogen pressure, through a porous plate.

The solutions of sodium hydrosulphide, and sodium hydrosulphide containing hydro-disulphide, were prepared from the 0.960 M sodium sulphide stock solution, by appropriate addition of elemental sulphur in the latter case, and then suitable acidification with hydrochloric acid during the dilution, to give the final concentration of 0.160 mole per liter.

Iodometric titrations were carried out by standard procedures.

RESULTS AND DISCUSSION

A method similar to that devised by Ogata et al. (9) was used to follow the reduction of nitrobenzene.

The absorption of nitrobenzene in aqueous ethanol was found to follow Beer's law over the concentration ranges studied.

Although reduction of nitrobenzene in alkaline media is known to yield bimolecular reduction products (azoxybenzene and azobenzene), a careful examination of a typical reaction at the $\lambda_{m \cdot x}$ at which these compounds absorb showed conclusively that bimo-lecular reduction products were not present nor were they involved in the reaction. Azoxybenzene has been converted to azobenzene by sulphide (13, 14). We have found that a 0.005 M solution of azoxybenzene in aqueous ethanol made 0.150 M in sodium sulphide gave approximately 1% conversion to azobenzene in 200 minutes, but only when elemental sulphur was added to form the more actively reducing polysulphide species. Hence, had such bimolecular reductions been involved in our sulphide reductions, azobenzene would surely have accumulated and been detected. Thus the only organic products found at any time during the reaction were nitrobenzene and aniline, in agreement with the observations of previous investigators (9, 10) and with the scheme of reduction given by Haber (8).

Bullock and Forbes (10) have suggested that the over-all reaction for the reduction of nitrobenzene as expressed by equation (b):

$$RNO_2 + S_2^- + H_2O \rightarrow RNH_2 + S_2O_3^-, \tag{b}$$
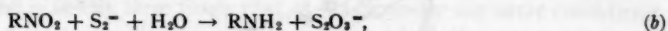
can be broken into three separate reactions as follows:

$$RNO_2 + 3S_2^- + 4H_2O \rightarrow RNH_2 + 3S_2^0 + 6OH^- \tag{c}$$

$$S^0 + S^- \rightarrow S_2^- \tag{d}$$

$$4S^0 + 6OH^- \rightarrow S_2O_3^- + 2S^- + 3H_2O. \tag{e}$$
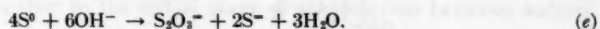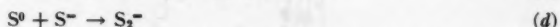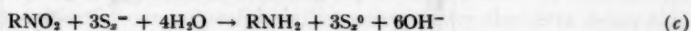
Of these products, only polysulphide interfered at 265 mμ. However, this could be estimated from suitable Beer's law plots (see Experimental).

Ogata's method (9) of allowance for polysulphide absorption was considered unsatisfactory for our work since polysulphide does not absorb to the same extent at 265 mμ and 240 mμ. This is illustrated in the following table for different concentrations of sodium disulphide.

Absorption at 265 mμ	Absorption at 240 mμ
0.098	0.125
0.213	0.260
0.361	0.412
0.510	0.580

Hence for the present work the actual absorption of the disulphide at 265 mμ was determined in each case.

On the assumption that a 10-fold excess of sodium sulphide over nitrobenzene would give a pseudo-first-order reaction, data for the disappearance of nitrobenzene with time were obtained for the reaction of 0.015 M nitrobenzene with 0.160 M sodium sulphide in aqueous ethanol (approximately 61:39 water:alcohol, by weight) at 50° C, carefully protected by an atmosphere of nitrogen. The data is shown conveniently in Fig. 1, plot I, and in Fig. 2. The existence of an induction period and an autocatalytic reaction, clearly shown here, has been observed previously by Bullock and Forbes (10) in their experiments on sulphide reduction of nitro compounds in aqueous solution. They discovered that, of the products obtained from these reactions (equations $(c-e)$), only polysulphide was responsible for the autocatalytic reaction. This has been supported by our observation that replacement of some of the sodium sulphide by disulphide shortened or practically eliminated the induction time (Fig. 1, plots II–IV). When 2% of the sodium sulphide was present as disulphide, the induction period was reduced to about 25 minutes, while a molarity of added elemental sulphur greater than 0.0075 (4.7%) gave a reaction practically devoid of an induction period.

Corroboration that the reactive species is, in fact, an increasing quantity of polysulphide was found by simultaneously following the change in polysulphide concentration during the course of the reduction. Polysulphide absorbs quite strongly over a broad region but is quite measurable at 450 mμ. In a plot of concentration of sulphur as polysulphide in 0.160 M sodium sulphide in aqueous ethanol versus absorption at 450 mμ at 25° and at 50° C, it was found that Beer's law held remarkably well even up to a molarity of 0.08 for elemental sulphur.

The exact composition of a combination of elemental sulphur with sodium sulphide,
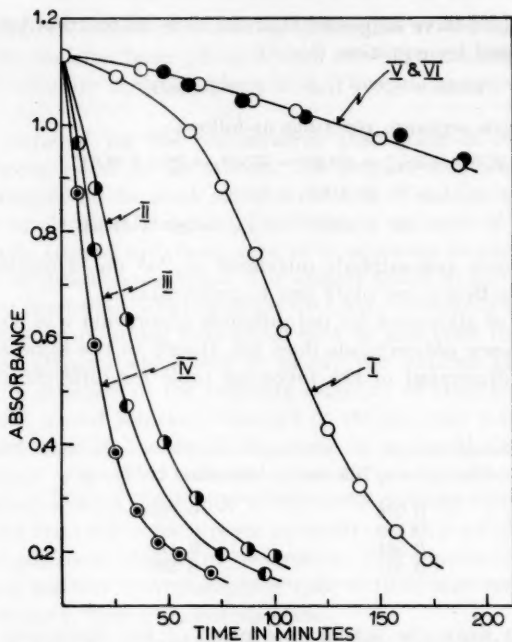
FIG. 1. The change in absorbance of nitrobenzene at 265 mμ with time during the reduction at 50° C of 0.015 M nitrobenzene by aqueous ethanolic sodium sulphide. I to IV have a Na$_2$S concentration of 0.160 M; II, III, and IV are 0.0075 M, 0.015 M, and 0.030 M respectively in dissolved sulphur; V and VI plots both contain 0.160 M NaHS, VI (●) being also 0.015 M in sulphur.
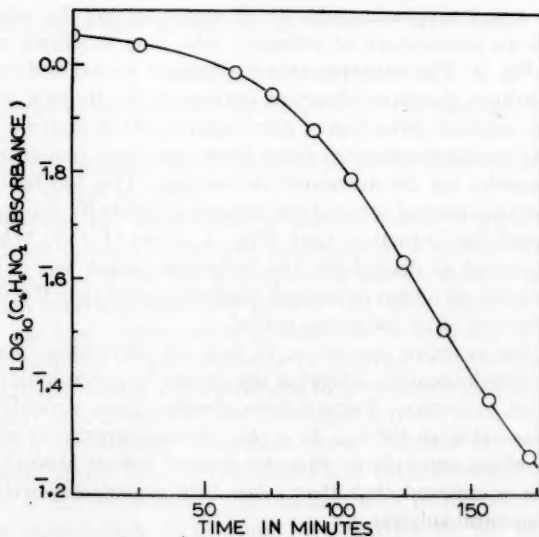

FIG. 2. A plot of log$_{10}$ of the nitrobenzene absorbance at 265 mμ vs. time for the reduction of 0.150 M nitrobenzene by 0.160 M Na$_2$S in aqueous ethanol at 50° C.

and hence the nature of the absorbing species, is uncertain (15–18). The adherence to Beer's law noted above, and our finding that the intensity of absorption of Na_2S_3 in the aqueous ethanol employed is nearly *three* times that of Na_2S_2 under the same conditions, favors the view that S_2^- is essentially the species present when the concentration of sulphur is considerably less than that of the sodium sulphide. However, in view of the uncertainty of the composition of our polysulphide, for convenience the term *disulphide* will be used.

From Fig. 3, plot I, it is seen that in the initial stage of the reaction between sodium
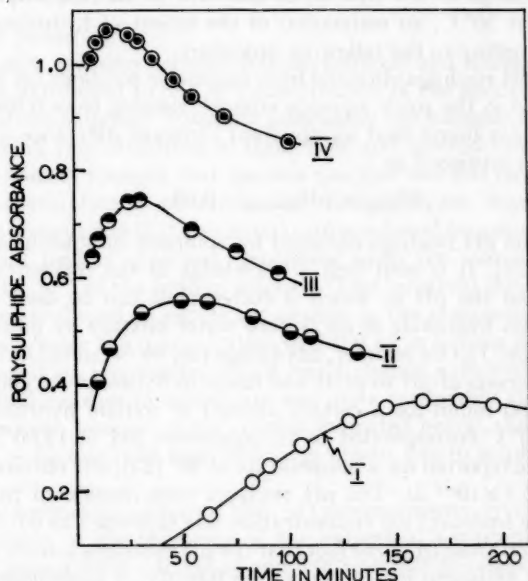
FIG. 3. The change in absorbance at 450 mμ with time during the reduction at 50° C of 0.015 M nitrobenzene in aqueous ethanolic sodium sulphide. I to IV have a Na_2S concentration of 0.160 M; in addition II, III, and IV are 0.0075 M, 0.015 M, and 0.030 M respectively in dissolved sulphur.

sulphide and nitrobenzene, the disulphide concentration was indeed quite small, but increased to a maximum at about 175 minutes of reaction, slowly decreasing thereafter. This value became constant when the reduction had been completed, a fact not shown in the plot but actually determined in two separate cases. When sulphur was added initially, not only was the rate of increase of disulphide greater with larger initial concentration of disulphide, but so was the rate of loss of disulphide. Furthermore, from the pseudo-first-order logarithmic plot (Fig. 2) it is seen that no truly linear section occurred.

In an attempt to rationalize these findings the following aspects of the reaction were considered.

The Probable Extent of Hydrolysis of Sodium Sulphide in Aqueous Ethanol

An aqueous solution of sodium sulphide is considered to be extensively hydrolyzed (17). Kuster and Heberlein (19, compare also 17) indicate that a 1 M solution of sodium sulphide is hydrolyzed to about 50%. Ogata (9) has used a figure of 10 for the hydrolysis constant for a solution of sodium sulphide in aqueous media. However, disagreement

concerning the value of the second ionization constant of hydrogen sulphide (20, 21) makes the value of the concentration of sulphide and hydrosulphide ions, calculated by the use of the value 10, somewhat uncertain.

Little is known about the extent of hydrolysis of sodium sulphide in aqueous ethanol. The reasoning presented by Ogata *et al.* (9) indicates that the hydrolysis constant of sodium sulphide in aqueous methanol at room temperature is somewhat less than the value of 10.[2] It is reasonable that a similar decrease in magnitude of the hydrolysis constant applies to the aqueous ethanol employed in our work. But, in view of the lack of more precise knowledge of the hydrolysis constant of sodium sulphide in aqueous ethanol, particularly at 50° C, an estimation of the extent of hydrolysis was made by pH measurements according to the following procedure.

In a comparison of pH readings obtained from equimolar solutions (at 50° C) of sodium hydroxide in water and in the stock aqueous ethanol, ranging from 0.050 to 0.500 M in sodium hydroxide, it was found that an apparent constant difference of 0.60 pH units occurred, and could be expressed as

$$pH_{H_2O} = pH_{H_2O-alc} - 0.60.$$

This "alcohol effect" on pH readings obtained for solutions in aqueous alcohol has been recorded previously (22). It is seen that a knowledge of the concentration of sodium hydroxide in water and the pH to which it corresponds can be used to estimate the concentration of sodium hydroxide in an alcohol–water mixture by measurement of the pH of the latter solution. In this manner, advantage can be taken of the known values of pK_w in water for conversion of pH to pOH and hence to hydroxyl ion concentration. For example, a pH of 12.60 found for a certain amount of sodium hydroxide dissolved in aqueous ethanol at 50° C corresponded to an equivalent pH of 12.00 in water. Using $pK_w = 13.26$, the value reported for a temperature of 50° (23), one obtained the hydroxyl ion concentration of 5.5×10^{-2} M. The pH readings were considered to be accurate to ± 0.02 units, hence the hydroxyl ion concentration was expressed as 0.055 ± 0.002 M.

A further complication arose from the fact that the pH measures *activity* of the hydrogen ion and not the actual hydrogen ion concentration directly. A knowledge of the activity values would permit calculation of the hydrogen ion, and hence hydroxyl ion, concentration. The lack of such data led to the following evaluation.

A 0.050 M solution of sodium hydroxide in *water* at 50° C gave a pH reading of 11.90 whereas the calculated figure, using pK_w at 50° C = 13.26, was 11.96—a difference of 0.06 units. Sodium hydroxide solutions, 0.1 and 0.5 M in strength, showed respectively the difference of 0.160 and 0.260 between calculated and observed values of pH. Thus the pH value found for aqueous alcoholic solutions of sodium hydroxide, even though corrected for the alcohol effect, gave an apparent hydroxyl ion concentration which was, in the region of 0.050 molarity, about 0.06 pH units lower than that actually present.

The foregoing considerations and observations were then applied to the problem of determining the sulphide ion concentration of a 0.160 M sodium sulphide solution in aqueous ethanol at 50° C. The pH of this solution was found to be 12.60 ± 0.02. When corrected for the alcohol effect, the value was 12.00 ± 0.02. This was identical with the pH found for a 0.160 M solution of the same concentration of sodium sulphide in water

[2]*These authors show a ratio of hydrolysis constants in aqueous media of $K_{S^-}/K_{S_2^-} = 4$. Since S_2^- should hydrolyze less than does S^-, either in water or in aqueous ethanol, and since Ogata obtained a value of 1.4 for the hydrolysis constant, K_h, of S_2^- in aqueous methanol, the K_h of sodium sulphide in aqueous methanol may also be approximately four times this figure, i.e. 5.6. If aqueous ethanol and aqueous methanol are comparable, the K_h of Na_2S in aqueous ethanol then might be about 5.*

at 50° C. Using the pK_w value of 13.26, the hydroxyl ion concentration was estimated at 0.055 ± 0.002 M. Allowing for the "activity measurements" indicated above, the hydroxyl ion concentration was estimated to be 0.063 ± 0.002 M.

On the basis of the above calculations of the hydroxyl ion concentration, the extent of hydrolysis of a 0.160 M solution of sodium sulphide in the aqueous ethanol at 50° C was $39 \pm 2\%$. The sulphide ion concentration was therefore 0.097 ± 0.002 M. From these figures a value of 4.1×10^{-2} was obtained for the hydrolysis constant of sodium sulphide in the aqueous ethanol at 50° C. It is realized that these calculations are approximations. However, they do supply us with a rough estimate of the sulphide ion concentration.

The Initial Slow Reduction

The initially slow reaction between sodium sulphide and nitrobenzene (Figs. 1 and 2, plot I) might be attributed to one or a combination of the species present as a result of hydrolysis of sodium sulphide. These are principally the sulphide and hydrosulphide ions with possibly small concentrations of disulphide and hydrodisulphide ions as contaminants. It was originally thought that the slow reaction was due largely, if not completely, to the small concentration of contaminating disulphide ion. Support for this view was obtained by the observation that this initial rate was found occasionally to be considerably greater than that usually observed, depending upon the source (and hence extent of contamination by S_2^-) of the sodium sulphide. This apparent doubling of the initial rate could hardly be attributed to significant change in the monosulphide ion concentration due to hydrolysis, since the concentration of 0.160 M in sodium sulphide was adhered to as closely as possible. The species which could change sufficiently in concentration to effect this twofold increase in initial rate was more reasonably the contaminating disulphide ions. However, because of the reasons indicated below, the view is now held that the initial slow reduction is at least to a large extent due to sulphide and hydrosulphide species.

The extent of hydrolysis, obtained from pH measurements, gives for a 0.160 M solution of sodium sulphide, at the beginning of the reduction, a concentration of sulphide and hydrosulphide ions of 0.097 ± 0.002 M and 0.063 ± 0.002 M respectively. It is reasonable to assume that of these two ions, the sulphide ion should possess the greater capability for reduction. But the fact that the initial reduction rate by a solution which contains only hydrosulphide ions (Fig. 1, plot V) is not much different from that found when more than half of the hydrosulphide is converted to sulphide ion (Fig. 1, plot I) indicates that the sulphide and hydrosulphide (and also hydrodisulphide, Fig. 1, plot VI) ions are all of the same order of reducing power.

The extremely slow reduction by the sulphide ion might be due to the fact that it is much more strongly hydrated than is the hydrosulphide ion (23). The displacement of the water to allow association of the sulphide ion with the nitro group for the subsequent electron transfer occurs with difficulty. In contrast, disulphide and polysulphide ions reduce nitrobenzene much more rapidly, no doubt due in part to the lower degree of hydration of these ions (18). Furthermore, it is not unreasonable to assume that the conversion $:\ddot{S}:\ddot{S}:^- \rightarrow 2e + \ddot{S}::\ddot{S}$ is more facile than is the analogous change of $:\ddot{S}:^- \rightarrow 2e + \ddot{S}:$ on the basis that the combination of the two sulphur atoms yields a more stable product.

In this connection it is of interest to record the observation that the rate of reduction of nitrobenzene by a dilute, aqueous ethanolic solution of sodium *tri*sulphide was

approximately the same as, although constantly slightly lower than, that found for an equal concentration of sodium *di*sulphide under otherwise identical conditions. This agrees with the view expressed by Ogata (9) that attack by disulphide ion is on the nitrogen atom of the nitro group. The bulkier trisulphide ion would find such an approach somewhat more difficult.

The Autocatalytic Reaction

Since the effective reducing species is the disulphide ion, and this is present in a concentration less than or comparable with that of the nitrobenzene, although increasing as the reaction progresses, it is obvious that a pseudo-first-order reaction cannot be obtained. The data shown in Figs. 1 and 3 indicate an autocatalytic reaction; hence it might be possible to apply the equation for such a reaction (24) and thus evaluate the rate constant, providing the concentrations of both reactants are known or can be measured.

The concentration of one reactant, nitrobenzene, is easily and accurately determined by absorption measurements, and is found to decrease continually with time. However, the concentration of disulphide ion is governed by several factors. The process of reduction itself (equation (c)) with simultaneous production and reaction of elemental sulphur (equations (d) and (e)) is one factor which must be considered. When this is coupled with the unknown extent of hydrolysis of the disulphide ion, which, in turn, is affected by the change in hydroxyl ion concentration,[3] the task of measuring the disulphide ion concentration is indeed quite formidable. Since, to our knowledge, the hydrolysis constant of the disulphide ion is unknown either in aqueous media or in aqueous ethanolic solution at 50° C, the determination of the disulphide ion concentration by this route is not feasible.

The Relative Absorbances of Disulphide and Hydrodisulphide Species and the Attempt at Estimation of Disulphide Ion Concentration by Absorption Measurements

During the course of these experiments it was also shown that the absorption of "disulphide ion" at 450 mμ does not give a direct measure of the disulphide ion concentration since both disulphide and hydrodisulphide species contribute to this absorption, although to different extents.

An attempt was made to convert a solution of sodium disulphide, on the one hand, to one containing entirely unhydrolyzed disulphide ion (and sulphide ion), and, on the other hand, to a solution containing only hydrodisulphide ion (and hydrosulphide ion). Measurement of the absorption would then provide a means of estimating the extent of hydrolysis of sodium disulphide in our reduction mixture.

A series of aqueous ethanolic solutions, 0.160 *M* in sodium sulphide, containing 21.4% of sulphur as disulphide, were made up to contain progressively greater concentrations of sodium hydroxide. The results of absorbance measurements, made at 25° C at 450 mμ, are shown in Fig. 4. The absorbance rose from 1.013 units for the unbasified equilibrium mixture to a maximum of 1.820 units when the molarity of added base reached 4.0. Further addition of base produced no change in absorbance. The most reasonable explanation of these results is that of repression of hydrolysis by the added base to produce essentially disulphide ion, which must then absorb to a greater degree than does an equal amount of hydrodisulphide ion.

When the aqueous ethanolic solution, 0.160 *M* in sodium sulphide and containing

---

[3]*In one experiment involving the reduction of nitrobenzene by sodium sulphide at 50° C, the changes in* pH *were found to be: initial* pH, *12.60; after 45 minutes of reaction, a maximum* pH *of 12.95; and after 130 minutes, well beyond one half life, a* pH *of 12.50.*
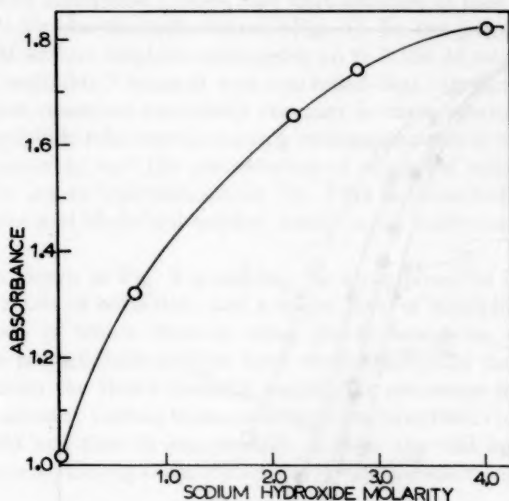
Fig. 4. The effect of the addition of NaOH on the absorbance at 450 mμ of a solution of sulphur in 0.160 M Na$_2$S (in aqueous ethanol).

elemental sulphur as disulphide, was treated so as to convert sulphide and disulphide ions to hydrosulphide and hydrodisulphide ions (see Experimental) the absorption *increased* rather than decreased as would be expected from the results of the work involving basified solutions. No constant value for absorption was obtained since the extent of absorption increased with increasing amounts of hydrochloric acid added. No explanation could be found for this phenomenon.

From these experiments, it is obvious that the ratio HS$_2^-$/S$_2^-$ could not be calculated from absorbance measurements. Hence the concentration of disulphide ion could not be found, thus making a satisfactory kinetic study of the reduction of nitrobenzene by sodium sulphide under our conditions quite difficult.

The Effect of Addition of Base on the Reduction of Nitrobenzene by Sodium Sulphide

The addition of sodium hydroxide increased the rate of reduction of nitrobenzene by sulphide (Fig. 5, plots I–IV), but not in proportion to the amount of base added. Eventually a state was reached where further addition of base actually had the reverse effect (Fig. 5, plot V). The increased rate was no doubt due to the conversion of the relatively unreactive HS$_2^-$ to the much more reactive species, S$_2^-$. A large concentration of base would convert essentially all the polysulphide to the unhydrolyzed state and result in a maximum rate of reduction. However, the increased concentration of base caused greater reaction between hydroxyl ion and the "active sulphur" (10), hence less disulphide was formed, thus leading to a lower acceleration of rate. With sufficiently high concentration of base it is expected that most if not all of the active sulphur would be lost as thiosulphate and no autocatalysis would be observed. This could not be tested in our solutions since a concentration of base significantly greater than 4 M resulted in a salting out of the ethanol.

The changes in "polysulphide concentration" accompanying the reductions in each of these cases are shown in Fig. 6. It has been shown that this absorption is due to both
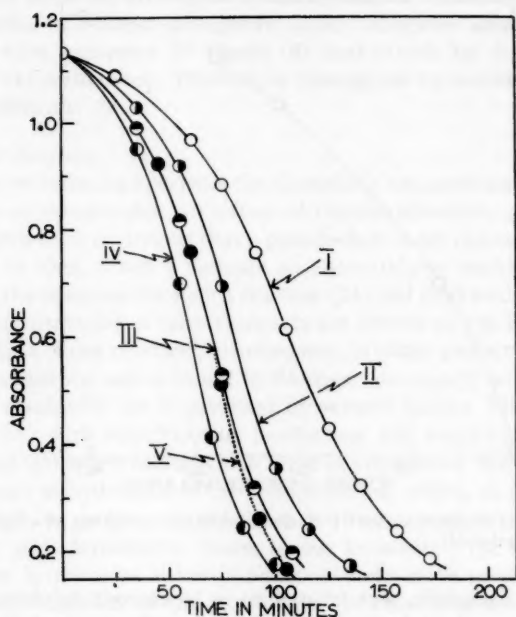
Fig. 5. Absorbance at 265 mμ vs. time during the reduction of 0.015 M nitrobenzene in aqueous ethanol at 50° C by 0.160 M Na$_2$S. I contains no added NaOH; II, III, IV, and V are 0.160 M, 0.320 M, 0.800 M, and 1.600 M in NaOH respectively.
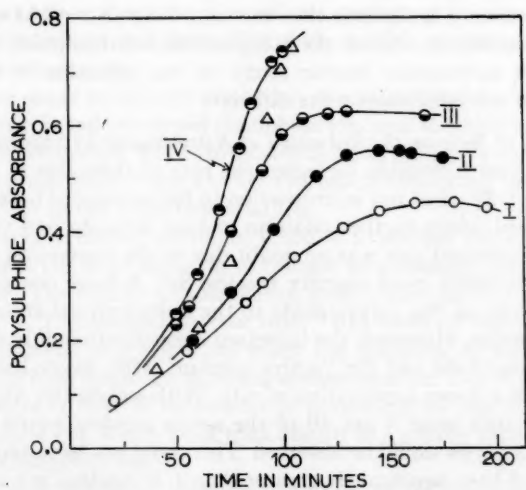
Fig. 6. The absorbance at 450 mμ vs. time during the reduction of 0.015 M nitrobenzene in aqueous ethanol at 50° C by 0.160 M Na$_2$S. I contains no added NaOH; II, III, IV, and V (△) are 0.160 M, 0.320 M, 0.800 M, and 1.600 M in NaOH respectively.

hydrodisulphide and disulphide species, and that addition of base changes their relative proportion and hence the total absorption (Fig. 4). In the preparation of solutions of sulphur in 0.160 M sodium sulphide, containing up to 0.160 M sulphur, it was found that the pH changed negligibly,[4] hence it was concluded that the ratio of disulphide ion to hydrodisulphide ion remained essentially constant in these solutions. Absorption of the 0.160 M sodium sulphide solutions containing various amounts of sulphur as polysulphide then reflected reasonably well the *concentration* of elemental sulphur, although not the *ratio* of disulphide ion to hydrodisulphide ion. This is embodied in the linear relation between absorbance and elemental sulphur found in the calibration plot which followed Beer's law.

The absorption shown in Fig. 6 must then be a composite of increased polysulphide concentration as result of reduction, and a larger ratio of disulphide to hydrodisulphide ion, the magnitude of which depends upon the hydroxyl ion concentration. Hence, calculation of the polysulphide sulphur from these absorption measurements, using the calibration data from the Beer's law plot would give erroneous results. With the aid of Fig. 4, the absorbances at various base concentrations have been converted to those where no base was added and thus it was possible to show the real increase of polysulphide sulphur which occurred during these reductions in basified solutions. Figure 7 shows more
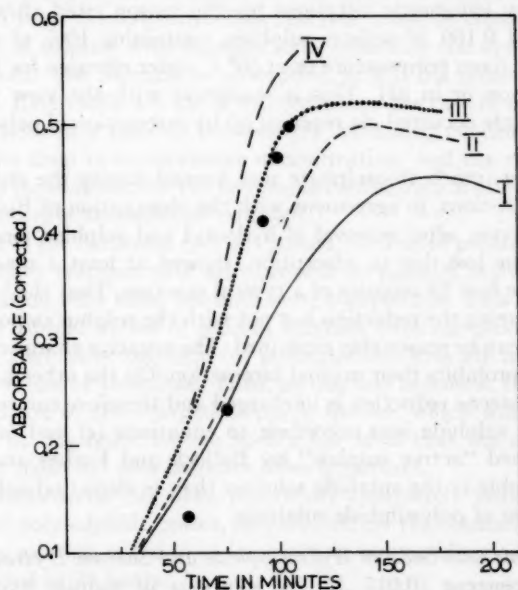
FIG. 7.   The corresponding absorbances at 450 mμ from Fig. 6 corrected for the effect of increased OH ion concentration on the absorbance at 450 mμ (here ● represents 1.600 M NaOH).

clearly the diminishing increase of polysulphide sulphur as the initial concentration of base is increased and thus the greater extent of loss of sulphur by reaction with base.

Figure 4 was obtained by progressive basification of a sodium sulphide solution

[4] *A decrease in pH was expected since the disulphide ion should hydrolyze to a lower extent than does the sulphide ion (9). However, these results were repeatable using several different electrodes to avoid the chance that an electrode might have become contaminated or unreliable.*

containing *one* specific concentration of polysulphide, and gave a figure of 1.80 for the ratio of absorbance of basified (4 *M*) solution to that of the unbasified solution. The same figure of 1.80 was obtained when a number of solutions were prepared, differing only in concentration of polysulphide, and made 4 *M* in sodium hydroxide. Hence the use of Fig. 4 and the ratio 1.80 for conversion of absorbances of the basified polysulphide solutions shown in Fig. 6 is justified.

The Formation of Thiosulphate during the Course of the Reduction

The possibility of air oxidation of sulphide to thiosulphate was avoided by careful deaeration of all solutions and by use of a nitrogen atmosphere. Iodometric titration of thiosulphate (25) requires preliminary removal of both sulphide and hydroxide ions. The addition of cadmium sulphate, rather than cadmium carbonate (10), accomplished this satisfactorily. However, it was found that the precipitated cadmium sulphide adsorbed some of the thiosulphate, thus giving low results in spite of attempts at recovery of adsorbed thiosulphate by extractions. Hence small changes in thiosulphate concentration during a reaction might easily be missed.

There existed the possibility of thiosulphate formation in our solutions due to the interaction of polysulphide sulphur with hydroxyl ions formed as a result of hydrolysis, especially since the pH of the solutions were well above 8 (10). This could not be determined satisfactorily by iodometric titrations for the reason cited above. However, an oxygen-free solution of 0.160 *M* sodium sulphide, containing 10% of sulphur as polysulphide, when kept at room temperature or at 50° C under nitrogen for 12 hours, showed no change in absorption or in pH. This is consistent with the view that little or no formation of thiosulphate occurred via reaction (*e*) by interaction of polysulphide sulphur and hydroxyl ion.

However, in contrast, much thiosulphate was formed *during* the reduction of nitrobenzene by sulphide solutions, in agreement with the observation of Bullock and Forbes (10). Iodometric titrations, after removal of hydroxyl and sulphide ions with cadmium sulphate, in spite of the loss due to adsorption, showed at least a ninefold increase of thiosulphate during the first 70 minutes of a typical reaction. That the base should react with sulphur formed *during* the reduction but not with the sulphur in polysulphide when nitrobenzene is absent can be reasonably explained. The negative charge on both hydroxyl and polysulphide ions prohibits their mutual interaction. On the other hand, the sulphur released during nitrobenzene reduction is uncharged and therefore can react readily with hydroxyl ions or with sulphide ions according to equations (*e*) and (*d*). This form of sulphur has been termed "active sulphur" by Bullock and Forbes and appears to be much more readily soluble in the sulphide solution than is elemental sulphur, ordinarily used for the preparation of polysulphide solutions.

Reduction of Nitrobenzene with Sodium Hydrosulphide and Sodium Hydrodisulphide

Reduction of nitrobenzene (0.015 *M*) by solutions of sodium hydrosulphide and sodium hydrodisulphide were carried out at 50° C. The results, shown in Fig. 1, plot V, indicate that during the initial stage of the reduction by hydrosulphide the rate was only ½ to ⅓ that found for the reduction with sodium sulphide. The marked autocatalytic effect observed in the latter case did not occur in hydrosulphide reduction of nitrobenzene. The addition of enough sulphur to convert about 10% of the sodium hydrosulphide to the hydrodisulphide gave no apparent increase in initial rate of this slow reaction and thus shows that sodium sulphide, sodium hydrosulphide, and the hydrodisulphide have

apparently the same order of reducing capacity. The slow increase in rate shown in Fig. 1, plot V, could be ascribed to a gradual shift in the equilibrium $S_2^- + H_2O \leftrightarrows HS_2^- + OH^-$ to the left due to the increase in hydroxyl ion concentration resulting from the slow reduction. The observation that the pH rose from 10.0 to 10.9 over a period of 630 minutes of reaction supports this point of view. This is further supported by the observation of a greater rate of reaction in one preparation of hydrosulphide wherein only enough hydrochloric acid had been added to reduce the pH of the solution to 12.1 rather than the usual 10.0 to 10.2.

Summary of the Course of Reduction of Nitrobenzene by Sodium Sulphide in Aqueous Ethanol

The studies described in the preceding sections assist in clarifying the course of the reduction of nitrobenzene by sodium sulphide solution.

As the reaction progresses, to the initial, slow reduction by sulphide and hydrosulphide ions is added the much faster reduction due to polysulphide formed by the sulphur produced during the reduction. Since the conversion of *one* molecule of nitrobenzene to aniline forms *three* atoms of sulphur, which then rapidly react preferentially with sulphide or hydrosulphide ions present, an exponential increase of polysulphide occurs, accounting for the rapid autocatalysis. At the same time some of this active sulphur reacts with the hydroxyl ions to form thiosulphate. This reaction must be considerably slower than is the combination of sulphur with sulphide ions, otherwise the autocatalytic effect would be less pronounced. The increase in absorption at 450 mμ reflects an increase in polysulphide species. Eventually a state is reached where the rate of reduction appears to be constant, as a result of a balance between the increasing concentration of active polysulphide ions, the drop in nitrobenzene concentration, and the removal of some of the active sulphur as thiosulphate by the increasing concentration of hydroxyl ions. Following this, the reduction rate decreases as expected.

After the peak of the reduction rate has passed, the loss of polysulphide as thiosulphate, through preliminary reaction with nitrobenzene to produce active sulphur and its subsequent combination with base, becomes more competitive. This is no doubt due to the fact that only a 10-fold excess of sodium sulphide over nitrobenzene was employed as well as the fact that three sulphide (or polysulphide) ions are necessary to reduce one molecule of nitrobenzene to aniline. Thus, as reaction proceeds, there is a rapid decrease in the concentration of the charged sulphide species, which will react with the active sulphur formed by the reduction, to such a low level that the competitive reaction of sulphur with the hydroxyl ions becomes more important.

When the nitrobenzene has been practically completely reduced, the formation of thiosulphate and polysulphide ceases, as indicated by the constancy of the absorption of the polysulphide solution noted in at least two instances where such measurements were made over a period of 24 hours.

REFERENCES

1. R. ANSCHUTZ and F. HEUSLER.   Ber. **19**, 2161 (1886).
2. H. H. HODGSON.   J. Soc. Dyers Colourists, **62**, 114 (1946).
3. H. H. HODGSON.   J. Chem. Soc. 242 (1948).
4. H. H. HODGSON.   J. Chem. Soc. 2017 (1948).
5. S. A. NEWTON, F. J. STUBBS, and SIR C. HINSHELWOOD.   J. Chem. Soc. 3384 (1953).
6. M. J. STEPHEN and SIR C. HINSHELWOOD.   J. Chem. Soc. 1393 (1955).
7. Y. OGATA and I. SUGIYAMA.   Science (Tokyo), **19**, 232 (1949). Chem. Abstr. **45**, 5116 (1951).
8. F. HABER.   Z. physik. Chem. **32**, 193 (1900).
9. M. HOJO, Y. TAKAGI, and Y. OGATA.   J. Am. Chem. Soc. **82**, 2459 (1960).
10. J. L. BULLOCK and G. S. FORBES.   J. Am. Chem. Soc. **55**, 232 (1933).
11. R. G. BATES, V. E. BOWER, and R. E. SMITH.   J. Research Natl. Bur. Standards, **56**, 305 (1956).
12. H. H. HODGSON and E. R. WARD.   J. Chem. Soc. 242 (1948).
13. S. GABRIEL.   Ber. **9**, 1406 (1876).
14. H. H. HODGSON, W. H. NORRIS, and G. R. WOOD.   J. Soc. Dyers Colourists, **66**, 473 (1950).
15. F. FEHRER.   Angew. Chem. **67**, 337 (1955).
16. D. PESCHANSKI.   Compt. rend. **227**, 770 (1948).
17. G. SATYANARAYANA RAO and G. GORIN.   J. Org. Chem. **24**, 749 (1959).
18. H. GERISCHER.   Z. anorg. Chem. **259**, 220 (1949).
19. F. W. KUSTER and E. HEBERLEIN.   Z. anorg. u. allgem. Chem. **43**, 53 (1905).
20. H. KUBLI.   Helv. Chim. Acta, **29**, 1962 (1946).
21. P. SOUCHEY and R. SCHAAL.   Bull. soc. chim. France, 819 (1950).
22. I. M. KOLTHOFF and C. ROSENBLUM.   Acid base indicators. The MacMillan Co., New York. 1937. p. 356.
23. HANDBOOK OF CHEMISTRY AND PHYSICS.   37th ed. Chemical Rubber Publishing Co., Cleveland, Ohio. 1955–56.
24. A. A. FROST and R. G. PEARSON.   Kinetics and mechanism. John Wiley & Sons, Inc., New York. 1956.
25. W. W. SCOTT.   Standard methods of chemical analysis. D. Van Nostrand & Co., New York. 1917. p. 408.

HYDROGEN BONDING IN SOLUTIONS OF SUBSTITUTED ACETIC ACIDS[1]

LEONARD W. REEVES

ABSTRACT

The changes in chemical shift of the acid proton in some simple carboxylic acids on dilution in four solvents has been studied. The existence of chainlike hydrogen-bonded polymers in solution is suggested by the results. The association of the monomer molecules in dilute solution with donor centers in the solvent molecules is suggested from a study of the —O—H monomer stretching bond in the vapor and in two solvents. There is a difference in the behavior of acetic and trifluoroacetic acid in N-methyl and N,N-dimethyl formamide, which has been explained in terms of protonation of the amides in trifluoroacetic acid solutions.

INTRODUCTION

The proton resonance technique has been a useful tool in measuring changes in the amount of hydrogen bonding in fluid systems (1, 2, 3, 4). The changes in chemical shift with the amount of hydrogen bonding are often very large. Recent improvements in standardization of chemical shifts and their measurement and the introduction of 60 Mc/s as a proton high-resolution frequency have made the sensitivity for detection of very weak interactions of the hydrogen-bonding type superior to any other technique (5, 6). The short lifetime of the hydrogen bond association compared to the inverse frequency shift due to various environments results in an averaging of the varying proton-shielding parameter, and one signal is observed (1, 7). The position of this signal corresponds to the average environment of the various equilibrium processes involved in the hydrogen bonding. This is a particular disadvantage in a system in which polymeric association via hydrogen bonds occurs, since the variation of averaged nuclear-shielding parameter with concentration or temperature does not provide enough information for the obtaining of a true association chemical shift, or equilibrium constants (8, 9). Some attempt has been made to calculate equilibrium constants for the monomer–dimer equilibrium in dilute alcohol solutions in CCl₄ using a region of concentration known to involve only monomers and dimers (10, 11).

The study of strong dimer associations such as carboxylic acids or intramolecular hydrogen bonds has been pursued in an attempt to avoid some of the above difficulties (12, 13, 14, 15). It has been suggested that acetic acid forms polymeric hydrogen-bonded associations in concentrated nonpolar solutions (15) while longer-chain acids show only dimer associations in the same concentration regions (13). The present study of substituted acetic acids was undertaken to investigate possible polymeric hydrogen bonding and to try to provide an explanation for the difference in behavior of acetic acid (15).

EXPERIMENTAL

Dichloroacetic acid, trifluoroacetic acid, and α-bromo- and α-chloro-proprionic acid were purified by fractional distillation in a dry atmosphere. A small middle cut was taken in each case. Monochloroacetic, trichloroacetic, trimethyl acetic, phenyl acetic, bromo-acetic, and β-bromoproprinic acids were either recrystallized from chloroform or taken as reagent grade chemicals. The acids which are deliquescent were handled in a dry box.

The solvents used, carbon tetrachloride and 1,2-dichloroethane, were fractionally distilled in a dry atmosphere. The dilution chemical shift studies were made using 0.5

mole% cyclohexane in each solvent as an internal reference signal. The mole fraction of solute was computed using the total moles of solvent, solute, and internal standard.

The measurements were made with a V-4300 Varian 40-Mc spectrometer with field stabilizer V.K. 3506. An audio-oscillator was calibrated using Lisajoux figures at multiples of 60 c.p.s. mains frequency and the later measurements of audio frequencies were calibrated by a Hewlitt Packard Electronic Counter. The side-band technique of measurement was used in all cases. Chemical shifts are accurate to ±1.5 c.p.s. in this work. Solutions were made up by weighing the liquids in capped vials.

RESULTS

Chemical shift measurements of the carboxyl proton resonance, using an internal cyclohexane reference, are plotted in Fig. 1 for various concentrations of acid in carbon tetrachloride. The acids measured were mono-, di- and tri-chloroacetic, α-chloro- and α-bromo-proprionic, trifluoroacetic, and trimethyl acetic acid. As the solid acids were not completely soluble at 28° C, the dilution shift curves are not complete for these acids. Monochloroacetic acid is soluble to about 10 mole% and the dilution shift curve is coincident as far as it goes with dichloroacetic acid. Trichloroacetic acid shows distinct behavior (see curve 2) in dilute solution but, between 8 mole% acid and the solubility limit, 20 mole%, the dilution shift curve is the same as that for the other chloroacetic acids. All dilution chemical shifts except that for trimethyl acetic acid showed a low-field movement with decreasing acid concentration. The change in chemical shift to low-field ranges from 19 cycles in dichloroacetic to 9 cycles in trifluoroacetic. Figure 1 also shows the carboxyl proton resonance in trifluoroacetic acid as a function of concentration in n-methyl formamide (curve 7), and the dilute regions are continued and shown as curve 7 in Fig. 2. In even more dilute solutions, the carboxyl proton in this system is found at -170 c.p.s. in 3.00 mole% solution compared to the proton resonance in cycloC$_6$H$_{12}$. This constitutes a shift of 320 c.p.s. (8 p.p.m.) from the chemical shift of the same proton in a 50:50 mole mixture with N-methyl formamide (Fig. 1). The N-methyl peak is a doublet in the amide because of indirect spin–spin coupling with the N-proton; and the other peak in the spectra of these mixtures corresponded to the aldehyde proton (16). Significant changes in chemical shift were obtained in the chemical shift of these protons; this is shown in an inset of Fig. 2(b and c). The chemical shift scale is the same but the concentration axis is halved in length for the same concentration change. Figure 2 also shows the dilution chemical shifts for three acids in 1,2-dichloroethane. Figure 3 shows a comparison of the dilution chemical shifts for the acid proton in acetic and trifluoroacetic acid dissolved in N-methyl and N,N-dimethyl formamide.

The infrared spectra of the —OH stretching region was investigated for CCl$_3$COOH and CF$_3$COOH in various solvents and in the vapor phase. The spectra for CCl$_3$COOH are shown in Fig. 4(a) and those for CF$_3$COOH are shown in Fig. 4(b). The frequency shifts from the vapor phase monomer frequency are shown in Table I together with values of the half widths of the single peak and details of concentration. In addition to these, reliable values for the vapor phase frequency from the literature (25, 26) for the —OH stretching in monomeric acetic and formic acid are shown, and the value for this frequency for iodoacetic acid in CCl$_4$ is also measured and quoted in this work. Spectra were recorded on a Perkin–Elmer 21 double-beam spectrometer with sodium chloride optics on the normal automatic 927 program. The wavelength calibration was carefully performed with the water vapor spectrum in this same region. Wave numbers quoted are accurate to ±2 cm^{-1}. Solution spectra were taken using balanced 0.1-mm cells or a
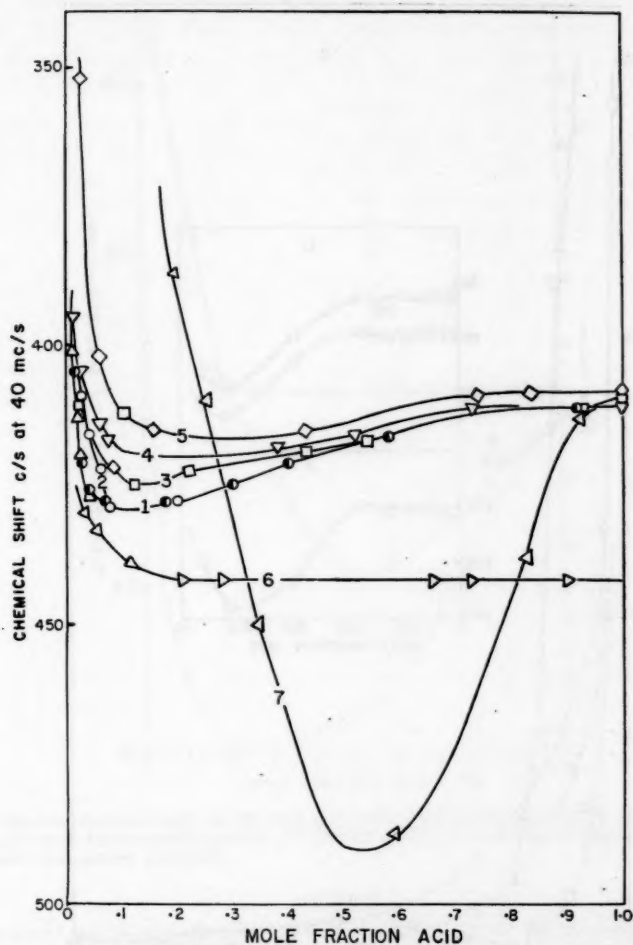
FIG. 1. Dilution chemical shifts of acids in 99.5 mole% CCl_4 and 0.5 mole% cycloC_6H_{12} as solvent: O CCl_3COOH (curve 2); ◑ $CHCl_2CO.OH$ (curve 1); △ $CH_2ClCO.OH$ (curve 1); □ $CH_3.CH.Cl.CO.OH$ (curve 3); ▽ $CH_3CHBr.CO.OH$ (curve 4); ◇ CF_3COOH (curve 5); ▷ $C.(CH_3)_3.CO.OH$ (curve 6). Curve 7 shows changes in chemical shift of the carboxyl proton of $CF_3.CO.OH$ as a function of concentration in N-methyl formamide. In all cases, chemical shifts are referred to an internal cyclohexane reference.

3-mm cell with a variable-length cell for balancing solvent absorptions. No solvent had a seriously large absorption at exactly the region required for accurate wave-number measurements on the acids. The vapor spectrum of CF_3COOH was obtained by using a 10-cm gas cell which was equilibrated with liquid CF_3COOH under vacuum conditions at 25° C, and the vapor obtained in the cell was expanded into a volume about 3 times the volume of the cell. The cell was closed off and spectra run using two blank sodium chloride windows of the same thickness as those in the gas cell in the compensating beam. The spectrum of CCl_3COOH vapor at 25° C was obtained using a 5-meter compensated gas
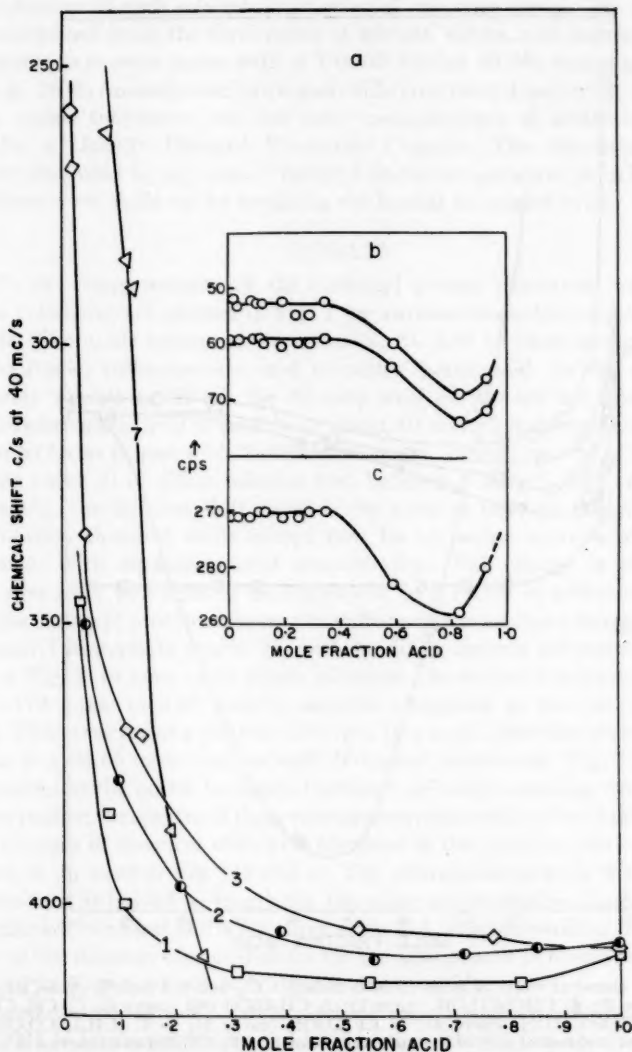
FIG. 2. (a) Dilution chemical shifts of acids in 1,2-dichloroethane: $\bullet$ CHCl$_2$CO.OH (curve 2); $\square$ CH$_3$CHClCO.OH (curve 1); $\diamond$ CF$_3$CO.OH (curve 3). The dilute region for carboxyl protons in the CF$_3$CO.OH – N-methyl formamide system appears as curve 7, a continuation of the same curve in Fig. 1.
(b) Dilution shifts of methyl doublet of N-methyl formamide in CF$_3$CO.OH system.
(c) Dilution shifts of aldehyde proton in N-methyl formamide in CF$_3$CO.OH system.

cell. Dry nitrogen flowed through CCl$_3$COOH which had been recrystallized from chloroform in a dry atmosphere and stored in a desiccator; the vapor of the acid was carried through a Perkin–Elmer 5-meter gas cell and recorded with the Perkin–Elmer 21 spectrometer.*
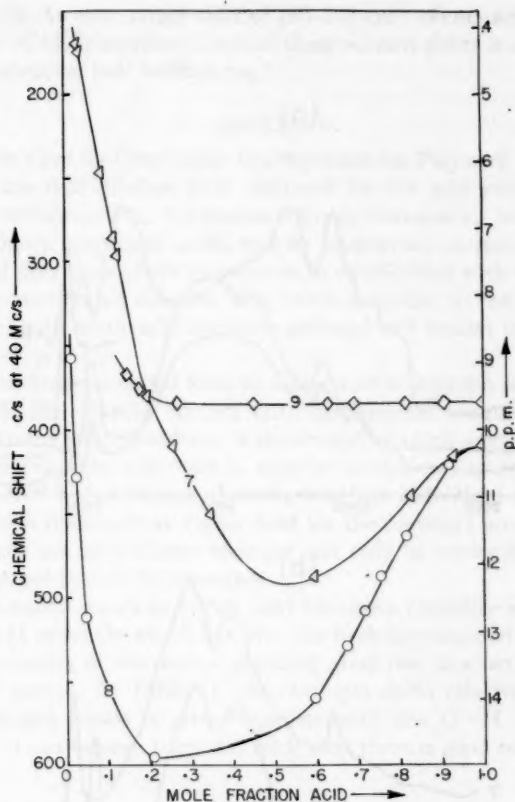
FIG. 3. Dilution chemical shifts for the acid proton in $CH_3CO.OH$ and $CF_3CO.OH$ in amide solvents: CF_3COOH in N-methyl formamide (curve 7); CF_3COOH in N,N-dimethyl formamide (curve 8); $CH_3CO.OH$ in N,N-dimethyl formamide (curve 9).

TABLE I

Hydroxyl stretching frequencies in simple carboxylic acids for the monomer molecules

Mole fraction concentration	Solvent	Acid	Hydroxyl stretching frequencies (cm^{-1})		
			$\Delta\nu_{\frac{1}{2}}$*	ν_{OH}	$\Delta\nu_{vap}$†
4.2×10^{-3}	CCl_4	$CCl_3CO.OH$	6	3490	90
6.4×10^{-4}	CCl_4	$CCl_3CO.OH$	6	3490	90
1.6×10^{-3}	$C_2H_4Cl_2$	$CCl_3CO.OH$	21	3378	202
Vapor	—	$CCl_3CO.OH$	3.5	3580	0
1.7×10^{-2}	$C_2H_4Cl_2$	CF_3COOH	18	3390	180
1.9×10^{-2}	CCl_4	CF_3COOH	6.5	3485	85
2.6×10^{-3}	CCl_4	$CF_3CO.OH$	7.0	3485	85
Vapor spectrum	—	CF_3COOH	4	3570	0
Vapor	—	CH_3COOH (21)	—	3577	
Vapor	—	HCOOH (22)	—	3567	
Vapor	—	DCOOH (22)	—	3567	
10^{-2}	CCl_4	CH_2ICOOH	—	3505	

*Half width of monomer O—H absorption.
†Difference between values of OH in the vapor and in the solvent under study for the particular acid.
NOTE: Other work is referred to the tabulation of literature at the end of the paper.
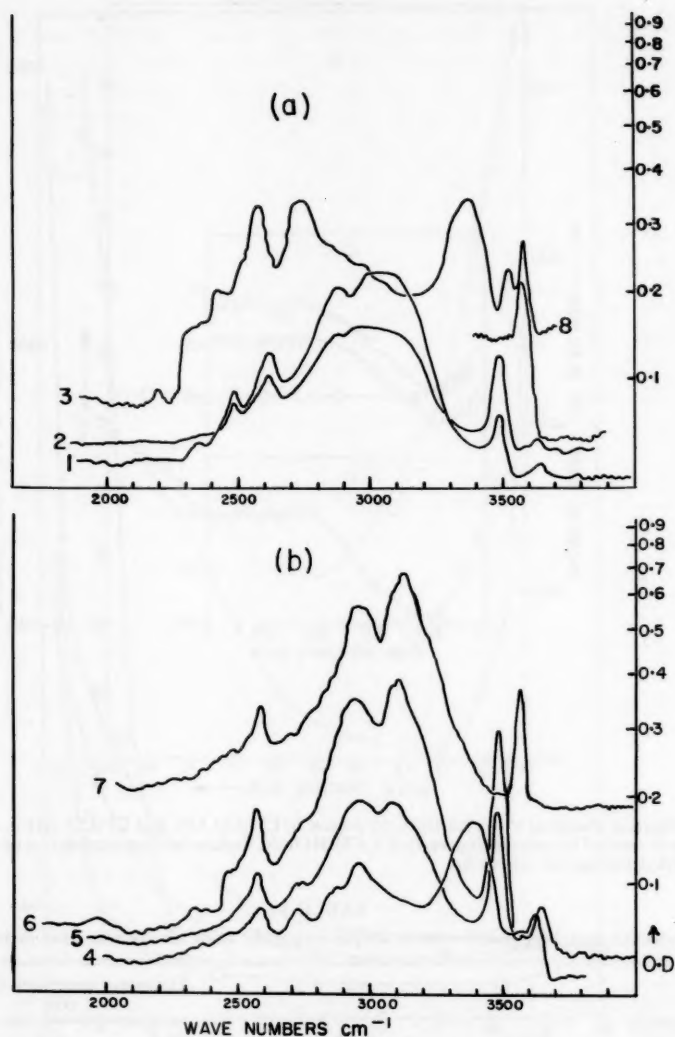
FIG. 4.   (a) Infrared spectra of the —O—H stretching region for CCl₃COOH. Curves are identified by numbers: (1) 4.2×10^{-3} mole fraction in CCl₄, 0.1-mm cell; (2) 6.4×10^{-4} mole fraction in CCl₄, 3.0-mm cell; (3) 1.4×10^{-3} mole fraction in 1,2-dichloroethane, 3-mm cell; (8) vapor spectrum CCl₃COOH at 35° C, 5-m gas cell.

(b) Infrared spectra of —O—H stretching region for CF₃CO.OH. Curves are identified by numbers: (4) 1.7×10^{-2} mole fraction in 1,2-dichloroethane, 0.1-mm, cell; (5) 1.904×10^{-3} mole fraction in CCl₄, 3.0-mm cell; (6) 2.9×10^{-3} mole fraction in CCl₄, 3.0-mm cell; (7) vapor spectrum of CF₃COOH at 25° C, 10-cm gas cell.

The —OH monomer stretching frequency occurs in the vapor phase for all acids measured at 3574 ± 6.5 cm⁻¹. The frequency difference from acid to acid is significant but quite small compared to a shift of 85–90 cm⁻¹ to the monomer absorption in CCl₄

solution for all acids. An even larger shift of 180–202 cm^{-1} occurs when the acid monomer absorbs in CH_2Cl—CH_2Cl solution. Each of these solvent shifts is accompanied by large changes in the absorption half widths, $\Delta\nu_{\frac{1}{2}}$.

DISCUSSION

Consideration of the Case for Open-chain Hydrogen-bonded Polymers

In Fig. 1, the low-field dilution shift obtained for the acid proton resonance in the following acids: trifluoroacetic, trichloroacetic, dichloroacetic, monochloroacetic, and α-bromo- and α-chloro-proprionic acids, will be interpreted as resulting from the occurrence of open- and polymeric-chain association in equilibrium with the cyclic dimer form of these acids in concentrated solution. The result is similar to that obtained by Reeves and Schneider (15) with acetic acid solutions although not similar to the curves obtained for the acids C_3 to C_{17} (13).

The polymeric hydrogen-bonded form of acetic acid in solution suggested by dielectric measurements (23, 28), Raman spectra (19), and nuclear magnetic resonance (15) is probably related to the polymeric form in the crystal of acetic acid (18). The order introduced by cyclic or chainlike polymers in solution as opposed to cyclic dimer formation must be compensated by an increased strength of the individual hydrogen bonds. The occurrence of proton resonance at higher field for the carboxyl proton and the fact that the hydrogen bonds are individually stronger can only be reconciled by chainlike polymerization as opposed to a cyclic structure.

The proton resonance occurs at higher field because a chainlike structure involves one terminal acetic acid molecule which has one non-hydrogen-bonded proton. It is possible that the rapid averaging of the proton shielding gives rise to a net displacement to high field for the acid proton. In Table II, the chemical shifts relative to water of various O—H - - - O hydrogen bonds is given together with the O—H - - - O distance where data is available. It can be seen from this table that there is good correlation between the

TABLE II

Comparison of chemical shifts in O—H - - - O hydrogen-bonding systems and bond distances when available

Compound	Concentration dependent?	Chemical shift, H_2O, p.p.m.	O—H - - - O distance in crystal, Å	Reference to chemical shifts
Pure acetic acid	Yes	−6.8	—	15
Pure substituted acetic acids	Yes	−6.9	—	Present work
Pure C_2–C_{10} acids	No	−7.2	—	13
Pure trimethyl acetic acid	No	−7.5	—	Present work
$CF_3CO.OH$ – N-methyl formamide 1:1 complex	Yes	−8.7	—	Present work
Calculated acetic acid dimer shift from K_{dimer}	No	−9.7	2.76$^+$	24
Acetylacetone-enol form	No	−10.0	—	12
Calculated benzoic acid dimer shift	No	−10.25	2.64$^+$	24
$CF_3CO.OH$–N,N-dimethyl formamide, lowest field position acid proton	Yes	−12.0	—	Present work
Triacetylmethane-enol form	No	−12.6	—	25
Potassium hydrogen maleate	No	−15.4	—	26
Sodium hydrogen maleate	No	−15.03	2.41$^+$ to 2.43	26
Potassium hydrogen phthalate	No	−15.15	—	26

NOTE: Uncertainties of ±0.2 p.p.m. exist in any given chemical shift due to varying referencing procedures. "+" bond distances obtained from reference 20.

hydrogen-bond strength and the paramagnetic chemical shift of the hydrogen-bonded proton. This supports the suggestions of Pople and Marshall (31) that the strongest hydrogen bonds have the largest negative chemical shifts, and the experimental measurements of Reeves, Allan, and Strømme (14, 27).

The suggestions of Pitzer and Davis (24) that the reduction of the O—O distance across the hydrogen bond eventually causes increased shielding due to electrons of the noncovalently bonded oxygen is not experimentally proved. The only explanation therefore of the low-field shift on dilution of some carboxylic acids is the occurrence of chainlike polymers.

The careful experimental work of Pitzer and Davis (24) warrants some discussion since the calculated dimer chemical shift in their work lies considerably to low field with respect to the dimer shifts assumed in the work of Reeves and Schneider (15) and, later, Reeves (13). The occurrence of abnormally large variations of monomer chemical shift with temperature (24) using equilibrium constants obtained from infrared measurements and the extremely large absolute magnitude of the monomer–dimer chemical shifts must reflect some uncertainty in either the equilibrium constants used or the basic assumptions that only monomers and cyclic dimers exist at the concentrations studied. A variation of 400 cycles in chemical shift due to a neighboring ring current effect (24) over an 80° C range is almost one order of magnitude too large (5). Even when the equilibrium constants are adjusted so as to obtain constant values of $\delta_{monomer}$ and δ_{dimer} with temperature, the uncertainty about the existence of open dimers, trimers, or higher polymers renders this adjustment of the value of $\delta_{monomer}$ somewhat artificial. Recent dielectric measurements (28) suggest the existence of polymers of the open-chain type in concentrated solutions of n-caproic and cyclohexane carboxylic acid in nonpolar solvents. The complicated question of species present in nonpolar solutions of long-chain acids is not resolved but in acetic acid and the substituted acetic acids measured here, the occurrence of open-chain polymers is indicated.

Association of the Monomer Form of Carboxylic Acids with Solvents

A weak hydrogen-bond acceptor such as chloroform forms hydrogen-bonded complexes with donor solvents such as acetone (4) and even with weak donor systems such as benzene or olefins (5). It is to be expected that a much stronger acceptor such as the acid proton of the monomer form of carboxylic acids will form a stronger hydrogen-bond association than chloroform, with the same donor solvents. The position of the monomer acid proton chemical shift is shown to be strongly temperature dependent in the work of Pitzer and Davis (24) but the calculated position of the signal is subject to large systematic errors. The interpretation suggested by several workers (13, 15, 17) that the monomer form appears in solutions of higher dielectric constant merely because of the higher dipole moment of the monomer is not entirely true. Recent work on the infrared spectra of solute molecules has shown conclusively that spectral shifts can be associated with specific association with a solvent molecule through a hydrogen bond (30, 29). The figures in Table I are evidence for the specific association of the acid monomers with solvent molecules on this basis. The frequency shift of the monomer —O—H stretching frequency between the vapor phase and essentially infinite dilution in CCl_4 is about 80–90 cm^{-1}. This is too large to be accounted for on the basis of dispersion forces alone. At the same time the half width of the single line observed increases markedly between the vapor and the solution as seen from Table I. The frequency shift and increase in

half width of the monomer —O—H absorption is much more marked in 1,2-dichloro-ethane (Fig. 4 and Table I), indicating a stronger hydrogen-bonded complex with the monomer in this case. The frequency shift of the monomer absorption in the vapor phase amongst a series of acids is quite small, ± 6.5 cm^{-1}, compared with the change between vapor and solvent. The variation of monomer absorption frequency in CCl$_4$ amongst three acids measured (Table I) is also quite small. The weak hydrogen-bond association of carbon tetrachloride with carboxylic acid monomers is to be expected since this molecule is a very weak donor.

The dimer band is considerably more intense than the monomer even at the concentrations studied, but an intensification factor of $37 \times$ on dimer formation suggested by Pimentel and McClellan (32, Table 3-VIII) indicates that little dimer is present.

The Chemical Shift Changes in 1,2-Dichloroethane

The dilution chemical shifts of three acids in 1,2-dichloromethane indicate that the polymeric hydrogen-bonded forms and the dimer form are dissociated appreciably at much higher acid concentrations. The situation at infinite dilution of acid will correspond to some kind of hydrogen-bonded complex between the acid monomer and dichloromethane. The behavior of the substituted acids in this solvent is very similar to that reported previously for other carboxylic acids in dichloroethane, acetone, and acetonitrile. The dissociation at higher concentrations of acid is encouraged in a solvent of higher dielectric constant.

The Behavior of Carboxylic Acids in Basic Solvents

The changes in chemical shift of the acid proton of trifluoroacetic acid in N-methyl and N,N-dimethyl formamide (Figs. 1, 2, and 3) are of some interest since the low-field extremes of these shifts are quite remarkable. Such a low-field shift is consistent only with the formation of a very strong hydrogen bond. There is considerable heat evolution on making up the solutions, which is not usually detectable when there is a change in the strength and number of hydrogen bonds formed.

The formation of a stronger hydrogen bond in a 1:1 complex could conceivably occur between trifluoroacetic acid and N-methyl formamide in a configuration similar to an acid dimer, as shown below.

$$\begin{array}{ccc}
 & \overset{\displaystyle CH_3}{\underset{|}{}} & \\
O\cdots H-N & & \\
F_3C-C & & C-H \\
O-H\cdots O & &
\end{array}$$
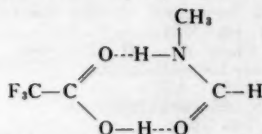
This particular form of a 1:1 complex depends on the existence of both donor and acceptor ends of the hydrogen bond in the correct spatial arrangement on the amide molecule. This is excluded in N,N-dimethyl formamide but the extreme low-field chemical shift of the acid proton becomes greater in these solutions as shown in Fig. 3. The form of the 1:1 complex above is not therefore the cause of this extreme low-field shift.

The form of these dilution chemical shift curves are explicable in terms of proton transfer to the amide.

$$CF_3CO.OH + NMe_2CHO \rightleftharpoons CF_3COO^- + NMe_2CH_2O^+$$
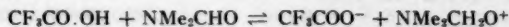
The strength of trifluoroacetic acid is sufficient to cause proton transfer to the amide,

although in such concentrated solutions the medium effects prohibit quantitative prediction of the extent of protonation. The addition of amide to the acid causes the chemical shift of the acid proton to move to low field. This can be explained in terms of the protonation of almost all amide molecules and the formation of a very strong hydrogen bond between the conjugate acid of the amide and the trifluoroacetate anion. This is equivalent to the formation of ion pairs in moderately concentrated solution. The chemical shift of the acid proton observed is an average of the various environments since rapid proton exchange is evident from the single sharp line observed. In a 1:1 mole ratio of acid to amide it is expected that almost all the molecules present are involved in ion-pair formation. Addition of further amide will raise the dielectric constant of the solution and cause dissociation of the ion pairs. The breaking of the strong hydrogen bond in the ion pairs in dilute solution causes the very large chemical shift change in the high-field direction. The nature of the amide conjugate acid is not indicated by these results.

The dilution chemical shift of acetic acid in the N,N-dimethyl formamide is quite small and not detectable until dilute acid solutions. The strength of acetic acid is much smaller so it is expected that protonation of the amide is inappreciable.

The chemical shift in dilute solutions of acetic acid in N,N-dimethyl formamide is not measurable ($\sim$15 mole% acid) because of broadening of the acid proton resonance below noise level. This is indicative of proton exchange in the critical region for n.m.r. measurements (7). Further studies of these processes are being made.

REFERENCES

1. J. T. ARNOLD and H. G. PACKARD. J. Chem. Phys. 19, 1608 (1951).
2. U. LIDDEL and N. F. RAMSEY. J. Chem. Phys. 19, 1601 (1951).
3. W. G. SCHNEIDER, H. J. BERNSTEIN, and J. A. POPLE. J. Chem. Phys. 28, 601 (1958).
4. G. KORINEK and W. G. SCHNEIDER. Can. J. Chem. 35, 1157 (1957).
5. L. W. REEVES and W. G. SCHNEIDER. Can. J. Chem. 35, 251 (1957).
6. T. SCHAEFER and W. G. SCHNEIDER. J. Chem. Phys. 32, 1218, 1224 (1960).
7. H. S. GUTOWSKY and A. SAIKA. J. Chem. Phys. 21, 1688 (1956).
8. E. D. BECKER, U. LIDDEL, and J. N. SHOOLERY. J. Mol. Spectroscopy, 2, 1 (1958).
9. E. D. BECKER. J. Chem. Phys. 31, 269 (1959).
10. M. SAUNDERS and J. B. HYNE. J. Chem. Phys. 31, 270 (1959).
11. C. REID and T. M. CONNOR. Private communication.
12. L. W. REEVES. Can. J. Chem. 35, 1351 (1957).
13. L. W. REEVES. Trans. Faraday Soc. 55, 1684 (1959).
14. L. W. REEVES. Can. J. Chem. 38, 748 (1960).
15. L. W. REEVES and W. G. SCHNEIDER. Trans. Faraday Soc. 54, 314 (1958).
16. A. BERGER, A. LOEWENSTEIN, and S. MEIBOOM. J. Am. Chem. Soc. 81, 62 (1959).
17. G. ALLEN and E. F. CALDIN. Quart. Revs. (London), 7, 255 (1953).
18. R. E. JONES and D. H. TEMPLETON. Acta Cryst. 11, 484 (1958).
19. M. I. BATUEEV. Compt. rend. acad. sci. U.R.S.S. 52, 401 (1946).
20. INTERATOMIC DISTANCES. Chem. Soc. (London), Spec. Publ. No. 11 (1958).
21. J. K. WILMSHURST. J. Chem. Phys. 25, 1171 (1956).
22. J. K. WILMSHURST. J. Chem. Phys. 25, 478 (1958).
23. R. J. W. LE FEVRE and H. VINE. J. Chem. Soc. 1795 (1938).
24. J. C. DAVIS and K. S. PITZER. J. Phys. Chem. 61, 886 (1960).
25. S. FORSEN and M. NILSONN. Acta Chem. Scand. 13, 1383 (1959).
26. S. FORSEN. J. Chem. Phys. 31, 852 (1959).
27. L. W. REEVES, E. A. ALLAN, and K. O. STRØMME. Can. J. Chem. 38, 748 (1960).
28. G. LOVELUCK. J. Phys. Chem. 64, 385 (1960).
29. L. J. BELLAMY, H. E. HALLAM, and R. L. WILLIAMS. Trans. Faraday Soc. 54, 1120 (1958).
30. G. L. CALDOW and R. W. THOMPSON. Proc. Roy. Soc. (London), A, 254, 1 (1960).
31. J. A. POPLE and T. W. MARSHALL. Mol. Phys. 1, 199 (1958).
32. G. C. PIMENTEL and A. L. McCLELLAN. The hydrogen bond. W. H. Freeman Co. 1960. p. 102.

NOTES

SAPONINS AND SAPOGENINS
XI. ON THE PRESENCE OF ECHINOCYSTIC ACID AND QUERCETIN IN FLOWERS OF ALBIZZIA LEBBEK BENTH.*

I. P. Varshney and Mohd. S. Y. Khan

Seeds of *Albizzia lebbek* Benth. from Utter Pradesh have previously been reported to yield saponin from which oleanolic acid and echinocystic acid have been obtained (1), while the complete beans of *A. lebbek* Benth. from Bengal yield, in addition to these two acids, another isomer of echinocystic acid named albigenic acid (2). Another species, *Albizzia anthelmintica* (3), yields echinocystic acid alone. *Albizzia procera* from Madhya Pradesh (4) and *Albizzia odoratissima* seeds from Maharashtra (5) yield machaerinic acid.

Although much work has been done on the seeds from various species, no work seems to have been done on the flowers of any of the species of *Albizzia* and therefore the work on the flowers of *A. lebbek* Benth. was undertaken.

The flowers of *A. lebbek* Benth., collected locally from the university campus, yielded, by alcoholic extraction and subsequent treatment, a colorless hygroscopic powder giving all the tests for saponins. The sulphuric acid hydrolysis of the saponin gave the sapogenin (acid), m.p. 297–301°. It gave a diacetate, m.p. 257–262°, and diacetyl methyl ester, m.p. 201–202°. It is a pentacyclic triterpenic acid belonging to the β-amyrin group and has been identified as echinocystic acid ($3\beta,16\alpha$-dihydroxy-Δ^{12}-oleanene-28-oic acid) by mixed melting point with authentic samples of echinocystic acid and derivatives (c.f. echinocystic acid, m.p. 305–312°; acetate, m.p. 272–275°; acetyl methyl ester, m.p. 200–201° (1, 6)). The infrared spectra of the acetyl methyl ester, which is superimposable with that of an authentic sample, confirmed its identity as echinocystic acid.

The flowers also yield an anthoxanthin glycosidic fraction. The product did not crystallize and therefore was hydrolyzed. The aglycone obtained was then chromatographed on filter paper. The chromatogram showed the presence of at least three components quite different from each other. One of the components was identified as quercetin by chromatography with an authentic sample of quercetin.

EXPERIMENTAL

All the melting points recorded have been taken on a Kofler hot microscopical stage and are corrected. The infrared spectra have been taken in these laboratories by one of the authors (I. P. V.) using a Perkin–Elmer spectrometer model 137 (Infracord) in nujol mull.

Saponin and sapogenin.—The flowers (200 g), after being exhausted with light petroleum ether, were extracted with 95% alcohol and the saponin (10.5 g) was obtained as a colorless hygroscopic powder in the usual manner (4). It gave all the tests for saponin, i.e. it foams copiously when shaken with water, is toxic to fishes in dilute concentrations, and haemolyzes red blood corpuscles in dilute solutions (7). The saponin (5 g) was hydrolyzed with sulphuric acid (7%) (4) and the genin obtained (1.5 g) was then transformed into the potassium salt by being refluxed with methyl alcoholic potassium

hydroxide. The solution of the potassium salt was extracted with ether to remove any neutral sapogenin present. Hydrochloric acid, added to the alkaline solution remaining after ether extraction, precipitated the acid sapogenin, which was filtered, washed free of the acid, and dried.

Acetate.—The genin (200 mg) was acetylated hot, in the usual manner, with pyridine and acetic anhydride. The acetate obtained was crystallized from methyl alcohol as colorless needles, m.p. 257–262° (cf. diacetyl echinocystic acid, m.p. 272–275° (6); 248–249° (1)). The melting point was not depressed when a mixed melting point was taken with an authentic sample of diacetyl echinocystic acid. I.R. spectra: λ_{max}^{nujol} 5.81, 5.90, 8.09 μ.

Genin.—The acetate (100 mg) was deacetylated with methyl alcoholic potassium hydroxide (10%) and the free genin (80 mg) obtained was crystallized from isopropyl alcohol as colorless crystals, m.p. 297–301° (cf. echinocystic acid, m.p. 305–312° (6); 291–293° (1)). No depression was noted when a mixed melting point was taken with an authentic sample of echinocystic acid. I.R. spectra: λ_{max}^{nujol} 2.87, 5.97 μ.

Acetyl methyl ester.—The acetate (100 mg) was methylated with diazomethane and the methyl ester obtained was crystallized from methyl alcohol as colorless fine needles (90 mg) melting at 201–202°. It was found to be identical with acetyl methyl echinocystate as no depression was observed in the mixed melting point with an authentic sample of diacetyl methyl echinocystate and the infrared spectra were identical (cf. echinocystic acid diacetyl methyl ester, m.p. 200–201° (1, 6); I.R. spectra: λ_{max}^{nujol} 5.75, 8.09 μ). I.R. spectra: λ_{max}^{nujol} 5.75, 8.09 μ.

Anthoxanthin glycosides.—The residue obtained after the evaporation of the alcoholic extract was dissolved in water and the solution extracted with *n*-butyl alcohol. The recovery of the butyl alcohol gave a mixture of the saponin and the glycoside. It was dissolved in alcohol, filtered, and then added dropwise into a large volume of acetone to precipitate the saponin. The saponin was filtered off and the acetone solution was evaporated to dryness and then again dissolved in alcohol and reprecipitated with acetone. This operation was repeated twice to remove the saponin completely. The acetone, after the removal of the saponin, was evaporated to dryness and the product obtained gave a salmon-pink coloration with magnesium and hydrochloric acid (8). All attempts to crystallize the glycoside were fruitless.

Aglycone.—The aqueous solution of the glycoside containing a little alcohol was hydrolyzed by refluxing with sulphuric acid (10%) for 3 hours. The aglycone obtained was filtered and washed free of acid. It was dissolved in alcohol and two drops of dilute lead acetate solution added to it precipitated the impurities. It was then filtered and the filtrate was treated with hydrogen sulphide to remove any lead which might have passed into the filtrate. The solution thus obtained was evaporated to dryness under reduced pressure. The product (aglycone) obtained gave acidic cyanidin and Wilson's boric acid tests (8, 9).

Paper chromatography.—The aglycone dissolved in a few drops of alcohol was deposited on Whatman filter paper No. 1 and chromatographed beside an authentic sample of quercetin (L. Light & Co. Ltd., England). An acetic acid:water (60:40) (10) solvent mixture and the ascending technique were used. The chromatogram was run for 16 hours and then dried and sprayed with sodium carbonate solution, ferric chloride solution, or examined under ultraviolet light and ultraviolet light and ammonia (10, 11) vapors. It showed three clear spots, one of which was found to be identical with quercetin. All attempts to crystallize the aglycone failed.

The authors are thankful to the Council of Scientific and Industrial Research, New Delhi, for the award of a junior research fellowship to one of them (M. S. Y. K.).

1. I. P. VARSHNEY. D.Sc. Thesis, Université de Paris, Paris, France. 1956. CH. SANNIÉ, H. LAPIN, and I. P. VARSHNEY. Bull. soc. chim. France, 1440 (1957).
2. A. K. BARUA and S. P. RAMAN. Tetrahedron, 7, 19 (1959).
3. R. TSCHESCHE and D. FORSTMANN. Ber. 90, 2383 (1957).
4. M. O. FAROOQ, I. P. VARSHNEY, and H. HASAN. Arch. Pharm. 292, 57 (1959); Compt. rend. 246, 3261 (1958); Current Sci. (India), 27, 489 (1958).
5. I. P. VARSHNEY and MOHD. S. Y. KHAN. J. Pharm. Sci. In press.
6. I. BERGSTEINSSON and C. R. NOLLER. J. Am. Chem. Soc. 56, 1403 (1934).
7. CH. SANNIÉ. Exposés ann. biochim. méd. 9, 175 (1948).
8. Y. ASAHINA and M. INUBUSE. Ber. B, 61, 1646 (1928).
9. C. W. WILSON. J. Am. Chem. Soc. 61, 2303 (1939).
10. T. B. GAGE, C. D. DOUGLASS, and S. H. WENDER. Anal. Chem. 23, 1582 (1951).
11. E. C. BATE-SMITH and R. G. WESTALL. Biochim. et Biophys. Acta, 4, 427 (1950).

PREPARATION OF UNDECENOL AND UNDECENYL BROMIDE

D. G. M. DIAPER

Although complex hydrides have revolutionized the preparation of primary alcohols from acids and esters, the Bouveault–Blanc procedure may still be preferable for preparative work on the grounds of expense, especially when catalytic hydrogenation cannot be employed. To prepare undecenol (undec-10-en-1-ol) in quantity (1), sodium–ethanol reduction of ethyl undecylenate (undec-10-enoate) was used. Yields previously reported for this and other Bouveault–Blanc reductions vary widely, and rarely exceed 80%. Smith (2) obtained undecenol in 76% yield by sodium and ethanol reduction and only 30% was obtained (3) in butanol. Poor yields have been attributed to the presence of water, which gives sodium hydroxide, destroying the ester by conversion to the sodium salt, which is not attacked by the reagent. In long-chain ester reductions this concurrent production of the sodium salt of the acid is doubly serious since it not only reduces the yield but complicates isolation of the alcohol which is entrained in the soapy aqueous layer. Intensive drying of the ethanol is the customary solution of this problem—a tedious affair which must be repeated at intervals if the stock of ethanol is exposed to air in intermittent use. Even so, Darzens (4) contends that reaction of the ester with sodium thus,

$$R.COOEt + 2H_2 \rightarrow RCH_2OEt + H_2O, \qquad [1]$$
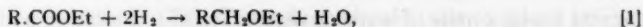
inevitably produces some water and thus sodium salt. This interpretation implies a stoichiometric equivalence of ethyl ether production, water formation, and ester destruction.

In an attempt to assess the effects of traces of water (such as are removed in an intensive drying operation) upon the reaction, progressive amounts were added to the solvent in successive reductions under standard conditions. The saponification yield was found by titration and the results are represented in Fig. 1, curve A. The first part of the curve is steep, demonstrating that the effect of water upon the saponification reaction is catalytic
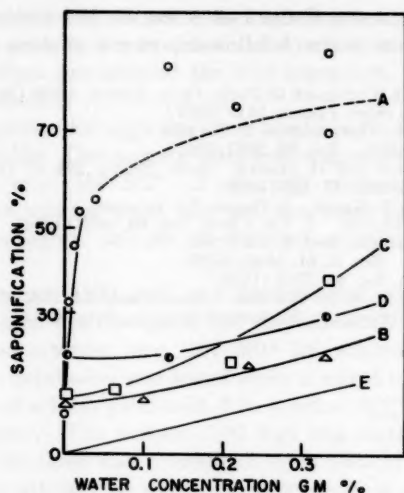
FIG. 1. Saponification of ethyl undecylenate during Bouveault–Blanc reduction as a function of water concentration. Curve A (open circles), ethanol alone; curve B (triangles), ethanol (30 ml) and acetic anhydride (1 ml); curve C (squares), ethanol (30 ml) and acetic acid (0.5 ml); curve D (half-filled circles), ethanol (30 ml) and acetic acid (1 ml); curve E, theoretical saponification yield.

and not stoichiometric. Curve E represents stoichiometric utilization of water in saponification (by calculation). It is suggested that the latter part of curve A (dotted) is indefinite for the following reason. The Bouveault–Blanc reaction is performed extremely rapidly and there must be a competition between two rapid reactions. Reduction probably occurs principally at or near the sodium surface; saponification, in all regions of the ethanol phase. The competition will therefore be controlled by the effective surface area of the molten metal and therefore by the degree of turbulence of the mixture during a brief critical period of time. This condition is hard to control or reproduce.

The use of ammonium chloride (5) and trialkyl borates (6) as additives to suppress saponification in sodium reductions has been advocated. We find that acetic anhydride (curve B, Fig. 1) and acetic acid (curves C and D) have similar effects. Such a result for acetic anhydride is not unexpected, for this reagent can effectively diminish water concentration by conversion to acetic acid. The product, acetate ion in this case, would attack the ester starting material much more slowly than the hydroxide ion. The acetic acid result is more surprising, for it must react with hydroxide ion as follows:

$$OH^- + CH_3.COOH \rightarrow H_2O + CH_3.COO^-. \tag{2}$$

On this basis, a mole of water is regenerated for a mole of hydroxide ion destroyed. This can react further with sodium giving a mole of hydroxide back again, so the effect of acetic acid is not expected to destroy water or hydroxide but to keep the amounts of these constant in a cyclic process. Possibly the acetic acid functions, with its ion, as a buffer, diminishing hydroxide concentration during the early critical part of the reaction. An increased acetic acid concentration (curve D, compare C) actually leads to a poorer result with traces of water. This is attributed to precipitation of sodium salts on the sodium surface, hindering migration of ester to the site of reduction and exposing it for a relatively longer time to saponification.

The Darzens hypothesis (equation [1]) would require that the crude undecenol should contain some of its ethyl ether as an impurity. It was found that a single peak was obtained in gas chromatographic analysis and it was shown that an authentic sample of 1-ethoxy-10-undecene can be separated from undecenol under the conditions employed. To prepare the ether, undecenyl bromide was made by an improved method which incorporates removal of starting material (which boils close to the product) as acidic phosphate esters.

While the evidence now available confirms catalytic rather than stoichiometric participation of water and rules out significant formation of ethyl ether as a side reaction, it sheds little light on the mechanism of the reduction process. It is demonstrated, however, that the necessity for "super-dry" ethanol as a solvent in this instance may be avoided.

EXPERIMENTAL

Undecenol—Preparative Method

Ethyl undecylenate (46 g, 0.22 mole, n_D^{20} 1.4390) was mixed with ethanol (200 ml) which had been drawn from the stock of absolute ethanol without special drying. Acetic acid (3 ml) was added. The solution was poured, as rapidly as possible without loss, down an inclined condenser attached to a flask containing sodium (40 g, 1.7 moles, cut in several large pieces under xylene and melted under nitrogen) and heated in a salt bath at 160°. After the reaction had moderated, the solution was boiled under reflux for 5 minutes in a dry nitrogen atmosphere. A steam inlet was then quickly attached and the bulk of the ethanol was removed by steam distillation while the unreacted sodium was simultaneously destroyed. It is important that air is not allowed to enter the system until all the sodium has been destroyed. The residual liquid was extracted with ether, washed once with water, and dried. Upon distillation, undecenol was obtained in three runs of similar scale in yields of 78, 84, and 82%, b.p. 134–139° at 12 mm. Scale-up to 100 g of ester diminished this to 74%. The discrepancy between these yields and those indicated in Fig. 1, curve C, may be due to scale-up or distillation loss. The undecenol in each case gave a single peak in gas chromatographic analysis as described below.

Undecenol—Estimation of Concurrent Saponification

A 500-ml three-necked flask was fitted with an inlet tube for dry nitrogen, a large-liquid-capacity Allihn condenser, arranged for reflux somewhat inclined from the vertical, and a stopper. The condenser was capped with a drying tube. All apparatus was standard taper glassware, oven dried at 120° and quickly filled with nitrogen after assembly, while still hot. Sodium metal (approximately 9 g, 0.39 mole) was cut in a single lump, under xylene, with a knife and a large, warm, lightly greased cork borer. It was pressed out of the cork borer directly into the flask while a vigorous stream of nitrogen emerged. The flask was then immersed in a salt bath at 170°. The sodium should melt to give a bright globule with a thin broken black film. There should be no visible pieces of white crust. Dry ethyl undecylenate (10 g, 0.047 mole) was quickly weighed into a flamed flask while still hot, and dry ethanol (30 ml) was siphoned in. The ethanol stock had been dried by the magnesium ethoxide method; it was then collected in hot glassware previously filled with dry nitrogen, and stored in a ground-joint apparatus fitted with a siphon and drying tube. Immediately before being poured onto the sodium, the required additives (acetic acid, water, or acetic anhydride (see Fig. 1)) were added by pipette in the form of freshly prepared ethanol or benzene solutions of accurately known concentration in the

1–10% range. The nitrogen stream was interrupted while the solution was poured down the condenser and restarted immediately after. A few minutes were allowed to elapse after the reaction subsided and the apparatus was then quickly fitted with a steam inlet, care being taken to avoid ingress of air. When all the sodium had been destroyed, the solution was acidified with sulphuric acid and ice, and continuously extracted with ether. The ether extract was made up to 100 ml with ethanol and an aliquot was neutralized to bromcresol green. Sodium hydroxide (0.0486 N in ethanol) was added from a burette in excess, and, after it had been allowed to stand several hours under nitrogen to ensure saponification of ester, the alkali was back-titrated with standard acid. Solvent blank reactions were performed (ethanol, sodium, acetic acid or anhydride, but no ethyl undecylenate), giving titration values within 0.2 ml of the theoretical figures. Curves B, C, and D were plotted using titration values corrected for acetic acid content. All points represent single determinations, except the first point (water concentration = 0) on curve A, which was the mean of a triplicate determination (7.0, 7.6, and 8.3%).

Undecenyl Bromide (11-Bromo-1-undecene)

Conversion of undecenol to the bromide (6) is complicated by the fact that starting material and product boil at nearly the same temperature. The following modification ensures freedom from undecenol. After undecenol (86 g, 0.51 mole) was treated with phosphorus tribromide (50 g, 0.18 mole) in toluene (250 ml) at −5° and then at 90° for 3 hours, toluene was removed under reduced pressure and the solution was diluted with dry ether (150 ml). It was treated with phosphorus pentoxide (two 20-g portions) and next day decanted into 250 ml of 50% aqueous methanol. Ammonia was quickly added until the mixture was alkaline to phenolphthalein and, after it was washed with a similar portion of aqueous methanolic ammonia and with water, the ether solution was dried and distilled, giving 57 g (48%) of undecenyl bromide, b.p. 136–141° at 15 mm, n_D^{20} 1.4638. By vapor phase chromatography in hydrogen at 160 ml/minute and 183° on an Apiezon grease column the bromide came through as a single peak with a retention time of 15.6 minutes. Under similar conditions undecenol had a retention time of 8.4 minutes and a sample of undecenyl bromide, prepared as above but omitting the phosphoric anhydride – ammonia purification, showed two peaks. The infrared absorption spectrum of this sample had a peak in the O—H region, absent from the purified sample.

1-Ethoxy-10-undecene

By condensation of undecenyl bromide with one equivalent of sodium ethoxide in dry ethanol or by condensation of ethyl bromide with one equivalent of sodium undecenoxide in dry benzene, a liquid product was obtained, boiling at 114–115° at 4 mm, n_D^{21} 1.4344. Although it analyzed correctly for $C_{13}H_{26}O$ (found: C 79.1, H 12.9; calc: C 78.8, H 13.1%), the vapor chromatogram (in hydrogen at 160 ml/minute over Apiezon at 220°) showed two peaks at 3.25 and 4.0 minutes. The latter was identified as undecenol by admixture with an authentic sample and accounted for about 5% of the product. The fact that both methods of preparation gave a similar proportion after distillation indicates that an azeotropic mixture is formed. Separation was achieved by column chromatography over alumina and the purified ethoxy undecene gave a single vapor phase chromatograph peak. After distillation it had n_D^{21} 1.4336.

1. D. G. M. DIAPER and D. L. MITCHELL. Can. J. Chem. **38**, 1976 (1960).
2. R. ASHTON and J. C. SMITH. J. Chem. Soc. 1308 (1934).
3. T. F. DANKOVA, E. I. GENKIN, and N. A. PREOBRAZHENSKII. J. Gen. Chem. (U.S.S.R.), **15**, 189 (1945).
4. G. DARZENS. Compt. rend. **224**, 570 (1947).
5. P. ANGLARET and L. PALFRAY. Compt. rend. **223**, 205 (1946).
6. C. G. TOMECKO and R. ADAMS. J. Am. Chem. Soc. **49**, 527 (1927).

THE CRYSTALLIZATION OF POLYAMINO POLYACETIC ACIDS
IN AN ION EXCHANGE MEMBRANE CHAMBER

R. A. KUNTZE

Ethylenediamine tetraacetic acid (EDTA) as represented by the formula $(HOOCCH_2)_2N(CH_2)_nN(CH_2COOH)_2$, where $n = 2$, has received considerable attention because of its ability to form highly stable chelates with a variety of metal ions. It is generally synthesized by condensation of sodium chloracetate and ethylenediamine (1) or by modifications of the Strecker-type synthesis (2). The free acid can be crystallized from the alkaline reaction mixtures by acidification to pH 1.5–2 with a mineral acid.

In the course of an investigation of the properties of polyamino polyacetic acids as inhibitors of the precipitation of calcium salts, the methods of synthesis and crystallization of several acids similar to EDTA were examined. It was found that diethylenetriamine pentaacetic acid (DTPA), with the formula $(HOOCCH_2)_2N(CH_2)_2NCH_2COOH(CH_2)_2$-$N(CH_2COOH)_2$, can be synthesized by both the Strecker-type synthesis and the chloracetate method, although it has been claimed that the latter method cannot be used for this purpose (3). The chloracetate method is preferred since the accompanying impurities are well known, whereas those of the Strecker-type synthesis have not been determined (4).

Attempts to obtain the free acid of DTPA by crystallization from the reaction mixture on acidification with a mineral acid were unsuccessful. Similarly, no success was encountered with crystallization methods used for other polyamino polyacetic acids (5). It is apparently necessary to remove the majority of the sodium ions from the reaction mixture before crystallization can take place.

Subsequently, an ion exchange membrane method was developed which permits crystallization in a simple and efficient manner. The apparatus employed (Fig. 1) was
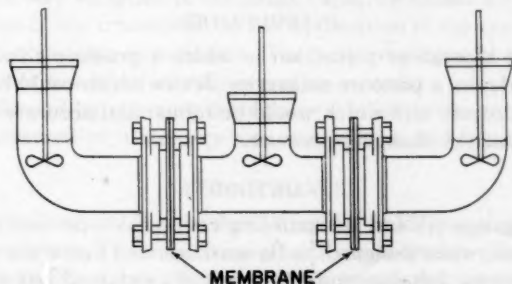
MEMBRANE

FIG. 1. Ion exchange membrane vessel.

assembled from standard 3-in. glass pipe using two 90° elbows and one T piece. This results in a W-shaped vessel whereby each of the two elbows are on the outside separated from the T piece in the center by a No. 3142 Permutit cation exchange membrane inserted between two polyethylene gaskets. Thus, three compartments in series are formed, the outer two containing dilute hydrochloric acid and the center compartment containing the alkaline reaction mixture. The membranes permit the passage of sodium ions from the center compartments into the outer compartments but prevent migration of chloride, chloracetate, or polyamino polyacetate ions from one compartment into the other. In this way, sodium ions are gradually removed from the reaction mixture, the speed of which depends upon the amount of sodium ions and the strength of the hydrochloric acid solution. For example, if 0.75 liter $N/5$ hydrochloric acid is used in each outer compartment (renewed every 4 hours), and if the concentration of the reaction mixture is adjusted to contain 2.5 mole NaOH, the crystallization of DTPA can be expected to occur within 24 hours. The DTPA obtained in this manner melted with decomposition at 224° C. Calculated for $C_{14}H_{23}O_{10}N_3$: C, 42.75; H, 5.89; N, 10.68%. Found: C, 42.81; H, 5.93; N, 10.63; Cl, <0.05; Na, <0.05%. This crystallization is quantitative, as shown by control experiments, and can be accelerated by renewing the hydrochloric acid solution at shorter intervals and by applying a potential across the compartments.

The higher homologues of EDTA such as trimethylenediamine to hexamethylenediamine tetraacetic acids ($n = 3$–6) were also prepared by the chloracetate method and crystallized in the ion exchange vessel.

1. F. MÜNZ. U.S. Patent No. 2,130,505 (September 20, 1938).
2. R. SMITH et al. J. Org. Chem. 14, 355 (1949).
3. F. C. BERSWORTH. U.S. Patent No. 2,407,645 (September 17, 1946).
4. R. SMITH. Master's Thesis, Clark University, Worcester, Mass. 1942.
5. G. SCHWARZENBACH et al. Helv. Chim. Acta, 31, 1029 (1948).

A RECORDING GLASS SPIRAL MANOMETER

F. H. C. EDGECOMBE AND D. A. JARDINE

INTRODUCTION

In a study of the kinetics of a reaction in which a pressure change occurred, it was found necessary to devise a pressure-measuring device which could be used in an atmosphere corrosive to mercury and which would be robust and accurate and able to provide a continuous record of the changing pressure.

METHOD

The glass spoon gauge (1) and its recording counterpart devised by Hooley (2) were not sufficiently robust, when designed, to be sensitive, and hence the stronger glass spiral manometer described by Johnson and McIntosh (3) was modified to make a recording instrument.

In Fig. 1, a schematic representation of the manometer, B and C form the plates of a
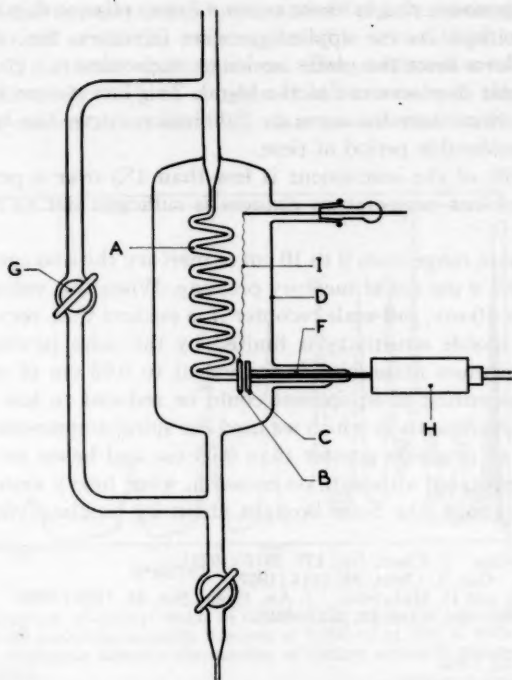
FIG. 1. Schematic diagram of the recording glass spiral manometer.

simple parallel condenser; B, a thin brass plate attached to the glass spiral, is grounded through a wire I. I should be preferably very flexible, e.g. Litz wire, in order to eliminate, so far as possible, drag on the spiral. C is another brass plate attached to a metal rod which, in turn, is sealed in wax to permit adjustment of the distance between the plates. Connected to C through the metal rod is H, the capacitance transducer, obtained from the Decker Corporation of Bala-Cynwyd, Pennsylvania. D is a vacuum-tight glass envelope and G a shorting stopcock through which the envelope may be evacuated when the gauge is used as a differential manometer. The transducer probe, H, is described in detail by Lion (4). Every variation of the gauge capacitor causes a corresponding change in the output voltage of the transducer. In our application of the system the plates C and B of Fig. 1 form the variable capacitance. The voltage output of the transducer is fed through an attenuator to a continuously operating recorder.

The spiral is calibrated by referring the voltage applied to the recorder to the pressure on the spiral, as measured on a mercury manometer by a cathetometer.

PERFORMANCE

The glass spiral used is capable of withstanding the sudden application of a differential pressure of one atmosphere. The sensitivity of such a manometer when used in the system described is very high. By fabrication of thinner spirals, increased sensitivity may be obtained but only at the expense of increasing the "noise level" caused by vibration of the building, which is transmitted to the spiral.

Over small pressure ranges there exists a linear relationship between pressure applied and output voltage. As the applied pressure increases, the calibration curve becomes hyperbolic in form since the plates no longer approximate a parallel relationship due to increased angular displacement of the spiral. This fact cannot be counted as too great a disadvantage, since once an accurate calibration curve has been obtained it remains valid for a considerable period of time.

The zero drift of the instrument is less than 1% over a period of 24 hours and its stability to ambient temperature changes is sufficient not to require any thermostatic control.

Over a pressure range from 0 to 10 cm of mercury the average voltage output from the transducer is 0.2 v per cm of mercury pressure. When this voltage is applied through an attenuator to a 10-mv, full-scale recorder it is evident that very high sensitivities can be obtained. The usable sensitivity is limited by the noise produced by vibration of the spiral. The maximum noise level is equivalent to 0.05 cm of mercury, and by suitable location and mounting of equipment could be reduced to less than that equivalent to 0.01 cm. The experiments in which we used the spiral manometer did not require pressure measurements of precision greater than 0.05 cm and hence no special mounting of the gauge was necessitated although, on occasion, when heavy motors were operating in the vicinity of the gauge, the noise brought about by building vibration was troublesome.

1. R. G. W. Norrish.   J. Chem. Soc. 127, 2316 (1925).
2. J. G. Hooley.   Can. J. Chem. 35, 1414 (1957).
3. F. M. Johnson and D. McIntosh.   J. Am. Chem. Soc. 31, 1138 (1909).
4. K. S. Lion.   Rev. Sci. Instr. 27, 222 (1956).

APPLICATION OF THE VARRENTRAPP REACTION TO THE PREPARATION OF LONG-CHAIN DICARBOXYLIC ACIDS

R. G. Ackman, M. A. Bannerman, M. E. Retson, and F. A. Vandenheuvel

Aliphatic dicarboxylic acids with 11 or more carbon atoms were required for gas–liquid chromatographic identification of similar materials produced by ozonolysis of marine-oil fatty acids. Aside from brassylic acid, prepared by oxidative fission of erucic acid, these acids are not conveniently available. As an alternative to individual syntheses, modification of the Varrentrapp reaction (1–4) by limiting it to redistribution of the 13:14 double bond in erucic acid into adjacent positions, followed by oxidative fission and recovery of the dicarboxylic acids, offered a means of obtaining a number of these acids in one preparation.

The product of alkali fusion at 320° C was selected for oxidative fission as the iodine value of 60 indicated that the Varrentrapp reaction proper, production of the saturated acid two carbon atoms shorter than the original monounsaturated acid, had proceeded only to a limited extent. Since double bonds migrating to the 6:7 or 7:8 positions rapidly participate in the final stages of this reaction (2), it was expected that the residual double bonds in the fusion product would be in positions more remote from the carboxyl group.

The petroleum-ether-soluble ozonolysis product contained chiefly monocarboxylic acids such as palmitic, stearic, and arachidic, with appreciable amounts of odd-numbered monocarboxylic acids of 11 or fewer carbon atoms. The methanol-soluble ozonolysis product contained approximately 60% of roughly equal amounts of the dicarboxylic acids with 7 to 16 and 17 carbon atoms and 40% of monocarboxylic acids with 7 to 16 carbon atoms (Fig. 1).
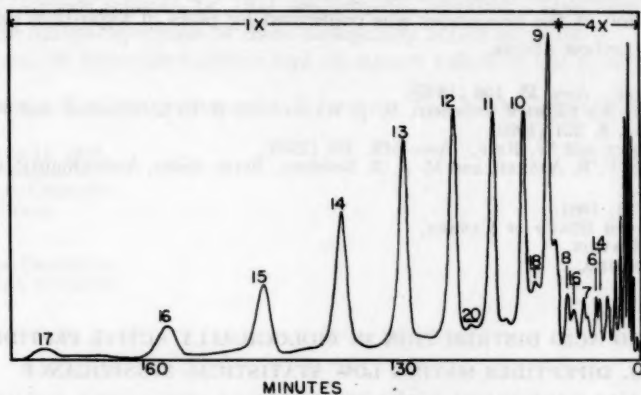

FIG. 1. Gas–liquid chromatogram of methyl esters of dicarboxylic acids. Column, 10 ft × ¼ in., packed with 25% LAC-3R-728 on 60-80 mesh Chromosorb. Analysis of 0.005 ml at 200° C with hydrogen carrier gas flowing at 80 ml/minute. Numerals indicate the number of carbon atoms in the acid chains, monocarboxylic acids being underlined.

Since double bonds are increasingly less susceptible to the Varrentrapp reaction when more remote from the carboxyl group, a higher proportion of long-chain dicarboxylic acids with 15 or more carbon atoms could be obtained by prolonged fusion at lower temperatures. The over-all dicarboxylic acid yield would, however, be diminished as a consequence of further completion of the Varrentrapp reaction.

EXPERIMENTAL

A technical erucic acid, iodine value 85, was employed in this reaction. Gas–liquid chromatography indicated a composition of 72.8% erucic acid, 12.4% eicosenoic acid, 6.7% oleic acid, and minor amounts of palmitic, stearic, linoleic, and arachidic acids. Alkali fusions were carried out in a covered iron vessel fitted with a nitrogen inlet and a stirrer of iron pipe. Equal weights of erucic acid, sodium hydroxide, and potassium hydroxide were placed in this vessel, and it was then placed in a Wood's metal bath preheated 40° C above the reaction temperature. The mixture was stirred continuously for ½ hour and intermittently for a further half hour. The cooled reaction mass was dissolved in water, acidified, and the fatty acids extracted with petroleum ether. Weight recoveries were approximately 80%, with iodine values of 38, 60, and 69 from fusions at, respectively, 360, 320, and 300° C for 1 hour. Gas–liquid chromatography indicated almost complete destruction of the oleic, linoleic, and eicosenoic acids, the products thus consisting chiefly of saturated acids and docosenoic acids.

The alkali fusion product of iodine value 60 (5 g) was ozonized in glacial acetic acid and the ozonide decomposed with hydrogen peroxide (2). The final solution was diluted

to 400 ml with water and extracted with diethyl ether (400 ml). The ether solution was washed with water (50 ml), and the aqueous phases discarded. The ether was removed and the product (5.7 g) was dissolved in 90% methanol (200 ml) and extracted with petroleum ether (b. p. 40–60° C, 200 ml). The petroleum-ether-soluble material (0.9 g) and the methanol-soluble material (4.8 g) were converted to methyl esters with diazomethane. Identification of certain components was effected through mixed gas–liquid chromatograms with authentic materials employing both silicone grease and polyester substrates. The identification of the remainder was confirmed by plots of logarithm retention time vs. number of carbon atoms.

1. F. VARRENTRAPP. Ann. **35**, 196 (1840).
2. R. G. ACKMAN, SIR PATRICK LINSTEAD, B. J. WAKEFIELD, B. C. L. WEEDON, and R. A. DYTHAM. Tetrahedron, **8**, 221 (1960).
3. A. LUTTRINGHAUS and W. REIF. Ann. **618**, 221 (1958).
4. A. V. RONCERO, F. R. AYERBE, and M. A. A. ROMERO. Fette, Seifen, Anstrichmittel, **61**, 900 (1959).

AMINO ACID DISTRIBUTION IN BIOLOGICALLY ACTIVE PEPTIDES
II. DIPEPTIDES HAVING LOW STATISTICAL SIGNIFICANCE

SAUL B. NEEDLEMAN

In the previous publication of this series (1), the amino acid sequences of a number of biologically active proteins were examined for the occurrence of relative chain position preferences of the individual constituent amino acids and for statistically significant repeating amino acid sequences comprising dipeptidic couplet units. Thirty-five dipeptide structures were found for which the chi-square values exceeded the 90% confidence limits for one degree of freedom (2.706). The study is now extended to dipeptide sequences which occur at a very low level of statistical significance.

A total of 10 couplets, listed in Table I, occurred only once in the proteins included in

TABLE I

Dipeptide couplets having low chi-square values

Dipeptide couplet	χ^2 *	Dipeptide couplet	χ^2 *
Ala–Phe	0.000	Cys–Lys	0.013
Asp–Gly	0.003	Cys–Pro	0.013
Asp–Lys	0.000	Gly–Phe	0.015
Cys–Ser	0.001	Leu–Cys	0.013
Glu–Gly	0.002	Lys–Cys	0.013
Glu–Thr	0.000	Lys–Thr	0.016
Leu–Asp	0.000	Phe–Asp	0.023
Pro–Asp	0.000	Phe–Tyr	0.023
Pro–Tyr	0.000	Ser–Asp	0.019
Tyr–Val	0.003	Ser–Gly	0.013
		Ser–Val	0.015
Asp–Ser	0.023	Thr–Lys	0.019
Asp–Phe	0.023	Tyr–Phe	0.023
Cys–Leu	0.013	Val–Ala	0.015

*The chi-square value is calculated from the formula, $\chi^2 = \Sigma (A - C)^2/C$, where A is the "actual" occurrence of a particular dipeptide unit and C is the "chance" occurrence of that couplet.

this study. All had chi-square values of less than 0.00393 at the 0.95 probability level and for one degree of freedom.

If the data are randomly or normally distributed and agree with the null hypothesis, one should expect to get χ^2 values greater than 0.00393 95% of the time. Since these values are much lower, it is possible that the data for these couplets, as well as for the 106 dipeptide combinations (of 400 possible combinations for 20 amino acids) which did not appear at all, are not random, or, that the couplets, somehow, have been preselectively avoided in the natural synthesis of these biologically active proteins.

An additional 18 dipeptide couplets had chi-square values of less than 0.025.

1. S. B. NEEDLEMAN, R. Q. BLACKWELL, and L. S. FOSDICK.   Can. J. Chem. 38, 477 (1960).

SOME NEUTRAL AND ACIDIC EXTRACTIVES FROM CEANOTHUS AMERICANUS L.

R. A. ABRAMOVITCH AND G. TERTZAKIAN

The extractives from *Ceanothus americanus*, also known as New Jersey tea, have been the subject of many investigations (for a survey of the literature on this subject see ref. 1). A number of alkaloidal and acidic constituents have been isolated from the root bark, and some of the fatty and dicarboxylic acids have been identified (2). Bertho and Liang (3) reported the isolation of an alkaloid, ceanothin, for which they gave the molecular formula $C_{29}H_{36}N_4O_4$. On the other hand, Julian, Pikl, and Dawson isolated a high-melting monohydroxydicarboxylic acid which they called ceanothic acid and to which they assigned the molecular formula $C_{29}H_{44}O_5$ (4). The fact that both this acid and the above alkaloid were reported to be C_{29} compounds might indicate a possible structural relationship between them and it was thought to be of interest to examine systematically the composition of the neutral and acidic extractives from *Ceanothus americanus* root bark.

When the ground root bark (kindly supplied by Flint, Eaton and Co., Decatur, Illinois) was percolated and worked up as described by Julian, Pikl, and Dawson (4) no ceanothic acid could be isolated. A crude acid mixture was in fact isolated from which betulic acid was obtained as the main component (the fatty acids and simple dicarboxylic acids being eliminated in the work-up procedure). The same mixture of acids could be obtained by ether extraction. Betulic acid was characterized further as the methyl ester, the methyl ester acetate, and the acetate. A red pigment, believed to be a tannin, can also be isolated in relatively large quantities (11.5% based on dry root bark). Chromatography of the crude high-melting acids on silica gel gave betulic acid as well as a yellow amorphous acid, m.p. 250–260° (decomp.), which could not be purified but whose infrared spectrum indicated the presence of a $\diagdown$C=CH$_2$ group.

The root bark was continuously extracted with ether and the brown oil obtained was saponified with aqueous ethanolic potassium hydroxide (ammonia was evolved during the saponification and identified as ammonium picrate). Steam distillation gave a very small quantity of a saturated aliphatic alcohol which has been tentatively identified as 2-nonanol by comparison of its relative retention time (relative to ethanol) on vapor phase chromatography on two different columns (silicone on firebrick and Apiezon "N" on firebrick) with that of an authentic sample, as well as by a comparison of their infrared spectra. From the steam distillation residue a small amount of β-sitosterol glucoside could be extracted out. Working up the non-saponifiable fraction led to the isolation of (a) β-sitosterol, characterized as its acetate and its benzoate, and (b) lupeol, characterized further as lupeol acetate and dihydrolupeol acetate. A mixture of saturated hydrocarbons was also isolated chromatographically but not characterized further as were also a number of minor compounds.

EXPERIMENTAL

Melting points are uncorrected. Petroleum ether refers to the fraction, b.p. 40–50°, which had been freed of unsaturation. All yields are given as a per cent of dry root bark.

Isolation of the Acidic Components

Dry root bark (2.25 kg) was continuously extracted with ether (8 l.) in a Soxhlet extractor for 3 days. The solution was concentrated to 1 l. and kept in the refrigerator for a few days. The white, oily solid which separated was filtered and extracted exhaustively with petroleum ether. The residue was a tan-colored powder (A). This was dissolved in ether (250 ml), extracted with 10% sodium carbonate solution, and the ether layer dried (Na$_2$SO$_4$) and evaporated to give whitish crystals (15.3 g; 0.69%), which after numerous recrystallizations from methanol yielded betulic acid,* m.p. 312°, $[\alpha]_D^{25}$ +6.04° (pyridine). Found: C, 78.71; H, 10.85. Calc. for C$_{30}$H$_{48}$O$_3$: C, 78.89; H, 10.59. Robertson, Soliman, and Owen give m.p. 317°, $[\alpha]_D$ +7.8° (pyridine) for betulic acid (5). The melting point was undepressed on admixture with an authentic sample of betulic acid. This acid gave the acetate, m.p. 290° (reported (5) m.p. 289–291°); the methyl ester with diazomethane, m.p. 222–223°, $[\alpha]_D^{25}$ +3.5° (pyridine) (reported (5) m.p. 223–224°, $[\alpha]_D$ +8.01° (pyridine)) (found: C, 78.88; H, 10.68; calc. for C$_{31}$H$_{50}$O$_3$: C, 79.10; H, 10.71); and the methyl ester acetate, m.p. 203° (reported (5) m.p. 201–202°).

The crude mixture of acids (A) (2.55 g) was chromatographed on a column of silica gel (70 g). Elution with petroleum ether–benzene (1:2) (3900 ml) gave betulic acid (1.078 g), m.p. 295–300° after recrystallization from aqueous acetone. The infrared spectrum of this acid was identical with that of authentic betulic acid. Elution with benzene–ether (1:1) (2500 ml) gave an amorphous yellow powder (369 mg) m.p. 250–260° (decomp.). Infrared spectrum (main peaks): 3400 (br)(m), 1680 (s), 1635 (m), 1603 (w), 1508 (w), 1280 (br)(m), 1230 (br)(s), 1190 (br), 1105 (m), 1030 (m), and 880 (m) cm^{-1}. This product could not be purified by recrystallization and was not examined further at this stage.

Saponification of the Ether Extractives—The Non-saponifiable Fraction

The viscous, brown ether extractives after removal of betulic acid (16.81 g) were boiled under reflux with 7% aqueous ethanolic (2:3) potassium hydroxide solution (250 ml) for 24 hours. The solution was concentrated at atmospheric pressure at 80° and water was then added and the mixture steam distilled. The distillate was saturated with salt,

*Betulic acid is insoluble in sodium carbonate solution.

extracted with ether, and the dried ether layer evaporated. Distillation of the residue gave 2-nonanol, b.p. 82° at 12 mm, $[\alpha]_D^{25}$ +0.74° (methanol), n_D^{21} 1.4320. Vapor phase chromatography on 6-ft columns of silicone on firebrick and Apiezon "N" on firebrick respectively indicated that this product had the same relative retention times as authentic 2-nonanol. The infrared spectra of the two samples were identical. The reported (6) boiling point of 2-nonanol is 81–83° at 15 mm.

The residue from the steam distillation was continuously extracted with ether. White, needle-like crystals (40 mg), m.p. 310°, separated in the extraction flask and were shown to be identical with β-sitosterol glucoside by comparison of the infrared spectrum with that of an authentic specimen and by a mixed melting point determination. Evaporation of the ethereal extract gave a yellow wax (1.75 g, 0.13%) which crystallized from methanol to give β-sitosterol, m.p. 133.5–135.5°, $[\alpha]_D^{25}$ −31.2° (chloroform). The melting point was undepressed on admixture with an authentic specimen of β-sitosterol. Found: C, 83.55; H, 12.16. Calc. for $C_{29}H_{50}O$: C, 83.99; H, 12.15. The sterol gave the acetate, m.p. 123.5–124.5°, $[\alpha]_D^{26}$ −39.2° (chloroform) (found: C, 81.72; H, 11.07; calc. for $C_{31}H_{52}O_2$: C, 81.52; H, 11.48) (lit. (7) m.p. 126.5–127.5°, $[\alpha]_D$ −36.56°) and the benzoate, m.p. 142–143°.

The crude, non-saponifiable, non-steam-volatile fraction (5 g) after extraction with ether was chromatographed on a column of alumina (28 cm × 2.2 cm). Elution with petroleum ether gave a colorless oil (309 mg), b.p. 200–240° at 0.5 mm (with darkening), n_D^{25} 1.4795, $[\alpha]_D^{26}$ +1.16° (chloroform). Found: C, 86.82, 86.12; H, 13.11, 13.77; mol. wt. (ebullioscopic), 226. Calc. for $C_{20}H_{36}$: C, 86.86; H, 13.14; mol. wt., 276. Calc. for $C_{18}H_{34}$: C, 86.32; H, 13.68; mol. wt., 250. Infrared spectrum (liquid film): 2900 (s), 2860 (s), 1462 (m), and 1371 (m) cm^{-1}. This oil did not take up hydrogen on shaking in the presence of Adams' catalyst even in dioxane – glacial acetic acid solution (20:1) at 2 atm. It did not consume any peracid on treatment with monopherphthalic acid but did decolorize bromine water. In view of the inconsistent analyses this product was not examined further at this stage.

Elution with petroleum ether – benzene (1:2) gave at first a mixture (587 mg) of a ketonic and a non-ketonic compound. The ketonic portion was removed with Girard's reagent "T" giving the non-ketonic portion (493 mg) as a yellow solid which, on recrystallization from methanol, gave lupeol, m.p. 203–204°, $[\alpha]_D^{26}$ +29.5° (chloroform). Found: C, 84.66; H, 12.06; mol. wt. (Rast), 437. Calc. for $C_{30}H_{50}O$: C, 84.44; H, 11.81; mol. wt., 427. The melting point was undepressed on admixture with an authentic specimen of lupeol kindly supplied by Dr. T. R. Govindachari. It formed an acetate, m.p. 204–205°. Found: C, 82.03; H, 11.07. Calc. for $C_{32}H_{52}O_2$: C, 81.99; H, 11.18. Heilbron, Kennedy, and Spring (8) give m.p. 214–215° for lupeol acetate. This acetate was hydrogenated over Adams' catalyst to give dihydrolupeol acetate, m.p. 241–242° (lit. (8) m.p. 245–246°).

Further elution with petroleum ether – benzene (1:2) gave β-sitosterol (980 mg). Elution with somewhat more polar solvents gave intractable materials. Finally, methanol (6750 ml) eluted a brown solid (1.063 g), m.p. 250° (decomp.), which could not be recrystallized.

ACKNOWLEDGMENTS

supply of plant material, to Dr. T. R. Govindachari (Madras) for a sample of lupeol, and to Dr. R. E. Corbett for an authentic sample of betulic acid.

1. G. TERTZAKIAN. M.Sc. Thesis, Saskatchewan. 1960.
2. C. W. ROSCOE and N. A. HALL. J. Am. Pharm. Assoc. 49, 108 (1960).
3. A. BERTHO and W. S. LIANG. Arch. Pharm. 271, 273 (1933).
4. P. L. JULIAN, J. PIKL, and R. DAWSON. J. Am. Chem. Soc. 60, 77 (1938).
5. A. ROBERTSON. G. SOLIMAN, and E. C. OWEN. J. Chem. Soc. 1267 (1939).
6. G. V. NAIR and E. VON RUDLOFF. Can. J. Chem. 38, 177 (1960).
7. J. W. COOK and M. F. C. PAIGE. J. Chem. Soc. 336 (1944).
8. I. M. HEILBRON, T. KENNEDY, and F. S. SPRING. J. Chem. Soc. 329 (1938).

DECARBOXYLATION OF AROMATIC CARBOXYLIC ACIDS IN ISOTOPIC STUDIES

F. B. FISHER AND A. N. BOURNS[1]

It is occasionally necessary in C^{13}-isotopic studies to isolate in a form suitable for mass spectrometric analysis a carbon atom attached directly to an aromatic nucleus. This may be accomplished by oxidation of the compound in question to an aryl carboxylic acid which, on decarboxylation, furnishes carbon dioxide derived exclusively from the carbon whose isotopic abundance is to be determined. When precise isotopic ratios are required, as in kinetic isotope effect studies, it is essential that these degradative reactions proceed with high conversion, otherwise they may give rise to isotopic fractionation which could introduce a serious error in the results.

The two principal decarboxylation methods used in isotopic studies are the copper chromite – quinoline reaction and the Schmidt reaction. The former has given variable yields (1) and, in our hands, contamination from extraneous carbon has been difficult to avoid. The Schmidt reaction has been reported (2) to give carbon dioxide in 55% yield from benzoic acid. By making certain modifications in the original procedure, we have been able to increase the yield to 95% for benzoic and p-anisic acid. When, however, the method was applied to aromatic acids containing electronegative substituents the yield of carbon dioxide fell drastically.

A further method of decarboxylation of value in preparative organic chemistry is the Hunsdecker reaction involving the action of bromine on the silver salt of a carboxylic acid. The higher yields of aryl halide reported for the nitrobenzoic acids compared to benzoic acid (3, 4, 5) suggested that this reaction might be satisfactorily applied to the production of carbon dioxide from aromatic carboxylic acids containing electron-withdrawing groups. This has indeed proved to be the case, yields of over 90% having been obtained from m-nitrobenzoic acid and p-trifluoromethylbenzoic acid. The two reactions, therefore, provide complementary methods for the decarboxylation of aromatic carboxylic acids in isotopic investigations.

[1]To whom all correspondence should be addressed.

EXPERIMENTAL

Hunsdecker Reaction

The silver salts were prepared by the method outlined by Cason and Rapoport (6), collected on a sintered-glass funnel, and dried in a vacuum desiccator. Yields were 90% for benzoic acid and better than 95% for the substituted benzoic acids.

The apparatus for the decarboxylation consisted of a 200-ml three-necked flask fitted with a dropping funnel, nitrogen-inlet tube, and a reflux condenser. Nitrogen gas, used to sweep carbon dioxide from the reaction mixture, was purified by passing through Fieser's solution and concentrated sulphuric acid and was led to the top of the dropping funnel as well as to the inlet tube. The condenser was connected to a CO_2-absorption train consisting of a dry ice – acetone trap and a CO_2 absorber described by Calvin et al. (7).

Silver salt, sufficient to produce approximately 100 mg of barium carbonate, and 60–80 ml of dry carbon tetrachloride were placed in the reaction flask, which was fitted temporarily with a downward distillation assembly in place of the reflux condenser and CO_2-absorption train. The system was flushed with nitrogen and about one third of the carbon tetrachloride removed by distillation. The condenser and absorption train were quickly replaced and, with a slow stream of nitrogen passing through the apparatus, the suspension was heated to the boiling point and stirred magnetically. Bromine (10% in carbon tetrachloride) was added a few drops at a time to the reaction mixture, with time being allowed between successive additions for the solution to decolorize. When the reaction was essentially complete, as usually indicated by the flocculation of silver bromide, a further three to five drops of bromine solution were added and heating continued for an additional 20–30 minutes. Barium carbonate was precipitated by the usual procedure (7). Blank experiments carried out in the absence of silver salt gave less than one milligram of precipitate.

Schmidt Reaction

The procedure described by Doering et al. (2) was used with minor modification. Ethylene dichloride was used as solvent instead of chloroform and the effluent carbon dioxide was passed through a dry ice – acetone trap and 5% permanganate in $1 N$ sulphuric acid (8) and absorbed in sodium hydroxide (7). Sodium azide was added over a period of 40 minutes at 40° C, and stirring and heating were continued an additional 50 minutes. Contamination with extraneous carbon dioxide was found in blank experiments to be less than one per cent.

RESULTS

The per cent yields of barium carbonate from each of four acids using the two methods of decarboxylation are shown in the following table:

Acid	Per cent yield of $BaCO_3$	
	Hunsdecker*	Schmidt
p-Anisic	61	95
Benzoic	90	95
p-Trifluoromethylbenzoic	93	28†
m-Nitrobenzoic	98	9

*Based on silver salt.
†Reaction temperature of 56–60° C.

1. W. G. DAUBEN, J. C. REID, P. E. YANKWICH, and M. CALVIN. J. Am. Chem. Soc. 72, 121 (1950).
2. W. v. E. DOERING, T. I. TAYLOR, and E. F. SCHOENEWALDT. J. Am. Chem. Soc. 70, 455 (1948).
3. W. G. DAUBEN and H. TILLES. J. Am. Chem. Soc. 72, 3185 (1950).
4. R. A. BARNES and R. J. PROCHASKA. J. Am. Chem. Soc. 72, 3188 (1950).
5. J. W. H. OLDHAM. J. Chem. Soc. 100 (1950).
6. J. CASON and H. RAPOPORT. Laboratory text in organic chemistry. Prentice-Hall, Inc., New York. 1950. p. 271.
7. M. CALVIN, C. HEIDELBERGER, J. C. REID, B. M. TOLBERT, and P. E. YANKWICH. Isotopic carbon. John Wiley & Sons, Inc., New York. 1949. p. 83.
8. E. F. PHARES. Arch. Biochem. Biophys. 33, 173 (1951).

NOTES TO CONTRIBUTORS

Canadian Journal of Chemistry

MANUSCRIPTS

General.—Manuscripts, in English or French, should be typewritten, double spaced, on paper $8\frac{1}{2} \times 11$ in. **The original and one copy are to be submitted.** Tables and captions for the figures should be placed at the end of the manuscript. Every sheet of the manuscript should be numbered. Style, arrangement, spelling, and abbreviations should conform to the usage of recent numbers of this journal. Greek letters or unusual signs should be written plainly or explained by marginal notes. Characters to be set in bold face type should be indicated by a wavy line below the characters. Superscripts and subscripts must be legible and carefully placed. Manuscripts and illustrations should be carefully checked before they are submitted. Authors will be charged for unnecessary deviations from the usual format and for changes made in the proof that are considered excessive or unnecessary.

Abstract.—An abstract of not more than about 200 words, indicating the scope of the work and the principal findings, is required, except in Notes.

References.—These should be designated in the text by a key number and listed at the end of the paper, with the number, in the order in which they are cited. The form of the citations should be that used in this journal; in references to papers in periodicals, titles should not be given and only initial page numbers are required. The names of periodicals should be abbreviated in the form given in the most recent *List of Periodicals Abstracted by Chemical Abstracts*. All citations should be checked with the original articles and each one referred to in the text by the key number.

Tables.—Tables should be numbered in roman numerals and each table referred to in the text. Titles should always be given but should be brief; column headings should be brief and descriptive matter in the tables confined to a minimum. Vertical rules should not be used. Numerous small tables should be avoided.

ILLUSTRATIONS

General.—All figures (including each figure of the plates) should be numbered consecutively from 1 up, in arabic figures, and each figure referred to in the text. The author's name, title of the paper, and figure number should be written in the lower left corner of the sheets on which the illustrations appear. Captions should not be written on the illustrations.

Line drawings.—Drawings should be carefully made with India ink on white drawing paper, blue tracing paper, or co-ordinate paper ruled in blue only; any co-ordinate lines that are to appear in the reproduction should be ruled in black ink. Paper ruled in green, yellow, or red should not be used. All lines must be of sufficient thickness to reproduce well. Decimal points, periods, and stippled dots must be solid black circles large enough to be reduced if necessary. Letters and numerals should be neatly made, preferably with a stencil (**do NOT use typewriting**), and be of such size that the smallest lettering will not be less than 1 mm high when the figure is reduced to a suitable size. Many drawings are made too large; originals should not be more than 2 or 3 times the size of the desired reproduction. Wherever possible two or more drawings should be grouped to reduce the number of cuts required. In such groups of drawings, or in large drawings, full use of the space available should be made; the ratio of height to width should conform to that of a journal page ($5\frac{1}{4} \times 7\frac{3}{4}$ in.), but allowance must be made for the captions. **The original drawings and one set of clear copies (e.g. small photographs) are to be submitted.**

Photographs.—Prints should be made on glossy paper, with strong contrasts. They should be trimmed so that essential features only are shown and mounted carefully, with rubber cement, on white cardboard, with no space between those arranged in groups. In mounting, full use of the space available should be made. **Photographs are to be submitted in duplicate;** if they are to be reproduced in groups one set should be mounted, the duplicate set unmounted.

REPRINTS

A total of 100 reprints of each paper, without covers, are supplied free. Additional reprints, with or without covers, may be purchased at the time of publication.

Charges for reprints are based on the number of printed pages, which may be calculated approximately by multiplying by 0.5 the number of manuscript pages (double-space typewritten sheets, $8\frac{1}{2} \times 11$ in.) and including the space occupied by illustrations. Prices and instructions for ordering reprints are sent out with the galley proof.

Contents